
Morphology, Taxonomy, and Phylogeny of Triassic Pholidophorid Fishes (Actinopterygii, Teleostei)

Author(s): Gloria Arratia

Source: Journal of Vertebrate Paleontology, 33(S1):1-138. 2013.

Published By: The Society of Vertebrate Paleontology

URL: <http://www.bioone.org/doi/full/10.1080/02724634.2013.835642>

BioOne (www.bioone.org) is a nonprofit, online aggregation of core research in the biological, ecological, and environmental sciences. BioOne provides a sustainable online platform for over 170 journals and books published by nonprofit societies, associations, museums, institutions, and presses.

Your use of this PDF, the BioOne Web site, and all posted and associated content indicates your acceptance of BioOne's Terms of Use, available at www.bioone.org/page/terms_of_use.

Usage of BioOne content is strictly limited to personal, educational, and non-commercial use. Commercial inquiries or rights and permissions requests should be directed to the individual publisher as copyright holder.

MORPHOLOGY, TAXONOMY, AND PHYLOGENY OF TRIASSIC PHOLIDOPHORID FISHES (ACTINOPTERYGII, TELEOSTEI)

GLORIA ARRATIA

Biodiversity Institute, The University of Kansas, Dyche Hall, Lawrence, Kansas 66046, U.S.A., garratia@ku.edu

ABSTRACT—This study presents the first comprehensive revision of ‘pholidophoriform’ fishes, which are a key taxon for understanding the early diversification of teleost fish. Systematic revisions of Triassic pholidophorids, which are based on numerous well-preserved specimens, include †*Annaichthys*, gen. et sp. nov., †*Knerichthys*, gen. nov., †*Parapholidophorus*, †*Pholidoctenus*, †*Pholidophoretes*, †*Pholidophorus*, †*Pholidorhynchodon*, and †*Zambellichthys*, gen. et sp. nov. The morphological descriptions presented support a phylogenetic analysis that proposes a new hypothesis for character evolution within basal Teleostei, with implications for holosteans and teleosteans. The phylogenetic analysis resolves traditional ‘pholidophoriform’ species as a paraphyletic assemblage, with some grouped in a monophyletic †Pholidophoridae and others more closely related to crown-group teleosts. The monophyletic Family †Pholidophoridae is restricted to European Triassic taxa and is the sister group of the Jurassic genus †*Eurycornus* plus all other teleosts. The latter clade is supported by several synapomorphies, such as an elongate posteroventral process of the quadrate, long epineurial processes, and seven or more ural neural arches modified as uroneurals. †*Pholidophorus bechei* is removed from †Pholidophoridae and recognized as the new genus †*Dorsetichthys*. Current evidence indicates that the Upper Triassic †*Pholidophoretes salvus* and †*Knerichthys bronni* represent the oldest known pholidophorids, and †*Prohalecites* from the Middle/Upper Triassic boundary represents the oldest stem teleost. Aspidorhynchiforms, pachycormiforms, and †*Prohalecites* are resolved as stem teleosts. The monophyly of Teleostei, which now includes Triassic pholidophorids, is supported by numerous synapomorphies, such as one suborbital, two supramaxillae, and the articular fused to the angular and retroarticular bones—with further transformations within more advanced teleosts. Synapomorphies of Teleosteomorpha, the clade including crown-group teleosts and all fish more closely related to them than to their closest extant relatives, include the autosphenotic lacking a dermal component, an unpaired vomer, and one long, toothed, serrated appendage on the cleithrum.

INTRODUCTION

†Pholidophoriformes Berg (1937) is a poorly known assemblage of Mesozoic actinopterygian fishes whose close association with teleosts and their closest relatives makes them an important group for the understanding of the modern radiation of fishes. The several families that are included within †Pholidophoriformes range from the Late Triassic (Carnian) to the Late Cretaceous (Cenomanian; Arratia, 2000) and share a common body shape and scale type. More recently, however, the monophyly of †Pholidophoriformes and the relationships of its constituent families have been cast into doubt. The rhombic ganoid scales with peg-and-socket articulation and the elongate or fusiform body shape shared by †pholidophoriforms are now recognized to have a broad distribution within primitive actinopterygians (e.g., Schultze, 1966; Schultze and Cumbaa, 2001; Zhu and Schultze, 2001; Cloutier and Arratia, 2004; Grande, 2010). As a result, the nature and phylogenetic affinities of the various taxa constituting †Pholidophoriformes (collectively referred to here as ‘pholidophoriforms’) are uncertain.

The importance of ‘pholidophoriforms’ to understanding the origin and evolution of Teleostei, a group that includes over half of all living vertebrate species, is underscored by continued use of the type species of the genus, †*Pholidophorus latiusculus*, as a temporal calibration point for molecular trees of Teleostei (e.g., Alfaro et al., 2009; Betancur-R. et al., 2013; Broughton et al., 2013). Although *P. latiusculus* has been interpreted as one of the oldest teleosteans (Arratia, 2000, 2004), this has not yet been evaluated within a broader phylogenetic context of ‘pholidophoriforms’ and basal teleosts.

In this memoir, osteological data from hundreds of well-preserved specimens are presented through detailed descriptions and illustrations. The morphological patterns presented by these fish specimens, part of which were previously undescribed, provide new information to better understand the phylogenetic

relationships of basal teleosts and their immediate outgroups. The morphological data presented here form the basis of an integrative evolutionary study that will draw on comparative osteology to analyze and understand (a) the characteristics of Triassic ‘pholidophoriform’ taxa; (b) their basic taxonomy; (c) the relationships of holosteans, ‘pholidophoriforms,’ and teleosts; and (d) how their traits impacted evolutionary history.

TAXONOMIC BACKGROUND

The taxa included within †‘Pholidophoriformes’ have changed considerably over the years, and it is difficult to find arguments explaining the changes, which makes interpretation of the group problematic and confusing. In this section, I provide background on the taxonomic content and phylogenetic affinities of ‘pholidophoriform’ fish.

Taxonomic Content of †Pholidophoriformes

In the 19th century, only a single family of ‘pholidophoriforms’ was recognized, the family †Pholidophoridae (Woodward, 1890). †Pholidophoridae was originally included within the suborder Isospondyli, together with the families †Oligolepididae and †Leptolepididae, based on characters such as “notochord varying in persistence, the vertebral centra usually complete, but none coalesced; tail homocercal, but hemal support not much expanded or fused; symplectic bone present; scales ganoid only in the less specialized families” (Woodward, 1895:440). About 50 years later, the order †Pholidophoriformes was erected by Berg (1937) to contain the families †Pholidophoridae, †Archaeomaenidae, and †Oligolepididae within subclass Actinopterygii. Later, the order was renamed †Pholidophorida and its constituency broadened to include †Pleuropholidae, in addition to the original families (Danil’chenko and Yakolev, 1964). †Pholidophorida was included within the superorder Holostei, or the ‘bony ganoids’

(Danil'chenko and Yakolev, 1964). This approach was partially followed by Lehman (1966), who maintained the group as part of Holostei and added the families †Majokiidae, †Ligullelidae, and †Galkiniidae within the order, which he referred to †Pholidophoriformes. In subsequent studies, †Oligopleuridae was removed from the ‘pholidophoriforms,’ and its content was split into different major actinopterygian groups that had no close relationship to †Pholidophoriformes. For example, †*Oligopleurus esocinus* was interpreted as a member of Halecostomi (Patterson, 1973), †*Oligopleurus vectensis* (= †*Arratiaelops vectensis*) was included in Teleostei (Elopomorpha; Taverne, 1999), and †*Ionoscopuss* was placed in Halecomorphi (e.g., Grande and Bemis, 1998).

†Pholidophoriformes is currently interpreted as a non-monophyletic group (Arratia, 2000) that informally includes the families discussed below.

†Pholidophoridae—This important family has a history as complicated as †Pholidophoriformes, due mainly to the content of †*Pholidophorus* and its somewhat vague original definition (Agassiz, 1832), which has led to it becoming a taxonomic wastebasket for fish possessing rhombic ganoid scales. †*Pholidophorus* is “one of the most extensive holostean genera,” including taxa from all over the world, ranging from the Late Triassic of Europe to the Early Cretaceous of South America (Nybelin, 1966:354).

Pholidophoridae was erected originally by Woodward (1890) to contain the genus †*Pholidophorus*. A few years later, it was expanded to also include †*Thoracopterus*, †*Pholidopleurus*, †*Peltopleurus*, †*Pleuropholis*, †*Archaeomaene*, and †*Ceramurus* (Woodward, 1895). Eventually, Woodward (1941) divided the genus †*Pholidophorus* into four genera: †*Pholidophorus* Agassiz, †*Pholidophoroides* Woodward, †*Pholidophoristion* Woodward, and †*Ichthyokentema* Woodward. The content of †Pholidophoridae during the 50 years spanned by Woodward (1890, 1941) grew from a single genus to 10 genera, all of which possess rhombic ganoid scales. Subsequent to that, various members of the family were removed to different fish groups. For instance, the gliding fish †*Thoracopterus* from the Triassic of Europe and Asia was removed from ‘pholidophoriforms’ and assigned, in succession, to the order †Perleidiformes (Lehman, 1966), order †Peltopleuriformes (Tintori and Sassi, 1992), and stem Neopterygi (Yu et al., 2012). Similarly, †*Peltopleurus* was removed from ‘pholidophoriforms’ and placed in a newly created order, †Perleidida (Berg et al., 1964) before being assigned to the order †Peltopleuriformes (e.g., Lehman, 1966; Bürgin, 1992). †*Pholidopleurus* was placed in the new order †Pholidopleurida (Berg et al., 1964) before Lehman (1966) changed the ordinal name to †Pholidopleuriformes. †*Pleuropholis*, †*Archaeomaene*, †*Ceramurus*, †*Ichthyokentema*, and †*Pholidophoristion* are currently included in separate non-pholidophorid families within †Pholidophoriformes (see below).

To further complicate the history of the family, Nybelin (1966) restricted the family †Pholidophoridae to include only a few European species of †*Pholidophorus* (from the Late Triassic and Early Jurassic), †*Pholidolepis* (Early Jurassic), †*Pholidophoroides* (Early Jurassic), and †*Pholidophoropsis* (Early Jurassic). Here and elsewhere, this will be referred to as †Pholidophoridae sensu stricto. This was modified by Zambelli (1980c, 1986, 1990), who added the Late Triassic Italian genera †*Parapholidophorus*, †*Pholidoctenus*, †*Pholidorhynchodon*, and †*Eopholidophorus*. Consequently, †Pholidophoridae sensu stricto only contains some of the European Triassic and Early Jurassic species previously described as †*Pholidophorus*, but leaves out all non-European species, which according to Nybelin (1966) were in need of revision because most of them were poorly known or based on fragments (see below). Later studies of some of the Late Jurassic European species previ-

ously identified as †*Pholidophorus* from France and Germany led Gaudant (1978) to use the term †Pholidophoridae sensu lato to designate more species than those considered by Nybelin (1966). As result of this revision, some Late Jurassic species previously identified as †*Pholidophorus* were assigned to the new genera †*Ankylophorus*, †*Lemanophorus*, and †*Pholidorichthys* (Gaudant, 1978). Recently, the revision of †*Pholidophorus macrocephalus* resulted in creation of a new genus, †*Siemensichthys* (Arratia, 2000). At the same time it was proposed that all Late Jurassic and Cretaceous species included in †*Pholidophorus* be identified as †*Pholidophorus* to note that they were in need of revision and that the genus is not monophyletic (Arratia, 2000; see below, description of †*Pholidophorus*, ‘Taxonomic Comments,’ and ‘Concluding Remarks’).

In sum, the family †Pholidophoridae sensu lato is currently interpreted to contain †*Pholidophorus* from the Late Triassic of Europe; †*Pholidophorus*, an unnatural assemblage of species from the Early Jurassic to the Early Cretaceous of Europe, Asia, and Gondwanan continents; †*Parapholidophorus*, †*Pholidorhynchodon*, †*Eopholidophorus*, †*Pholidoctenus*, and †*Pholidophoretes* from the Late Triassic of Europe; †*Jianligichthys* from the Late Triassic of China; †*Pholidophoroides* and †*Pholidophoropsis* from the Early Jurassic of Europe; †*Hengnania* from the Early Jurassic of China; and †*Hungkuichthys* and †*Baleichthys* from the Middle Jurassic of China (Chang and Jin, 1996). Pholidophoridae sensu lato or ‘Pholidophoridae’ is a non-monophyletic family (Arratia, 2000, 2004).

†Ichthyokentemidae—This family includes †*Ichthyokentema purbeckensis* Davies from the Upper Jurassic of England, which is one of the best-known ‘pholidophoriforms’ due to the extensive revision by Griffith and Patterson (1963). This species is included here as part of the ingroup in the phylogenetic analysis. The genus †*Elpistioichthys* from the Carnian of Lunz, Austria, was tentatively assigned to this family by Griffith (1977). It has not been revised after its original description, and its taxonomic position remains uncertain.

†Archaeomaenidae—This family includes at least four genera (†*Archaeomaene*, †*Madariscus*, †*Wadeichthys*, and †*Oreochima*) from the Lower Jurassic of Antarctica (†*Oreochima*), and Upper Jurassic and Lower Cretaceous of Australia (Lehman, 1966; Waldman, 1971; Schaeffer, 1972; Babcock et al., 2006). The Late Jurassic genera †*Aphnelepis* and †*Aetheolepis* from Australia were assigned to separate families—†*Aphnelepidae* and †*Aetheolepidae* by Wade (1941). For a long time, this assignment was not accepted, and the genera were retained in Archaeomaenidae. Recently, though, Taverne (2011a) validated these two family names, in addition to †*Archaeomaenidae*, with no explanation. None of the four genera have been revised after their original descriptions, although that new material of †*Oreochima* has been collected (Babcock et al., 2006).

†Catervariolidae—This monotypic family is based on †*Catervariolus* from the Middle Jurassic of the Democratic Republic of Congo (Taverne, 2011b). Recently, the family was included as the most basal family within †Pholidophoriformes (Taverne, 2011b), but it was previously listed as Teleostei incertae sedis by Schaeffer and Patterson (1984).

†Ankylophoridae—A poorly known family comprising †*Ankylophorus* and †*Lehmanophorus* from the Upper Jurassic of France (Gaudant, 1978) was recently enlarged (Taverne, 2011b) to contain other genera previously included in the †*Siemensichthys* group of Arratia (2000). †*Pholidophorus aequatorialis* from the Middle Jurassic of Congo is now assigned to a new genus, †*Steurbautichthys*, which is interpreted as a member of †Ankylophoridae together with †*Pholidophoristion* and †*Lemanophorus* (Taverne, 2011a). Diagnostic features of †Ankylophoridae and its content are discussed below.

†Pleuropholidae—This very poorly known family includes at least four genera (*†Pleuropholis*, *†Parapleuropholis*, *†Austropleuropholis*, and *†Gondwanapleuropholis*) from the Upper Jurassic to the Lower Cretaceous of Europe and the Gondwanan continents (Janensch, 1925; Saint-Seine, 1955; Chiappe et al., 1998; Brito and Gallo, 2002). They are easily distinguished by the presence of a single row of deepened ganoid scales covering almost the whole side of the body. A comprehensive study of the family is not available yet.

Other Families—The poorly known monotypic families *†Lombardinidae* and *†Signeuxellidae* (Saint-Seine, 1955) from the Middle Jurassic of Central Africa (Congo) are doubtfully assigned to †Pholidophoriformes' (Taverne, 2011b). Both families are in need of revision to test their validity and their position among neopterygians. *†Oligopleuridae*, from the Upper Jurassic of France, known by *†Oligopleurus esocinus*, was recently revalidated as a 'pholidophoriform' family by Taverne (2011b); however, diagnostic characters supporting the family—which is based on poorly preserved material—were not presented by Taverne (2011b). The monotypic family *†Majokiidae* from the Upper Jurassic of Congo and *†Galkiniidae* (known from two genera, *†Galkinia* and *†Ceramurus*) from the Upper Jurassic of Russia and the English Purbeck were interpreted as pholidophoriforms by Berg (1937), and later by Lehman (1966). However, the *†Majokiidae* was removed from *†Pholidophoriformes* without explanation by Schaeffer and Patterson (1984). The two families are very incompletely known and have not been revised after their original descriptions.

The Early Cretaceous family *†Siyuichthyidae* from China includes the genera *†Siyuichthys*, *†Wukungia*, *†Dsungarichthys*, *†Bogdaichthys*, and *†Manasichthys* (Chang and Jin, 1996), all of which are based on poorly preserved material in need of revision. The monotypic family *†Ligulellidae* from the Upper Jurassic of Congo was recently revised, removed from 'pholidophoriforms,' and included in a new order, Ligulelliformes, whose described relationship was inconsistent within the paper (Taverne, 2011c). For instance, it was presented as a new order within Halecostomi in the paper's title, and then stated as having "an intermediate position between Pachycormiformes and 'Pholidophoriformes' in the evolutionary tree of actinopterygians" (Taverne, 2011c:230). For this reason, the phylogenetic position of *†Ligulellidae* is in need of revision.

One genus, *†Pholidophorichthys*, from the Upper Jurassic of France was not assigned to any family and is considered a 'pholidophoriform' incertae sedis (Gaudant, 1978).

The oldest members of the †Pholidophoriformes' are known from marine Upper Triassic localities of Europe and Asia. The European 'pholidophoriforms' come from the Carnian and Norian of Austria and the Norian and Rhetian of Italy (e.g., *†Pholidophoretes* Griffith, 1977; *†Pholidophorus* Agassiz, 1832; *†Parapholidophorus* Zambelli, 1975). Asian 'pholidophoriforms' have been assigned to *†Pholidophoridae* and come from the continental Xujiaje Formation of Sichuan Province, China (e.g., *†Jialingichthys*; Su, 1983; Chang and Fan, 1996). A recent review of the fossil fishes of Gondwana suggested that the oldest 'pholidophoriform' is from the Triassic of Gosford, Australia (López-Arbarello et al., 2008). This refers to *†Pholidophorus gregarius* (Woodward, 1890) from Gosford, New South Wales, a taxon later considered by Wade (1940) to be a member of *†Perleididae* and renamed *†Chrotichthys*. *†Chrotichthys gregarius* is not a 'pholidophoriform' and is currently interpreted as a subholostean belonging within the order Perleidiformes sensu Lombardo and Tintori (2004) and Lombardo et al. (2011). A ?Middle Triassic 'pholidophoriform,' *†Pholidophorus vallejensis*, was described based on a poorly preserved specimen from the Cuyana Basin (Agua de la Zorra Formation), Argentina (Rusconi,

1947). It was assigned to *†Pholidophorus* because of certain similarities to *†Ph. micronyx* from the Upper Jurassic of Germany (Rusconi, 1947). However, "there is no meaningful anatomical similarity" between *†Ph. vallejensis* and *'Ph' micronyx*, and currently *†Pholidophorus' vallejensis* cannot be diagnosed beyond Actinopterygii incertae sedis (López-Arbarello et al., 2010:264). *†Pholidophorus dentatus* from the lower Upper Triassic Potrerillos Formation, Cuyana Basin, Argentina, was described as a new species based on two isolated scales, identified as holotype and paratype (Rusconi, 1946). The material was never illustrated and is currently lost. *†Pholidophorus' dentatus* currently cannot be diagnosed beyond Actinopterygii incertae sedis (López-Arbarello et al., 2010).

Diagnoses of *†Pholidophoriformes*, *†Pholidophoridae*, and *†Pholidophorus*

†Pholidophoriformes—This order was erected by Berg (1937) based on 12 characters that are currently interpreted to be primitive or incorrect:

- (1) scales and bones built as in *Lepidosteus*;
- (2) small, anteriorly positioned premaxilla;
- (3) maxilla covered by two supramaxillae;
- (4, 5) lower jaw without prearticular, coronoid, and surangular;
- (6) vertebral centra absent;
- (7) ossified ribs present;
- (8) intermuscular bones absent;
- (9) dorsal and anal fins with each radial bearing one lepidotrichium;
- (10) abbreviate heterocercal caudal fin present;
- (11) unfused or enlarged hypurals; and
- (12) scales covered with ganoine.

Feature 1, scales and bones built as in *Lepidosteus* (= *Lepidosteus*), is difficult to evaluate because it could refer to many different aspects of the scale (e.g., thickness, ornamentation). Even so, there are major differences in the scales and bones of taxa identified as pholidophoriforms by Berg (1937), so it is not clear how this feature unites the group. Feature 2, small, anteriorly positioned premaxilla, is found in pholidophoriform taxa, but it is also found in other taxa, such as the Actinopterygii incertae sedis *†Prohalecites* (Tintori, 1990; Arratia and Tintori, 1999), basal teleosts such as *†Leptolepis coryphaenoides*, *†Varasichthys*, *†Tharsis*, *†Ascalabos*, and others (Arratia, 1994, 1997, 1999). Additionally, some Triassic 'pholidophoriforms' lack this feature (see below). Feature 3, maxilla covered by two supramaxillae, characterizes some 'pholidophoriforms' (e.g., *†Pholidophorus latiusculus* [Nybelin, 1966; Arratia, 2000], *†Ph. bechei* [e.g., Nybelin, 1966; Arratia 1999, 2000], *†Eurycornus* [e.g., Wenz, 1968; Patterson, 1973; Arratia and Schultze, 2010], *†Pholidophoroidea* [Nybelin, 1966], *†Pholidolepis* [Nybelin, 1966], *†Catervariolus* [Taverne, 2011b]), but others have only one supramaxilla (e.g., *†Siemensichthys* [Arratia, 2000], *†Ankylophorus* [Gaudant, 1978; Arratia, 2000]; see below, 'Analysis of Some Morphological Characters Used in Diagnoses and Phylogenetic Analysis'). Two supramaxillae are also found in most basal teleosts such as *†Leptolepis coryphaenoides* (Nybelin, 1974; Taverne, 1975; Arratia, 1996), *†Tharsis* (Nybelin, 1966), *†Ascalabos* (Arratia, 1997), *†Varasichthys* (Arratia, 1981, 1994), ichthyodectiforms, and elopiforms, and in various extant clupeocephalans (e.g., Gregory, 1937; Grande, 1985; see Arratia, 1997 and 2010, for references). Features 4 and 5, lower jaw without prearticular, coronoid, and surangular, are not present in 'pholidophoriforms,' as it will be demonstrated below (see also Patterson, 1973; Arratia, 2000; Arratia and Schulze, 2010; Taverne, 2011a, 2011b).

The absence of coronoid and surangular bones are currently interpreted as synapomorphies of Teleostei (e.g., Patterson, 1977; Pinna, 1996; Arratia 1997, 1999, 2000, Arratia and Tischlinger, 2010). Feature 6, vertebral centra absent (pleurocentra plus hypocentra) or retained as rings or amphicoelous, is partially correct. Information on vertebrae is scarce in ‘pholidophoriforms’ because scales cover the vertebral column and obscure structure. In those species where the condition has been observed, the vertebrae have thin-walled, ring-like chordacentra surrounding an unconstricted notochord (e.g., †*Pholidophorus bechei* [Nybelin, 1966; Arratia, 1991], †*Pholidoropsis* [Nybelin, 1966], †*Pholidophoroides* [Nybelin, 1966], †*Parapholidophorus* [Zambelli, 1975], †*Pholidoctenus* [Zambelli, 1977], †*Pholidophoretes* [Griffith, 1977], †*Ichthyokentema* [Griffith and Patterson, 1963], †*Eurycornus* [Arratia and Schultze, 2010], †*Siemensichthys* [Arratia, 2000]; and see descriptions below). Amphicoelous vertebrae have not been observed in ‘pholidophoriforms,’ and this particular type of vertebra (compact centrum with concave anterior and posterior articular surfaces that give an hour-glass shape to the centrum) is unique to Teleostei (e.g., Goodrich, 1909; Arratia, 1997, 1999; Arratia et al., 2001). The presence of ring-like chordacentra is a widespread feature observed in a variety of neopterygians, e.g., macrosemiiforms (e.g., Lehman, 1966; Bartram, 1977; Arratia and Schultze, 2012), some halecomorphs (e.g., Lehman, 1966; Grande and Bemis, 1998; Arratia et al., 2001), aspidorhynchiforms (Brito, 1997; pers. observ.), and †*Atacamichthys* (Arratia and Schultze, 1987). Feature 7, presence of ossified ribs, is a generalized feature among neopterygians (e.g., lepisosteiforms [e.g., Grande, 2010], halecomorphs [e.g., Goodrich, 1909; Grande and Bemis, 1998], pycnodontiforms [e.g., Nursall, 1996, 1999], pachycormiforms [e.g., Arratia and Schultze, 2013], aspidorhynchiforms [e.g., Brito, 1997], and basal teleosts [e.g., Arratia, 1997; pers. observ.]) and does not support a grouping of pholidophoriforms. Feature 8, absence of intermuscular bones, is imprecise because there are different kinds of intermuscular bones—supraneurals, epineurals, epipleurals, epicentrals—and the character does not specify which intermuscular bone is supposed to be absent in ‘pholidophoriforms.’ Supraneurals are found in all neopterygians so far as is known (e.g., Grande and Bemis, 1998; Arratia et al., 2001; Grande, 2010; pers. observ.). The absence of epineural processes or bones is the generalized condition present in most neopterygians (pers. observ.). Long epineurals and epipleurals are considered synapomorphies of Teleostei (e.g., Patterson and Johnson, 1995; Arratia, 1997, 1999, 2000; Arratia and Tischlinger, 2010). In contrast, epicentrals are found only in certain teleostean lineages (e.g., Patterson and Johnson, 1995). Feature 9, dorsal and anal fins with each radial bearing one lepidotrichium, may represent a misinterpretation of anatomy. The first and last radials in pholidophoriforms bear more than one lepidotrichium, as described below, which is observed in other neopterygians, such as macrosemiiforms (e.g., Lehman, 1966; Bartram, 1977; Arratia and Schultze, 2012), halecomorphs (e.g., Grande and Bemis, 1998; Arratia and Schultze, 2010), pycnodontiforms (e.g., Nursall, 1996, 1999), and teleosts (Arratia, 2008; 2012). Feature 10, presence of an abbreviate heterocercal caudal fin, is broadly distributed among basal neopterygians (e.g., Lehman, 1966; Bartram, 1977; Grande and Bemis, 1998; Arratia, 2008; pers. observ.). Feature 11, unfused or enlarged hypurals, are only known from a few ‘pholidophoriforms,’ because the presence of scales frequently obscures the caudal endoskeleton. However, the few known caudal skeletons of ‘pholidophoriforms’ show small and unfused hypurals (see below, descriptions of †*Parapholidophorus* and †*Pholidoctenus*). This feature is not unique to ‘pholidophoriforms,’ because small and unfused hypurals are broadly distributed among neopterygians (e.g.,

lepisosteiforms [e.g., Schultze and Arratia, 1986], halecomorphs [Schultze and Arratia, 1986], aspidorhynchiforms [e.g., Brito, 1997, 1999], and basal teleosts, such as †*Leptolepis coryphaenoides* [Wenz, 1968; Taverne, 1975; Arratia, 1991], †*Tharsis* [Arratia, 1991, 1997, 1999], and †*Ascalabos* [Arratia, 1991, 1997]). Feature 12, scales covered with ganoine, is considered a synapomorphy of Actinopterygii (e.g., Schultze, 1977; Patterson, 1982).

Danil'Chenko and Jakolev (1964) proposed an abbreviated list of diagnostic characters, several of which overlap with those of Berg (1937). Some of the proposed features are anatomical misinterpretations of the group:

- (1) premaxilla small, extensible;
- (2) lower jaw composed of a maximum of two or three elements;
- (3) branchial operculum complete, with numerous branchiostegal rays;
- (4) pleurocentra and hypocentra usually present, either annular, amphicoelous, or opisthocelous;
- (5) fused or enlarged hypurals absent;
- (6) fulcra present; and
- (7) scales covered with ganoine.

Features 2, 4, 5, and 6, as already discussed above, have a widespread distribution among actinopterygians and cannot diagnose ‘pholidophoriforms.’ Feature 1, premaxilla small, extensible, is not present in any ‘pholidophoriform,’ halecostome, halecomorph, or basal teleost. I am uncertain whether the authors interpret ‘extensible’ as a synonym of ‘mobile’; but if this is the case, teleosts have a premaxilla capable of a certain degree of mobility. Feature 3, branchial operculum complete, with numerous branchiostegal rays, is also present in other neopterygians, e.g., halecomorphs and basal teleosts (e.g., McAllister, 1968; Arratia, 1997, 1999, 2000; Grande and Bemis, 1998). Feature 6, fulcra present, is present broadly in actinopterygians, with some exceptions (e.g., *Amia*, pycnodontiforms, and most crown-group teleosts; e.g., Patterson, 1982; Cloutier and Arratia, 2004; Arratia 2008, 2009).

Lehman (1966) offered a slightly modified diagnosis of pholidophoriforms, which for him included additional families, with the addition of the following characters:

- (1) elongate, independent maxilla; and
- (2) lower jaw lacking certain dermal ossifications (e.g., splenial, surangular).

The first feature is indeed present in ‘pholidophoriforms,’ but it is not unique to the group because it is a synapomorphy of Halecostomi (including Halecomorpha and Teleostei; Patterson and Rosen, 1977; Grande and Bemis, 1998; Grande, 2010). The second character is not unique to ‘pholidophoriforms,’ because it is also found in teleosts and other neopterygians, which lack independent splenials (Wenz, 1968; pers. observ.), but possess a surangular, as described below.

The three diagnoses presented above were published as part of paleontological treatises illustrating the knowledge of the time concerning taxonomic interpretation of fossil fishes. None of the authors was a specialist on pholidophoriforms, and their diagnoses can be read as elaborated interpretations of the available literature at the time. The three diagnoses did not have the benefit of Hennig's (1966) approach to the interpretation of characters in phylogenetic systematics. Unfortunately, as the analysis of characters presented above demonstrates, not a single character nor combination stands as a synapomorphy supporting the monophyly of †‘Pholidophoriformes,’ because all possible combinations are present in one or another neopterygian group.

†Pholidophoridae—The Family †Pholidophoridae was erected by Woodward in 1890. The characters used to diagnose the family hold similar problems as those of the order †Pholidophoriformes, as explained above, because they are broadly distributed among

actinopterygians. In Woodward's (1890) original diagnosis, these included body elongate or fusiform; head with well-developed membrane bones, externally enameled; snout not pronounced; gape of mouth wide; teeth small and conical; fin fulcra present, but usually small; and upper lobe of the tail externally inconspicuous or slightly pronounced. Later, Woodward (1895) provided a more extended diagnosis that added the following features: suborbital and circumorbital plates completely covering the cheek; mandibular suspensorium almost vertical or inclined forwards; premaxilla very small; maxilla large, loosely attached and with two well-developed supramaxillary plates; opercular apparatus complete; vertebral centra never advanced beyond the annular stage; ribs delicate; no fused or expanded hemal arches at the base of the tail; intermuscular bones absent; dorsal and anal fins small, the former above or behind the pelvic fins; and scales ganoid, more or less rhombic, but deeply overlapping, with the hinder margin often somehow rounded. Within the family, seven genera were recognized by Woodward (1895): †*Pholidophorus*, †*Thoracopterus*, †*Pholidopleurus*, †*Peltopleurus*, †*Pleuropholis*, †*Archaeomaene*, and †*Ceramurus*. With the exception of †*Pholidophorus*, the other genera have since been removed from the family.

Nearly 70 years after the initial diagnosis, Nybelin (1966) revised a few selected European Triassic and Early Jurassic genera and proposed a new concept of the family, his '†*Pholidophoridae sensu stricto*,' to include only a few European species of †*Pholidophorus*, †*Pholidolepis*, †*Pholidophoroides*, and †*Pholidophoropsis* (see above). This grouping was based on a mostly new set of characters. Like those used by his predecessors, many of these are general features present in a range of actinopterygians, including rostral toothless and not separating premaxillaries; nasals not in contact in midline; five to seven infraorbitals, infraorbital 3 the largest; one or two supraorbitals; two supramaxillaries (a character of the order after Berg, 1937; see above); single gular; suture between opercle and subopercle oblique; and supraorbital sensory canal ending in parietal bone (of traditional terminology) and having no anastomosis with infraorbital canal. All of these characters are present in basal teleosts, such as †*Proleptolepis* (e.g., Nybelin, 1974), †*Leptolepis coryphaenoides* (e.g., Wenz, 1968; Nybelin, 1974), †*Tharsis* (e.g., Nybelin, 1974; Arratia, 1997, 1999), varasichthyids (Arratia, 1991, 1994, 1997), †*Allothrissops* (e.g., Patterson and Rosen, 1977; Arratia, 1999), and fossil and extant elopiforms (e.g., Forey, 1973; Arratia, 1981, 1987, 1997, 1999). Some characters, such as the presence of one or two supraorbitals, one gular, and trajectory of the supraorbital canal, are also found in neopterygians outside teleosts (e.g., semionotids [e.g., Lehman, 1966; Grande, 2010], macrosemiids [Bartram, 1977; Cavin, 2010; Grande, 2010; Arratia and Schultze, 2012], halecomorphs [e.g., Maisey, 1991; Grande and Bemis, 1998; pers. observ. on all these groups]). Furthermore, the presence of a single gular (median element) is common in basal actinopterygians (e.g., Cloutier and Arratia, 2004, and cited literature therein). A toothed rostral separating premaxillaries is described below as a unique feature of one species.

More recently and based on a series of studies on Triassic fishes from northern Italy, Zambelli (1986), an autodidact who dedicated many years to the study of Triassic fishes of Italy, added to the content of †*Pholidophoridae sensu stricto* of Nybelin (1966): the Triassic †*Pholidophorus gervasutti* (see description below) and the Triassic genera †*Parapholidophorus*, †*Pholidoctenus*, and †*Pholidorhynchodon*. Zambelli (1986) discussed previously used characters of Nybelin (1966) and listed a combination of characters to diagnose the family. These included some broadly distributed characters and characters that have an ambiguous definition, such as rostral bone with or without teeth, which may or may not separate the premaxillary bones; nasal bones in contact

to each other or separated medially; and vertebral centra in some forms diplospondylous, in others monospondylous. All characters mentioned above will be redescribed and analyzed in later sections of this memoir.

†*Pholidophorus*—The genus †*Pholidophorus* was erected by Agassiz in 1832 to include two species from the Upper Triassic of Seefeld in Tyrol, Austria, †*Pholidophorus latiusculus* (Fig. 1) and †*Ph. pusillus*. The original diagnosis included the following features: herring-like shape; large rhomboidal scales; caudal fin with nearly equal lobes; scales reach onto the upper lobe; dorsal fin opposite to pelvic fins; and very small anal fin (Agassiz 1832:145; translated from the German by H.-P. Schultze). All these features are found in all pholidophorid species studied below, and except for the rhomboidal scales, they are broadly distributed among basal teleosts, e.g., †*Proleptolepis* (Nybelin, 1974), †*Leptolepis* (e.g., Wenz, 1968; Nybelin, 1974; Arratia, 1997, 1999), †*Tharsis* (Nybelin, 1974; Arratia, 1997, 1999), †*Ascalabos* (e.g., Arratia, 1997), and others. Rhomboidal scales are commonly found in most basal neopterygians (e.g., macrosemiids [e.g., Lehman, 1966; Schultze, 1966; Bartram, 1977], semionotids [e.g., Lehman, 1966; Schultze, 1966; Grande, 2010], lepisosteiforms [e.g., Schultze, 1966; Grande, 2010], aspidorhynchiforms [e.g., Schultze, 1966; Brito, 1997]), including other 'pholidophoriforms' (e.g., †*Ichthyokentemidae* [Griffith and Patterson, 1977], †*Catervarioliidae* [Taverne, 2011]). Later, emended diagnoses provided by Agassiz (1833–1844) and Woodward (1895) were based on broadly distributed features among actinopterygians.

By 1895, more than 50 species of †*Pholidophorus* had been described—mainly from the Jurassic of Europe. Of these, 41 were recognized to be valid species by Woodward (1895). However, most of the species described by Kner (1866, 1867; Fig. 1), such as †*Ph. bronni*, †*Ph. dorsalis*, and †*Ph. microlepidotus*, were not included in Woodward's (1895) revision or any revision since. Exceptions include †*Pholidophorus latiusculus* (Nybelin, 1966; Zambelli, 1986), †*Ph. pusillus* (Nybelin, 1966), and scales of some Triassic pholidophorids from Austria (Schultze, 1966; see below). Among those species described by Kner (1866, 1867), only †*Ph. bronni* will be redescribed here, because †*Ph. pusillus* Agassiz is too fragmentary. Other species not included in Woodward's (1895) catalog will be left out of the present study, including species from the Triassic of Italy (e.g., †*Ph. barazzettii* Bassani, †*Ph. deeckeii* de Zigno, †*Ph. kneri* de Zigno, †*Ph. oblongus* Bellotti, and others), which were founded on poorly preserved and incomplete specimens, some of which were apparently lost during World War II.

In the last 50 years, Lehman (1966), Nybelin (1966), and Zambelli (1986) provided revised diagnoses of the genus †*Pholidophorus*, which like previous ones were based solely on characters that currently are interpreted as primitive among different levels of actinopterygians. As a consequence of the inadequacy of the existing diagnoses, many species all over the world have been erroneously assigned to the genus. For instance, some Triassic species described from South America (listed in Arratia and Cione, 1996), such as †*Pholidophorus dentatus* and †*Pholidophorus vallejensis* from Argentina, are represented by undiagnosable material that cannot be referred to the 'Pholidophoriformes' and have been interpreted as Actinopterygii incertae sedis by López-Arbarello et al. (2010; see above). Numerous species of the Upper Jurassic of Europe, previously assigned to †*Pholidophorus*, are currently under revision and treated provisionally as '†*Pholidophorus*,' as proposed by Arratia (2000). A few Jurassic species from the Gondwanan continents have been revised. For instance, †*Pholidophorus aequatorialis* from the marine Middle Jurassic Stanleyville Beds at Songa, Democratic Republic of Congo, was recently included in a new genus in the family †*Ankylophoridae* (Taverne, 2011b; see above). †*Pholidophorus*

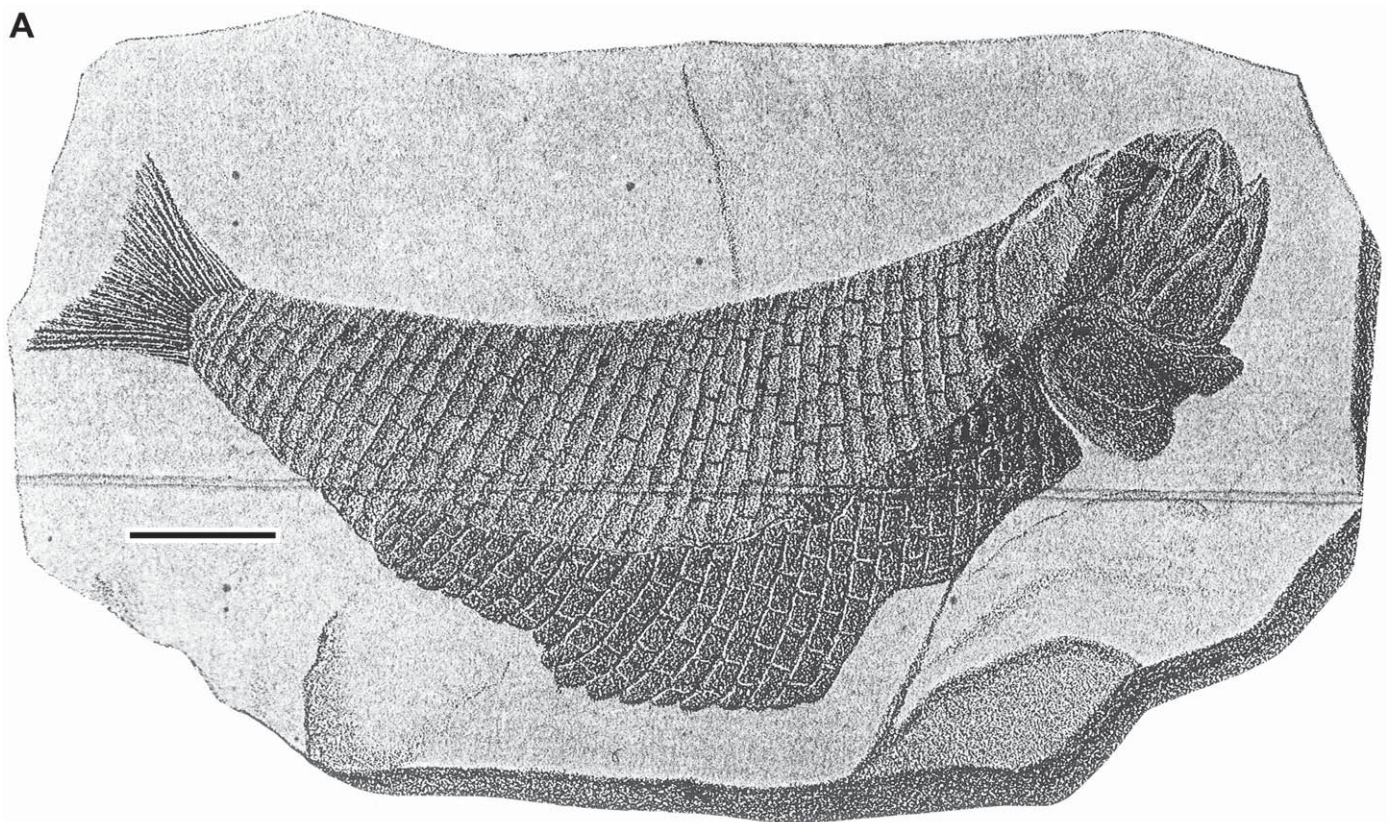
A**B**

FIGURE 1. \dagger *Pholidophorus latiusculus* Agassiz, 1832, from Seefeld in Tirol, Austria. **A**, drawing of specimen Innsb. 123 (from Kner, 1866). **B**, photograph of specimen Innsb. 123 designated as neotype by Nybelin (1966). Scale bars equal 10 mm. Note the damage that the specimen has undergone in the past 150 years. (Color figure available online.)

domeykanus, known from incomplete material from the Oxfordian of Quebrada del Profeta in Chile (Arratia et al., 1975), is a non-pholidophoriform teleost that probably represents a member of the †Varasichthyidae, according to recent revisions (Arratia and Schultze, 1999; contra Taverne, 2011b). †*Pholidophorus argentinus* from the Tithonian Vaca Muerta Formation in Argentina has been recently reinterpreted as an aspidorhynchiform (Gouric-Cavalli and Cione, 2013). Some specimens from the Lower Cretaceous of San Luis, Argentina, were mentioned in the literature as ‘pholidophoriforms’ (identification of the fishes by A. Bocchino de Ringuelet, as cited in Flores, 1969) but never studied systematically. These are currently under revision. Preliminary results do not confirm them as ‘pholidophoriforms,’ but as basal neopterygians (Giordano, 2010; Giordano and Arratia, 2011).

PREVIOUS PHYLOGENETIC STUDIES

‘Pholidophoriform’ species have rarely been included in phylogenetic studies. Most commonly, one species was included (†*Pholidophorus bechei*; e.g., Patterson and Rosen, 1977; Grande and Bemis, 1998; Arratia, 1997, 1999), but occasionally several species were included (e.g., Patterson, 1977a; Arratia, 2000; Taverne, 2011a). Patterson (1977a; Fig. 2A) included seven ‘pholidophoriform’ species, recent halecomorphs, and certain fossil teleosts in an analysis of 52 characters. The analysis, which was done by hand, resolved ‘pholidophoriforms’ as a non-monophyletic group; not even the species of †*Pholidophorus* grouped together (Fig. 2A). According to this hypothesis, †*Pleuropholidae* is the most basally positioned ‘pholidophoriform’ taxon, followed by †*Ichthyokentema*. All of these fishes, as well as the pachycormiforms and aspidorhynchiforms, were interpreted as basal teleosts based on four questionable characters (e.g., presence of modified ural neural arches, four pectoral radials, propterygium fused with first pectoral ray) that are not present or are still unknown in those fishes (see Arratia 1997, 1999; ‘Phylogenetic Analysis,’ below).

The phylogenetic hypothesis proposed by Arratia (2000) was based on 141 characters and included six pholidophoriforms: the Late Triassic †*Pholidophorus latiusculus* (see †*Ph. gervasutii*, below), the Early Jurassic †*Ph. bechei*, and the Late Jurassic †*Ichthyokentema purbeckensis*, †*Eurycormus speciosus*, two species of †*Siemensichthys*, and †*Ankylophorus*. The resultant topology (Fig. 2B) placed †*Pholidophorus latiusculus* and †*Ph. bechei* at the base of Teleostei, followed by †*Ichthyokentema*, †*Leptolepis coryphaenoides*, and more advanced fossil teleosts. The other ‘pholidophoriforms’ were resolved as a new clade of Late Jurassic taxa, the †*Siemensichthys* group, which was found to be the sister group of the clade that includes †*Ph. latiusculus*, †*Ph. bechei*, and other teleosts. According to this phylogenetic hypothesis, both the order Pholidophoriformes and family †*Pholidophoridae* are paraphyletic (Fig. 2B, nodes B, C, and D). Subsequent phylogenetic studies have shown †*Ph. bechei* at the base of the apomorphy-based Teleostei (identified as †*Pholidophorus* s. str. in Fig. 3; Arratia, 2001, 2008, 2009). Characters supporting this node are a well-developed, elongate posteroventral process of quadrate, mobile premaxilla, pectoral propterygium fused with first pectoral ray, and coronoid bones absent, as well as several homoplastic characters.

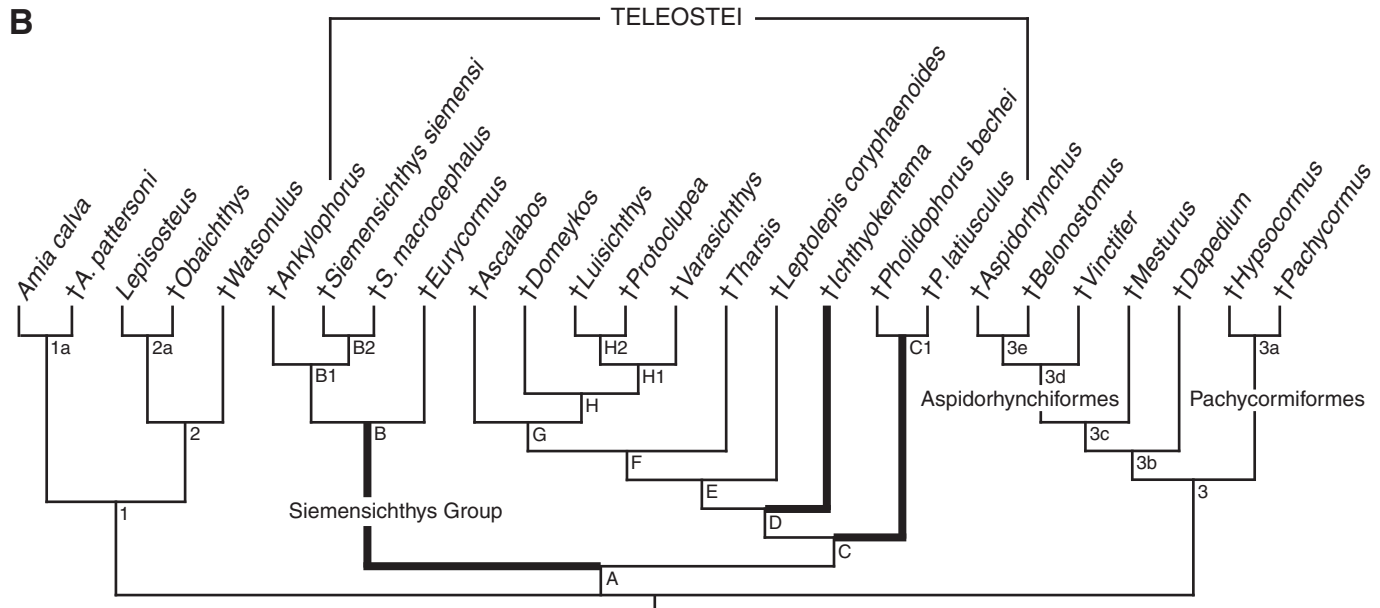
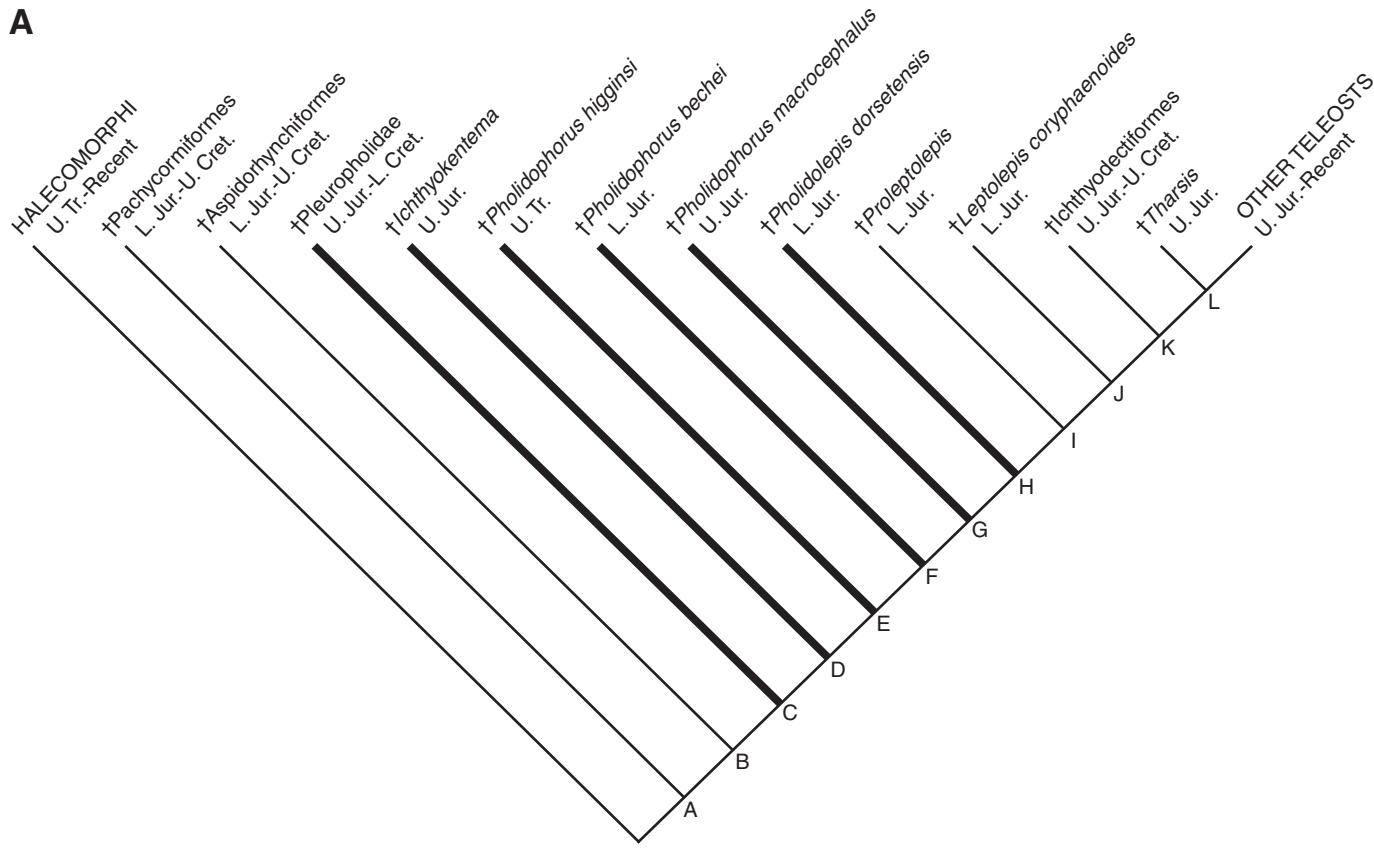
A recent study concerning the redescription of †*Pholidophorus aequatorialis* and its phylogenetic position included numerous taxa interpreted as ‘pholidophoriforms’ (Taverne (2011b; Fig. 2C). The manual-made phylogenetic analysis was based on 71 characters for which no character states are presented. Character polarity was authoritatively based on comparisons with †Pachycormiformes in general and with various neopterygians. The resultant topology places †Pachycormiformes as the most primitive teleosts, followed

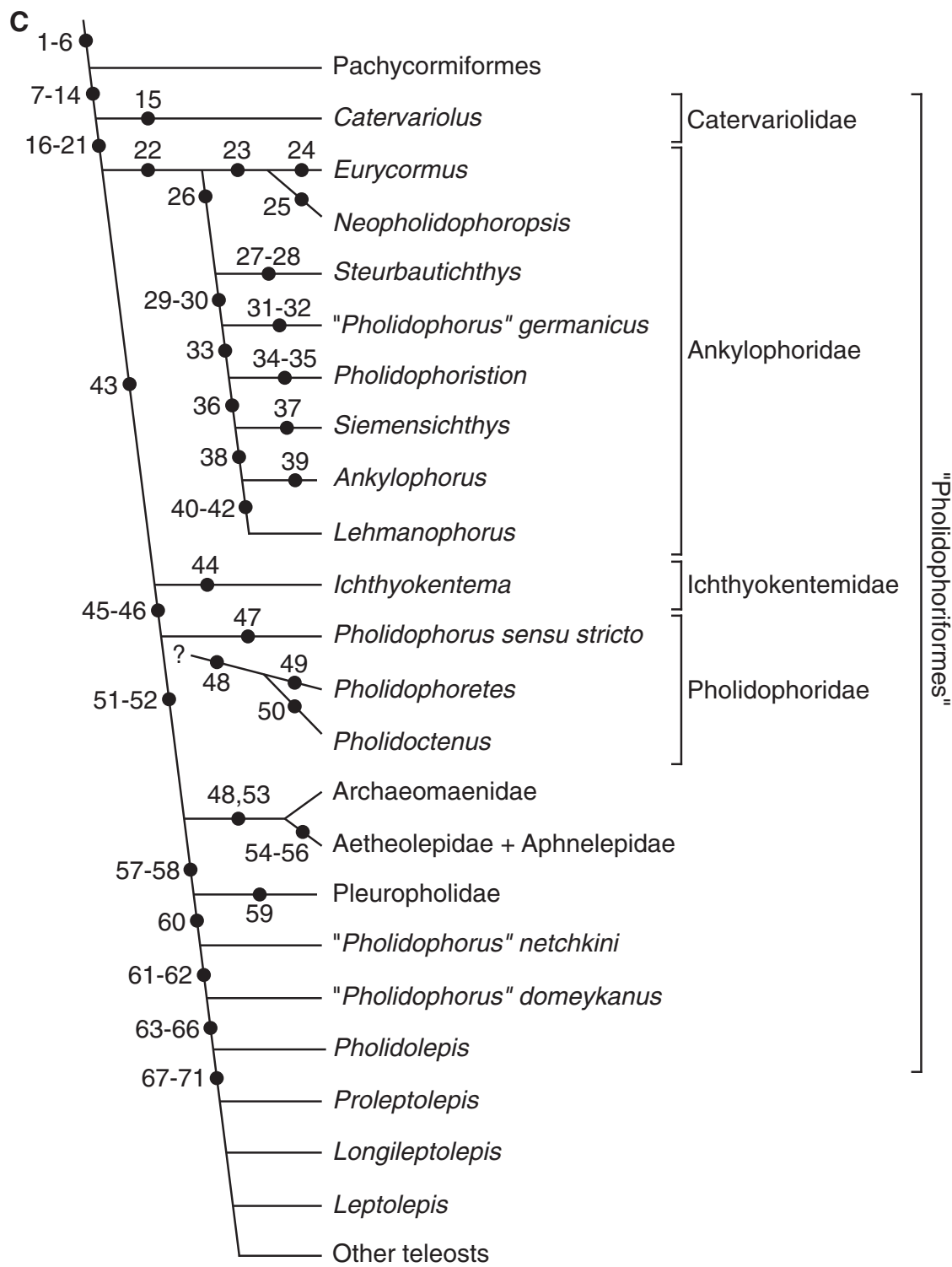
by a paraphyletic ‘Pholidophoriformes’ (Fig. 2C). Characters 1 to 6 of Taverne (2011b) are listed as shared by †Pachycormiformes and more advanced teleosts. However, the distributions of these six characters are problematic. For instance, characters 1 [premaxillaries possessing a nasal process more or less long in comparison with that in holosteans], 4 [pectoral fin with four radials and first pectoral ray fused to propterygium], 5 [neural arches of the last vertebrae elongated to form uroneurals], and 6 [caudal fin with branched and segmented principal rays, about 20 or more in number] are not found in most pachycormiforms and/or in most ‘pholidophoriforms’ mapped in Figure 2C (see morphological descriptions for ‘pholidophoriforms’ below and Arratia and Lammers, 1996; Friedman et al., 2010; and Arratia and Schultze, 2013, for analyses on pachycormiform characters). Characters 2 [internal carotid foramen in parasphenoid] and 3 [unpaired dentated basibranchial] are unknown for most pachycormiforms and most ‘pholidophoriforms.’ The seven characters proposed as supporting the phylogenetic position of †‘Pholidophoriformes’ plus more advanced teleosts do not stand up to an analysis either because the characters are unknown for most ‘pholidophoriforms’ (e.g., characters 7 [median vomer], 9 [foramen for pseudobranchial artery in parasphenoid], 12 [median dermobasihyal], 13 [urohyal], and 14 [long, thin epineural bones]) or the condition is variably present, as will be demonstrated below (e.g., characters 8 [medial contact between nasal bones], 10 [an ossified supraoccipital], and 11 [long posteroventral process of quadrate]). A further analysis of the ‘Pholidophoriformes’ sensu Taverne (2011a) will be presented in the section ‘Phylogenetic Analysis.’

Institutional Abbreviations—**AMNH**, American Museum of Natural History, New York, New York, U.S.A.; **ANSP**, Academy of Natural Sciences, Philadelphia, Pennsylvania, U.S.A.; **BGhan**, Bundesanstalt für Geowissenschaften und Rohstoffe, Niedersächsisches Landesamt für Bodenforschung, Hannover, Germany; **BSPG**, Bayerische Staatssammlung für Paläontologie und historische Geologie, Munich, Germany; **CAS(SU)**, California Academy of Sciences, Department of Ichthyology, San Francisco, California, U.S.A.; **CM**, Carnegie Museum of Natural History, Pittsburgh, Pennsylvania, U.S.A.; **DMNH**, Denver Museum of Natural History, Denver, Colorado, U.S.A.; **FMNH**, Field Museum of Natural History, Chicago, Illinois, U.S.A.; **GBA**, Geologische Bundesanstalt Wien Abteilung, Paläontologie und Sammlungen, Vienna, Austria; **GOE**, Institut und Museum für Geologie und Paläontologie, Georg-August Universität, Göttingen, Germany; **Innsb.**, Department of Geology, University of Innsbruck, Innsbruck, Austria; **IVVP**, Institute of Vertebrate Palaeontology and Palaeoanthropology, Beijing, China; **KUNHM**, Division of Ichthyology, Natural History Museum, University of Kansas, Lawrence, Kansas, U.S.A.; **KUVP**, Division of Vertebrate Paleontology, Natural History Museum, University of Kansas, Lawrence, Kansas, U.S.A.; **JFBM**, James Ford Bell Museum, Saint Paul, Minnesota, U.S.A.; **JME**, Jura Museum Eichstätt (SOS indicates that the fish was recovered in the Solnhofen Limestone), Eichstätt, Germany; **LACM**, Los Angeles County Museum of Natural History, Los Angeles, California, U.S.A.; **LBUCH**, Laboratorio de Biología, Universidad de Chile, Sede Santiago-Sur, Chile; **MB**, Museum für Naturkunde, Humboldt Universität, Berlin, Germany; **MCSNB**, Museo Civico di Scienze Naturali, Bergamo, Italy; **MCSNIO**, Civico Museo Insubrico di Storia Naturale, Unduno-Olona, Italy; **MNHN**, Muséum national d’Histoire naturelle, Paris, France; **MRAC**, Musée Royal de l’Afrique Centrale, Tervuren, Belgium; **NHMUK**, Natural History Museum, London, U.K.; **NHMW**, Natural History Museum, Vienna, Austria; **NMMNH**, United States National Museum, Smithsonian Institution, Washington, D.C., U.S.A.; **OS**, Department of Fisheries and Wildlife, College of Agricultural Sciences, Oregon State University,

Corvallis, Oregon, U.S.A.; **Pi**, Institut und Museum für Geologie und Paläontologie, Tübingen, Germany; **R-**, Paleontological Collection, Faculty of Geology, University of Chile, Santiago, Chile; **ROM**, Royal Ontario Museum, Toronto, Canada; **SenkM**, Senckenberg Museum, Frankfurt-am-Main, Germany; **SIO**, Scripps In-

stitution of Oceanography, University of California, La Jolla, California, U.S.A.; **SMNH**, Department of Paleozoology, Naturhistoriska Riksmuseet, Stockholm, Sweden; **SMNS**, Staatliches Museum für Naturkunde, Stuttgart, Germany; **TCWC**, Texas Cooperative Wildlife Collection, Department of Wildlife and





← FIGURE 2 Phylogenetic hypotheses, including some ‘pholidophoriform’ fishes. **A**, slightly modified from Patterson (1977a). **B**, Arratia (2000). Bold lines identify ‘pholidophoriform’ taxa. **C**, Taverne (2011b).

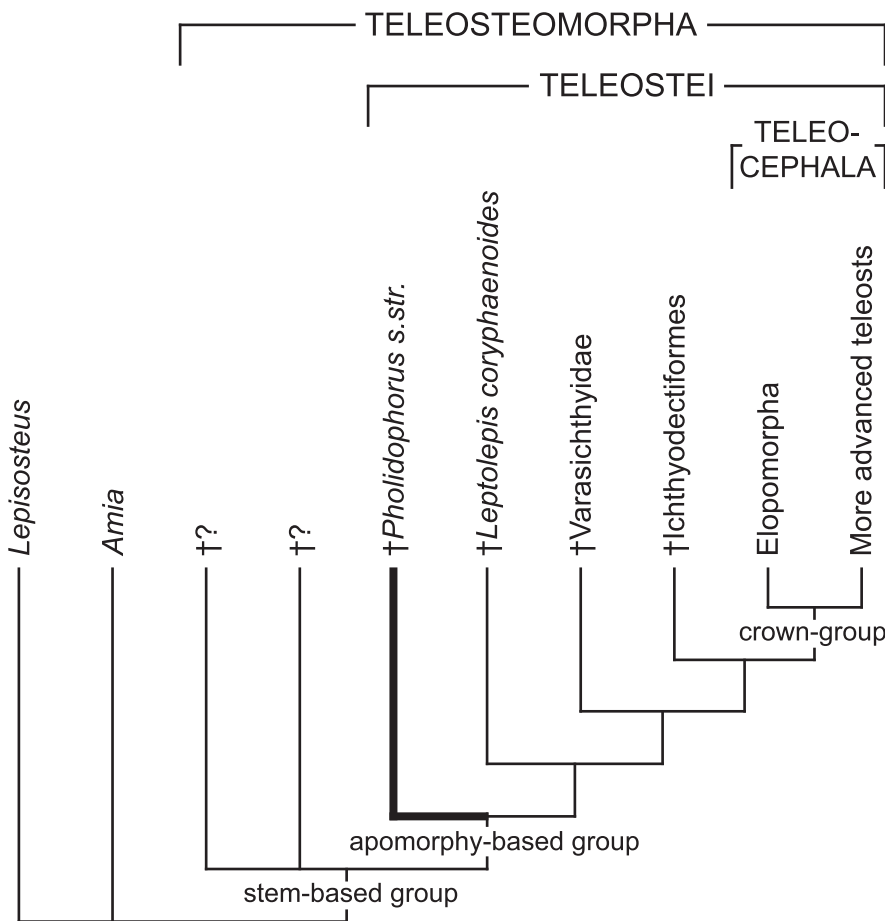


FIGURE 3. Phylogenetic hypothesis of major clades of Teleostei (Arratia, 2001). Bold line identifies a ‘pholidophoriform.’ †*Pholidophorus* sensu stricto included †*Ph. bechei*, following Nybelin (1966).

Fisheries Science, Texas A&M University, College Station, Texas, U.S.A.; **UALVP**, University of Alberta, Laboratory for Vertebrate Paleontology, Edmonton, Canada; **UCLA**, Department of Biology, University of California at Los Angeles, Los Angeles, California, U.S.A.; **UNC**, Institute of Marine Sciences, University of North Carolina, Morehead City, North Carolina, U.S.A.; **UMZC**, University Museum of Zoology, Harvard University, Cambridge, Massachusetts, U.S.A.

MATERIALS AND METHODS

Preparation

All Triassic specimens studied herein were prepared mechanically under a binocular microscope using needles. Abrasive machines were not used because of the fragile nature of the specimens. In most cases, the cleaning and preparation of the fossils was done by professionals working at the institutions listed above. However, in some cases further preparation of specific regions was done under my instructions. In the case of the fossil fishes studied by Griffith (1977) and deposited in MNHW (see †*Pholidophoretes*), permission to further prepare some specimens was not granted. Most Triassic fishes studied here are flatly preserved, so that acid preparation was not attempted. The acid-transfer preparation technique of Toombs and Rixon (1959) was performed on some of the Early and Late Jurassic specimens from Germany with a three-dimensional preservation.

All illustrations were prepared by the author using Wild FM5, Wild FM 8, and Leica MZ9 stereomicroscopes equipped with a camera lucida. Thus, illustrations are based directly on specimens rather than on photographs. The photographs of fossil ‘pholidophoriforms’ were done by professional photographers working for the museums listed above, as listed in ‘Acknowledgments.’ Small specimens (larvae) were studied and photographed using an Olympus microscope with normal optic, phase contrast, and polarized light with a Nikon camera attachment. Photographs are not retouched or manipulated with Photoshop. The latter was only used to label figures.

Material Examined

The Triassic specimens examined as part of this study are listed in their respective taxonomic description. Specimens used in comparisons and in the phylogenetic analyses are listed below. Most of the extant fishes included in this study are cleared and stained (cl&st) for both cartilage and bone, following a procedure described in Arratia and Schultze (1992). Others are prepared as dry skeletons (skl). Where possible, I list total length (TL) and standard length (SL) for fossil and Recent specimens, and notochordal length (NL) only for Recent larval specimens.

Holostei—Amiiformes: *Amia calva*: KUNHM 21290, 4 cl&st, 76, 79, 85, 86 mm TL; KUNHM 21261, skl, about 450 mm TL; KUNHM 3883, 5 cl&st, 41, 50, 53, mm TL. †*Caturus elongatus*: MB f.3851. †*Caturus furcatus*: MB f.2931. †*Caturus brevicostatus*: MB f.3849 and MB f.3850. †*Caturus* sp.: JME SOS 3344.

Lepisosteiformes: *Atractosteus macrobeccus*: KUNHM 21317, 1 skl; KUNHM 21372, 1 skl. *Atractosteus spatula*: KUNHM 18537; KUNHM 18540; KUNHM 18545; KUNHM 18548, dry crania. *Lepisosteus osseus*: KUNHM 3651, 3 cl&st, 60, 63, 70 mm TL; KUNHM 3677, 1 cl&st, 241 mm TL; KUNHM 8530, 1 cl&st, 139 mm TL; KUNHM 12645, 1 cl&st, 710 mm TL; KUNHM 16246, 1 cl&st, 50.5 mm TL; KUNHM 17935, 1 cl&st, 730 mm TL. *Lepisosteus platostomus*: KUNHM 16142, 1 cl&st, 455 mm TL; KUNHM 003137, 1 cl&st, 655 mm TL; KUNHM 003138, 1 cl&st, 626 mm TL. †Parasemionotiformes: †*Watsonulus eugnathoides*: UMCZ 13872, UMCZ 13876, UMCZ 13877, and UMCZ 13878; MNHN MAE58a, MNHN MAE58a363, MNHN MAE595a, b, MNHN MAE2481b, c, MNHN MAE2482a, MNHN MAE248a, b, MNHN MAE2485, and MNHN MAE2495.

Neopterygii incertae sedis—†*Prohalecites porroi*: MCSNIO P 15L, MCSNIO P 331, MCSNIO P 342, MCSNIO P 335, MCSNIO P 343, MCSNIO P 364, MCSNIO P 378-1, MCSNIO P 384, MCSNIO P 407, MCSNIO P 413, MCSNIO P 658, and many others. †*Prohalecites* indet.: MCSNIO P 378-1, MCSNIO P 657, and MCSNIO P 658.

Teleosteomorpha—(Sensu Arratia, 2001; Fig. 3.) †*Aspidorhynchiformes*: †*Aspidorhynchus acutirostris*: MB f.358, MB f.3529, MB f.3554, and MB f.3566. †*Aspidorhynchus* sp.: JME ETT 2006-2. †*Belonostomus muensteri*: MB f.3544. †*Belonostomus tenuirostris*: JME SOS 2339 and JME SOS 2844. †*Belonostomus* sp.: BSPG 1956 I 422. †*Pachycormiformes*: †*Asthenocormus titanius*: JME SOS 542 and JME SOS 3556. †*Euthynotus* sp.: SMNH P 1037. †*Hypsocormus insignis*: BSPG AS VI 4a, b (holotype); SMS P 5698; SenkM 1863. †*Orthocormus cornutus*: SenkM 1863 (holotype); JME SOS 3460 and JME SOS 3571a, b. †*Orthocormus roeperi*: BSPG 1993 XVIII-VFKO B16. †*Pachycormus* sp.: SMS P 6151 and SMNH P 6152; MB 2349. †*Protosphyraena tenuis*: KUVP 49419. †*Protosphyraena* cf. *Pernicosa*: KUVP 67877. †*Protosphyraena* sp.: KUVP 49418 and KUVP 55000. †*Pseudoasthenocormus retrodorsalis*: BSPG 1956 I 361. †*Sauropsis depressus*: CM 4766A/B (holotype). †*Sauropsis longimanus*: BSPG AS VII 1089 (holotype). †*Sauropsis* sp.: JME SOS 3336a, b; JME 2181a, b; MB 2348.

†‘*Pholidophoriformes*’ incertae sedis—†*Jianligichthys serratus*: IVVP 6353, IVVP V6353-1-2, IVVP V6354. †‘*Pholidophorus*’ *armatus*: MB f.7010. †*Pholidophorus* *dorsalis*: Innsb. 124. †‘*Pholidophorus*’ *furcatus*: UMCZ 9863. †‘*Pholidophorus*’ *germanicus*: UMCZ 9762. †‘*Pholidophorus*’ *granulatus*: NHMUK P3605, NHMUK P6378e, and NHMUK P6379. †‘*Pholidophorus*’ *hartmani*: NHMUK P605, NHMUK P3591a, and NHMUK 22527. †‘*Pholidophorus*’ *leptocephalus*: UMCZ 9761. †‘*Pholidophorus*’ *limbatus*: UMCZ 9763. †‘*Pholidophorus*’ *ornatus*: NHMUK P6378. †*Pholidophorus* *pusillus*: Innb. 115. †‘*Pholidophorus*’?: UMCZ 9764 and UMCZ 13661. †‘*Pholidophorus*’ sp.: UMCZ 10317. And many other specimens identified as ‘*Pholidophorus*’ from the Jurassic of Europe.

Basal Teleostei—†‘*Pholidophorus*’ *bechei*: FMNH 2137; MB f.3504, MB f.19219; SMNS P 944; UMCZ 9873, UMCZ 6301, and UMCZ 12056. †*Siemensichthys* Group: †*Ankylophorus similis*: NHMUK 1083. †*Eurycornus speciosus*: BSPG AS V510 and BSPG 1960 XVIII 106; JME SOS 2339 and JME SOS 2341. †*Siemensichthys macrocephalus*: BSPG AS I 1134; JME SOS 2812; MB f.7017, MB f.7018a, b, and MB f.7019. †*Siemensichthys siemensi*: JME SCHA 82. †*Ichthyokentema purbeckensis*: NHMUK P1073, NHMUK P1074, NHMUK P3607, NHMUK P6171, and NHMUK P12347. †*Leptolepis coryphaenoides*: BGHan 1931-4, BGHan 1956-8, BGHan 1957-2, BGHan 1957-5, and BGHan 1960 (acid-prepared specimens); GOE uncataloged, many articulated and disarticulated specimens. Many disarticulated bones prepared for SEM. †*Tharsis dubius*: BSPG 1964 XXIII 280; CM 4845; FMNH 25076 and FMNH 25124;

JME, many specimens from different localities. †*Ascalabos voithi*: CM 9491; JME 537, JME SOS 2363 and JME SOS 2497, and many other specimens from different localities deposited at the JME; NHMUK 3672, NHMUK 3673, and NHMUK 37062.

†*Crossognathiformes*—†*Bavarichthys incognitus*: JME SOS 4934a/b. †*Chongichthys dentatus*: LBUCH 021778a, b and LBUCH 15-010277a, b. †*Domeykos profetaensis*: LBUCH 12-260972a, b and LBUCH 01277-13a-b. †*Protoclupea atacamensis*: LBUCH 1-250277a. †*Protoclupea chilensis*: R-396a, R-396b; LBUCH 190179a, b. †*Varasichthys ariasi*: LBUCH 16-260972a, b, LBUCH 012378a, LBUCH 020778a, and LBUCH 020778b. And many other specimens of †*Varasichthys*.

†*Ichthyodectiformes*—†*Allothriissops mesogaster*: JME SOS 1941/17a; FMNH-PF UC 2021 and FMNH-PF UC 2082; SMNH P 976; SMNH P 2925, and SMNH P 7733. †*Pachythriissops propterus*: BSPG 1986 XXIII 154; JME SOS 741; MB. f. 3505. †*Thrissops* cf. †*T. formosus*: JME SOS 3024. †*Thrissops subovatus*: JME SOS 1953/14a. †*Thrissops* cf. *T. subovatus*: JME SOS 2557.

Elopomorpha—Elopiformes: †*Anaethalion angustum*: JME SOS 2271, JME SOS 2259, JME SOS 2260, JME SOS 2261a, and JME SOS 2261b. †*Anaethalion angustissimum*: JME SOS 2271; Pi F 891, Pi 1074/1, Pi 1074/2, and Pi Y 1930. †*Anaethalion knorri*: JME SOS 2267a, b, JME SOS 2270, and JME SOS 2282. *Elops affinis*: SIO 69-167, 1 cl&st, 121 mm SL; UCLA W 50-29, 4 cl&st., 121.3, 128.4, 157, and 165 mm SL. *Elops hawaiiensis*: CAS(SU) 35105, partially disarticulated skl, braincase of about 90 mm length; OS 5105, 2 cl&st leptocephalous larvae, 26.7 and 32.5 mm SL. *Elops saurus*: ANSP 147401, 2 cl&st, 97.8 and 99.1 mm SL; CAS(SU) 10847, skl, ca. 395 mm SL; TCWC 0503.1, 5 cl&st, 24.0, 24.0, 26, 30.0, and 35.0 mm SL; TCWC 0782.1, 3 cl&st., 35.7, 43, and 46.4 mm SL; TCWC 2452.2, 5 cl&st, 60.1, 97.3, 107, 110.4, and 154 mm SL; UNC 82/8, 2 cl&st, 57 and 76 mm SL. †*Elopsomolos frickhingeri*: JME SOS 4393. †*Elopsomolos* sp.: NMH 37048. *Megalops atlanticus*: UF 171286, 5 cl&st, 26.3, 27.8, 29.1, 29.8, and 40.5 mm SL; UF 208605, 5 cl&st, 25.5, 31, 32.7, 41.1, and 44.5 mm SL; UF 208780, 3 cl&st, 85, 90.4, and 122.5 mm SL. *Megalops cyprinoides*: CAS 145216, 2 cl&st, 17.5 and 34.5 mm SL. Albuliformes: *Albula vulpes*: AMNH 56840, skl, ca. 292 mm SL; AMNH 56743, skl, ca. 300 mm SL; AMNH 56878, skl, ca. 305 mm SL; UCLA W58-96, 2 cl&st, 195 and 220 mm SL; UCLA W49-122, 5 cl&st, 46.7, 54.6, 63.5, 72.7, and 88.8 mm SL; UCLA W49-122, 4 cl&st leptocephalous larvae. Anguilliformes: *Anguilla rostrata*: KUNHM 5029, 6 cl&st, 50, 50.4, 53.8, 55, 82.5, and 103 mm SL.

Osteoglossomorpha—†*Lycopteridae*: †*Lycoptera davidi*: LACM 4959-122316 and LACM 4959-122317; SMNH P 6553. †*Lycoptera* cf. *L. sinensis*: FMNH 1291a and FMNH 1291b. Hiodontidae: *Hiodon alosoides*: JFBM 43312, 1 skl, ca. 400 mm SL; JFBM 43306, 1 skl, ca. 380 mm SL; KUNHM 9618, 7 cl&st, from 22 to 55 mm SL; KUNHM uncataloged, 3 cl&st, 68, 70, and 72 mm SL; KUNHM 9661, 2 cl&st, 59 and 67 mm SL; KUNHM 13993, 2 cl&st, 200 and 305 mm SL. *Hiodon tergisus*: KUNHM 9662, 3 cl&st, 48.6, 51.8, and 55.7 mm SL. *Osteoglossum ferreri*: KUNHM 22650, 1 cl&st, 52.3 mm SL. *Pantodon buchholzi*: KUNHM 22651, 1 cl&st, 50 mm SL.

Clupeomorpha—Clupeiformes: *Alosa chryschloris*: KUNHM 9634, 2 cl&st, 43.7 and 54.3 mm SL. *Anchoa mitchilli*: KUNHM 7494, 2 cl&st, disarticulated specimens; KUNHM 17183, 2 cl&st, disarticulated specimens. *Brevoortia patronus*: KUNHM 15113, 5 cl&st, disarticulated specimens. *Coilia nasus*: KUNHM 40362, 33 cl&st (15 larvae between 10.2 and 22.7 mm SL; 9 between 16.6 and 30.1 mm SL; 9 specimens between 63.5 and 103.1 SL). *Dorosoma cepedianum*: KUNHM 12100, 3 cl&st, 30.5, 67, and 71.6 mm SL; KUNHM 16167, 1 cl&st, 46.9 mm SL; KUNHM 21801, 169 cl&st (100 specimens from 8 mm notochordal length (NL) to 15 mm SL and 69 specimens from 13.9 to 29.5 mm SL). *Dorosoma petenense*: KUNHM 9594, 2 cl&st, 27.3 and 34.5 mm SL. *Engraulis encrasicolus*: KUNHM 19941, 8 cl&st, 25 to 50 mm SL. *Engraulis*

ringens: KUNHM 19347, 10 cl&st, disarticulated specimens. *Ethmidium maculatum*: KUNHM 19349, 2 cl&st, disarticulated large specimens. *Jenkinsia lamprotaenia*: KUNHM 40364, 10 cl&st, from 34.5 to 49.1 mm SL. *Lile stolifera*: KUNHM 5411, 3 cl&st, 29.5, 45.6, and 52.2 mm SL; UCLA 58-307, 3 cl&st, 71.7, 80, and 88.1 mm SL. *Sardinops sagax*: KUNHM 19345, 6 cl&st larvae, 14 to 19 mm SL, and 4 cl&st disarticulated large specimens. Denticipitidae: *Denticeps clupeoides*: MRAC M.T. 76-32-P-4915-932, 1 cl&st, 29.1 mm SL; MRAC M.T. 76-44-P-7, 1 cl&st, 18.5 mm SL.

Ostariophysi incertae sedis—†*Tischlingerichthys viohli*: JME Moe 8.

Gonorynchiformes—*Chanos chanos*: CAS(SU) 35075, 1 skl, disarticulated, braincase of 148 mm length; KUNHM 39848 to 38796, day-to-day series of about 200 specimens from about 10 mm to 10 mm notochordal length and from 7.0 to 83.5 mm SL; KUNHM 40365, 2 skl, 370 and 376 mm SL and 4 cl&st, 150, 180, 330, and 400 mm SL; SIO 80-199, 7 cl&st, from 16.1 to 44.5 mm SL. *Gonorynchus abbreviatus*: CAS 30993, 1 cl&st, 150 mm SL.

Cypriniformes—*Aspius aspius*: ROM 52742, 4 cl&st, 26.7, 35.8, 51.8, and 59.8 mm SL. *Barbatula barbatula*: ROM 49713, 5 cl&st, 49.8, 60.9, 64.1, 66, and 75 mm SL. *Carpoides carpio*: KUNHM 21807, 24 cl&st, 13.3 to 42.3 mm SL. *Carpoides microstomus*: FMNH 35171, 4 cl&st, 34.8, 38.8, 40.5, and 45.7 mm SL. *Catostomus commersoni*: JFBM 11495, 7 cl&st, from 22.3 to 31 mm SL; JFBM 41727, skl, ca. 278 mm SL; KUNHM 38655, >100 cl&st, between 12 to 21.3 mm SL. *Cobitis lutheri*: KUNHM 38976, 2 cl&st, 55.6 and 81.5 mm SL. *Cyclopterus elongatus*: KUNHM 40695, 1 cl&st, 148 mm SL. *Cyprinus carpio*: FMNH 42392, 1 cl&st, 85.5 mm SL; KUNHM 3739, 1 cl&st, 80.0 mm SL; JFBM, skl, ca. 354 mm SL. *Danio rerio*: KUNHM uncataloged, 10 cl&st; KUNHM 40245, day-to-day ontogenetic series of about 100 specimens, between 6 to 27.9 mm SL. *Hemiculter leuciscus*: UMCZ 32394, 2 cl&st, 90.8 and 97.2 mm SL. *Labeo batesi*: NMNH 303704, 4 cl&st, 89.7, 95, 195.5, and 197.4 mm SL. *Lepidomedra mollispinus*: KUNHM 11768, 20 cl&st, from 54.8 to 68.7 mm SL. *Misgurnus anguillicaudatus*: FMNH 57343, 5 cl&st, 47, 50.1, 50.7, 53, and 80.5 mm SL; KUNHM 21447, 2 cl&st, 96.2 and 100.3 mm SL. *Notropis atherinoides*: FMNH 72149, 20 cl&st, from 20.2 to 55.5 mm SL. *Opsariichthys bidens*: CAS(SU) 32512, 2 cl&st, 81.9 and 117.6 mm SL. *Opsariichthys uncirostris*: KUNHM 21448, 4 cl&st, 25, 29.6, 36.6, and 70.4 mm SL. *Parabramis pekinensis*: NMNH 86494, 5 cl&st, 49, 50.5, 54.7, 58.5, and 59.1 mm SL. *Sabanajewa balcanica*: FMNH 63814, 3 cl&st, 33.9, 36.8, and 58 mm SL. *Semonotilus atromaculatus*: KUNHM 12594, 5 cl&st, 39, 41, 42, 42, 45, and 47 mm SL. *Squalibarbus curriculus*: AMNH 10890, 2 cl&st, 112.6 and 136 mm SL. Characiformes: *Astyanax* sp.: KUNHM 20099, 6 cl&st, between 19.9 and 18.8 mm SL. *Xenocharax spilurus*: CAS(SU) 15639, 2 cl&st, 74.7 and 92 mm SL.

Siluriformes—*Diplomystes nahuelbutaensis*: MNHN-Stg uncataloged, 4 cl&st, 150 to 180 mm SL. *Diplomystes viedmensis*: FMNH 58004, 2 cl&st, 80.5 and 91.7 mm SL. *Noturus exilis*: KUNHM 17229a, 10 cl&st larvae, from 10 to 12.0 mm SL.

Euteleostei—Esociformes: *Esox americanus*: KUNHM 5227, caudal skeleton only, cl&st; KUNHM 17864, 4 cl&st, 82.7, 89.5, 112, and 123 mm SL. *Esox lucius*: KUNHM 19092, disarticulated skull, lower jaw 120 mm length, and caudal skeleton. Salmoniformes: †*Erichalcis arcta*: UALVP 8598, UALVP 8602, UALVP 8606, and UALVP 8612. †*Humbertia* sp.: DMNH 2518-1. †*Leptolepides haertesi*: JME SOS 2473, JME SOS 2474, and JME SOS 2554. †*Leptolepides sprattiformis*: FMNH-PF 10984 and FMNH-PF 10986; JME SOS 2956; KUVP 60722 and KUVP 96128; SMNH P 1891, SMNS P 1894, SMNS 55106, and SMNS 55928. †*Orthogonikleithrus hoelli*: JME ETT 2301, JME ETT 2632, JME ETT 3954, JME ETT 3955, and JME ETT 3956. †*Orthogonikleithrus leichi*: JME SOS 2301 and JME SOS 2632.

†*Orthogonikleithrus* sp.: JME ETT 30 and JME ETT 216. *Oncohynchus mykiss*: KUNHM 12463, 7 cl&st, from 28.0 to 43 mm SL; KUNHM 21936, 20 cl&st, 290 to 300 mm SL; OS uncataloged, day-to-day ontogenetic series of about 200 cl&st, from 13 mm NL to 73 mm SL. *Prosopium cylindraceous*: KUNHM 15417, 2 cl&st, 300 and 310 mm SL. *Prosopium williamsoni*: KUNHM 11817, 13 cl&st, 12 larvae between 20 and 33.6 mm SL and 1 specimen of 230 mm SL. *Thymallus arcticus*: KUNHM 15419, 3 cl&st, 151, 166, and 177 mm SL. *Umbra limi*: KUNHM 10370, 6 cl&st, 22.5, 26.3, 27, 27.8, 52, and 54.4 mm SL. Argentiniformes: *Argentina sialis*: SIO 66-4, 3 cl&st, 119, 140, and 121.2 mm SL. SIO CR 5208, 4 cl&st, 3 larvae of 9.0 to 14 mm NL, and 1 specimen of 13.5 mm SL.

Measurements

Standard measurements taken in teleosts (see Hubbs and Lagler, 1947) are used here, except in instances where the particular anatomical characteristics of ‘pholidophoriforms’ required that these standards be modified. These modifications are explained below.

Total length (TL) is the distance from the anterior tip of the snout to the posterior tip of the caudal fin. The total lengths given for the ‘pholidophoriforms’ are approximate because the distal tips of the caudal fin rays are commonly not preserved, displaced, or broken. Notochordal length (NL) is the distance from the anterior tip of the snout to the posterior tip of the caudal fin measured in larval specimens prior to the notochordal flexion.

Standard length (SL) is the distance from the anterior tip of the snout to the posterior tip of the hypurals. Standard length can be measured only in fishes showing the endoskeleton of the caudal fin. It cannot be measured in the Triassic pholidophorids studied with the whole squamation in situ or in the many fishes whose hypural region was not preserved. To make measurements comparable with those in previous descriptions of pholidophorids, I designated the last scale of the middle lateral flank bearing the lateral line canal as the end point of the measurement of the standard length.

Head length is the distance between the most anterior tip of the snout to the most posterior margin of the opercle, which is commonly the largest bone of the opercular apparatus. However, in some of the taxa described below, the subopercle extends further posteriorly than the opercle. In those cases, the head length was measured to the posterior margin of the subopercle.

Snout length is the length of the skull in front of the eye. That is, the distance between the anterior tip of the snout and the anterior margin of the orbit.

Eye diameter is the greatest diameter of the orbit as measured from the anterior inner margin to the posterior inner margin.

The anterior skull roof width is compared with the posterior width by measuring at the anterior tip and posterior margin of the nasal bones. The maximal skull roof width is in the region posterior to the posterodorsal corner of the orbit, which remained constant in the Triassic fishes, with one exception (†*Pholidorhynchodon malzani*; see below).

Phylogenetic Methodology

The phylogenetic analyses were conducted using PAUP (Phylogenetic Analysis Using Parsimony) software (version 4.0b10) for 32-bit Microsoft Windows operating system (Swofford, 2000). The character matrices were constructed using MacClade for the analysis to run in PAUP. All characters are unweighted, unordered, and considered to be independent of one another. The phylogenetic analysis used the list of characters of Arratia (2000) with the addition of 29 new characters (Appendix 1). The outgroups used in the analysis are fossils and extant holosteans, including the basal paracanthopteriform †*Watsonulus*,

the amiiforms *Amia calva* and †*A. pattersoni*, and the lepisosteiforms †*Obaichthys* and *Lepisosteus*. †Aspidorhynchiformes and †Pachycormiformes—interpreted as possible teleostean morphs (Arratia, 2004)—are included as part of the ingroup together with Triassic pholidophorids, some Early and Late Triassic ‘pholidophoriforms’, †*Leptolepis coryphaenoides*, and more advanced teleosts. †*Prohalecites*, previously proposed as a taxon possibly related to teleosts (Tintori, 1999) or as an actinopterygian incertae sedis (Arratia and Tintori, 1999), is also included in the analysis (as an outgroup). The data matrix with scoring of characters is presented in Appendix 2.

In addition to my own study of specimens, the following literature was used to score the following ‘pholidophoriforms’: †*Catervariolus* (Taverne, 2011b); †*Eurycornus speciosus* (Patterson, 1973; Arratia and Schultze, 2007; Schultze and Arratia, 2013); †*Parapholidophorus* (Zambelli, 1975); †*Pholidophoretes* (Griffith, 1977); †*Pholidoctenus* (Zambelli, 1977); †*Pholidophorus bechei* (Nybelin, 1966; Patterson, 1968, 1973, 1975, 1977b; Patterson and Rosen, 1977; Arratia, 2000); †*Pholidophorus bronni* (Kner, 1866; Schultze, 1966); †*Pholidophorus gervaisii* (Zambelli, 1980a); †*Pholidophorus latiusculus* (Agassiz, 1832; Kner, 1866; Nybelin, 1966; Schultze, 1966; Arratia, 2000); †*Pholidorhynchodon* (Zambelli, 1980b); and †*Siemensichthys macrocephalus* (= †*Pholidophorus macrocephalus*; Schultze, 1966; Patterson, 1975; Grande and Bemis, 1998; Arratia, 2000).

Interpreting Homologies—My understanding of homologous features follows ideas extensively discussed by different authors and were clearly summarized by Ax (1987:159): “Homologous features are features in two or more evolutionary species, which go back to one and the same feature of a common stem species. They may have been taken over from the stem species unchanged or else with evolutionary transformations.” To investigate what features can be primary homologues or non-homologues, I use the classic criteria set up by Remane (1952, 1955) and followed later by others (e.g., Pinna, 1991; Rieppel, 1994; Wiley and Lieberman, 2011). For instance, position or spatial relationships, origin, ontogenetic development, and structure of the features under study. These primary interpretations are tested in the phylogenetic hypothesis and discussed below in the section ‘Phylogenetic Analysis’.

TERMINOLOGY

Anatomical Terminology—The terminology of the skull roof bones follows Westoll (1943), Jollie (1962), and Schultze (2008). This terminology is based on study of bones in Osteichthyes and differs from traditional skull roof terminology, which is fundamentally based on human anatomy. For instance, the bone called ‘frontal’ in traditional terminology actually corresponds to the parietal bone in actinopterygians. To avoid confusion, all figures show in square brackets the names of bones in the traditional terminology, e.g., parietal bone [= frontal]: pa [= fr].

The skull roof of basal teleosts includes a series of dermal bones, such as the medial rostral, paired nasals, paired parietals [= frontals], paired postparietals [= parietals], paired autosphenotics or sphenotics, paired pterotics or autopterotics in †*Leptolepis coryphaenoides* and more advanced teleosts (e.g., Patterson, 1975; Arratia, 1997, 1999, 2000; Arratia and Tischlinger, 2010; or dermopterotics in more primitive forms), paired epiotics, median occipital, paired extrascapulae, and paired posttemporals. The Triassic pholidophorids studied here are characterized by a tendency to fuse partially or completely the parietals, postparietals, autosphenotics, and dermopterotics. The fusion of these elements results in one bony plate. To facilitate the reading, I identify it as the ‘skull roof plate’ in the text. The supraoccipital and epiotic bones have not been found in any of the Triassic pholidophorids described below.

The posterior opercular bones (i.e., opercle, subopercle, interopercle), branchiostegal rays, and median gular plate form the operculogular series. The preopercle is not part of this series; it lies just anterior to the other opercular bones, but it is described below together with the operculogular series.

The identification and terminology of the cephalic sensory canals follows Northcutt (1989). In basal actinopterygians, the lateralis system includes a complete cephalic sensory system and a complete body lateral line. The cephalic sensory canal system comprises the supratemporal or extrascapular commissure, postotic or temporal, otic, supraorbital, infraorbital, preopercular, and mandibular canals. Identification of some of the pit-lines present in the fishes studied here is based on Coombs et al. (1988). The pit-lines were set in well-defined grooves within the layer of ganoine that are easily identifiable in ‘pholidophoriforms.’ All cephalic sensory canals observed in the studied pholidophorids are simple, with very short tubules opening on the surface; the tubules may open directly perpendicular to the canal, or they may be inclined and open superior to the canal. These canal pores are typically round and small, but can also be larger and oval. All cephalic sensory canals observed in the studied pholidophorids are enclosed by bone and not visible, but their trajectory can be traced by the sensory pores on the surface of the bones.

The structure of the vertebral column is one of the major sources of characters in the evolutionary history of holosteans and teleosts (Schultze and Arratia, 1989; Arratia et al., 2001; Arratia, 2008). ‘True’ teleosts, which include †*Leptolepis coryphaenoides* and more advanced teleosts (Arratia, 1999, 2000, 2008), are characterized by the presence of an autocentrum (an ossification that forms outside the external sheath of the notochord). This contrasts with non-teleostean fishes, which possess a chordacentrum (mineralization of the middle sheath of the notochord; e.g., Schultze and Arratia, 1989; Arratia et al., 2001). In the present study, special attention has been given to the constitution of the vertebral centra in all studied fishes. The term ‘vertebra’ includes all serially repeated ossified, cartilaginous, and ligamentous elements around the notochord, consisting of centrum, neural arch and spine, and hemal arch and spine (Schultze and Arratia, 1988; Arratia et al., 2001).

Vertebrae formed by a single central element are called monospondylous, and those formed by more than one element are called diplospondylous or polyspondylous (see Arratia et al., 2001:103 for further details). The central element can be formed by mineralized, calcified, or ossified portions that surround the notochord. The centrum is termed chordacentrum, arcocentrum, or autocentrum, depending on its origin and structure (see Arratia et al., 2001:103–106). These terms will be used here in the descriptions of the vertebral centra and also in the lists of characters used in the phylogenetic analyses.

The posttemporal is the dorsal-most element attaching the pectoral girdle to the cranium. Because of its position, the posttemporal can be described as an element of the skull roof or as part of the pectoral girdle. The posttemporal will be described together with other bones of the pectoral girdle in the sections below. The terminology of the pectoral and pelvic axillary processes follows Arratia (1997, 1999). The terminology of the pectoral girdle follows mostly that of Jessen (1972). The structure identified here as a serrated appendage is fused along the anterior surface of the cleithrum; as described in *Amia calva* by various authors, it has some similarities to the ‘posterior flagellum’ of Allis (1897) and Jessen (1972), ‘posterior serrated appendage’ of Wilder (1877), ‘serrated appendage’ of Arratia and Schultze (1987), or ‘posterior clavicle element’ of Grande and Bemis (1998). See discussion on this element in the section ‘Analysis of Morphological Characters Used in Diagnoses and Phylogenetic Analysis’.

The terminology of the caudal endoskeletal elements (e.g., preural centrum, ural centrum, parhypural) and of types of caudal

skeletons (e.g., polyural, diural) follows Nybelin (1963), Schultze and Arratia (1986, 1989, 2013), and Arratia and Schultze (1992). ‘True’ uroneurals are elongated, paired ural neural arches extending along the dorsolateral walls of the neural cord and the notochord; ‘uroneural-like’ elements resemble true uroneurals, but are actually modified preural neural arches and their spines. The terms ‘uroneural-like’ or ‘uroneural of a particular type’ found in certain fishes (e.g., ‘pachycormiform uroneural’) are included here in the phylogenetic analysis, and usage of these terms follows Arratia and Lambers (1996) and Arratia and Schultze (2013).

Fin rays, scutes, fulcra, and spines have been traditionally interpreted as modified scales, but their morphological diversity has been ignored. In the present study, special attention will be given to each of these elements and also to the differences between procurent rays, epaxial rudimentary rays, and principal rays following the definitions provided by Arratia (2008, 2009). The identification of pectoral and pelvic axillary processes, and their structures in different fishes, follows Arratia (1997).

Following Arratia (2008, 2009), procurent rays are interpreted as short rays, shorter than the principal rays, which form the anterior series of lepidotrichia of median fins and that are associated with endoskeletal elements (e.g., pterygiophores, neural and hemal spines, epurals, uroneurals). The most anterior rays are usually unsegmented, but the posterior ones are segmented. Most or all procurent rays may become segmented during growth.

Principal rays have slightly different definitions in dorsal and anal fins compared with the caudal fin. Principal rays of the dorsal and anal fins are the series of rays comprising the first segmented but unbranched ray, followed by all branched and segmented rays of the fin (Arratia, 2008). These elements are associated with endoskeletal elements (pterygiophores). Principal rays of the caudal fin are all segmented and branched rays plus one unbranched but segmented ray located at the leading margin in each lobe of the fin (Hubbs and Lagler, 1947). These elements are associated with endoskeletal elements (e.g., hypurals and hemal spines of preural centra 1 and 2).

The ‘pholidophoriforms’ studied in the present contribution may have one or two rudimentary rays in the caudal fin. A rudimentary ray, as defined by Arratia (2008), is a small ray with a short base not reaching endoskeletal bones. It is positioned between the epaxial basal fulcra and the first principal ray of the caudal fin. A rudimentary ray may be distally segmented or not. This interpretation of a rudimentary ray differs from that of Grande and Bemis (1998:figs. 84, 86).

The ‘pholidophoriform’ fishes may have basal fulcra associated with the paired and unpaired fins. Following Arratia (2008, 2009), basal fulcra are defined as large, laterally expanded, paired or unpaired scale-like structures that precede the bases of both paired and median fins. Basal fulcra may be lanceolate, leaf-like, or arrow-like in shape. Each fulcrum broadly overlaps the following one. Epaxial or dorsal basal fulcra are the series of fulcra positioned at the dorsal or anterodorsal margin of the caudal fin, whereas hypaxial or ventral basal fulcra are placed at the anteroventral margin of the fin (Arratia, 2008). The term fringing fulcra follows Arratia (2008, 2009). They are paired structures associated with the leading rays of paired and/or unpaired fins. In the fishes studied here, they form a series of small elements lying on the surface of a marginal leading ray, developing from anterior to posterior (rostrad to caudad), and appear in combination with accessory fulcra and the distal segment of the procurent rays that resemble a fulcrum.

The terminology of scales follows Schultze (1966, 1996). The Triassic and most Jurassic ‘pholidophoriforms’ studied here possess ganoid scales. Ganoid scales are rhomboidal, and their shape varies from deeper than long in the anterior lateral side of the body to longer than deep in the dorsal, ventral, and cau-

dal regions. Peg-and-socket articulation and connective fibers (Sharpey’s fibers) connect each scale to adjacent scales above and below. The ganoid scales of the Triassic pholidophorids are of lepisosteoid type, which means that the basal lamellar bone layer directly overlain by ganoine without an intercalated dentine layer; the canals of Williamson extend inward from the base to the ganoine layer). Other fishes studied here have elasmoid scales, a term used for flexible, round scales. Elasmoid scales can be subdivided into those with ridges (amiod scale; e.g., *Eurycormus*) on the overlapped field and those with circuli (cycloid scale; e.g., *Leptolepis*) on the anterior overlapped field (Schultze, 1966).

Anatomical Abbreviations—**ac.dor**, accessory dorsal elements placed between dorsal procurent rays and first dorsal principal ray; **a.cer**, anterior ceratohyal; **a.gu**, additional gulars (paired); **all.sc**, scales carrying additional segments of the lateral line; **a.nao**, anterior nasal opening; **ang**, angular; **an.r**, anal fin rays; **ANT**, anterior; **antb**, antorbital or anterodorsal dermal bone of the circumorbital series, which may or may not carry the infraorbital sensory canal; **a.pl**, anterior pit-line commonly located in a groove in the postparietal bone or postparietal region, just in front of the middle pit-line groove; **a.pop**, anterior preopercular bone or accessory preopercle; **a.ro**, accessory rostral bone, a small bone placed posterior to the main rostral bone; **ar+rar**, articular plus retroarticular; **art.f**, articular facet or fossa; **art.pr**, articular process; **art.s**, articular surface; **a.sclr**, anterior sclerotic bone; **a.sob**, accessory suborbital bone(s), which may lie on the dorsolateral surface of the suborbital; **asc.p**, ascending process or ramus of the parasphenoid; **asp**, autospheophotic; **b**, broken element (e.g., b.sop = broken subopercle); **bd.chc**, basidorsal chordacentrum; **bfu**, basal fulcra; **bhc**, buccohypophyseal canal; **b.mc**, broken mandibular canal; **br**, branchiostegal rays; **brc**, fused cranial bones forming part of the lateral walls of the braincase; **brch.b**, broken branchial arches; **btg**, basipterygoid process; **bv.chc**, basiventral chordacentrum of vertebral centrum; **chc**, chordacentrum; **chcPU1**, hemichordacentrum of preural centrum 1; **chcU1–3**, hemichordacentrum of ural centra 1–3; **cl**, cleithrum; **clv**, clavicle; **cor.b**, coronoid bone(s); **cor.p**, coronoid process of the lower jaw; **d**, hypural diastema; a space between hypurals 2 and 3; **de**, dentary; **df.scu**, scute preceding dorsal fin; **dor**, dorsal fin rays; **d.pcl**, dorsal postcleithrum; **dpt**, dermopterotic; **d.scu**, dorsal caudal scute; **dshp**, dermosphenotic; **ebfu**, epaxial basal fulcra; **end.p.lj**, endochondral portion of lower jaw; **ent**, entopterygoid; **et.c**, ethmoidal or rostral commissure; **etmv**, ethmovomerine region; **exc**, extrascapular bone; **f.fu**, fringing fulcra; **fica**, foramen for internal carotid artery; **fpsa**, foramen or notch for optic artery; **gan.ri**, ganoine ridges of serrated appendage; **gu**, median gular plate; **H**, hypurals; **H1–6**, hypurals 1–6; **haPU1**, PU6, hemal arch of preural centrum 1, 6; **hbfa**, hypaxial basal fulcra; **hml**, hemilepidothrichia forming a lepidotrichium or fin ray; **hpr.r**, hypaxial procurent rays; **hs**, hemal spine; **hy**, hyomandibular bone; **hys.c**, hyosymplectic cartilage; **id.chc**, interdorsal chordacentrum of vertebral centrum; **ihy**, interhyal; **io?**, infraorbital bone?; **io1–6**, infraorbital bones 1–6; **io3–5**, infraorbital bones 3–5; **iop**, interopercular bone or interopercle or interoperculum; **iv.chc**, interventral chordacentrum of vertebral centrum; **l**, left (used as a prefix, e.g., ‘Lang’); **lat.ri**, protruding bony lateral ridge separating dental and splenial regions of dentary; **lj**, lower jaw; **llc**, lateral line canal; **ll.sc**, lateral line scales; **l.no**, ‘leptolepid’ notch; **Mc?**, partially ossified Meckel cartilage; **me.sp**, median neural spines; **m.pl**, middle pit-line groove; **m.sc**, modified scales; **mtg**, metapterygoid; **mx**, maxilla; **na**, neural arch; **nab**, nasal bone; **naPU6–4**, neural arches of preural centra 6–4; **naU**, neural arches of ural vertebrae; **ns**, neural spines; **o.c**, otic sensory canal; **op**, opercular bone or opercle; **o.pl**, oral pit-line groove; **op.p**, opercular process of hyomandibula; **pa [= fr]**, parietal bone [= frontal bone of traditional terminology]; **pa.ns**, paired neural spines; **par**, paras-

phenoid; **pax.p**, pelvic axillary process formed from one or more modified scales; **pec.f**, pectoral fin; **pec.r**, pectoral fin rays; **pec.ra**, proximal pectoral radials; **pecx.p**, pectoral axillary process; **pel.p**, pelvic plate or basipterygium; **pel.r**, pelvic fin rays; **pel.sp?**, pelvic splint?; **p.excc**, pores of extrascapular canal; **PH**, parhypural; **pl**, pit-line groove; **p.ll**, pores of lateral line; **p.msc**, pores of mandibular sensory canal; **pmx**, premaxilla; **pop**, preopercular bone or preopercle; **popsc**, preopercular sensory canal; **potc**, pores of otic sensory canal; **ppa [= pa]**, postparietal [= parietal of traditional terminology]; **p.pl**, posterior pit-line groove; **p.poc**, pores of the preopercular sensory canal; **plqc**, palatoquadrate cartilage; **pr.dor**, procurent rays in dorsal fin; **pear**, prearticular bone; **pr.r**, procurent rays; **p.sclr**, posterior sclerotic bone; **p.sorb**, pores of the supraorbital sensory canal; **pt**, pterotic; **ptt**, posttemporal; **qu**, quadrate; **r**, right (used as a prefix, e.g., 'r.ang'); **rar**, retroarticular process; **r.epr**, rudimentary epaxial caudal ray; **r.hpr**, apparently a hypaxial rudimentary ray; **ro**, rostral bone; **rodet**, rostrodermethmoid or dermethmoid; **rscm**, recess on parasphenoid housing origin of subcephalic muscles; **sang**, surangular or supraangular or suprangular; **sc**, scales; **scl**, supracleithrum; **sclrb**, sclerotic bone(s); **smx**, only one supramaxilla present; **smx1–2**, supramaxillary bones 1–2; **sob**, suborbital bone(s); **sop**, subopercular bone or subopercle; **sorb**, supraorbital sensory canal; **sup**, supraorbital bone; **sup1–3**, supraorbital bones 1–3; **sy**, symplectic; **t.mc**, trajectory of mandibular sensory canal; **tsobc**, trajectory of supraorbital canal; **vpcl**, ventral postcleithrum; **vscu**, ventral caudal scute; **1st dor**, first dorsal principal ray; **1st dptg**, first dorsal pterygiophore; **1st pecr**, first pectoral ray; **1st PR**, first principal caudal ray; **2nd dor**, second dorsal principal ray; **+**, fusion between two bones (e.g., 'ang+rar'); **?**, unknown or uncertain determination; **†**, extinct.

SYSTEMATIC PALEONTOLOGY

ACTINOPTERYGII Cope, 1887
NEOPTERYGII Regan, 1923

TELEOSTEI sensu Arratia, 1999

† **PHOLIDOPHORIFORMES**, new usage
 † **PHOLIDOPHORIDAE** Woodward, 1890, new usage

Diagnosis—Based on a unique combination of characters. Autapomorphies are identified with an asterisk [*]. Small teleostean fishes not exceeding about 140 mm total length. Layer of ganoine on cranial bones densely ornamented with ridges and/or tubercles of ganoine in basal forms. Interparietal suture absent [*]. Tendency to have skull roof bones (parietal, postparietal, autosphenotic, and dermopterotic) fused into a single bony plate [*]. Supraorbital and otic canals with rudimentary tubules, some of which open onto the surface [*]. Absence of a tooth patch on parasphenoid. Large, rectangular or square nasal bones present. Five or six infraorbital bones. Dentary with well-developed 'leptolepid' notch. Preopercle notched at anteroventral margin so that the bone resembles an inverted heart shape in basal forms [*]. Long, serrated appendage or interclavicular element covering medial surface of cleithrum [*]. Presence of a clavicle [*] suturing with anteroventral margin of cleithrum. Pectoral axillary process present. Elongate, leaf-like bony axillary process present [*]. Three horizontal rows of ganoid, lepisosteoid-type scales, deeper than long in predorsal region present. Thirty-four to 40 lateral line scales present.

Content—†*Annaichthys*, gen. nov., †*Knerichthys*, gen. nov., †*Parapholidophorus* Zambelli, †*Pholidoctenus* Zambelli, †*Pholidophoretes* Griffith, †*Pholidophorus* Agassiz, †*Pholidorhynchodon* Zambelli, and †*Zambellichthys*, gen. nov.

Type Genus—*Pholidophorus* Agassiz, 1832.

Geographical Distribution and Age—Europe; Late Triassic (Carnian–Norian).

†*PHOLIDOPHORUS* Agassiz, 1832

Pholidophorus: Agassiz, 1832:145.

Pholidophorus: Nybelin, 1966:356.

Diagnosis—Emended from Nybelin, 1966, and based on a unique combination of characters. Autapomorphies are identified with an asterisk [*]. Pholidophorids of small size, maximum length approximately 90 mm. Anterior width of parietal bones in front of posterior margin of nasals very narrow, about one-fifth or one-sixth of postorbital cranial width [*]. One to three supraorbitals present. Posterior margin of maxilla rounded or slightly acute. Elongate lower jaw. Quadrate-mandibular articulation below posterior half of the orbit or posterior margin of orbit. Preopercle expanded at its anteroventral limb, with or without a gentle notch at its anterior margin, and with a narrow, short dorsal limb. Well-defined notch present at the posterior margin of preopercle. Preopercular sensory canal running nearer to anterior than posterior margin of preopercle. Ganoid scales with smooth surface or surface ornamented with tubercles and ridges of ganoine. Posterior margin of scales smooth, with 38 to 40 rows of mid-flank scales.

Type Species—†*Pholidophorus latiusculus* Agassiz, 1832. This designation differs from Woodward (1895) and Nybelin (1966), both of whom considered †*Ph. bechei* Agassiz, 1837, to be the type species because it is better known than †*Ph. latiusculus*. The latter, however, is more appropriately the type species because †*Ph. latiusculus* is the first species described for the genus (Agassiz, 1832).

Comments—The diagnosis of the genus is difficult because the type species is incompletely known in comparison with the Late Triassic †*Pholidophorus gervasutti* and the Early Jurassic †*'Pholidophorus' bechei*, both of which are known from numerous specimens. Agassiz (1832) described a second species from the Triassic of Seefeld, Austria, that he named †*Pholidophorus pusillus*. The original material is lost, apparently since 1942 (see Nybelin, 1966:386). This species was not included in the present contribution because after checking specimens identified as possible †*Ph. pusillus* in different collections in Austria (including specimens previously studied by Kner in 1866), I could not make sense of the variation observed. Additionally, most of the material is incompletely preserved, and in some cases, type specimens have been lost, so revisions are difficult. Nybelin (1966:382) gave a preliminary diagnosis of †*Pholidophorus* cf. *pusillus* based on one specimen from the Natural History Museum in London, which is too poorly known and does not add any significant information to the understanding of †*Pholidophorus*. †*Pholidophorus bronni*, described by Kner in 1866, is removed from the genus and described here as a new genus (see below).

†*PHOLIDOPHORUS LATIUSCLUS* Agassiz, 1832 (Figs. 1, 4–6)

Pholidophorus latiusculus: Agassiz, 1832:145.

Pholidophorus latiusculus: Agassiz, 1833, v. 2, pt. I:287.

Pholidophorus fusiformis: Agassiz, 1844, v. 1, pt. I:271, 288.

Pholidophorus latiusculus: Kner, 1866, pt. I:328, pl. III, figs. 2, 3.

Pholidophorus latiusculus: Kner, 1867, pt. I:903, pl. II, fig. 1.

Pholidophorus latiusculus: Woodward, 1895 (in part):454, ?pl. 14, fig. 3.

Pholidophorus latiusculus: Nybelin, 1966:368, text-figs. 3, 4, pls. 4, 5, 15, figs. 1, 2, 6, 7.

Pholidophorus latiusculus: Schultze, 1966:fig. 37a.

Pholidophorus latiusculus latiusculus: Zambelli, 1986:8.

Pholidophorus latiusculus: Arratia, 2000 (in part):phylogenetic analysis.

Neotype—Innsb. F.123 (Fig. 1). Almost complete, but poorly preserved specimen in part and counterpart; the counterpart is broken in three pieces. Agassiz (1832) did not assign a holotype for this species, so that Nybelin (1966) selected one specimen illustrated by Kner (1866:pl. 3, fig. 3; Innsb. F123) and assigned it as neotype. The specimen has two old labels, written with the same handwriting: one identifies the fish as †*Pholidophorus latiusculus* Agassiz, and the other as †*Pholidophorus pusillus* Agassiz.

Additional Material Examined—Innsb. 6b, 6c; Innsb. 27a; Innsb. 126b; Innsb. Lit F; Innsb. 1028a, b; however, and independently of their catalog number, the two parts identified as ‘a’ and ‘b’ do not belong to the same specimen, but are the same species; Innsb. 1028a and 1028b are treated here as two separate specimens. Additionally, I have included other specimens: GBA 2006/096/0024 and NHMUK P1063 (Fig. 4). Although GBA 2006/096/0024 is incompletely preserved, it is one of the few specimens preserved in lateral view allowing observation of body shape.

Type Locality, Age, and Distribution—Seefeld in Tirol, Austria; Upper Triassic Seefeld Formation, upper part of the middle Norian (Brandner and Poleschinski, 1986), about 210 Ma.

Diagnosis—Emended from Nybelin, 1966, based on a unique combination of characters. Autapomorphies are identified with an asterisk [*]. Small fishes of about 85 mm total length. Supramaxilla 1 covered with a few, thick concentric ridges of ganoine [*]. Infraorbital 3 extends posteriorly below suborbital, reaching anterior margin of preopercle. Supramaxilla 2 about three times longer than supramaxilla 1. Supramaxilla 2 with rudimentary anterodorsal process. Lower jaw elongated; quadrate-mandibular articulation posterior to posterior margin of orbit. Preopercle moderately expanded at its anteroventral limb and moderately narrow dorsally. Preopercular dorsal limb short, not reaching the lateral margin of skull roof. Anteroventral margin of preopercle straight. Preopercle with 14 or 15 sensory tubules [*]. Body covered with ganoid scales with smooth surfaces [*].

Comments—Among the studied species presented here, †*Pholidophorus latiusculus* is poorly known. This fact, as explained in ‘Introduction,’ is largely based on the incompleteness of the neotype of †*Ph. latiusculus*, and of many specimens tentatively identified as †*Ph. latiusculus* that are incompletely preserved. These are critical shortcomings because †*Ph. latiusculus* is the type species of the genus †*Pholidophorus* and of the family †*Pholidophoridae*.

Nybelin (1966) was the first to provide a more complete revision of †*Pholidophorus latiusculus* after the brief original descriptions provided by Agassiz (1832) and Kner (1866). Kner (1866:pl. 3, figs. 2, 3) illustrated two specimens: one that is currently considered as the neotype and a second complete specimen that is apparently lost. In addition, Kner (1866:28) presented a hand-drawn figure showing the opercular bones and lower jaw, but the illustration has two important errors: the subopercle shows three large spines or serrations in its posterior margin, and the lower jaw bears long conical teeth. Neither the neotype nor any of the specimens considered in this revision have these features (pers. observ.). Nybelin’s (1966) description and illustrations of †*Ph. latiusculus* seem to be largely influenced by those of †*‘Pholidophorus’ bechei*, which is better known than †*Ph. latiusculus*. Nybelin (1966) suggested that four characters are diagnostic of †*Ph. latiusculus*:

- (1) Small size (about 85 mm in total length). In this case, the reported maximum length is a composite number determined from three incomplete specimens of the Innsbruck collection.

- (2) Nasal bone not very large and anteriorly pointed; dorsolateral surface of the nasal ornamented with “irregular streaks and tuberculations” (Nybelin, 1966:369). According to my investigation of the neotype and other specimens from Seefeld assignable to the species, this is incorrect. The nasal bone is not preserved in the neotype and is incompletely preserved in specimen NHMUK P.1063 studied by Nybelin (1966:figs. 3, 4, pls. 4, 5, fig.1).
- (3) Posterior margin of preopercle with a shallow notch. This trait is present in the neotype and other species of †*Pholidophorus*, as well as species outside the genus (see below).
- (4) Preopercular sensory canal with 14 or 15 tubules. The neotype shows 14 tubules. This feature seems to be unique to †*Pholidophorus latiusculus*.

Description

The description of certain body regions, as well as determination of morphometric and meristic traits, is difficult due to conditions of preservation. The vertebral column, ribs, supraneurals, and dorsal and anal pterygiophores are obscured by the squamation.

†*Pholidophorus latiusculus* has an elongate body (Fig. 4), with maximum depth in the predorsal region, as shown by specimen GBA 2006/096/0024. The pectoral fins are positioned nearer the ventral margin of the body than to the middle region of the flanks. The pelvic fins are positioned directly opposite the dorsal fin. The anal fin lies opposite and posterior to the base of the dorsal fin. All fins are small, with very delicate and slender rays, and bear small fringing fulcra associated with the leading margins. External cranial bones and scales are mainly covered by a thin, smooth layer of ganoine, with a few exceptions indicated below.

Braincase—The braincase seems to be short; its posterior margin is positioned at the level of the anterior margin of the opercle. Except for the skull roof bones and a piece of the parasphenoid, no other elements of the braincase are observed.

Skull Roof—The skull roof is incompletely preserved, especially posteriorly, in all available specimens. As far as preservation permits, no crestae, fontanelles, or pineal opening have been observed in the skull roof (Fig. 5). As indicated by a lack of sutures, all bones (parietals, postparietals, autosphenotics, and dermopterotics) are fused into a bony plate, although an incomplete suture is present between the parietals in specimen Innsb. Lit F. A. The medial rostral bone anterior to the skull roof plate, paired extrascapulae, and posttemporals are not preserved. The skull roof is very narrow anteriorly, ending in an acute tip. The width of the skull roof increases posteriorly, being very broad at the level of the posterior corner of the orbital margin, and maintains its breadth in the postorbital region, which gives the skull roof a characteristic outline (Fig. 5). The breadth of the skull roof at the level of the posterior tip of the nasal bones is about one-fifth of that of the postorbital region.

The cephalic sensory canals are tube-like and enclosed by bone. Only sections of the supraorbital canal are preserved, and I have not found evidence to support the presence of a postparietal branch joining the anterior pit-line groove, although preservation is poor. The middle pit-line groove is long, extending near the lateral margin of the skull roof plate, in the region where the dermopterotic is found in other neopterygians. Despite the incomplete preservation of the material of †*Pholidophorus latiusculus*, Nybelin (1966:figs. 4, 5; 369, 371) offered a complete restoration of the skull roof and lateral cranial bones, including the trajectories of the cephalic sensory canals with sensory tubules and pores; however, he presented them as ‘attempted restorations.’ Separated dermopterotics, postparietals [= his parietals], and extrascapulars were restored, but framed with dotted lines indicating

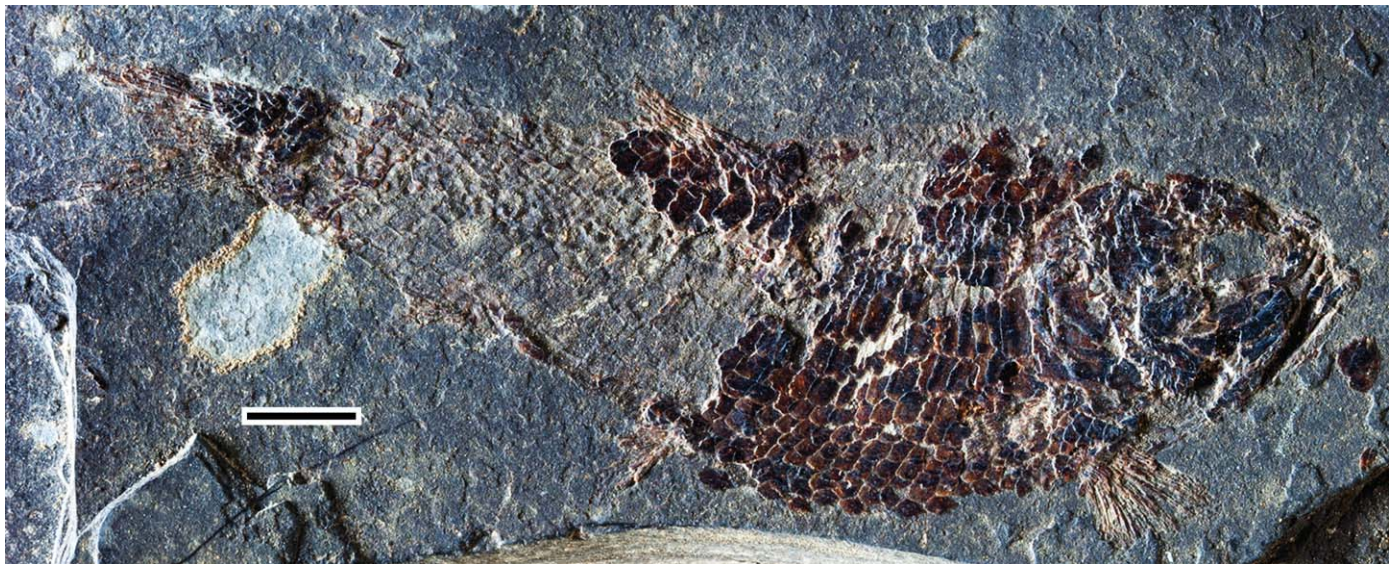


FIGURE 4. †*Pholidophorus latiusculus* Agassiz. Photograph in right lateral view (specimen GBA 2006/096/0024). Scale bar equals 5 mm.

that these were not observed. According to his restorations, the parietal bones [= his frontals] are independent bones, with well-defined posterior margins. This differs from the interpretation here, in which they are fused. He also restored the supraorbital and otic canals, including pores and short sensory tubules (Nybelin, 1966:text-figs. 3, 4), which I have not been able to observe in the studied specimens. Additionally, he restored the supraorbital sensory canal extending into the postparietals, a description that is not supported by available specimens.

The surface of the cranial roof is smooth, but a few ridges of ganoine are observed at the border where the autosphenotic would be in other neopterygians.

Circumorbital Series—The circumorbital ring is incompletely preserved in all specimens. It is known by infraorbitals 2 to 5, the

dermosphenotic, and two supraorbitals (Fig. 5). In addition, one large suborbital and remnants of sclerotic bones are present. The antorbital and infraorbital 1 are not preserved in the available material.

Remnants of two elongate, rectangular, thick bones are preserved lateral to the left side of the skull roof plate in the neotype. They are the supraorbitals 1 and 2.

Infraorbital 2 (Fig. 5) is a narrow, rectangular bone. The large infraorbital 3 (Fig. 5) is almost rhomboidal, with a slightly concave orbital margin, a straight dorsal margin, and a slightly rounded posteroventral margin. Infraorbital 3 contacts infraorbital 2 anteriorly, the preopercle and suborbital posteriorly, and infraorbital 4 dorsally. Infraorbital 3 extends posteriorly below the large suborbital and overlies slightly the anterior margin of the preopercle.

Infraorbitals 4 and 5 are small, slightly rectangular bones carrying the infraorbital canal close to their orbital margin (Fig. 5). Both infraorbitals contact the suborbital posteriorly, and infraorbital 5 also contacts the dermosphenotic dorsally.

The slightly triangular dermosphenotic is too poorly preserved to describe in detail.

A large, almost square suborbital (Fig. 5) occupies the space bounded by the lateral margin of the skull roof plate, the opercle posteriorly, the preopercle and posterodorsal margin of infraorbital 3, and the posterior margins of infraorbitals 4 and 5 anteriorly. An accessory suborbital has not been observed.

Upper Jaw—Only the maxilla and supramaxillae are preserved in the available material. The maxilla is incompletely preserved in the neotype (Fig. 5), as well as in all other studied specimens. The neotype preserves part of the maxillary blade. The posterior margin of the maxilla is incomplete in most specimens, but appears to be oblique in the neotype. Due to the destruction of the ventral margin of the maxilla, teeth have not been observed. The exposed surface is covered by thick ridges of ganoine, which are longitudinally oriented, giving the bone a characteristic aspect. A similar pattern of longitudinal ridges is on the surface of supramaxilla 2.

Two supramaxillary bones (Fig. 5) are preserved in the neotype. Supramaxilla 1 is a small, deep triangular bone that is covered by ridges of ganoine characteristically arranged in a concentric pattern. Supramaxilla 2 is an elongate bone, with its maximum depth about half of that of the maxilla. It has a rudimentary,

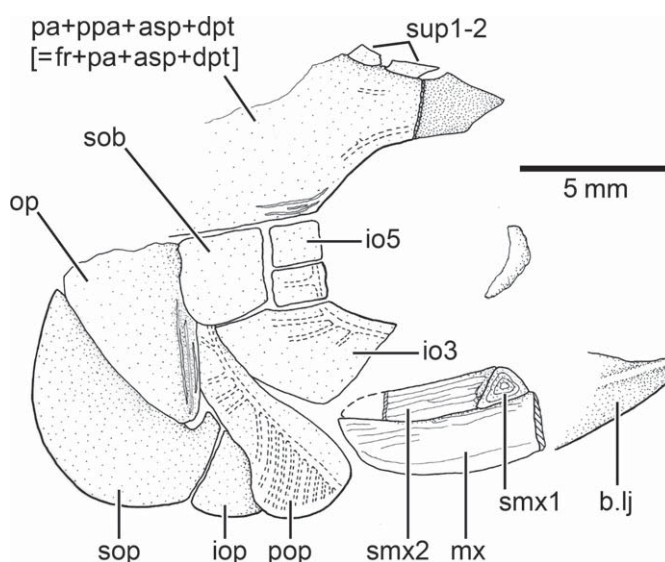


FIGURE 5. †*Pholidophorus latiusculus* Agassiz. Diagram of the head in right lateral view based on the neotype (Insb. 123).

slightly thickened anterodorsal process that barely overlaps the dorsal margin of supramaxilla 1.

Lower Jaw—The lower jaw (Fig. 5) is only partially exposed in the neotype and other specimens, or it is not preserved at all. The dentary forms most of the length of the lower jaw, but its suture with the angular is unclear. The dentary has a dental region lacking ganoine, located close to the oral margin above a well-exposed longitudinal ridge that protrudes along the length of the bone. The ventral region below the protruding longitudinal ridge corresponds to the splenial region of the dentary. Because of the damage to the oral margin, it is unclear whether teeth were present or not. The posterior margin of the jaw lacks a postarticular process.

The mandibular sensory canal, which is enclosed by bone, is positioned below the lateral bony ridge of the jaw in the splenial region. The canal is covered by longitudinal ridges and elongate tubercles of ganoine.

The articulation between the lower jaw and quadrate lies posterior to the orbital posterior margin. Only in one specimen (GBA 2006/096/0025) is it possible to observe the articulation of the lower jaw and quadrate. The bones are not preserved well enough to describe in detail.

Palatoquadrate, Suspensorium, and Hyoid Arch—Bones of the palatoquadrate, suspensorium, and hyoid arch, where preserved, are hidden by the opercular bones and lower jaw so that a description is not possible.

Opercular, Branchiostegal Series, and Gular Plate—The opercular bones (Fig. 5) are relatively well preserved in the neotype, whereas the branchiostegal rays and gular plate are not preserved. Together, the posterior margins of the opercle and subopercle plus the ventral margin of the interopercle produce a gently rounded profile of the opercular apparatus. All opercular bones are covered by a thin, smooth layer of ganoine, with an exception noted below.

The preopercle shows variation in its shape and size among specimens. In general, it is expanded ventrally and narrows slightly dorsally (Fig. 5). There is no clear distinction between dorsal and ventral arms, but a shallow notch at the posterior margin separates the bone into dorsal and ventral regions. The preopercle has no distinct dorsal arm, ventral arm, or anterior expansion—the anterior margin is smooth, slightly curvilinear, and inclines dorsoventrally. The ventral margin is also smooth, and lacks the deep, acute notch that is found in some of the species described below, so that the preopercle does not look like an inverted heart shape. The dorsal tip of the preopercle is covered by the suborbital. The anterior margin of the preopercle is narrowly covered by the posterior projection of infraorbital 3. Posteriorly, the preopercle overlaps the anterior margin of the opercle and the anterodorsal process of the subopercle. The interopercle abuts against the notch at the posterior margin of the preopercle.

The smooth anterior region of the preopercle is slightly expanded in front of the main course of the preopercular canal. The pathway of the preopercular sensory canal and its tubules is visible because the ganoine is thin and smooth. Ten sensory tubules are positioned in front and ventral to the notch, and four tubules are dorsal to the notch in the neotype. The sensory tubules end in small pores opening near the posterior and ventral margins of the bone.

The opercle (Fig. 5) is a moderately large, roughly triangular bone. Its dorsal margin is destroyed in the neotype. The anterior margin of the opercle nearly lies in a vertical plane; it is markedly thickened and covered by two or three ridges of ganoine. The ventral margin is long and lies in a plane approximately at 45 degrees to the anterior margin.

The subopercle (Fig. 5) is larger than the opercle. Its ventral margin is rounded and continues the rounded posterodorsal corner of the opercle. Its anterior margin is also slightly rounded

where it joins the interopercle and preopercle. The anterodorsal process of the subopercle is well developed. It projects dorsally in front of the anterior margin of the opercle, being partially hidden by the posterior margin of the preopercle.

The interopercle (Fig. 5), displaced and partially exposed in the neotype, is large and triangular. It is positioned between the posterior notch of the preopercle and the anterior margin of the subopercle. The anterior extension of the interopercle is covered by the preopercle in the neotype, so that the complete size of the bone is unknown. Considering the position and size of the anterodorsal process of the subopercle, the interopercle probably does not contact the anteroventral tip of the opercle.

Vertebral Column and Intermuscular Bones—Remnants of a few ring-like chordacentra are observed between scales. No other elements associated with the vertebral column have been observed.

Paired Girdles and Fins—Very little can be said about the paired girdles because they are incompletely preserved or are not exposed in the available material. Only a few lepidotrichia belonging to the pelvic fins are preserved, so the number of rays remains unknown. Additionally, it is unknown whether axillary processes are associated with the paired fins, as in other species described below.

No specimen preserves the complete series of dermal bones of the pectoral girdle. An incomplete supracleithrum, cleithrum, and dorsal postcleithrum have been observed in different specimens. The supracleithrum has a few ridges of ganoine.

The pectoral fin (Fig. 4) consists of at least 19 lepidotrichia. All pectoral rays are so poorly preserved that a description cannot be provided. Thus, it remains unknown whether the propterygium is fused to the proximal region of the first ray or not. The pectoral rays have long bases, and they are segmented and finely branched distally. A series of small, elongate fringing fulcra is associated with the leading margin of the fin.

Dorsal and Anal Fins—The dorsal fin is poorly preserved in most specimens so that a description is difficult. The fin is preceded by an unknown number of basal fulcra. There are about 18 rays with long bases that branch distally and are subtly segmented (in GBA 2006/096/0024). It is unclear if only the first principal ray forms the leading margin of the fin or whether the first and second principal rays form the leading margin. Small fringing fulcra lie between the last basal fulcrum and leading margin of the fin.

The short anal fin (Fig. 4), positioned posterior to the dorsal fin, is closer to the caudal fin than to the pelvic fins. It consists of an unknown number of small basal fulcra and about seven rays, a number that will likely be revised when better specimens become available. The anal fin rays are very delicate and are frequently broken. Small fringing fulcra are associated with the leading margin of the fin.

Caudal Fin—The caudal endoskeleton has not been observed because the squamation is *in situ* in most specimens, and a description of the tail cannot be provided due to poor preservation of the caudal region. The hemi-heterocercal caudal fin (Fig. 4) is deeply forked, with very short, middle principal rays in comparison with the rays forming the long leading margins of the dorsal and ventral lobes of the fin. The area covered by ganoid scales at the base of the caudal fin ends in two lobes formed by scales, slightly separated by a notch.

The caudal fin is incompletely preserved or not preserved at all in the available material. However, Innsb. 1028a, a poorly preserved specimen, provides information on the caudal fin rays. There are eight epaxial basal fulcra, a series of elongate epaxial fringing fulcra, a thin and short epaxial rudimentary ray, 22 principal rays, a series of elongate hypaxial fringing fulcra, three hypaxial segmented procurent rays, and three elements interpreted as hypaxial basal fulcra. The anterior-most epaxial

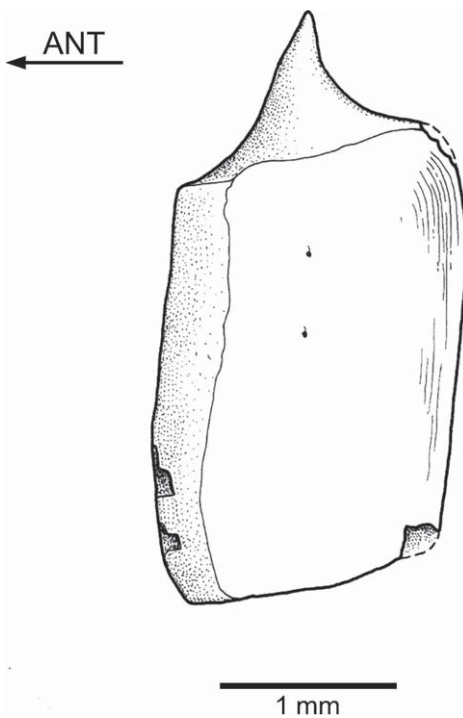


FIGURE 6. *†Pholidophorus latiusculus* Agassiz (Innsb. F126). Scale from the predorsal region of the right flank of the specimen, redrawn from Schultze (1966).

basal fulcra are unpaired (also in GBA 2006/096/0024), and the hypospinal basal fulcra seem to be unpaired as well. The segmentation of the delicate, thinly ossified principal rays is straight. The ventral leading margin of the caudal fin is formed by the posterior-most procurrent and the last two principal rays. The dorsal and ventral series of basal fulcra are preceded by two small scutes.

Scales—Ganoid scales (Figs. 1, 4, 6) of different sizes and shapes cover the body. They were described and illustrated by Schultze (1966:figs. 37a). Most scales of the dorsal and ventral rows of the flank are rhombic, slightly rectangular, or even square-shaped. However, the three main rows of the flank (the lateral line row plus the rows ventral and dorsal to it) up to the dorsal fin are comparatively deeper than broad and are larger than the other scales. The scales decrease in size posteriorly, and in the caudal peduncle they appear to be more uniform in size, but they are heterogeneous in shape (e.g., some are rhombic, others are rectangular, others have rounded posterior margins). A layer of ganoine with no ornamentation covers all scales.

Lateral Line—About 38 vertical rows of flank scales are observed in the neotype. Each of the scales carrying the main lateral line canal is rhombic, with a well-developed peg, smooth surface and margins, and a small notch at the posterior margin, which indicates the trajectory of the lateral line canal. It is unknown if there are additional lateral lines in the predorsal region near the dorsal margin of the body, as in some of the species described below.

†PHOLIDOPHORUS GERVASUTTII Zambelli, 1980a (Figs. 7–25)

Pholidophorus gervasutti: Zambelli, 1980a:7–8, figs. 1–3, pls. 1–3.
Pholidophorus latiusculus gervasutti Zambelli, 1986:8, fig. 1.

Pholidophorus latiusculus: Arratia, 2000:phylogenetic analysis (in part).

Holotype—MCSNB 4723a–c, an almost complete specimen preserved in part and counterpart; the positive is broken into three pieces (Fig. 7A–C). The head is preserved in dorsal view so that the bones of the cheek are lateral to the skull roof, with some being displaced, some in situ, and others destroyed.

Material Examined—There are more than 300 specimens cataloged in MCSNB. It is a common situation that four or more specimens (Fig. 8) are preserved together, indicating a mass mortality event. After checking all specimens, the following were selected for study because of the morphological information that they provide: MCSNB 3406a–b, MCSNB 3462d, MCSNB 4300a–c, MCSNB 4301a–d, MCSNB 4302a–b, MCSNB 4303a–d, MCSNB 4304a–d, MCSNB 4305, MCSNB 4306a–b, MCSNB 4308, MCSNB 4309, MCSNB 4310a–g, MCSNB 4311, MCSNB 4313, MCSNB 4317a–c, MCSNB 4318a, MCSNB 4329a–b, MCSNB 4330, MCSNB 4332, MCSNB 4334, MCSNB 4340a–d, MCSNB 4345a–b, MCSNB 4346a–d, MCSNB 4414, MCSNB 4416, MCSNB 4418, MCSNB 4425, MCSNB 4438, MCSNB 4453, MCSNB 4455, MCSNB 4469a–b, MCSNB 4470a–b, MCSNB 4473, MCSNB 4708c, MCSNB 4710, and MCSNB 4726a–b.

Type Locality, Age, and Distribution—*†Pholidophorus gervasutti* is only known from the type locality Ponte Giurino, about 18 km northwest of Bergamo, Lombardy, northern Italy. The age of these rocks is Late Triassic (Norian), about 210 Ma.

Diagnosis—Emended from Zambelli, 1980a, and based on a unique combination of characters. Autapomorphies are identified with an asterisk [*]. Small fishes of about 82 mm total length. Cranial bones, fin rays, and scales covered with thick layer of ganoine and ornamented with patches of tubercles and ridges [*]. Anterior tips of the parietal [=frontal] bones not fused medially, commonly asymmetric [*]. Large nasal bones, expanding broadly laterally and completely separated from each other by anterior tips of parietal bones. Large, rounded foramen placed near the lateral margin of nasal bone. Posterior margins of infraorbitals 3, 4, and 5 ending almost at the same level posteriorly [*]. Infraorbital 3 not extending below suborbital, and not reaching anterior margin of preopercle. Triangular suborbital [*], with ventral acute tip extending between posterior margin of infraorbital 3 and preopercle [*]. One or two additional suborbitals above dorsal margin of suborbital [*]. Supramaxilla 1 almost as long as supramaxilla 2 [*]. Supramaxilla 2 with well-developed anterodorsal process covering about half of dorsal margin of supramaxilla 1. Quadrato-mandibular articulation below posterior half of the orbit or posterior margin of orbit. Opercle slightly larger than subopercle. Additional lateral line canal extending between extrascapular bone and base of dorsal fin.

Comments—*†Pholidophorus gervasutti* is the most informative species within *†Pholidophorus* and one of the most informative among Triassic pholidophorids because there are many well-preserved specimens that provide important new morphological information.

†Pholidophorus gervasutti is a small-sized fish, reaching 82 mm total length (Zambelli, 1980a), which is similar in length to *†Pholidophorus latiusculus* from Seefeld, Austria, but comparatively larger than *†Parapholidophorus* and *†Pholidothenus* from northern Italy. Zambelli (1986:8) later designated *†Ph. gervasutti* a subspecies of *†Ph. latiusculus* (i.e., *†Ph. latiusculus gervasutti*) that is differentiated from *†Ph. latiusculus latiusculus* by differences in maximum length (82 vs. 85 mm) and thickness of ganoine covering bones ('molto sottili' or 'very thin' vs. 'robusti' or 'thick'). The features listed by Zambelli (1980a, 1986) provide subtle, if any, differentiation between these two taxa. Although many specimens of *†Ph. gervasutti* are available for study, maximum size of this species is reliably based on only a few specimens; many are missing the distal tips of the caudal rays, are bent, or are

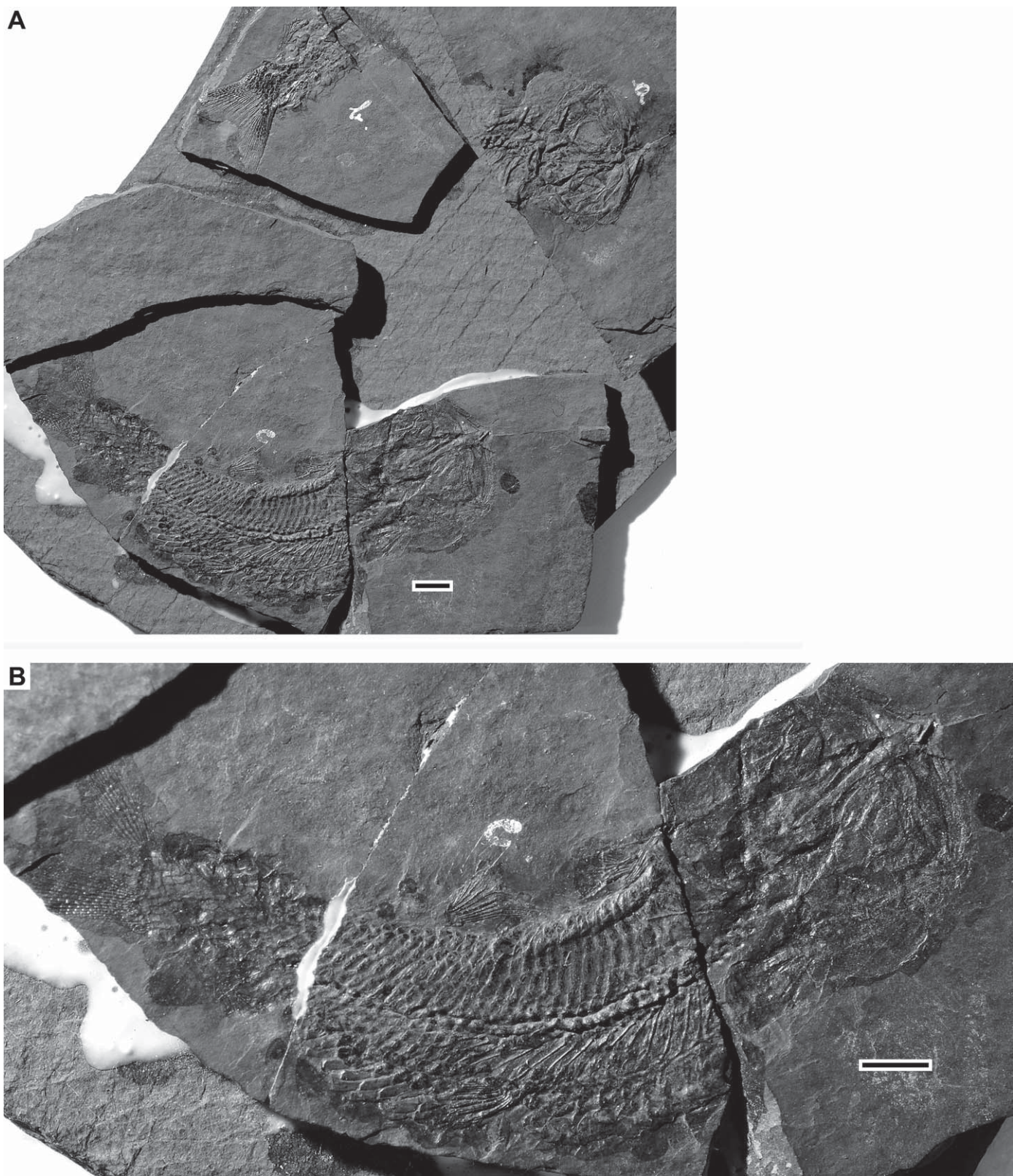


FIGURE 7. \dagger *Pholidophorus gervasutii* Zambelli (holotype; MCSNB 4723a–c). **A**, photograph of holotype separated in different pieces in right lateral view. **B**, enlargement of specimen 4723c. Scale bars equal 5 mm. **C**, drawing of the head preserved in dorsal view. Hatched lines indicate broken bone surface.

C

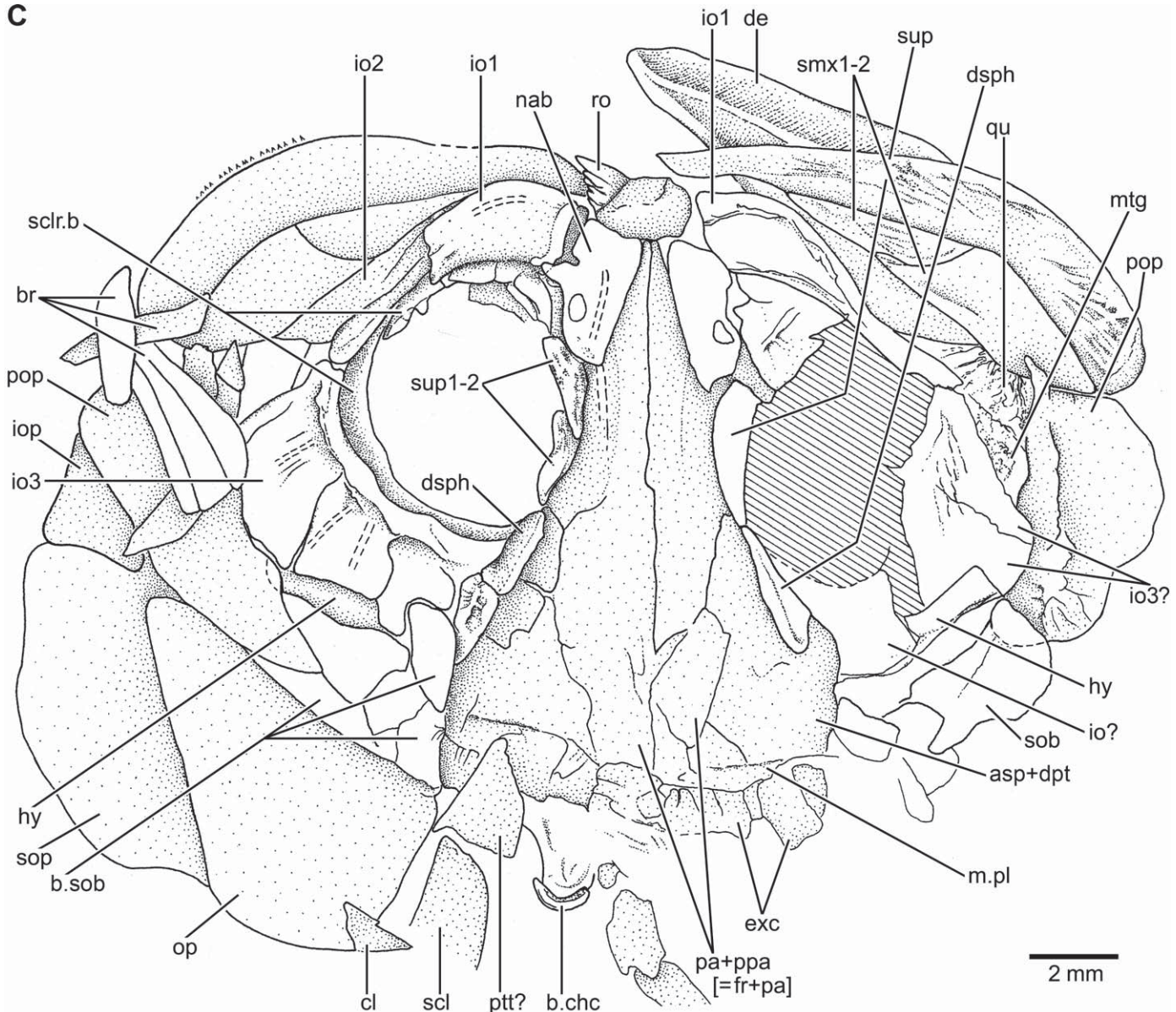


FIGURE 7. (Continued)

incomplete. The same is true for *†Ph. latiusculus*, whose maximum length of 85 mm is a composite value (Nybelin, 1966). Thus, a difference of 3 mm is within the range of variation and length estimation. Zambelli (1980a, 1986) correctly noted differences in ganoine thickness, which are minor, but he mixed up the attribution of the feature to the taxon.

In addition to these subtle distinctions, more significant, species-level differences are present in the ornamentation of the ganoine on cranial bones and scales, as well as the shape and position of cranial bones. *†Ph. latiusculus* has ornamentation on some cranial bones but the scales lack ornamentation, whereas *†Ph. gervasutti* has ornamentation on both (Fig. 6; see Schultz, 1966, and description of *†Pholidophorus latiusculus* above). The ganoine surface of these bones and scales forms thick patches of tubercles and ridges in *†Ph. gervasutti*, a uniquely derived feature among pholidophorids (see descriptions and illustrations below).

Additionally, in *†Ph. gervasutti* the anterior tips of the parietal [=frontal] bones are unfused medially and commonly asymmetric, the posterior margins of infraorbitals 3, 4, and 5 end at almost the same level posteriorly, infraorbital 3 does extend below the suborbital and does not reach the anterior margin of preopercle, and the suborbital is triangular. Based on these features, none of which are present in other 'pholidophorids,' and results presented in 'Phylogenetic Analysis,' I consider *†Pholidophorus gervasutti* Zambelli a valid species, not a subspecies of *†Ph. latiusculus*.

Description

The description of the braincase and the vertebral column and its associated elements is difficult due to poor preservation. The vertebral column, ribs, supraneurals, and dorsal and anal

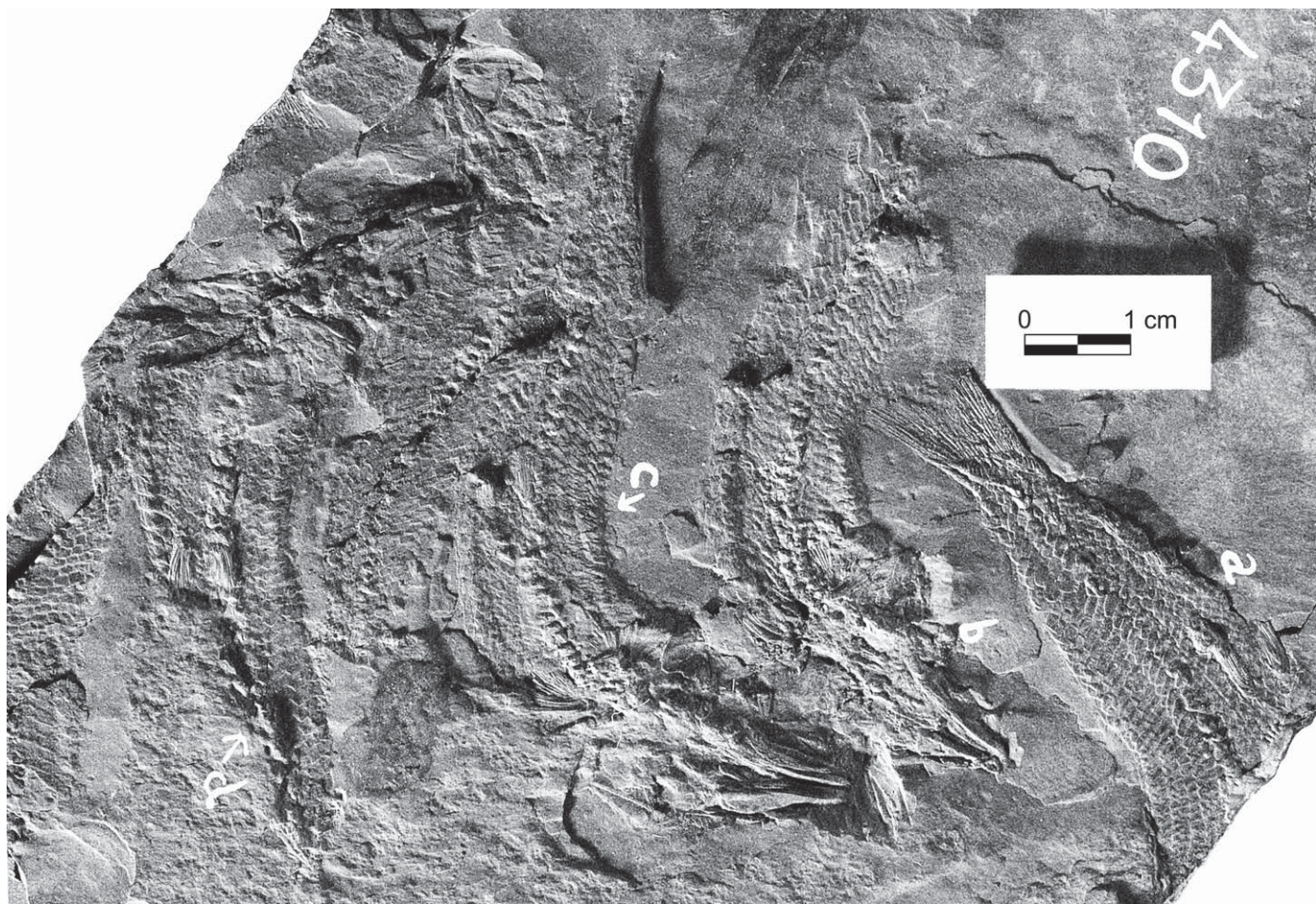


FIGURE 8. *†Pholidophorus gervasutti* Zambelli (MCSNB 4310a-d) from Ponte Giurino near Bergamo, northern Italy. Photograph of a group of specimens exemplifying the mass mortality event characterizing the locality.

pterygiophores are obscured by the presence of the squamation in most specimens; only in a few specimens where the scales are damaged, removed, or displaced is study possible on portions of the vertebral column.

Exemplars of *†Ph. gervasutti* are small, reaching about 70 mm SL, with a maximum total length of about 82 mm. The fishes have elongated bodies, with their maximum depth in the predorsal region. The snout length is short, being about 20–23% of the head length. The head is about 29–32% standard length, with relatively large eyes, which have a diameter of about 28–30% head length. The head is almost triangular in shape, with its deepest points at the posterior end of the cranial roof. The caudal peduncle is moderately narrower than the rest of the body. The pelvic and dorsal fins are positioned slightly posterior to the mid-length of the body. The pectoral fins are positioned nearer the ventral margin of the body than to the middle region of the flanks. The dorsal fin origin is almost at the level anterior to that of the pelvic fins. The anal fin is opposite and posterior to the base of the dorsal fin, almost midway between the pelvic fins and caudal fin. All fins are small, with very delicate and slender rays that have elongate fringing fulcra associated with their leading margins.

External cranial dermal bones, dermal bones of the pectoral girdle, and scales are covered with a thick layer of ganoin ornamentation.

mented with patches of tubercles of different sizes that are not positioned equidistantly from one another (e.g., Figs. 9, 10, 11). The maxilla and supramaxillae bear longitudinal ridges, as well as tubercles of different sizes arranged linearly. The detection of pores of the cephalic sensory canals and pit-lines grooves is difficult due to thick ornamentation. Cephalic sensory canals, tubules, and/or pores are observed in specimens with the layer of ganoin weathered away.

Braincase—The braincase seems to be short; its posterior margin reaches the level of the anterior margin of the opercle. With the exception of the skull roof bones and pieces of the parasphenoid, no elements of the lateral and ventral walls of the braincase are observed. The remains of the parasphenoid (Figs. 9, 10A) are uninformative.

Skull Roof—The skull roof lacks crestae or fontanelles, and its surface is uneven due to the ornamentation. The skull roof (Figs. 7C, 9, 10A, B, 11, 12, 13) is very narrow anteriorly, ending in an acute tip. From this point, the width of the skull roof increases posteriorly, being very broad at the level of the posterior corner of the orbital margin. This breadth is maintained in the postorbital region (Figs. 11, 12). The breadth of the skull roof in front of the posterior margin of the nasal bones is about five times narrower than that of the postorbital region. The surface of

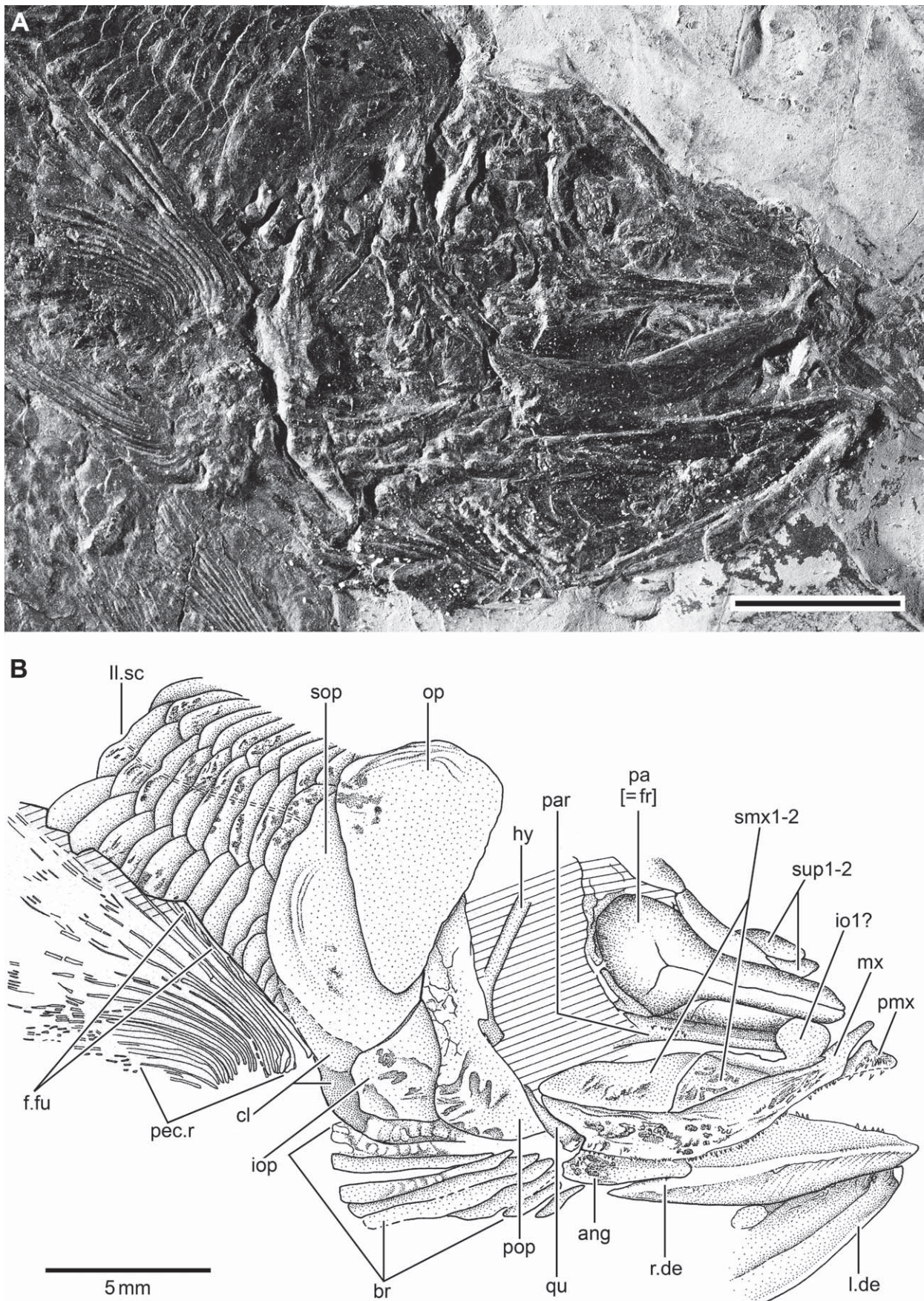


FIGURE 9. *†Pholidophorus gervasutti* Zambelli (MCSNB 4303b). **A**, photograph of head and anterior part of body in right ventrolateral view. Scale bar equals 5 mm. **B**, drawing of **A**. Hatched lines indicate broken bone surface.

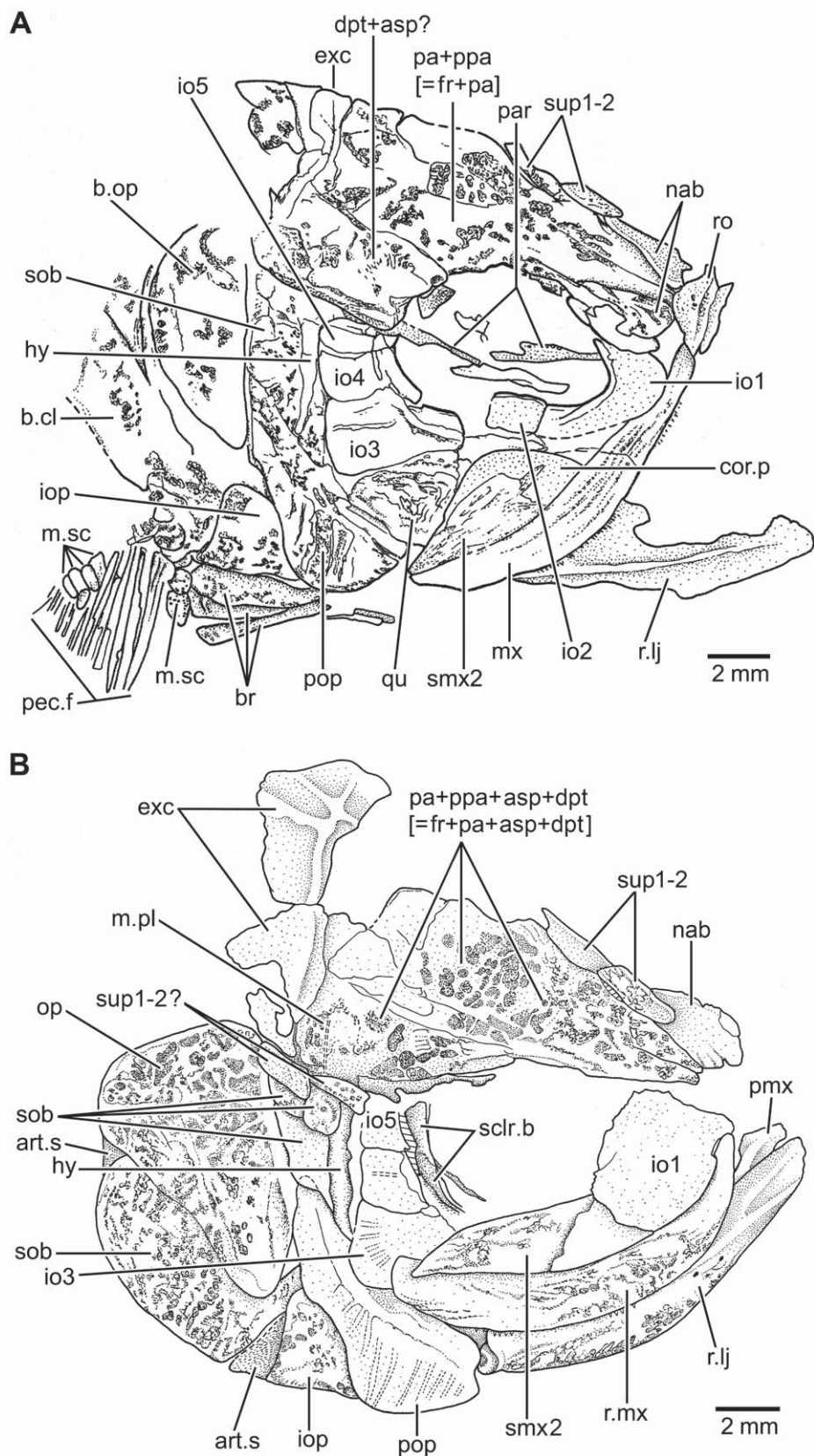
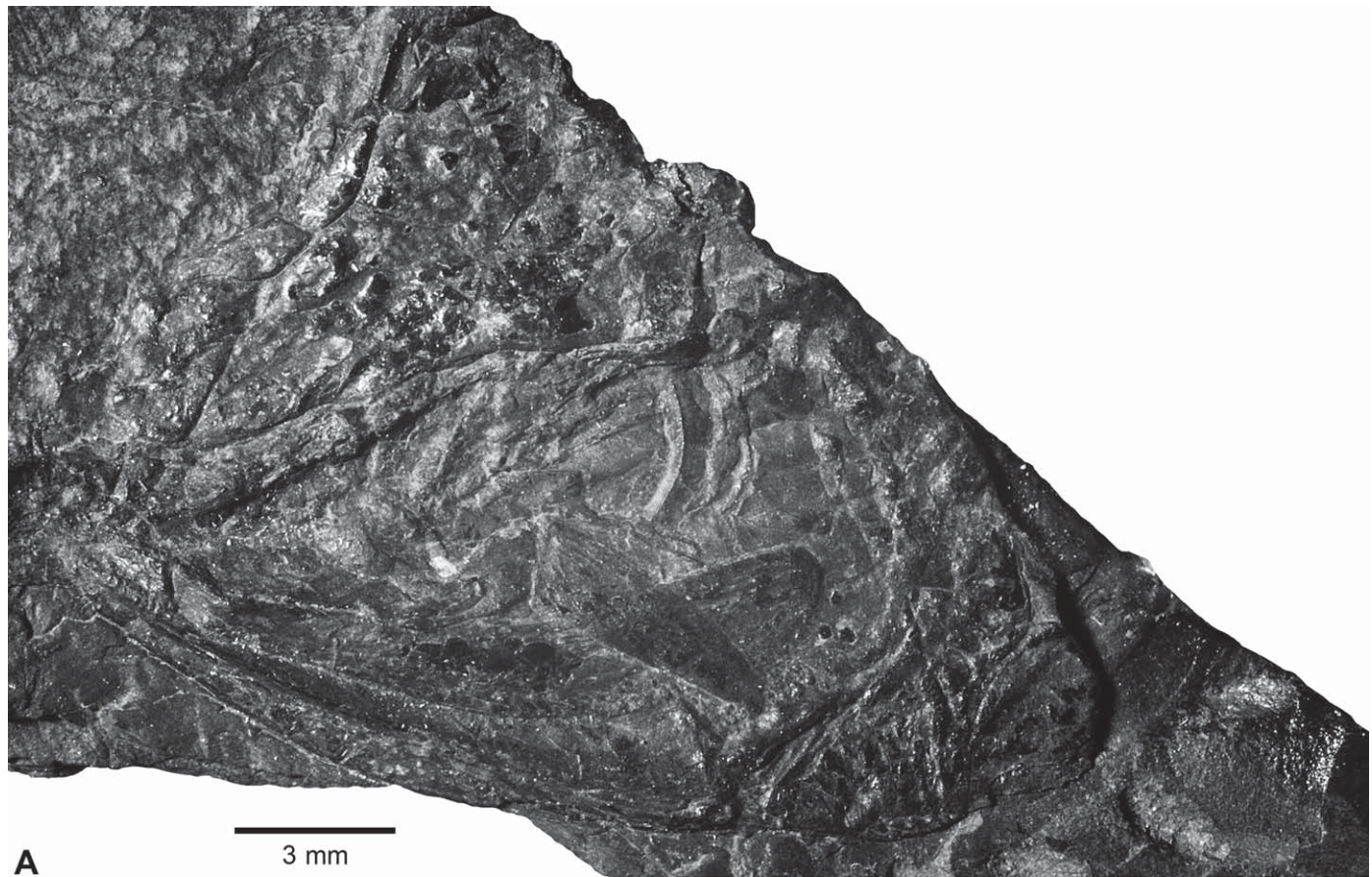


FIGURE 10. \dagger Pholidophorus gervasutti Zambelli. Drawings of crania in dorsolateral view. **A**, MCSNB 4340d. **B**, MCSNB 4346a.

**A**

3 mm

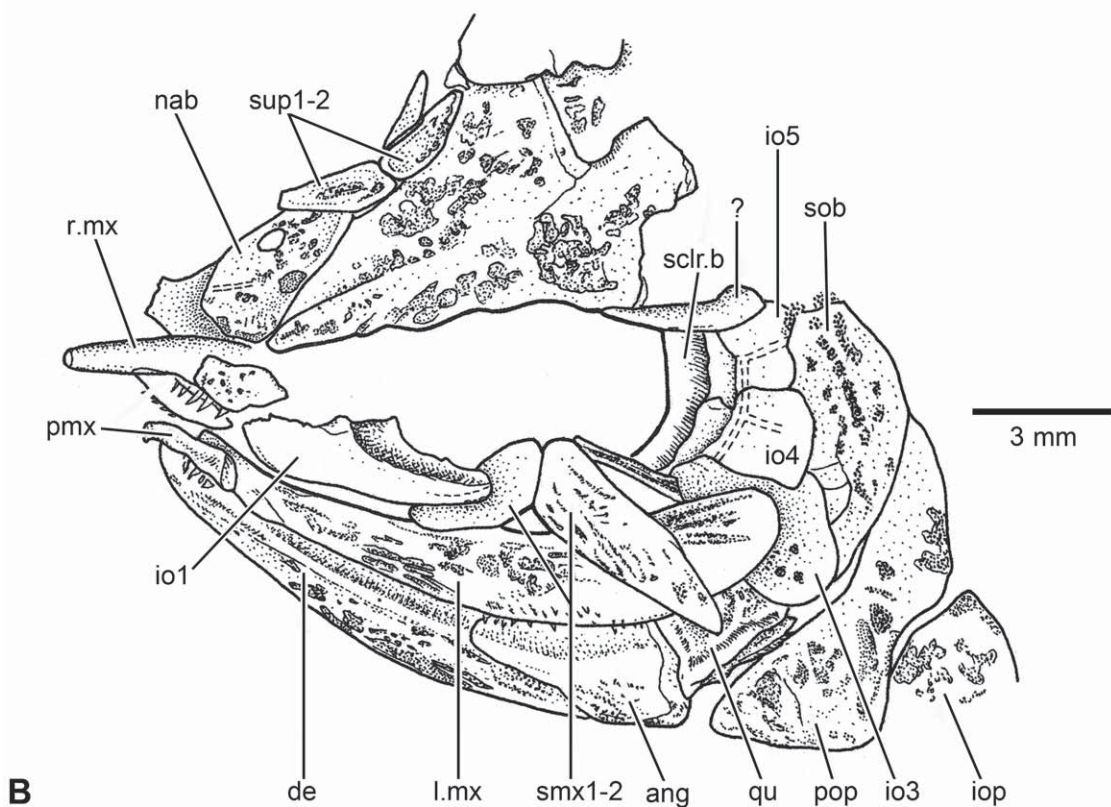
**B**

FIGURE 11. *†Pholidophorus gervasutti* Zambelli. **A**, photograph of cranium of specimen MCSNB 4311 in left dorsolateral view. **B**, drawing of the same specimen.

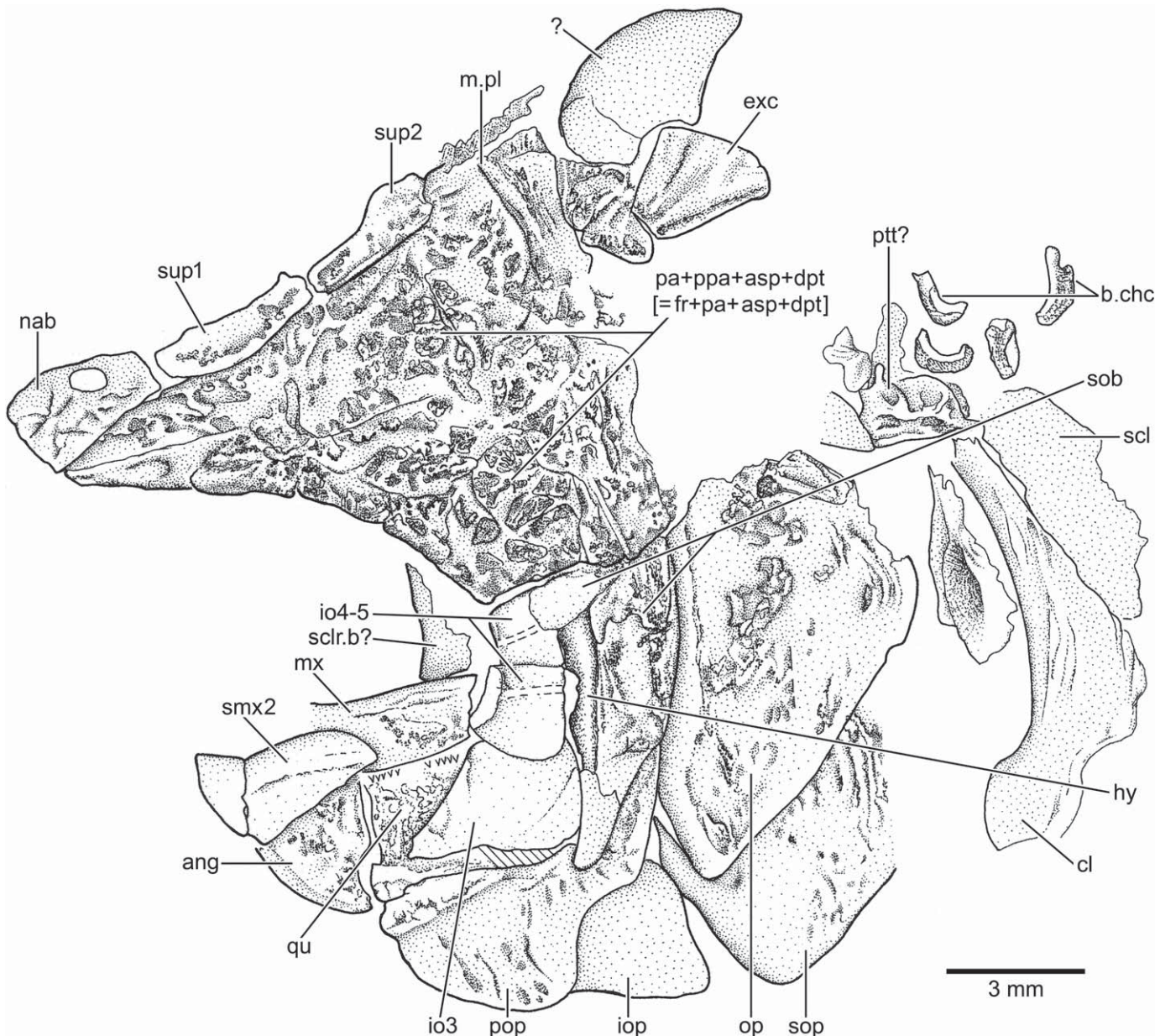


FIGURE 12. *†Pholidophorus gervasutti* Zambelli. Drawing of cranium, vertebral remnants, and pectoral girdle of specimen MCSNB 4317b in left dorsolateral view.

The cranial roof is completely covered with tubercles of ganoine (Figs. 10, 11, 12), which makes it difficult to identify sutures. However, the layer of ganoine is weathered away in some specimens so that bone surfaces are visible, providing good information concerning skull roof fusion. There is the tendency for the skull roof bones to fuse, with the exception of the anterior tips of both parietals [=frontals], which are divided in all skull roofs of *†Ph. gervasutti*. The anterior tips of the parietals (Figs. 9B, 10A, 11, 12, 13A–D) are usually asymmetrical in size so that the contact between the rostral and parietal bones is narrow and weak.

There is no evidence concerning the trajectory of the supraorbital canal or its pores because ornamentation obscures them. Where the layer of ganoine has been weathered away, they are

not observed either, with the exception of a small section of the canal in the holotype (Fig. 7C). Except for a section of the otic canal (Fig. 11A, D), no vestiges of other canals are observed either. A middle pit-line groove (Figs. 7C, 10B, 11A, B) is preserved in some specimens, and it ends near the lateral margin of the skull roof plate in the position where the dermopterotic would be. I have not observed anterior or posterior pit-line grooves, but their trajectories could be obscured by the ornamentation.

A median, well-developed, slightly rhomboidal rostral bone (Figs. 7C, 10A, 13C, 14A, B) occurs at the anterior-most region of the skull roof plate. The rostral has a bony anterior platform with an almost straight anterior margin (Figs. 10A, 11C, 14B), but part

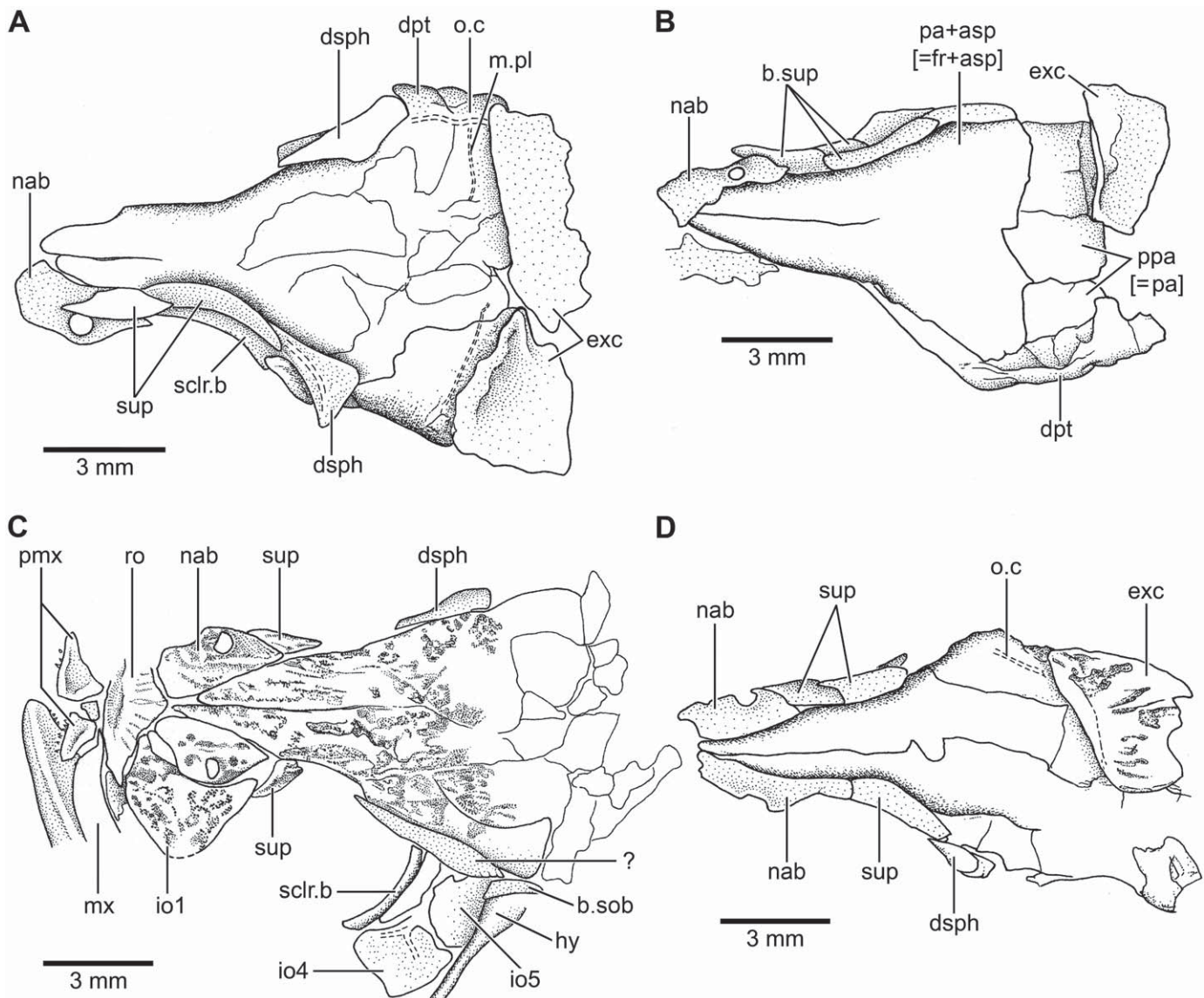


FIGURE 13. *†Pholidophorus gervasutti* Zambelli. Drawing of skulls in dorsal view. **A**, MCSNB 4773. **B**, MCSNB 3462. **C**, MCSNB 4346d. **D**, MCSNB 3462c.

of this anterior platform is broken in MCSNB 4346d (Fig. 11C). There are two well-developed lateral processes, which extend laterally to the anterior margin of the nasal bones. A comparatively large, triangular posterior region contacts the tips of the skull roof plate at the median plane and along the nasal bones laterally. The rostral bone anteriorly overlies the rudimentary ascending process of the small premaxilla. Apparently, the posterior articulation between the rostral and nasal bones is weak, because the rostral is usually displaced or lost. The ethmoidal or rostral commissure crosses the rostral from one lateral process to the other. No pores that could be associated with the commissure are observed on the surface of the rostral. It is unclear whether the ethmoidal commissure joins the anterior branch of the infraorbital sensory canal of the antorbital or not, because the few poorly preserved antorbital bones are displaced.

There are two large, slightly rectangular, plate-like nasal bones (Figs. 7C, 10, 12, 13). Their shape varies slightly, but the bone is

commonly broader anteriorly than posteriorly, projecting laterally to the skull roof plate and to the lateral margin of supraorbital 1, which is narrower than the nasal. The anterior margin of the nasal is usually straight or convex. The medial margin is almost straight, and the posterior margin may be straight or the bone may end in an acute tip. The lateral margin may be laterally notched at its anterior end, which forms part of the border of the anterior nostril. The rounded or oval foramen positioned close to the lateral margin represents the posterior nostril. Consequently, both nostrils were very close to each other. The supraorbital sensory canal (Fig. 7C) is closer to the medial margin of the nasal bone than to the lateral margin, as can be seen in the holotype.

There is no evidence of a supraoccipital bone, as is the condition described here for all other Triassic species. There is also no discernable evidence of chondral ossification. The dermal skull roof plate ends almost in a straight line at the posterior margins of the dermopterotic and postparietal bones.

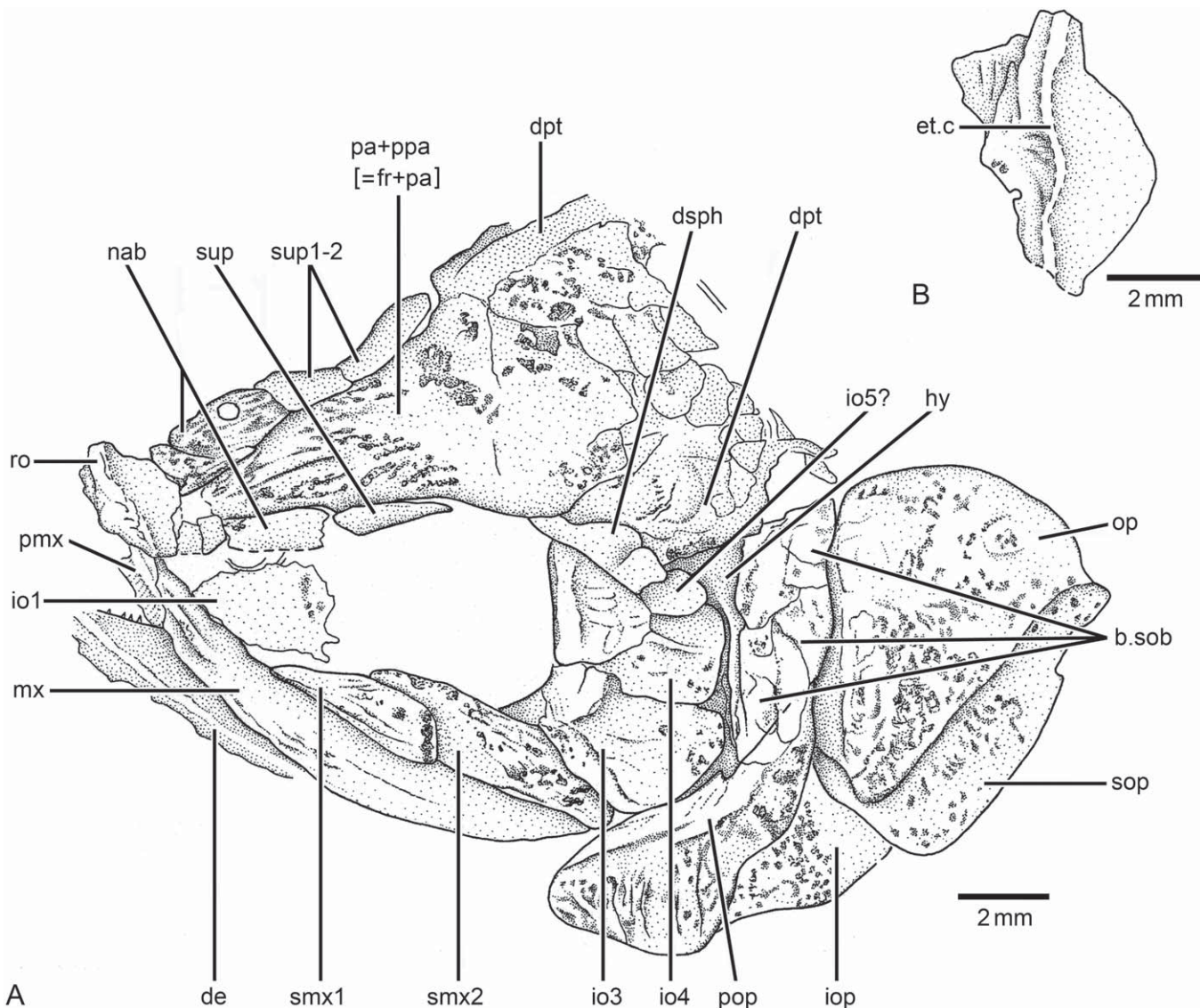


FIGURE 14. *†Pholidophorus gervasutii* Zambelli. A, drawing of cranium of specimen MCSNB 3406b in left dorsolateral view. B, enlargement of rostral bone.

Two large, roughly triangular, paired extrascapular bones (Figs. 10A, B, 12, 13A, B, D) cover the posterior region of the skull roof plate, just overlapping the posterior margin where the postparietals and dermopterotic would end. The extrascapulae are broken in most specimens, but according to the available information, each extrascapula has a slightly curved anterior margin, whereas its posterior region seems to be slightly triangular. The extrascapular canal or supratemporal commissure is nearer to the anterior margin than to the middle region of the bone and has a few sensory tubules extending posteriorly.

Although Zambelli (1980a:8, 16) recognized a tendency of the skull roof bones to become fused, describing it as the “fronto-parieto-dermopterotic,” he illustrated the three elements as separate bones (his fig. 2). Complete restorations of the supraorbital and otic canals, including pores and sensory tubules, can also be seen in the restorations of Zambelli (1980a:figs. 1 and 2). I have been unable to verify the suggested trajectory of both canals or

their pores, even in specimens with the ganoine removed, with one exception showing partial sections of the supraorbital and otic canals, as noted above.

Circumorbital Series—The circumorbital ring consists of one to three (commonly two) supraorbitals, one antorbital, five infraorbitals, and one dermosphenotic. Together with a skull roof element, the nasal bone, the circumorbital series completely surrounds each orbit. *†Pholidophorus gervasutii* has one large suborbital and one or two accessory suborbitals. All these bones, with the exception of the accessory suborbitals, are consistently present, but a certain degree of variation is observed for some of them (see description below). In addition, sclerotic bones are present.

Commonly, two elongate thick bones are lateral to the orbital margin of the skull roof plate and lie between the nasal bone anteriorly and dermosphenotic posteriorly. They are supraorbitals 1 and 2, but some specimens have only one elongate

supraorbital, whereas others have three; this variation is bilaterally asymmetrical.

Supraorbital 1 (Figs. 7C, 10A, B, 11, 12, 14A) is commonly roughly rectangular. It joins the posterior margin of the nasal bone anteriorly and the supraorbital 2 posteriorly; the posterior margin of supraorbital 2 joins the anterior tip of the dermosphenotic laterally. In a few specimens, a third, slightly triangular element may be present. Zambelli (1980a:fig. 1) interpreted this tiny element as an additional dermosphenotic, which he illustrated as a narrow fusiform element positioned anteroventral to the dermosphenotic. In light of the smaller sizes of supraorbitals 1 and 2 when this third element is present, the lack of sensory canals, and its position on the dorsal orbital margin, I identify it as a third supraorbital.

The dermosphenotic and supraorbitals are in direct contact, but a separation exists between the antorbital and supraorbital 1, and this space is filled by the lateral wall of the nasal bone.

The antorbital is lost or partially destroyed in many specimens. I am not able to provide an appropriate description of this bone, but it seems to be quite variable in size and shape. It is not as large as illustrated in the restoration of Zambelli (1980a:fig. 1).

Infraorbital 1 (Figs. 7C, 10A, B, 11, 14) is the largest bone of the infraorbital series, being uncommonly large in some specimens (e.g., Fig. 10B). Its shape may be rounded, rectangular, or triangular. The infraorbital sensory canal, partially seen in a few specimens, is positioned close to the ventral margin of the bone. Although the antorbital, infraorbital 1, and infraorbital canal (pores and tubules) are completely restored in Zambelli (1980a:fig. 1), I have been unable to find support for such a restoration in the available material.

Infraorbital 2 (Figs. 7C, 10A) is commonly a narrow, rectangular bone. The infraorbital sensory canal and its pores are not observed due to the fact that the external surface of the bone is ornamented with tubercles and ridges of ganoine that obscure any pores.

Infraorbital 3 (Figs. 7C, 10A, B, 11, 12) is almost rhomboidal, with a slightly concave anterior margin. In some exemplars, infraorbital 3 has almost straight dorsal and ventral margins, but in others the ventral margin is oblique. It is notable that the posterior margins of infraorbitals 3, 4, and 5 end almost at the same level. Consequently, infraorbital 3 is short and does not project posteriorly; together with infraorbitals 4 and 5 it just covers the anterior margin of the suborbital. This is a completely different arrangement of infraorbitals 4 and 5, which are smaller in *†Pholidophorus latiusculus* and other species described below. Infraorbital 3 contacts infraorbital 2 anteriorly, the suborbital posteriorly, and infraorbital 4 dorsally. The infraorbital sensory canal—enclosed by bone—is close to the orbital margin, and at least one long sensory tubule has been observed, contrary to the restoration by Zambelli (1980a:fig. 1), which shows five tubules of different sizes. A pit-line groove (anterior division of the supramaxillary pit-line) has been observed in some specimens.

Infraorbitals 4 and 5 (Figs. 7C, 10A, B, 11, 12, 13) are small, slightly square- or rectangular-shaped bones carrying the infraorbital canal close to their orbital margin. Both infraorbitals contact the suborbital posteriorly, and infraorbital 5 contacts the dermosphenotic dorsally and the accessory suborbital posteriorly.

The moderately large and triangular-shaped dermosphenotic (Figs. 7C, 13A, C, D, 14) is placed posterior to supraorbital 2 or 3, when the latter is present, anterolateral to the posterior corner of the dorsal orbital margin, and dorsal to infraorbital 5. The dermosphenotic does not fuse to the underlying skull roof plate and may extend posteriorly over its lateral margin, where it may contact the accessory suborbital. The dermosphenotic lacks well-defined processes, and it can be interpreted as type Ib in Poplin's (2004) classification of dermosphenotics (type Ib: dermosphenotic extends more or less over the orbit). The infraorbital and otic canals join in the dermosphenotic. There is no

evidence that the supraorbital canal joins the other two canals in the dermosphenotic.

The anterior and posterior sclerotic bones (Figs. 7C, 10B, 11) form a ring surrounding the eyeball, and dorsal and ventral sutures are visible.

One large suborbital (Figs. 10A, B, 12) occupies the space between the posterior margins of infraorbitals 3, 4, and 5 anteriorly, and the opercle and preopercle posteriorly. The suborbital has an almost straight margin dorsally, ending in an acute tip ventrally so that the bone appears as an elongate triangle in many specimens, an unusual shape among the species described here. A thick layer of ganoine with tubercles irregularly distributed covers the suborbital.

Commonly a small, triangular and narrow or ovoid accessory suborbital bone (Figs. 10B, 11, 12) is present dorsal to the large suborbital bone and lateral to the dermopterotic region of the skull roof plate and may extend posteriorly onto the opercle. Occasionally, a second small accessory suborbital is present overlying partially the anterior margin of the opercle. Both bones have their surfaces covered with tubercles of ganoine.

Upper Jaw—The upper jaw is composed of paired premaxillae and maxillae, and two supramaxillae on each side. The external surface of the maxilla and the supramaxillae are covered by a thick layer of ganoine, which is ornamented with irregular longitudinal ridges of ganoine of different lengths and tubercles of different sizes. Premaxillae are covered mainly by ganoine tubercles.

The premaxilla (Figs. 10B, 11, 13C, 14) is displaced in most specimens and is incompletely preserved. The bone is small, slightly triangular and with a very short ascending process; there is no evidence of a postpremaxillary or nasal process as the one present in amiiforms and parasemionotiforms. Tiny, conical teeth are placed on the oral margin of the bone. It is uncertain whether a single row of teeth or more teeth are present. A rostrodermethmoid has not been observed in any specimen, from which I conclude that it is absent.

The gently curved maxilla (Figs. 7C, 9, 10, 11) is as long as the lower jaw or slightly longer, with a moderately long articular process at its anterior end. The maxillary blade is shallow, becoming slightly deeper distally. The dorsal margin of the bone is slightly concave or almost straight in different specimens, whereas its ventral margin is gently convex at mid-length. The dorsal margin does not possess a well-defined supramaxillary process, but it has a narrow articular surface where the supramaxillary bones lie. The posterior margin of the maxilla is rounded in a few specimens (see Figs. 7C, 10B, 11), but it is notched in others (Fig. 9). Apparently, the rounded condition is the most common one, but I note that the posterior margin of the maxilla is completely preserved in only a few specimens, but damaged in many. A single row of very small conical teeth is present on the oral margin of the blade, ending just before the posterior margin of the bone (e.g., MCSNB 4311).

Two supramaxillary bones (Figs. 7C, 9, 10, 11, 12) cover the posterodorsal margin of the maxilla, just posterior to the rudimentary supramaxillary process. Both bones together represent about 75–80% of the length of the maxillary blade. Supramaxilla 1 is a slightly oval or fusiform bone and is about the half the length of supramaxilla 2. Supramaxilla 2 is a large and deep bone, with its maximum depth equal or even deeper than that of the maxilla. Its well-developed anterodorsal process overlaps half of the dorsal margin of supramaxilla 1 in the holotype, but it may be shorter in other specimens. Its posterior tip may be slightly acute or rounded and gives a gently sloped profile to both posterior tips of supramaxilla 2 and maxilla. Zambelli (1980a:fig. 1) restored supramaxilla 1 as a small element, about one-third of the length of supramaxilla 2, but both bones are of similar length in the holotype (Fig. 7C), and in other specimens supramaxilla 1 is about the one half the length of the supramaxilla 2 (Fig. 9).

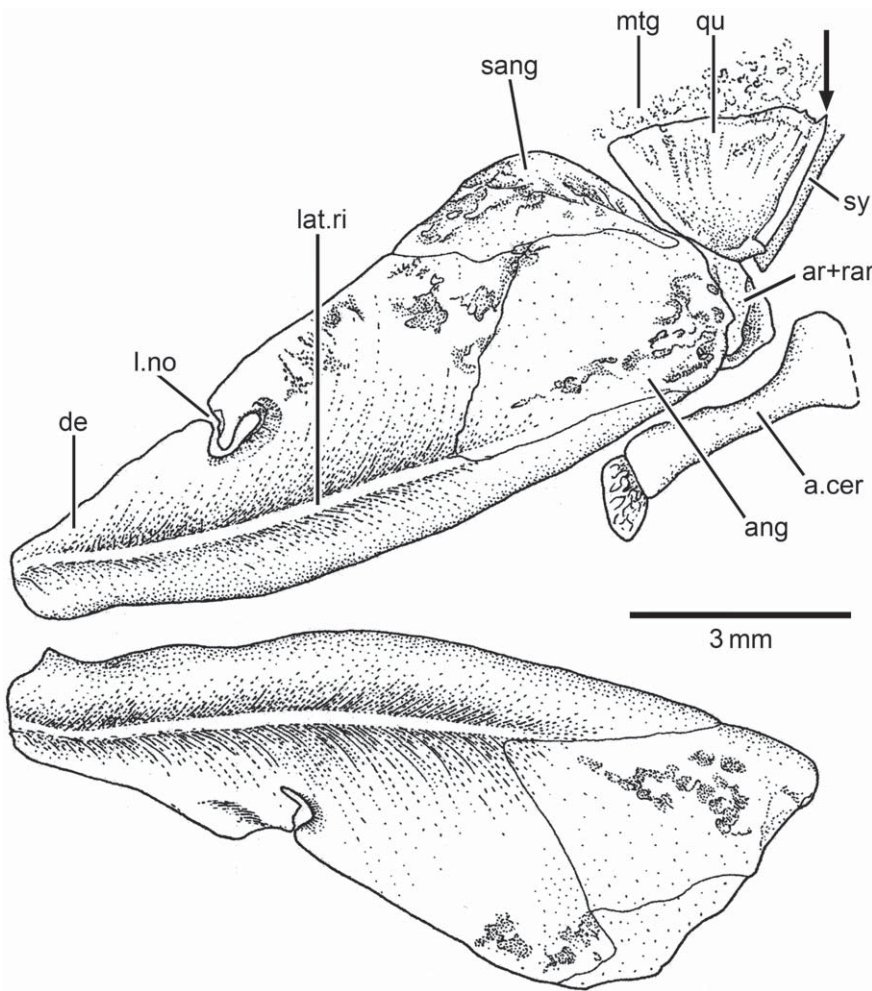


FIGURE 15. *†Pholidophorus gervasutti* Zambelli. Drawing of lower jaws, part of the suspensorium, and ceratohyal in ventral view with lateral surfaces exposed (MCSNB 4302). Arrow points to a tiny process.

Lower Jaw—The lower jaw (Figs. 10, 11) in many specimens is damaged or covered by the maxilla so that only the anterior part of the jaw and its ventral region are visible. However, the complete jaw (Figs. 15, 16, 17B) is observed in a few specimens. Laterally, each jaw is composed by the dentary, surangular, and angular. The dorsal margin of the jaw ascends in a linear fashion, with its highest point in the middle of the surangular. It then decreases abruptly posteriorly. A curiously shaped ‘leptolepid’ notch, similar in shape to that present in some Late Jurassic ‘pholidophoriforms’, is located at about the first third of the jaw (Fig. 15). Commonly,

the oral margin of the dentary is broken and the notch appears as a broad indentation (Fig. 16A), but this is an artifact of preservation. A similarly shaped notch is not present in other Triassic fishes studied here. Dorsal (or dental) and ventral (or splenial) regions of the dentary are separated by a well-developed, distinct lateral ridge protruding along the jaw and becoming inconspicuous in the anterior region of the angular. The anterior dorsal part of the dentary lacks ornamentation, but ridges and tubercles of ganoine are unevenly distributed, even in the surangular region, and are densely distributed in the ventrolateral surface of the jaw.

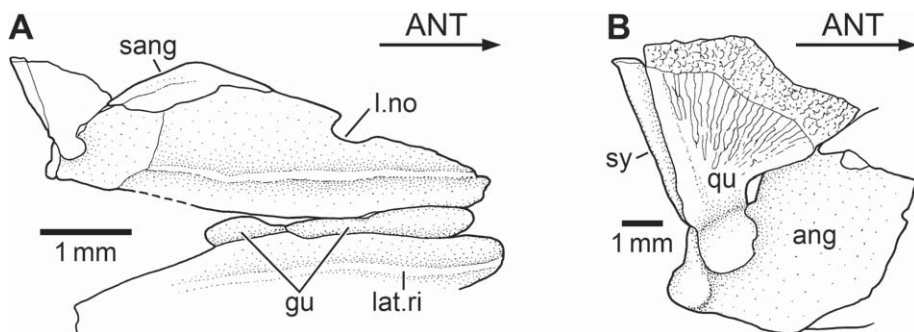


FIGURE 16. *†Pholidophorus gervasutti* Zambelli. **A**, drawing of right lower jaw, quadrate, and symplectic in lateral view, with gular in ventral view (MCSNB 4334). **B**, enlargement of posterior part of right lower jaw, showing its relationships to quadrate and symplectic. See photograph in Figure 17B.

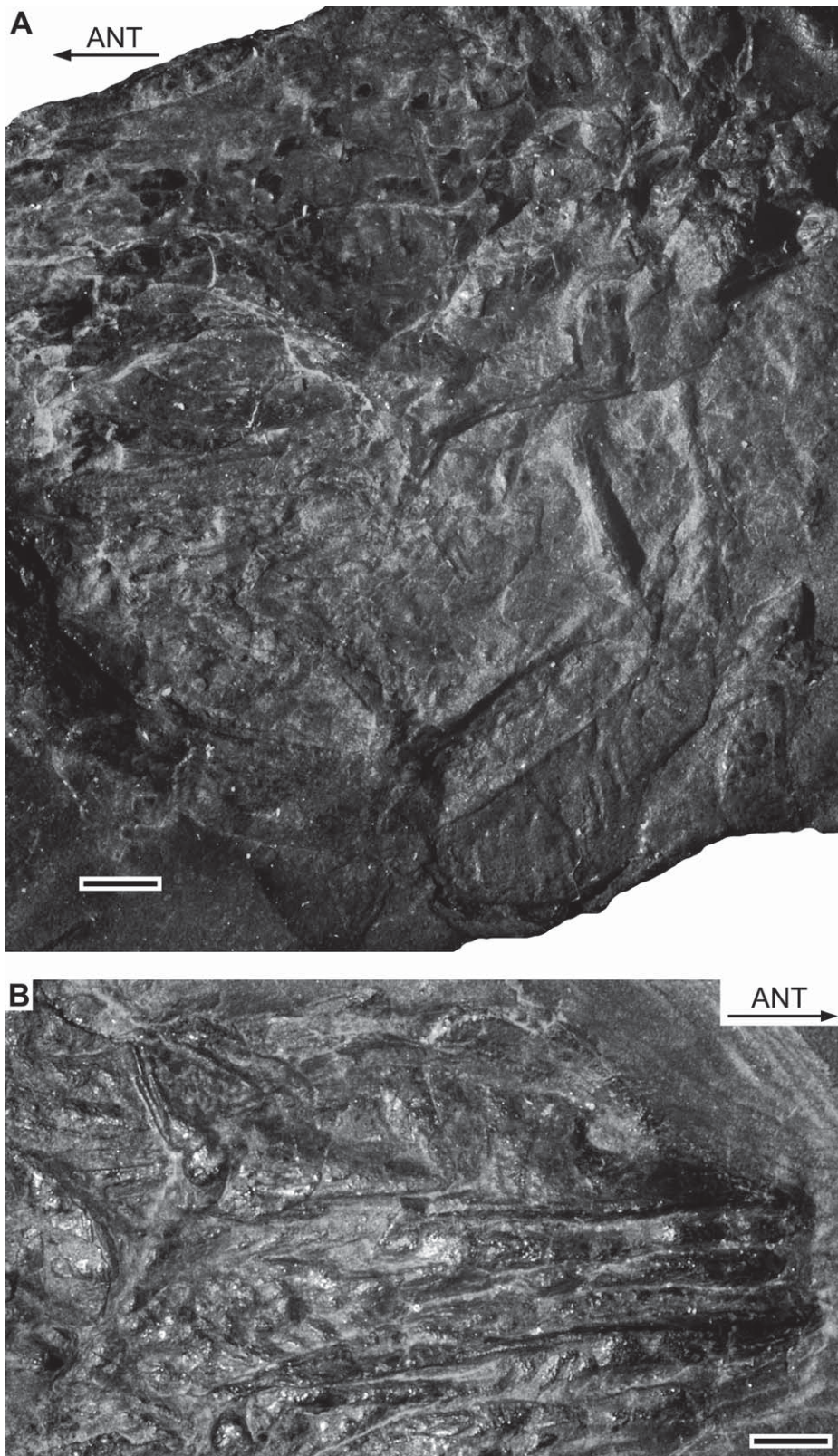


FIGURE 17. *†Pholidophorus gervasutti* Zambelli. **A**, photograph of suspensorium in left lateral view (MCSNB 4425). **B**, photograph of right lower jaw, quadrate, and symplectic in right lateral view, with gular in ventral view (MCSNB 4334). Scale bars equal 1 mm.

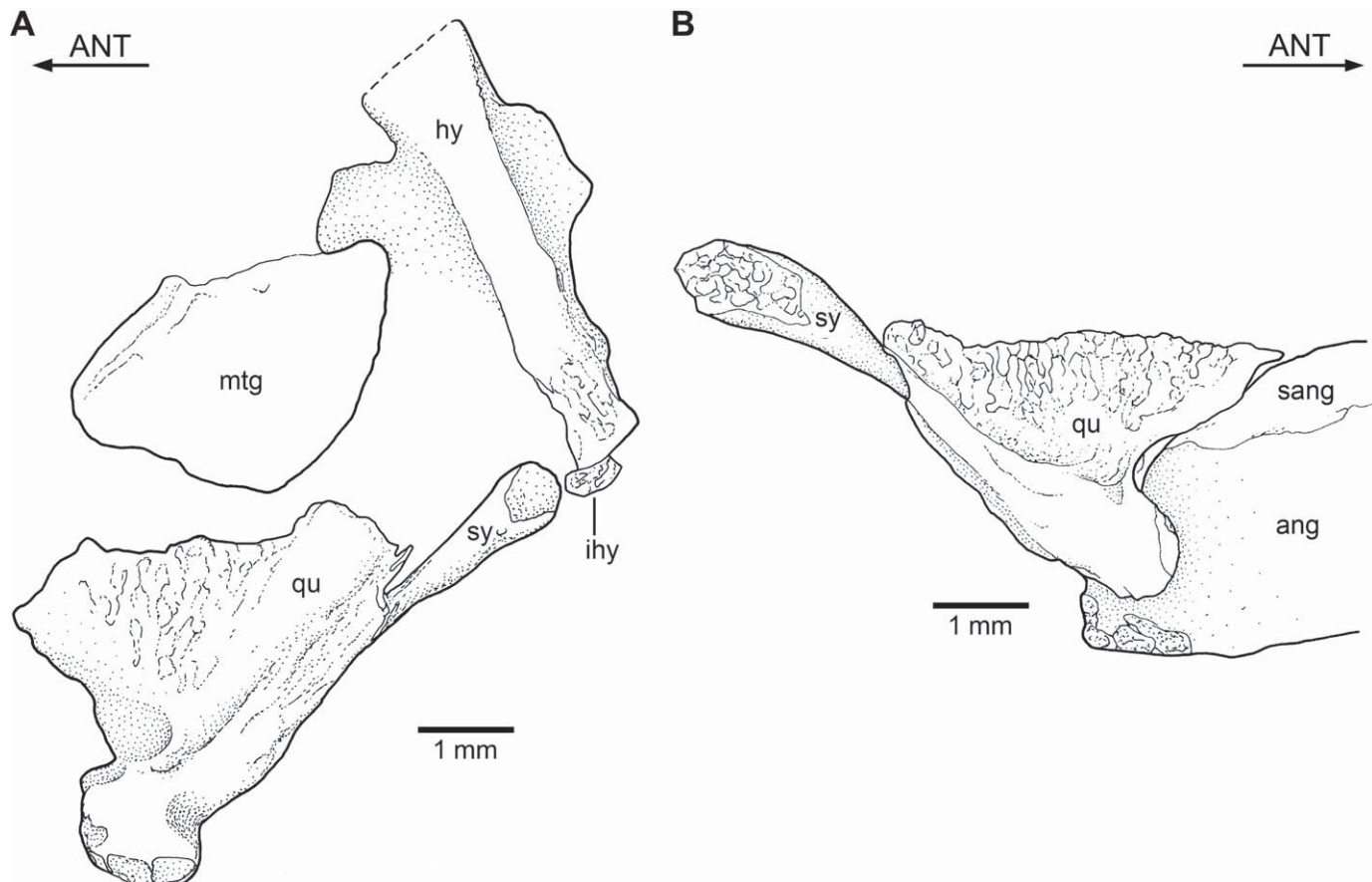


FIGURE 18. *†Pholidophorus gervasutii* Zambelli (MCSNB 4334). A, drawing of left suspensorium in lateral view (MCSNB 4425). See photograph in Figure 17A. B, drawing of posterior part of right lower jaw, quadrate, and symplectic in lateral view (MCSNB 4334).

The dentary (Figs. 7C, 9, 15) forms most of the lower jaw, extending below the angular. Both bones are sutured to each other, and no space is left between them at their ventral margins. The dentary bears very small, conical teeth on its oral margin; however, the teeth are usually damaged or not preserved. Specimen MCSNB 4303b preserves both jaws, with the left one displaced and visible in medial view. There is a small oval bone (Fig. 9) lying close to the oral margin of the left jaw. I am uncertain whether this element is an additional gular, as observed in some species described below (e.g., *†Parapholidophorus*, *†Pholidorhynchodon*).

The angular (Figs. 9, 15, 16B) forms the posteroventral lateral wall of the jaw. A thick layer of ganoin, commonly ornamented with irregularly distributed tubercles of different sizes, covers the angular. An elongate surangular (Figs. 15, 16A), tightly sutured with both the angular and dentary, forms the posterodorsal margin of the lower jaw. Although the surangular is the only element forming the coronoid process in most specimens, a small contribution of the dentary is observed occasionally.

The posterior margin of the jaw (Fig. 15) lacks a postarticular process. A chondral element placed medial to the angular is observed in a few specimens. I interpret this element to be the posterior part of a fused articular and retroarticular based on its position (Fig. 15).

The mandibular sensory canal apparently is positioned below the lateral bony ridge of the jaw. Its trajectory and pores are difficult to observe, but a short, vertical oral pit-line groove is visible

near the posterior corner of the angular. The posterior opening of the mandibular sensory canal is placed medially.

The articulation between lower jaw and quadrate (Figs. 10A, B, 11) is placed below the level of the posterior half of the orbit or slightly posteriorly.

Palatoquadrate and Suspensorium—Commonly, bones of the palatoquadrate and the suspensorium are hidden by bones of the cheek, so that portions of one or the other bone are only rarely observed. The quadrate (Figs. 15, 16, 17A, B, 18A, B) is mainly cartilaginous, except the articular condyle and both the anterior and posteroventral margins, which are heavily ossified. A well-developed posteroventral process is lacking, except in one specimen that has a tiny, acute process (Fig. 15) above the dorsal margin of the bone (Figs. 16, 18A, B). The articulation with the lower jaw involves a saddle-like articular surface, with two expanded lateral and middle regions that produce a strong joint with the jaw.

An elongate, triangular symplectic is positioned at the postero-lateral corner of the quadrate (Fig. 18A, B) in at least two specimens, but apparently it forms part of the articulation with the lower jaw in other specimens (Figs. 15, 16). The symplectic is narrow ventrally and expanded posterodorsally, retaining a considerable amount of partially ossified bone at its articulation with the hyomandibula. A small, partially ossified element is placed at the contact between the symplectic and hyomandibula. This element is interpreted here as the interhyal. There is no evidence of a quadratejugal.

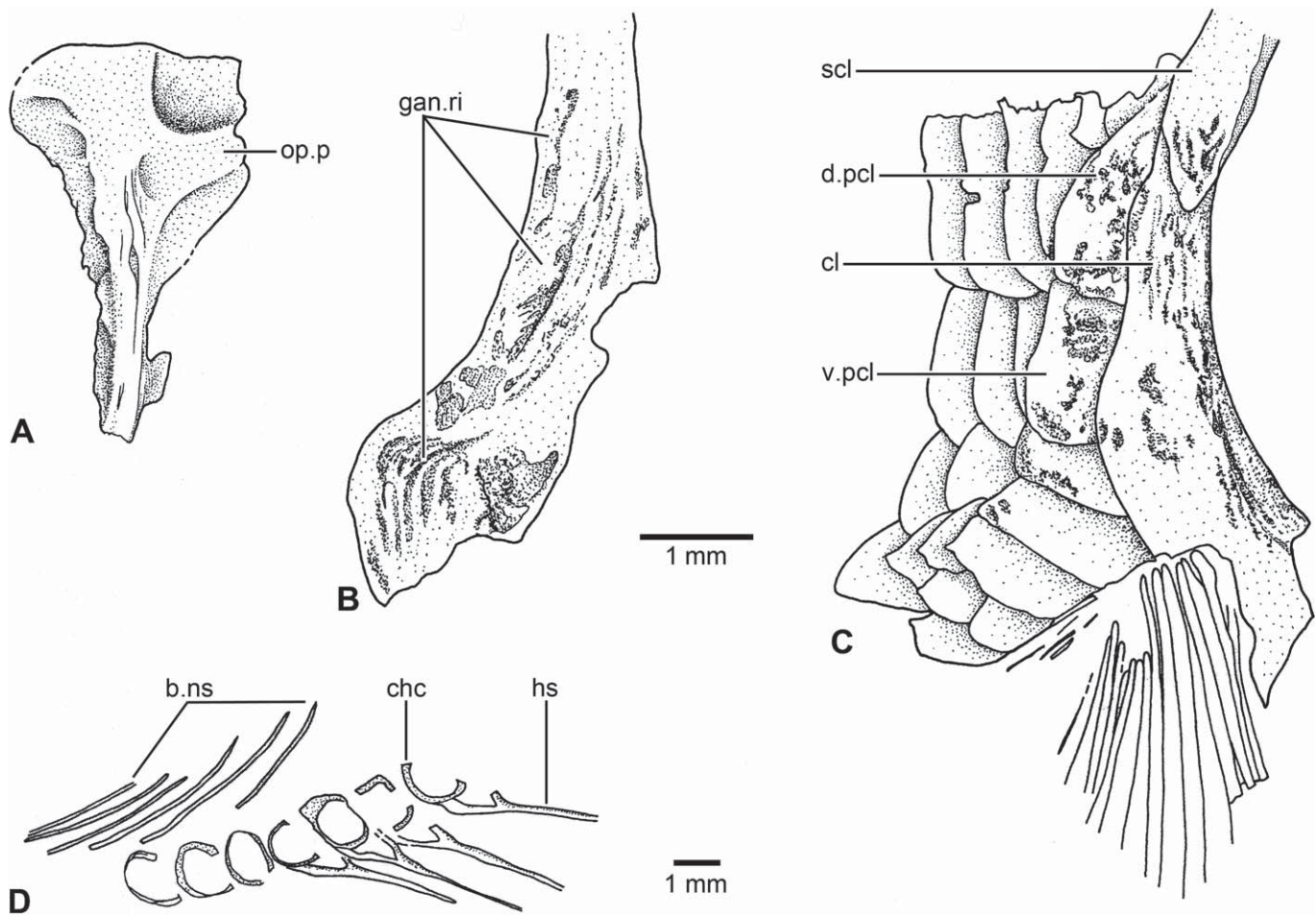


FIGURE 19. *†Pholidophorus gervasutii* Zambelli. **A**, left hyomandibula in lateral view (MCSNB 4448c). **B**, left cleithrum in lateral view (MCSNB 4305). **C**, part of right dermal pectoral girdle and scales in lateral view (MCSNB 4438). **D**, portion of vertebral column in right lateral view with chordacentra slightly displaced (MCSNB 10651b). Scale bar applies to **A–C**.

Apparently, the metapterygoid (Figs. 15, 17A, 18A) remains as a cartilaginous element in adult specimens. This statement is supported by the fact that an ossified bone has not been observed in the available specimens, but remnants of cartilage are dorsal to the quadrate (e.g., MCSNB 4303). It is notable that the entopterygoid has not been observed in any specimen. It could have been a very small bone that was covered by the infraorbitals, or it was so thinly ossified that is not preserved. An ectopterygoid has not been observed either.

Although the suborbital and dorsal part of the preopercle cover the hyomandibula laterally, it is possible to observe part of the hyomandibula when the suborbital is displaced or missing. The hyomandibula is partially preserved in some specimens (e.g., Figs. 17A, 18A, 19A). The hyomandibula has a well-developed dorsal margin and apparently has only one facet to articulate with the braincase. The bone is comparatively narrow ventrally, but is expanded in its antero- and posterodorsal regions, which are separated by the main shaft of the bone, which is perichondrally ossified. Between the main shaft of the hyomandibula and the posterior process for the opercle is a dorsally positioned, thinly ossified region. Another thinly ossified region is positioned ventral to the opercular process. Both regions seem to be formed by membrane bone, as well as the anterior expansion of the

hyomandibula. It is unclear whether a preopercular process at the posterior margin of the hyomandibula is present, because a small slightly rectangular bony projection at the posteroventral margin preserved in one specimen is missing in the others. A preopercular process has not been observed in other species studied here. The main shaft of the hyomandibula is heavily ossified. It is slightly inclined posteroventrally with respect to the skull roof bones.

Hyoid Arch—The anterior ceratohyal (Fig. 15) is tube-like, very delicate with only one articular surface anteriorly, and slightly expanded posteriorly. In front of the bone is a cartilaginous, partially ossified element that may correspond to the anterior articular cartilage of the ceratohyal (as in amiiforms; Arratia and Schultze, 1990; Grande and Bemis, 1998), or it may be the hypohyal. Considering the information from other pholidophorids, I identify this element as an unossified hypohyal.

Opercular, Branchiostegal Series, and Gular Plate—The opercular bones (Figs. 9, 10B, 13) are placed posterior to the margin of skull roof plate (the portion corresponding to the dermopterotic). A thick layer of ganoin that is heavily ornamented covers the opercular bones, as well as the branchiostegals. The posterior margins of the opercle and subopercle produce a gently rounded profile of the opercular apparatus that is notched at the articulation between both bones.

Although the preopercle (Figs. 9, 10, 11, 12, 14) shows variation in its shape and size, generally it is expanded ventrally and narrows slightly dorsally. A marked distinction between dorsal and ventral arms is missing, but there is a gentle inclination of the anterior margin from dorsal to ventral direction. Anteriorly, the anteroventral margin may present an acute notch where the preopercular canal exits the bone. This notch has differences in size but it gives the preopercle the shape of an inverted heart. In a few specimens the notch is absent, so that the anteroventral region of the preopercle is rounded. The posterior preopercular margin can be interpreted as having two arms due to the presence of a deep, large notch where the large interopercle abuts. The dorsal part of the preopercle is usually not observed because it is covered by the suborbital, but in the holotype the bone is completely exposed, revealing that the dorsal arm is short and the dorsal margin of the bone is quite distant from the lateral margin of the dermopterotic region of the skull roof plate. The anterior margin of the preopercle is partially covered by the suborbital and slightly by the posterior margin of infraorbital 3. Zambelli (1980a:fig. 4) illustrated the variability of the posterior margin of the preopercle and the size of the notch. Despite of the variability that the preopercle exhibits, I have not observed a preopercle with a dorsal arm ending in an acute tip, as was illustrated in the restoration of the head of *Pholidophorus gervasutti* (Zambelli, 1980a:fig. 1).

The anterior region of the preopercle is slightly expanded just anterior to the main course of the preopercular canal. The pathway of the preopercular sensory canal and its tubules is often not visible because of the thick layer of ganoine, but it is exposed in specimen MCSNB 4346a. Seven long tubules are observed in the ventral arm, and three short tubules are present in front of the posterior notch. The long tubules extend closer to the ventral margin rather than to the middle region the bone as illustrated by Zambelli (1980a:fig. 1). The dorsal connection between the preopercular and otic sensory canals has not been observed because the dorsal tip of the preopercle is hidden by the suborbital and opercle in all studied specimens, but a foramen for the exit of the preopercular canal on the lateral wall of the skull roof plate has not been observed either.

The opercle (Figs. 9, 10B, 12, 14) is a large, roughly triangular bone, gently curved at its expanded dorsal margin and slightly larger than the subopercle. The anterior margin of the opercle is markedly thickened and lacks ganoine where the suborbital, the preopercle, and the anterodorsal ascending process of the subopercle abut. The anterior margin is almost vertically oriented but ventrally, in front of the anterodorsal process, it is markedly oblique. The external surface of the bone is densely covered with tubercles of ganoine of different sizes and shapes.

The subopercle (Figs. 9, 10B, 12, 14) is a large bone that is slightly smaller than the opercle. Its posteroventral margin is gently rounded. Its anterior margin is obliquely oriented and extends dorsally as part of the well-developed anterodorsal process of the subopercle. The anterior margin joins both the interopercle extensively and the preopercle by a narrow portion. The anterodorsal process projects dorsally in between the anteroventral margin of the opercle and the posterior margin of the preopercle.

The interopercle (Figs. 7C, 9, 10A, B, 12, 14) is large and well exposed between the posterior notch of the preopercle and the anterior margin of the subopercle, but extends anteriorly medial to the preopercle. The exposed portion of the interopercle is triangular-like, with an acute or slightly rounded dorsal tip and a lightly curved ventral margin. The bone produces a broad articular surface for the anterior margin of the subopercle. The size of the interopercle is unknown because a complete disarticulated bone has not been observed among the available specimens.

There are nine branchiostegal rays preserved in the material illustrated here; however, the most anterior branchiostegals are

missing. Zambelli (1980a) reported that most specimens have incomplete series of branchiostegals rays, or the rays are damaged. He estimated there are 15 rays, and this is possibly correct. The branchiostegals (Figs. 9, 10A) are relatively narrow bones, including the most posterior one, and their lengths increase rapidly posteriorly. As far it can be observed, their exposed surfaces are ornamented.

As with the branchiostegals, the gular plate is not seen in most specimens because it is covered by the jaws. The gular plate (Figs. 16, 17B) is elongate, slightly oval-shaped, and about 50% of the length of the lower jaw.

Vertebral Column and Intermuscular Bones—Only a few elements of the vertebral column can be observed where the scales are displaced or lost (Figs. 7B, 19D). The abdominal region is formed by monospondylous chordacentra, but diplospondylous chordacentra are observed in the caudal region. Although Zambelli (1980a:8) wrote that some vertebrae of *†Pholidophorus gervasutti* were diplospondylous, he later wrote that members of *†Pholidophorus* have only monospondylous vertebrae (Zambelli, 1986). The latter is an incorrect statement, based on the specimens studied here.

In the abdominal region, each centrum is formed by basidorsal and basiventral hemichordacentra, which may become fused and form a thin-walled, ring-like chordacentrum. The neural arches and short spines are mostly not preserved in the abdominal region, but parapophyses, as well as short ribs, are observed in the holotype (Fig. 7B). The parapophyses are autogenous, and because of this they can be easily removed or lost during fossilization. The parapophyses are made of cartilage surrounded by a rim of bone. The thin and slender ribs are incompletely preserved, and some of the last ones are strongly inclined towards the horizontal. The first hemal arch is an expanded, large element mainly formed by cartilage with a thin rim of ossification. The arch bears a thin and slender hemal spine that is completely ossified.

Each mid-caudal centrum is formed by basidorsal and basiventral hemichordacentra and interdorsal and interventral hemichordacentra. The four elements commonly remain separated at their middle region so that a single ring-like centrum is not formed. A few thin, slender neural spines are observed in the caudal region in a few specimens. They are unpaired elements.

No other elements, such as epineurial or epipleural bones, have been observed associated with the vertebral column. They are interpreted as absent in *†Pholidophorus gervasutti*.

Paired Fins—Bones of the pectoral girdle and fins are preserved in many specimens, so that a satisfactory description can be presented. Nonetheless, some elements are obscured by the presence of displaced scales or fragmented. The structure of the posttemporal and the internal chondral elements of the girdle is unknown, and consequently, the number of radials is unknown. The following dermal elements of the pectoral girdle are preserved: supracleithrum, cleithrum, clavicle, and postcleithra. Typically, the bases of the rays are covered with a series of small rhombic or slightly oval scales, and even in the case where the scales are displaced, the radials are not preserved. It is unclear whether they remain as cartilaginous elements or are partially ossified.

The supracleithrum (Fig. 12) is a moderately broad, elongate bone that overlies the dorsal region of the cleithrum and part of the dorsal postcleithrum posteriorly. A thick layer of ganoine covers the supracleithrum. This layer is ornamented with tubercles and ridges of different sizes, which obscure the trajectory of the lateral line. However, following the position of the first scale bearing the lateral line, I can predict that the lateral line existed through the upper half of the supracleithrum.

Often, only a narrow portion of the cleithrum is exposed laterally in some specimens because most of its anterior region is

covered by the opercle and subopercle. The elongate cleithrum (Figs. 19B, C, 20) is almost vertically oriented so that dorsal and ventral arms are not clearly discernible. The dorsal region of the cleithrum is narrow, and the bone expands ventrally, producing a slightly sigmoid posterior margin. It continues as a narrow, short ventral region that ends in an almost abrupt vertical anteroventral margin. This margin articulates anteriorly with the narrow triangular clavicle (Fig. 20), which has a well-defined articular surface for the cleithrum. Its anterior margin is gently rounded, and both bones together produce an almost rounded ventral region of the dermal pectoral girdle. In contrast to the description above, Zambelli (1980a:fig. 1) restored the cleithrum with two well-defined arms and a sigmoid posterior margin, similar to the cleithrum of basal teleosts such as *†Leptolepis*, *†Tharsis*, and others (see below, 'Analysis of Some Morphological Characters Used in Diagnoses and Phylogenetic Analysis').

The anteromedial surface of the cleithrum is covered with long, toothed ridges that give the bone a serrated appearance. In *†Pholidophorus gervasutti*, the serrated ridges (Figs. 19B, C, 20) form a continuous element that is positioned on the surface of the cleithrum, near its medial margin. I am unable to identify them as separate elements because they are united with the surface of the cleithrum. Furthermore, the clavicular elements or serrated appendages differ from the clavicle sutured to the anteroventral part of the cleithrum.

Two postcleithra (Fig. 19C) are behind the cleithrum. The dorsal postcleithrum (Fig. 20) is the largest one and is located posterior to the ventral region of the supracleithrum and posterior to the cleithrum. An almost straight junction is present between the dorsal postcleithrum and the small, squarish ventral postcleithrum. Both bones are covered with a layer of densely ornamented ganoine. As with all species here described, the shape and size of the ventral postcleithrum make it difficult to separate it from the surrounding scales.

The pectoral fins are positioned low in the flank, close to the ventral margin of the body. Each pectoral fin consists of approximately 20 lepidotrichia. The first ray (Fig. 21) is the thickest. It is a compound element fused at least with one short basal fulcrum and a narrow, longer one. The proximal region of the first ray is massive and has an articular cavity. A propterygium is not fused with the base of the first ray. The pectoral rays have long bases; they are segmented and finely branched distally. A series of small, elongate fringing fulcra is associated with the leading margin of the fin. When the fin and scales are in situ, a moderately long, leaf-like pectoral axillary process lies above the insertion of the pectoral fin, just behind the posterior margin of the cleithrum. The proximal region of the axillary process lies on the first pectoral rays, and apparently its distal region was free, as in living fishes.

The pelvic girdles or basipterygia have not been observed because the scales cover them. The origin of the pelvic fin is positioned at the level of the 9th, 10th, or 11th vertical row of scales. The pelvic fins are poorly preserved, but specimen MCSNB 4318b displays both fins (Fig. 22) and surrounding scales. The pelvic fin consists of three to five leaf-like, elongate basal fulcra and 15 or 16 rays. The lateral rays have very long, narrow bases and are only segmented and distally branched. The length of the rays becomes considerably shorter medially, and the most internal rays are very short and thin. A series of small fringing fulcra are associated with the leading margin of the fin. A large, leaf-like (Fig. 22), and well-ossified pelvic axillary process lies at the base of the fin. The proximal region of the pelvic axillary process apparently is fixed to the girdle, because it is always observed in the same position. I assume that its distal region is free, as in the pectoral axillary process, which may have facilitated the flow of the

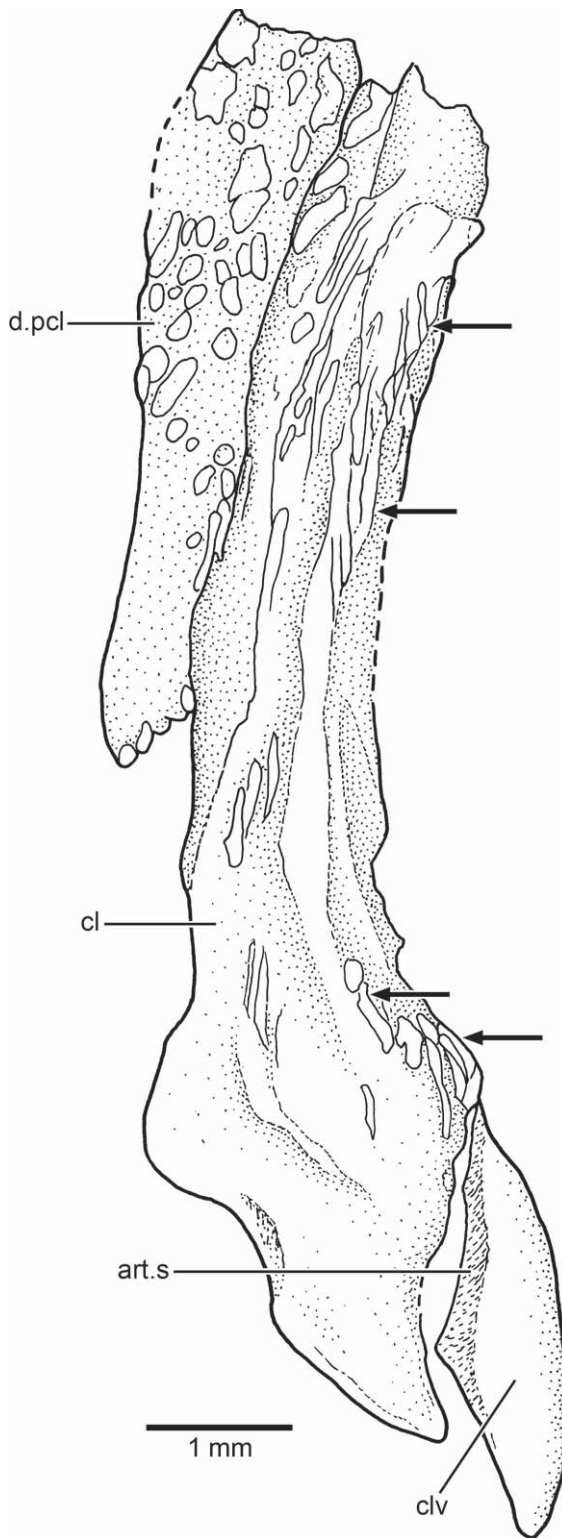


FIGURE 20. *†Pholidophorus gervasutti* Zambelli (MCSNB 4304c). Drawing of part of right pectoral girdle in lateral view. Arrows point to the remnants of the serrated appendage.

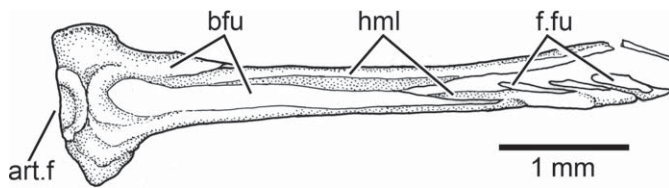


FIGURE 21. *†Pholidophorus gervasutti* Zambelli (MCSNB 4426). Drawing of left first pectoral ray in lateral view.

water along the body, as it does in some recent teleosts (see Arribalzaga, 1997:134, fig. 95). Although not well preserved in specimen MCSNB 4318b, the scales in front and around the base of the fins are slightly modified in shape and are smaller than the scales of the flanks.

Dorsal and Anal Fins—The origin of the dorsal fin is positioned about the level of the 18th vertical row of scales. The unpaired dorsal fin (Fig. 23) has long first principal rays and very short posterior ones, resulting in an almost triangular profile. At least eight pterygiophores, represented by their proximal radials, are preserved in MCSNB 3462b, a specimen with the scales partially removed at the base of the fin. Middle and distal radials have not been observed because these elements were apparently cartilaginous. The first proximal radial (Fig. 23) is bifurcated, with its anterior process shorter than the posterior one. The pterygiophores are short and apparently thicker than the bases of the rays.

The articular region of the rays is large in comparison with the fragile appearance of the rest of the ray. Five or six small basal fulcra precede the series of dorsal fin rays. The first fulcra are small, unpaired elements that are followed by fulcra whose depth increases caudodorsally. There are about 10 or 11 principal rays, including the first segmented but unbranched ray and 9 or 10 branched and segmented rays; all rays seem to be very fragile

and are usually broken. The principal rays have long bases and are scarcely segmented and branched distally. It is unclear if only the first principal ray forms the leading margin of the fin or whether the second principal ray forms also the leading margin. Small fringing fulcra lie between the last basal fulcrum and the leading margin of the fin.

The origin of the anal fin is about at the level of the 19th, 20th, or 21st vertical row of scales. The short anal fin is placed posteriorly to the dorsal fin and is closer to the caudal fin than to the pelvic fins. It consists of three or four small basal fulcra and eight or nine principal rays. The anal fin rays are also very delicate and thin and are broken in most specimens. Small and elongate fringing fulcra are associated with the leading margin of the fin.

Caudal Fin—The caudal endoskeleton is not visible in any specimen so that its internal composition remains unknown.

Although some of the distal tips of the caudal fin rays are broken, the tail is almost completely preserved in a few specimens. The hemi-heterocercal caudal fin (Figs. 24, 25) is deeply forked, with very long leading rays of the epaxial and hypaxial lobes of the fin. However, as the preserved caudal fins show, the middle rays are comparatively longer than those in other species here described. The terminal area covered by ganoid scales at the base of the caudal is divided into two well-defined regions formed by scales, separated from each other by a notch. Both areas are slightly triangular-shaped. The dorsal one is formed by a series of rhombic, rectangular, and even triangular scales that reach to the level of the last epaxial basal fulcrum, forming part of the margin of the epaxial lobe of the fin. The ventral region covered by scales is shorter than the dorsal one, and the scales are distributed in an almost round pattern. The posterior margins of the scales framing these dorsal and ventral regions are usually round, and as a whole the scales are more elongate than the preceding ones covering the caudal peduncle.

The caudal fin consists of nine epaxial basal fulcra (10 epaxial basal fulcra are rarely present), a series of elongate epaxial fringing fulcra, occasionally one epaxial rudimentary ray, 23 to 26

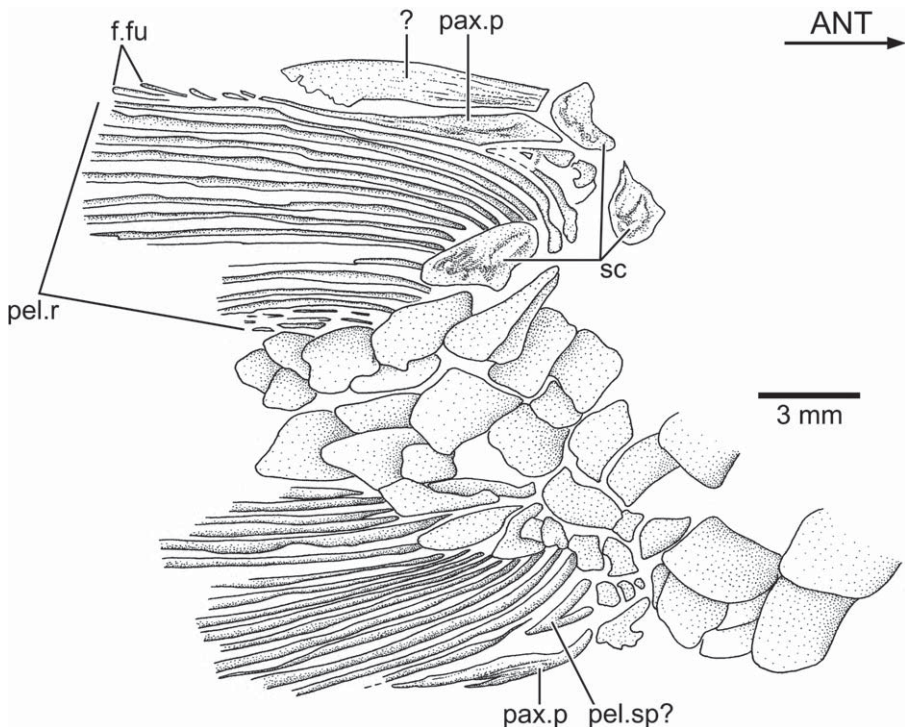


FIGURE 22. *†Pholidophorus gervasutti* Zambelli (MCSNB 4318b). Drawing of pelvic fins and associated scales in ventral view.

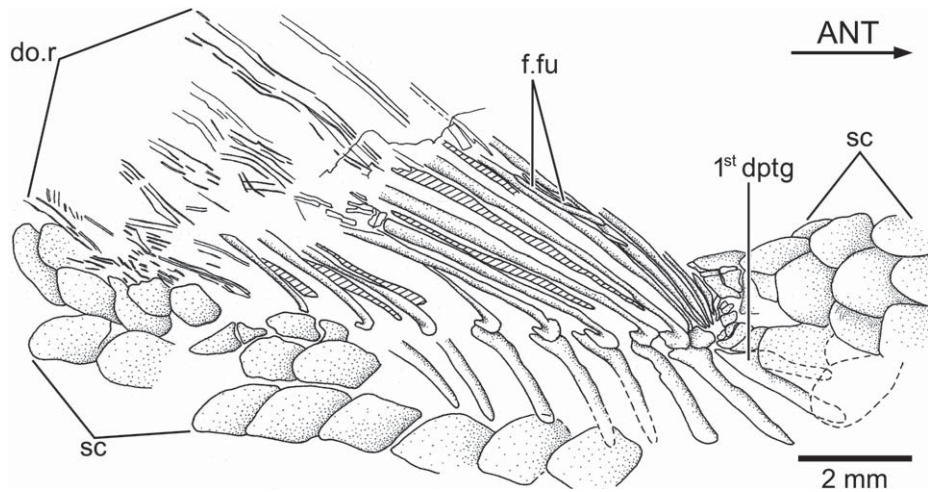


FIGURE 23. *†Pholidophorus gervasutti* Zambelli (MCSNB 3462b). Drawing of dorsal fin and associated scales in right lateral view.

principal rays, a series of elongate hypaxial fringing fulcra, three to four hypaxial segmented procurent rays, and two or three hypaxial basal fulcra.

The epaxial basal fulcra (Figs. 24, 25) are elongate, leaf-like elements that expand laterally, partially covering the next fulcrum. The anterior basal fulcra are unpaired, but the most posterior ones are paired. They are interpreted here as epaxial basal fulcra—and not as procurent rays—because of their shapes, relationship to each other, and lack of segmentation (Arratia, 2008, 2009). A short, thin, and segmented rudimentary ray lies dorsal to the first principal ray in specimen MCSNB 4312; two short and thin rudimentary rays were observed in other specimens (Fig. 25). The series of epaxial fringing fulcra is on the first and second principal rays, as well as the dorsal margins of the rudimentary ray where

it is present. The distal tip of the rudimentary ray resembles the shape of the fringing fulcra in MCSNB 4312 and is intercalated between the fringing fulcra, giving a continuous aspect to the dorsal margin of the fin.

The first principal ray (only segmented) and second principal ray (segmented and branched distally) form the dorsal leading margin of the fin. The segmentation of the principal rays is mainly straight. As far as preservation permits, no dorsal processes associated with the bases of the middle principal rays have been observed.

The hypaxial procurent rays (Figs. 24, 25) are segmented, and the terminal segment usually resembles the shape of the fringing fulcra. Accessory fringing fulcra lie between the terminal segment of a procurent ray and the next one. A series of elongate fringing

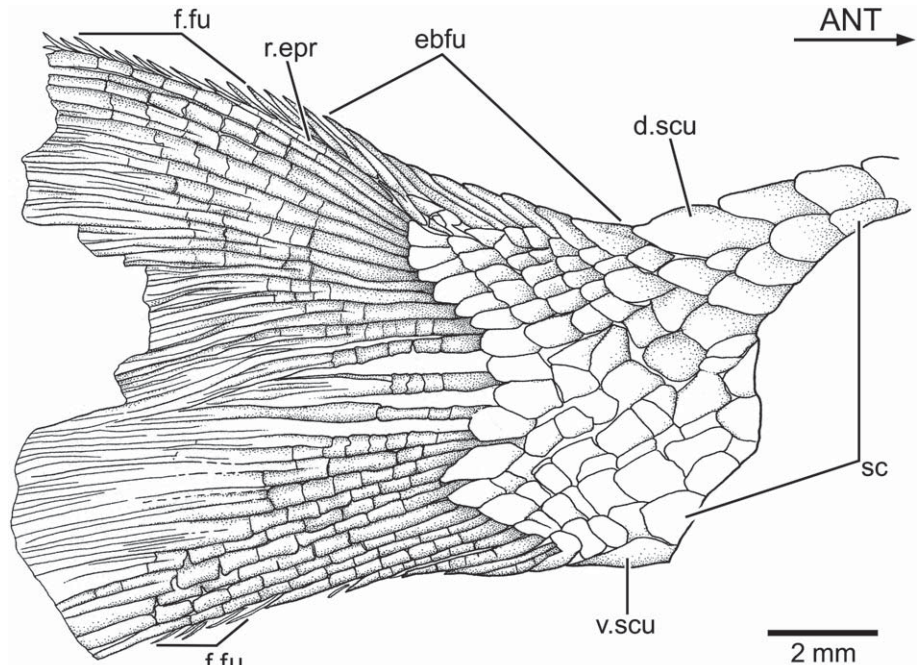


FIGURE 24. *†Pholidophorus gervasutti* Zambelli (holotype; MCSNB 4723b). Drawing of caudal fin in right lateral view.

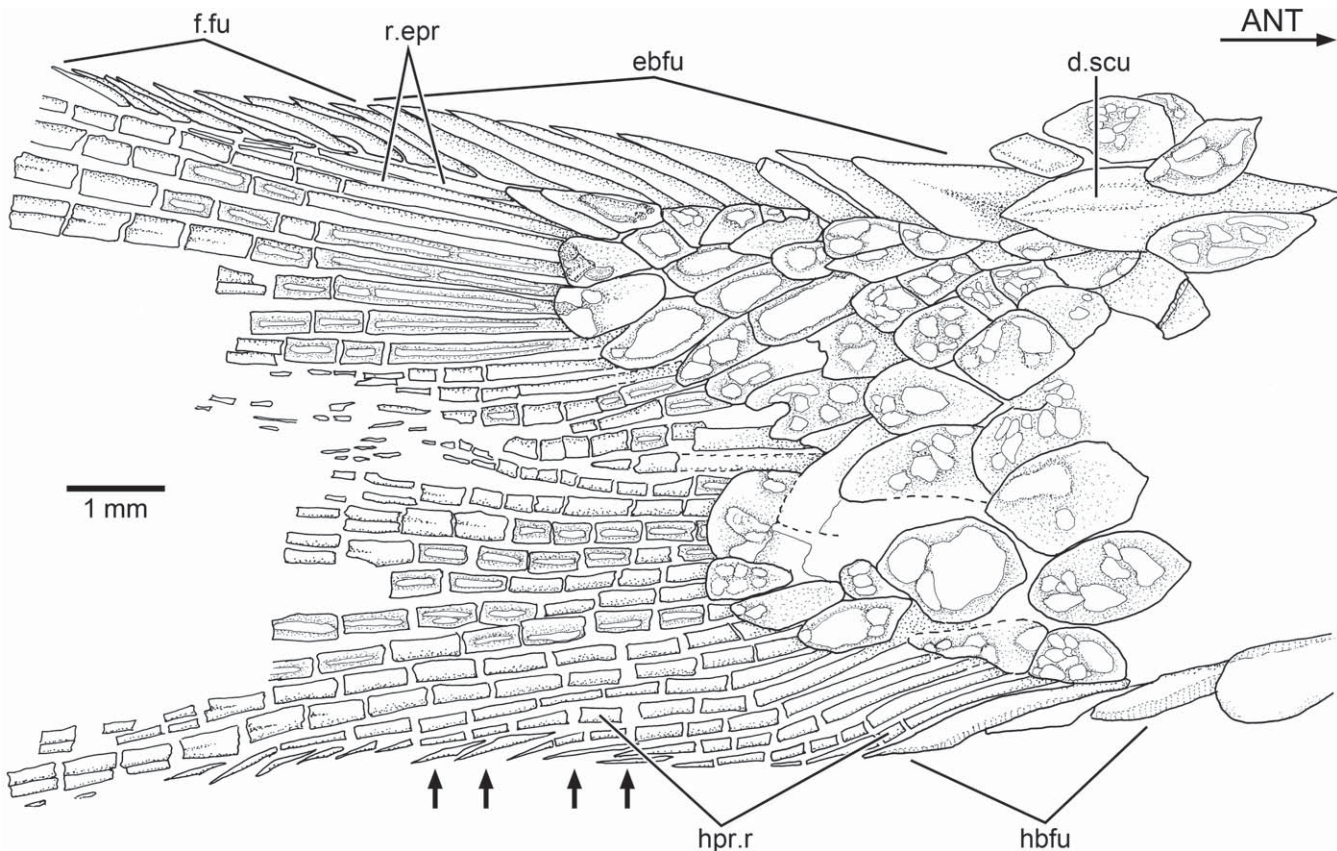


FIGURE 25. *†Pholidophorus gervasutii* Zambelli (MCSNB 4312). Caudal fin in right lateral view. Small arrows point to additional fringing fulcra intercalated between the tips of hypaxial procurent rays. Note the ornaments of ganoine covering scales and rays.

fulcra are positioned along the ventral margins of the last (only segmented) and penultimate (segmented and branched distally) principal caudal rays.

A thin layer of ganoine covers the fulcra and rays. This layer is ornamented with elongate ridges of ganoine that are observed on the surface of the base of the rays, as well as their segments (Fig. 25). A similar delicate ornamentation is observed on the lateral surface of the basal fulcra and also on the small fringing fulcra.

One slightly rhomboidal dorsal scute and another rhomboidal ventral one (Figs. 24, 25) precede the epaxial and hypaxial series of basal fulcra. The dorsal scute usually is covered by displaced scales and consequently is observed in a few specimens only. The ventral scute is smaller than the dorsal one. Both scutes may be covered by tubercles of ganoine.

Scales—Although numerous specimens are available for study, many have damaged scales. Thick ganoid scales (Figs. 7A, B, 9A, B, 19C, 25), of different sizes and shapes, cover the body. Most scales of the dorsal and ventral rows of the body are rhombic, slightly rectangular, or even square-shaped. However, the three main rows of the flank (the lateral line row and one dorsal and one ventral row) are comparatively deeper than broad in the predorsal region. The scales of the flank become smaller progressively posteriorly. In the caudal peduncle, the scales are more uniform in size, but they are very irregular in shape (Fig. 25). Some scales are rhombic, others are rectangular, and some even have slightly rounded posterior margins.

The scales are covered by a thick layer of ganoine that is ornamented with tubercles of various sizes, unevenly distributed on

the free field of the scales (Fig. 25). However, the ornamentation is very delicate and almost nonexistent on the scales covering the bases of the caudal rays.

Lateral Line—Thirty-eight to 40 flank scales carry the main lateral line canal. However, the trajectory of the lateral line is clearly observed only in a few scales, generally close to the pectoral girdle and some intermediate scales. Pores or the canal itself are difficult to observe, especially in the caudal peduncle. This could be due to the thickness of the ganoine cover.

†ZAMBELLICHTHYS, gen. nov.

Diagnosis—Based on a unique combination of characters. Autapomorphies are identified with an asterisk (*). Small pholidophorids reaching about 70 to 80 mm as maximum length. Cranial bones and scales covered with small tubercles and ridges of ganoine. Nasal bone with rounded foramen near lateral border. Numerous and irregularly shaped suborbital bones, arranged in two series, placed between infraorbitals 3 to 5, preopercle, and opercle (*). Long jaws extending posterior to orbit. Quadrato-lower jaw articulation positioned posterior to orbit. Deep and large preopercle almost reaching the dermopterotic region (*). Characteristically shaped preopercle lacking anteroventral expanded region (*). Preopercle almost vertically oriented (*) and with a well-pronounced notch at its posterior margin. Preopercular canal near anterior margin of preopercle.

Type Species—*†Zambellichthys bergamensis*.

Content—Type species only.

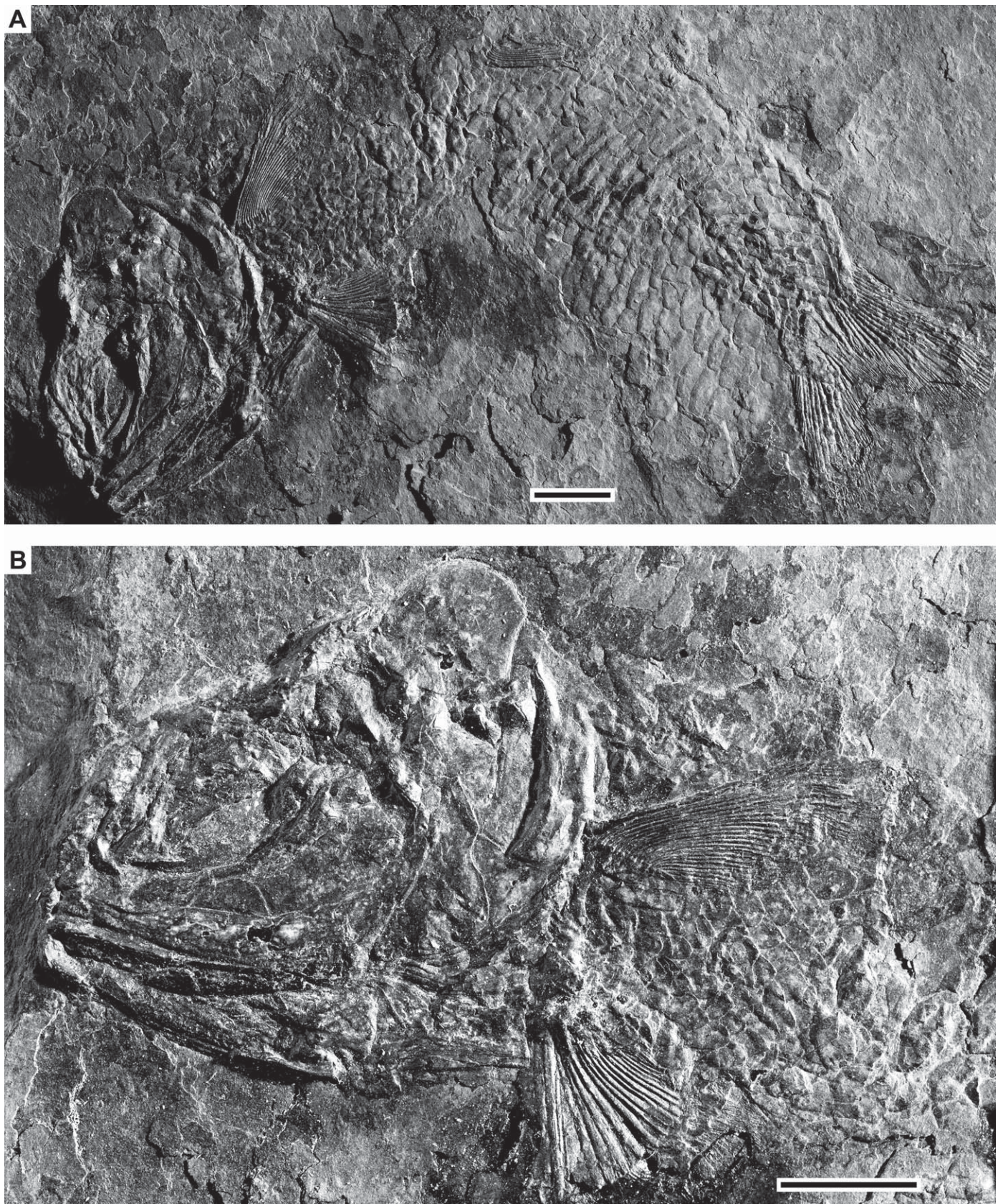


FIGURE 26. \dagger *Zambelichthys bergamensis*, gen. et sp. nov. **A**, photograph of the holotype (MCSNB 4446) in left lateral view. **B**, enlargement of head and anterior part of the body. Scales bars equal 5 mm.

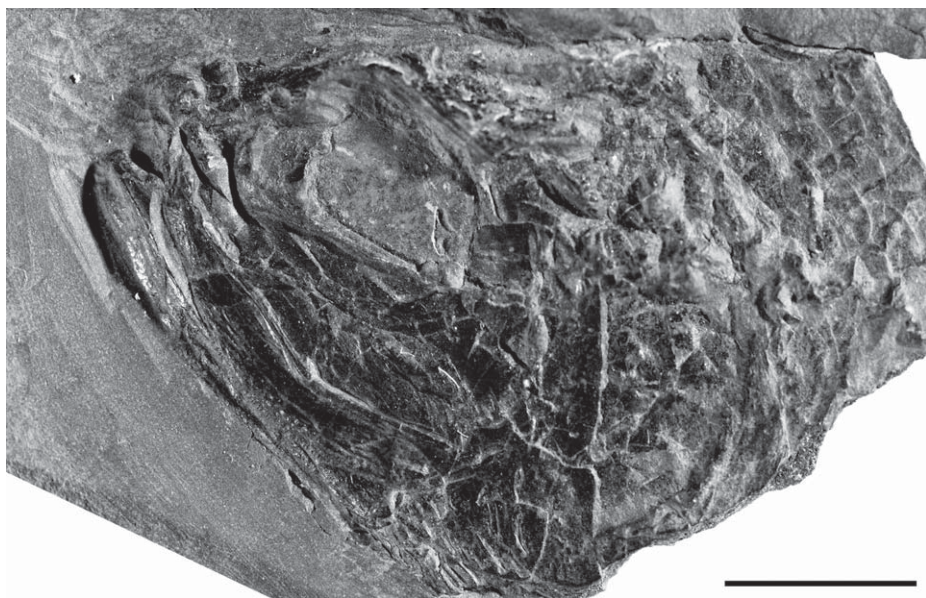


FIGURE 27. *†Zambellicthys bergamensis*, gen. et sp. nov. Photograph of the paratype (MCSNB 4332b) in left lateral view. Scale bar equals 5 mm.

†ZAMBELLICHTHYS BERGAMENSIS, gen. et sp. nov.
(Figs. 26–29)

Holotype—MCSNB 4446 (Fig. 26A), a complete specimen strongly bent at about mid-length and with body squamation partly displaced.

Paratype—MCSNB 4332b (Fig. 27), an incomplete specimen represented by head and anterior body squamation.

Type Locality, Age, and Distribution—Only known from the type locality Ponte Giurino, about 18 km northwest of Bergamo, Lombardy, northern Italy. The age of the sediments are Late Triassic (Norian), about 210 Ma.

Diagnosis—As for genus.

Etymology—*Zambellicthys*, honoring the contribution of the late Rocco Zambelli to the knowledge of fossil pholidophorid fishes in northern Italy, and *ichthys* (Greek, fish). The specific name *bergamensis* references the region in Italy he loved and where he collected fossils for many years.

Comments—The holotype and paratype were chosen by Zambelli (1980a:9) from a collection of 300 specimens that he considered to be a new species, *Pholidophorus gervasutti*, which he later interpreted as a subspecies of *Ph. latiusculus* and named it *Pholidophorus latiusculus gervasutti* (Zambelli 1986). M. Gersavutti, M. Pandolfi, and R. Zambelli collected these two specimens sometime between 1975 and 1980.

Description

Based on the size of the skull of the holotype and paratype in comparison with other species studied here, I assume that the fishes were small, reaching about 70 to 80 mm total length. The anterior profile of the head is somewhat triangular-shaped, with its maximum depth at the level of the preopercle. The snout is short, about 14% of the head length. The eyes are moderately large. The diameter of the orbit is about 30% of the head length. The jaws are elongated (Figs. 28, 29), extending caudad to the posterior margin of the orbit and reaching the anterior margin of the preopercle.

The ganoine layer is partially weathered out in the holotype, permitting a better understanding of the bones and scales.

Braincase—The braincase is as short or even shorter than most other pholidophorids studied herein. The posterior border of the braincase is almost at the level as the dorsal margin of the preopercle; consequently, the opercle and subopercle are positioned posterior to the braincase. Part of the parasphenoid and the ethmovomerine region is preserved in the paratype (Fig. 29). It is unclear whether the parasphenoid bears teeth or not. Part of the braincase (Fig. 28), together with part of the parasphenoid, is preserved in the holotype. No sutures are observed—the braincase is well ossified, as has been described for the Early Jurassic '*Pholidophorus*' *bechei* (Patterson, 1975:321).

Skull Roof—There are no crestae and fontanelles in the skull roof plate, which is preserved in lateral view in both the holotype and paratype. The surface of the cranial roof is smooth, and apparently, narrow at the level of the orbital margin. One pore and sensory tubule of the supraorbital canal and a small section of the otic canal are observed in the paratype (Fig. 29).

The parietal [= frontal of tetrapods], autosphenotic, and postparietals seem to be fused (Figs. 28, 29). The condition of the dermopterotic is unknown because the bone is broken in the paratype and is not preserved in the holotype. The parietal bone is broken, but no sutures are seen in the exposed skull roof. There is no evidence of a supraoccipital or any epiotics at the posterior region of the skull roof plate. The left extrascapula is incompletely preserved in the paratype. It is large and covered by small tubercles of ganoine. Neither the trajectory of the extrascapular commissure or supratemporal canal nor the pores and/or sensory tubules have been observed. A median rostral bone is not preserved.

The nasal bone is large, rectangular, and plate-like, and it always sutures with the anterolateral margin of the parietal bone (Figs. 27, 29). The nasals do not suture to each other medially, because they are separated by an acute anterior extension of the parietal region of the skull roof, similar to the pattern in *†Pholidophorus gervasutti*. The nasal has an emarginated or notched anterolateral margin that forms part of the anterior nostril opening. A large, rounded foramen perforates the nasal close to its lateral margin.

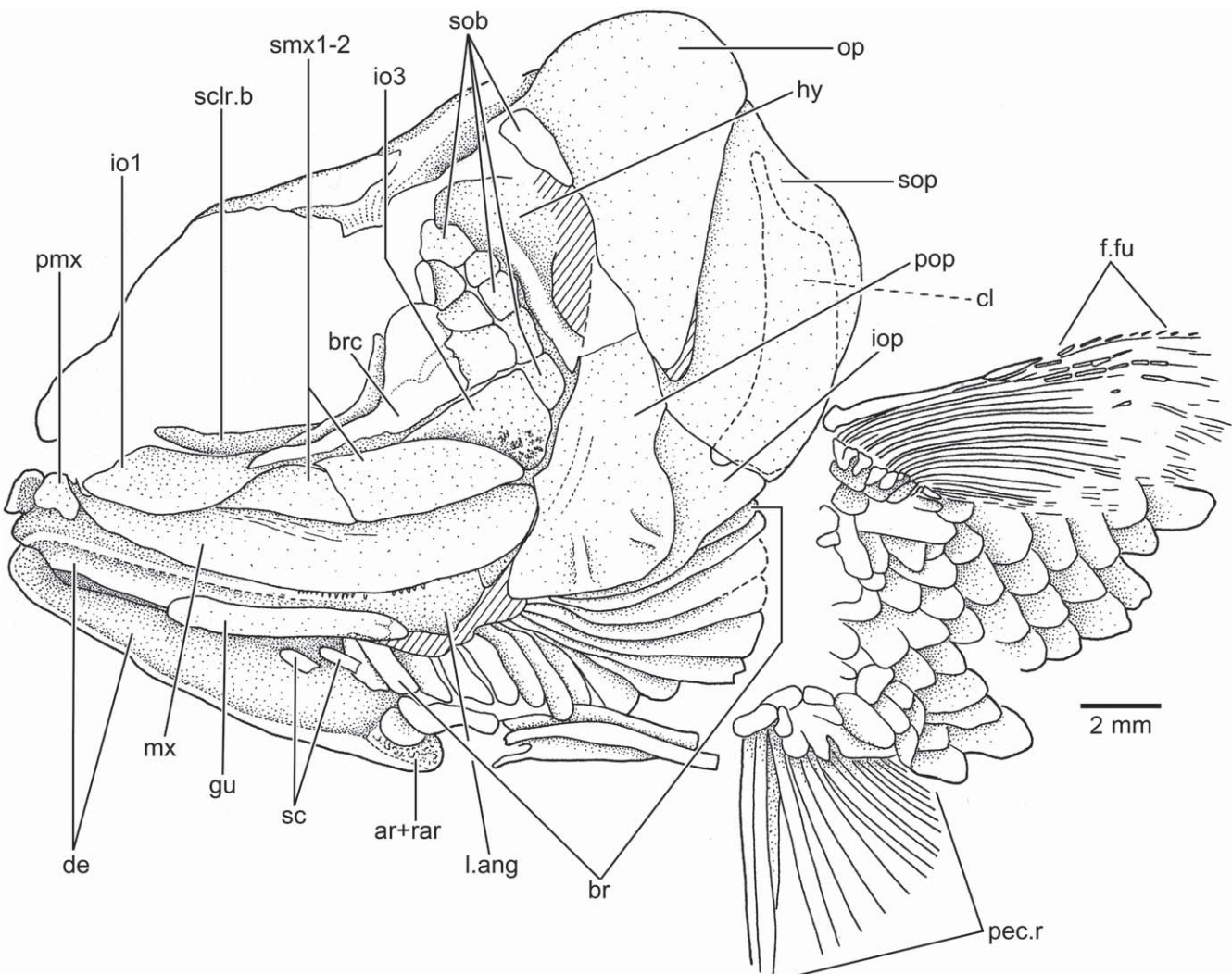


FIGURE 28. *†Zambelichthys bergamensis*, gen. et sp. nov. Drawing of head and anterior part of the body in left dorsolateral view (holotype; MCSNB 4446). Hatched lines indicate broken bone surface.

The lateral margin of the nasal is straight so that the foramen is interpreted here as the posterior nostril. Due to the presence of ornamentation, the trajectory of the supraorbital sensory canal is not discernable.

Circumorbital Series—It is unclear how many bones form the circumorbital ring because not even traces of the supraorbital bones or dermosphenotic are preserved. The circumorbital series has preserved one antorbital and five infraorbitals. In addition, *†Zambelichthys bergamensis* has numerous suborbitals and sclerotic bones.

The antorbital (Fig. 29) is a small triangular bone lying anterodorsally to the anterior margin of infraorbital 1. The layer of ganoine is eroded away, exposing the surface of the bone, and no sensory pores of the infraorbital canal are observed.

Infraorbital 1 (Figs. 28, 29) is a large, elongate bone, extending posteriorly, almost to the mid-region of the orbit. The bone has a well-defined, thick orbital margin, where the infraorbital canal apparently runs. No sensory pores or tubules are observed on the surface of the bone.

Infraorbital 2 (Fig. 29) is a tube-like bone surrounding the infraorbital canal. It is a short bone placed in between infraorbitals 1 and 3.

Infraorbital 3 (Figs. 28, 29) is a large bone, with a thickened tube-like orbital margin where the infraorbital canal passes. Its ventral margin is incompletely preserved in the paratype; thus, it is expected that the bone was larger, as it is illustrated in Figure 29. It has a marked concave orbital margin and is expanded posteriorly, extending to the anterior margin of the preopercle. No sensory pores or tubules are observed. The external surface of infraorbital 3 is covered with tubercles of ganoine.

Infraorbital 4 (Fig. 29) is incompletely preserved in the paratype. Infraorbital 5 is a comparatively large and almost square bone, carrying part of one sensory tubule.

Five to nine small, rectangular, square, or triangular suborbital bones (Figs. 28, 29) are present in the narrow space defined by the posterior margins of infraorbitals 4 and 5, dorsal margin of infraorbital 3, and anterior margins of both the preopercle and opercle. The suborbitals are arranged in two rows of bones. Some of the suborbitals cover the preopercle and anterior margin of opercle.

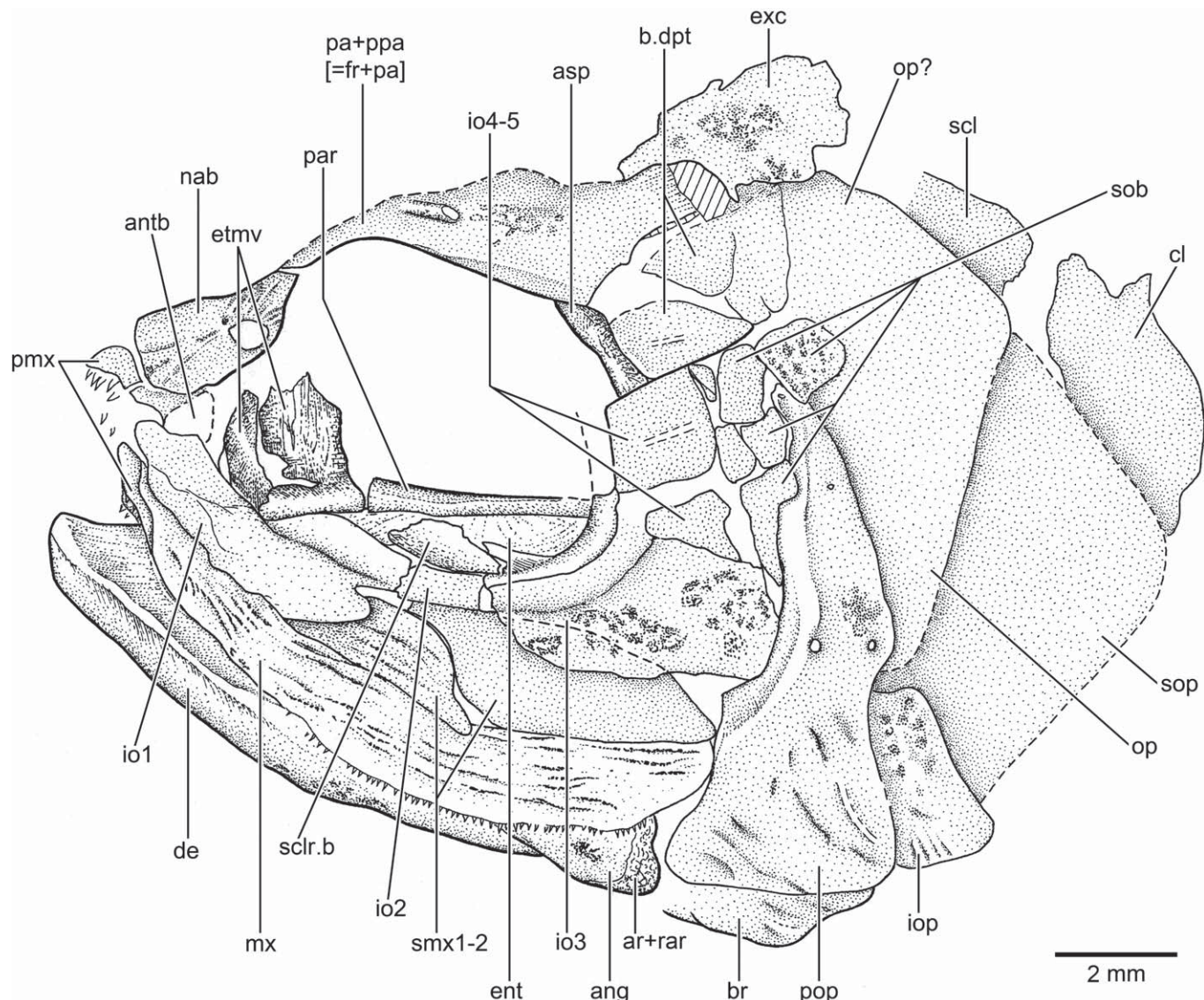


FIGURE 29. *†Zambelichthys bergamensis*, gen. et sp. nov. Drawing of head and anterior part of the body in left lateral view (paratype; MCSNB 4332b). Dashed lines indicate reconstructed margin of bone.

The surface of the bones is ornamented with small tubercles of ganoine. The small bone lying dorsally to the preopercle in the paratype is interpreted here as a suborbital and not as a suprapreopercular bone, because there is no evidence that the element carries the dorsal most portion of the preopercular canal, and the dorsal tip of the preopercle almost extends to the dermopterotic region of the skull roof plate.

There are remnants of both anterior and posterior sclerotic bones (Figs. 28, 29) medial to the infraorbital bones.

Upper Jaw—The external surfaces of the maxilla and the supramaxillae are covered by a thick layer of ganoine, which is ornamented with longitudinal ridges extending along the bones.

The premaxilla (Figs. 28, 29) is incompletely preserved in both specimens. The premaxilla is a small, triangular bone, with a short ascending process. Small conical teeth lie on the oral margin of the bone. Although the teeth are small, they seem to be comparatively

larger than the maxillary teeth. Evidence of a rostrodermethmoid has not been found.

The long, broad, and gently curved maxilla (Figs. 26–29) has a short anterior articular region. The maxillary blade is slightly shallow anteriorly, but its depth increases slightly distally; its ventral margin is gently convex. A single row of small conical teeth is present on the oral margin of the blade. The dorsal margin of the maxilla is covered by infraorbital 1 and supramaxillae 1 and 2. The posterior margin of the maxilla is gently rounded.

Two broad supramaxillary bones (Figs. 26–29) cover almost two-thirds of the posterodorsal margin of the maxilla. Supramaxilla 1 is a small, slightly triangular bone; it is about half the length of supramaxilla 2. In contrast, supramaxilla 2 is a longer, deeper, and larger bone that extends forward, overlapping supramaxilla 1 with its long anterodorsal process, as shown by the paratype.

Lower Jaw—Part of the left lower jaw is observed in the paratype, whereas both jaws are partially exposed in the

holotype. The dorsal part of the jaw is covered by other bones, so that only the ventral region of the dentary and the angular are exposed (Figs. 28, 29). The dentary forms most of the lower jaw, and the lateral portion of the angular is restricted to the posterior part, but the limit between both bones is not clearly seen in the available material. The dentary produces a marked border or ridge, protruding laterally, that separates the dorsal (dental) and ventral (splenial) regions of the bone, as in all other fishes here described. The dorsal region does not have ornamentation and is partially covered with ganoine. The trajectory of the mandibular sensory canal, its tubules, and pores are not observed in the available specimens due to the tubercles of ganoine covering the dentary. The posterior remnant of Meckel's cartilage (Fig. 28) is present medial to the angular. In other fishes where complete ossification occurs, this remnant corresponds to the fused articular and retroarticular bones.

Palatoquadrate and Suspensorium—Most bones of the palatoquadrate and suspensorium are hidden by other bones. Part of the dorsal region of the hyomandibula (Fig. 28) is preserved in the holotype. The bone is broadly expanded dorsally, with its ventral part slightly inclined posteroventrally, forming a peculiar angle with the lower part of the hyosymplectic. This pattern is similar to that observed in other long-jawed species here described, where the articulation of the lower jaw-quadrat is posteriorly placed in the head. Part of the entopterygoid (Fig. 29) is preserved in the large space of the orbit, below the parasphenoid. It is unclear whether the bone bears dentition.

Oculcular, Branchiostegal Series, and Gular Plate—All opercular bones, as well as the branchiostegals, are covered with a thick layer of ganoine, which is ornamented with a variable number of tubercles and ridges.

The preopercle (Figs. 26B, 28, 29) is a large bone that extends nearly to the lateral margin of the skull roof. Unlike other species here described, the preopercle is almost vertically oriented. The preopercle has a characteristic shape, with no differentiation between dorsal and ventral limbs, with the ventral part broader than the dorsal part and a deep notch at the posterior margin of the bone. The pathway of the preopercular sensory canal is visible closer to the anterior margin, but the number of sensory tubules the canal possesses remains unknown.

The opercle (Figs. 28, 29) is displaced in both specimens, but it is better preserved in the paratype. It is a large bone, approximately triangular in shape, but with a rounded posterodorsal margin. The anterior margin of the opercle is slightly irregular and is deeper than the posterior margin. The ventral margin of the opercle is markedly oblique. The external surface of the bone has tubercles of irregularly distributed ganoine.

The subopercle (Figs. 28, 29) is almost as deep as the opercle; its posteroventral margin is gently rounded. The anterodorsal process is short and sharp and projects dorsally in front of the anterior margin of the opercle.

The well-developed triangular interopercle (Figs. 28, 29) is expanded posteriorly and articulates with the subopercle. The bone narrows anteriorly and extends below and medial to the preopercle, but apparently it does not contact the anteroventral corner of the preopercle. The external surface of the bone is covered with tubercles of various sizes.

There are at least 16 branchiostegal rays (Figs. 26B, 28) preserved in the holotype. The anterior branchiostegals are short and broad, but become progressively longer and more slender posteriorly. The last branchiostegal rays are the longest, but apparently they do not extend below the subopercle.

The gular plate (Fig. 28) lies between both lower jaws, at about their posterior half. The gular is slightly oval and narrow.

Paired Fins—The pectoral girdle and fin are poorly preserved in both the holotype and paratype. The posttemporal has not been

identified among the broken bones at the posterior part of the skull roof. Parts of the supracleithrum and cleithrum (Figs. 28, 29) are preserved in the paratype, but part of the cleithrum is displaced in the holotype and looks like a moderately slender bone. No other bones can be identified.

The pectoral fins (Figs. 26B, 28) are positioned low in the flank, close to the ventral margin of the body. Both pectoral fins are preserved in the paratype. There are 17 or 18 lepidotrichia. The external ones are much longer than the internal ones. The rays have long bases and are finely segmented and branched distally. The first pectoral ray is short and stout at its proximal region and continues distally as a thin, segmented ray with no branching. The proximal region of the first ray is a compound structure formed by fusion of the base of the first ray and basal fulcra. There is a series of small fringing fulcra associated with the distal segmented region of the first ray. It is unclear if a propterygium is fused to the base of the first pectoral ray. The second ray is longer than the first ray and is branched and segmented distally.

Scales—The anterior region of the body is covered by thick ganoid scales, most of which are rhombic or square-shaped at the dorsal region of the flank in the holotype. These scales are poorly preserved. The scales of the ventral body region (Fig. 28), positioned between both pectoral fins, vary in shape from rectangular to oval, but they are mainly rhombic or square in the caudal peduncle.

†ANNAICHTHYS, gen. nov.

Diagnosis—Based on a unique combination of characters. Autapomorphies are identified with an asterisk [*]. Small pholidophorid of about 72 mm total length. Skull roof narrow anteriorly, then abruptly expanding in the posterior half of the orbital margin giving a peculiar shape to the skull [*]. Orbital width of skull roof plate moderately broad, about half the width of postorbital region [*]. Scattered, large and rounded tubercles of ganoine on cranial bones [*]. Skull roof bones, except the rostral and nasals, partially fused. Parietal [= frontal] bones ending in a moderately broad, straight anterior margin. Large nasal bones broadly separated from each other by the anterior tips of parietal [= frontal] bones. Parietal [= frontal] bones broadly sutured with rostral bone anteriorly. Large, rounded foramen at the lateral border of nasal bone. Eyes large, diameter about 36% of head length. Small infraorbital bones [*]. Infraorbital 3 slightly rounded [*]. Two suborbital bones [*]. Maxilla and supramaxillae almost vertically oriented [*]. Lower jaw with rudimentary postarticular process [*]. Quadrato-mandibular articulation below the level of anterior half of orbit [*]. Narrow and short crescent-shaped preopercle with indistinguishable dorsal and ventral arms, not extending to lateral margin of skull roof, and with a deep notch anteroventrally (inverted heart-like shape). Preopercle without a notch at its posteroventral margin. Body covered with rhombic or square ganoid scales. Scales with smooth posterior margins and covered with large and rounded tubercles of ganoine irregularly distributed [*].

Type Species—†*Annaichthys pontegiurinensis*.

Content—Type species only.

†ANNAICHTHYS PONTEGIURINENSIS, gen. et sp. nov. (Figs. 30–35)

Holotype—MCSNB 11282a, b, c (Figs. 30A, 31). MCSNB 11282a represents only the head, anterior part of the body squamation, and a few vertebrae, whereas MCSNB 11282b is the imprint of the whole specimen; 11282c represents a fragment of the vertebral column. The specimen was collected during the excavations organized by the Museo Civico di Scienze Naturali, Bergamo, in 1993.

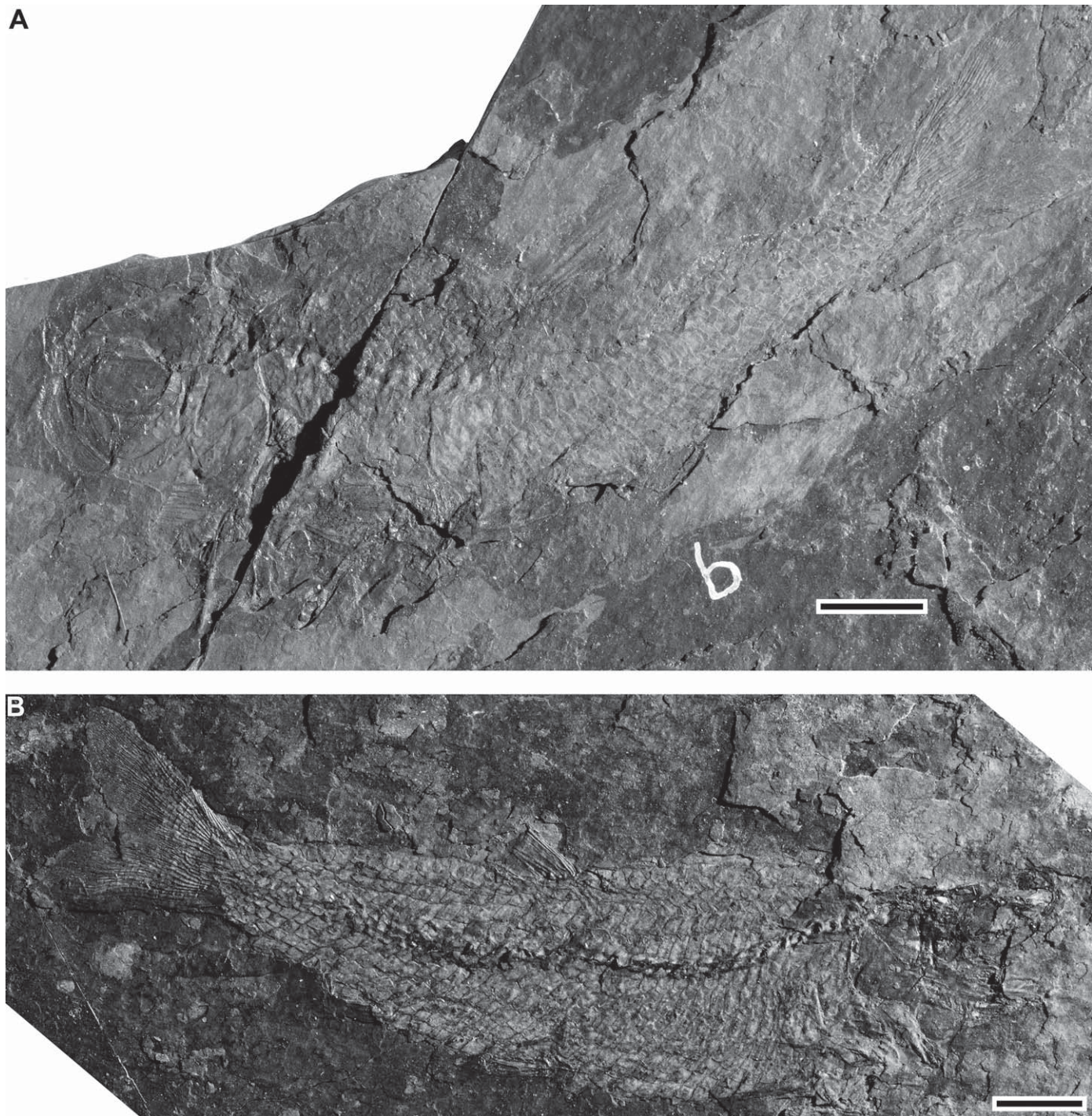


FIGURE 30. *†Annaichthys pontegiurinensis*, gen. et sp. nov. **A**, photograph of the holotype (MCSNB 18282b) in left lateral view. **B**, photograph of paratype (MCSNB 11283) in right lateral view. Scale bars equal 5 mm. (Color figure available online.)

Paratypes—In the same rock where the holotype is preserved was found a partial vertebral column (MCSNB 11283) that is very well preserved. Apart from the skull, which preserves only a few bones, the body and squamation are complete (Fig. 30B).

Type Locality, Age, and Distribution—Only known from the type locality, Ponte Giurino, about 18 km northwest of Berg-

amo, Lombardy, northern Italy; Late Triassic (Norian), about 210 Ma.

Diagnosis—As for genus.

Etymology—*Annaichthys*, honoring the contribution of Dr. Anna Paganoni to the development of paleoichthyology in northern Italy, especially the collection of new fossil material



FIGURE 31. †*Annaichthys pontegiurinensis*, gen. et sp. nov. Photograph of the head of the holotype in right dorsolateral view (MCSNB 18282a). Scale bar equals 5 mm.

including fishes, and *ichthys* (Greek, fish). The species name—*pontegiurinensis*—refers to the locality (Ponte Giurino) where the fish was recovered and where the team of the Museo Civico di Scienze Naturali (MCSNB) has collected fossils for many years.

Description

The members of this species are small, reaching about 59 mm SL, with a maximum total length of about 72 mm. The body is fusiform, with its maximum depth in the predorsal region. The snout length (calculated as the distance between the anterior margin of the orbit and the anterior margin of the premaxilla) is short, about 17% of the head length. The head is almost square in shape, with a short upper jaw that is almost vertically oriented (reminiscent of a bulldog's face), which gives a characteristic aspect to the fish. The caudal peduncle is moderately narrower than the rest of the body. All fins, except the caudal one, are damaged.

The ganoine layer is weathered out on certain bones and scales. Large, rounded and/or conical tubercles (Fig. 31) of ganoine are associated with most cranial bones.

Braincase—The braincase seems to be comparatively longer than the other species studied herein; however, its posterior region is damaged so that its limits and those of the extrascapulae are not distinguishable. Part of the parasphenoid is preserved in the counterpart, but the remnants are uninformative.

Skull Roof—There are no crestae, fenestrae, fontanelles, or pineal openings in the skull roof. The surface of the cranial roof (Figs. 31, 32) is smooth, and apparently slightly depressed medially. No traces of cephalic sensory canals are observed in MCSNB 11282a. The postorbital region seems to be comparatively longer than that in all other species described here, and the whole skull roof plate has a bottle-like shape. Because of the damage of the posterior part of the postorbital region, its length should be confirmed when more specimens become available for study. Both parietal bones [= frontals] are sutured medially and fused to the

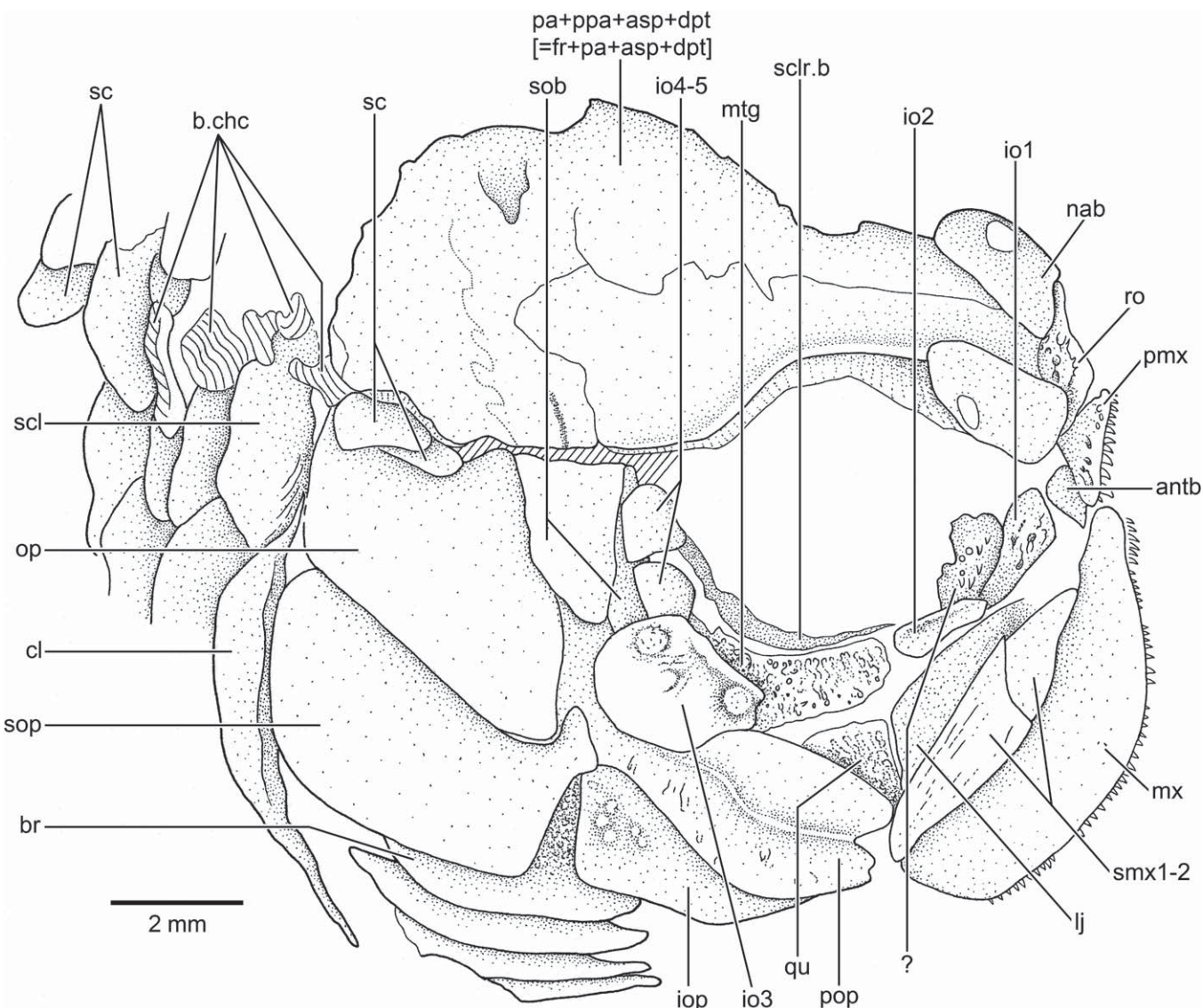


FIGURE 32. *†Annaichthys ponteigurinensis*, gen. et sp. nov. Drawing of the head of the holotype in right dorsolateral view (MCSNB 11282a). Hatched lines indicate broken bone surface. See photograph in Figure 31.

lateral autosphenotic. Whereas the right parietal sutures with the dermopterotic plus postparietals, the left parietal is almost completely fused to those bones. There is no evidence of a supraoccipital or epiotics in the posterior region of the skull roof plate. Remnants of the extrascapulae are scattered on the posterior part of the skull roof on MCSNB 11282a, but a large left extrascapula is preserved on the counterpart.

A median, moderately large, slightly rhomboidal-shaped rostral bone (Figs. 31, 32) is placed at the anterior-most region of the skull roof. The bone presents a slightly rounded anterior margin, two short lateral processes, and a short and broad posterior process. The surface of the bone is covered by large tubercles of ganoine, so that the trajectory of the ethmoidal or rostral commissure cannot be determined. The rostral bone overlies the anterodorsal part of the small premaxillae, and the small antorbital is positioned laterally and distant to the lateral process of the rostral. It is unclear whether a connection between the ethmoidal commissure and the

infraorbital canal was present. The posterior process of the rostral bone sutures with the anterior margin of the parietal region of the skull roof plate.

There are two large, slightly rectangular-shaped, plate-like nasal bones (Figs. 31, 32) that partially overlie the lateral margin of the parietal region at the anterolateral margins of the skull roof. They are posteriorly placed with respect to the lateral processes of the rostral bone. Each nasal has an emarginated or notched anterolateral margin that forms the posterior edge of the anterior nostril opening. A rounded or oval foramen perforates the nasal bone close to its lateral margin. The lateral margin of the nasal is straight so that the foramen is interpreted here as the posterior nostril. There is no evidence of the course of the supraorbital canal or its pores.

Circumorbital Series—It is unclear how many bones form the circumorbital ring because there is no evidence of supraorbitals or a dermosphenotic. The infraorbital series has five small

infraorbitals. In addition, *Annaichthys* presents two suborbitals and remnants of sclerotic bones.

The antorbital (Fig. 32) is a small, thick triangular bone lying anterodorsally to the anterior margin of infraorbital 1. The layer of ganoine is weathered away, exposing the surface of the bone. No traces of the infraorbital canal and sensory pores are present, but it is interesting to note that the antorbital is placed just in front of the anterior opening of the infraorbital canal in infraorbital 1. However, a branch of the infraorbital canal did not pass through the antorbital.

Infraorbital 1 (Fig. 32) is a moderately small bone, slightly oval and expanded anteriorly. The bone is dorsally expanded and covered with tubercles of ganoine of different sizes. The infraorbital sensory canal is positioned close to the ventral margin.

Infraorbital 2 (Fig. 32) is narrow and somewhat rectangular. The infraorbital sensory canal is enclosed in bone. No sensory pores or tubules are observed.

Infraorbital 3 (Fig. 32) is the largest bone of the series, but is the smallest of any species described here. Infraorbital 3 is positioned at the posteroventral corner of the orbit in all other pholidophorids described herein; although the bone in †*Annaichthys* is slightly displaced in the holotype, it still gives the impression that it has a loose connection to infraorbitals 2 and 4 and is broadly separated from the anterior margin of the preopercle. Infraorbital 3 has a slightly concave orbital margin, but it is moderately expanded and rounded posteriorly, unlikely any other infraorbital 3 described here for other species. The infraorbital canal is close to the orbital margin, and no sensory pores or tubules are observed. The surface of infraorbital 3 is covered by tubercles, with some of them being very large in comparison with the size of the bone.

Infraorbitals 4 and 5 (Fig. 32) are small and square. Information concerning the course of the infraorbital canal is not discernable.

Two suborbital bones are present. The anterior one is elongate and lies within the posterior margins of infraorbitals 4 and 5 and a large posterior suborbital. The larger suborbital, which is slightly triangular (Fig. 32), partially occupies the space defined by the opercle posteriorly, infraorbitals 4 and 5 anteriorly, the lateral margin of the skull roof plate dorsally, and the preopercle ventrally. Accessory suborbitals seem to be absent.

There are remnants of the anterior and posterior sclerotic bones (Fig. 32), which apparently form a complete ring surrounding the eyeball. Medial to infraorbitals 1 and 2, in the position of the anterior sclerotic bone, is an element with the exposed surface covered by small tubercles of ganoine. If this is part of the sclerotic ring, then it means that it was laterally exposed, forming a rim around the eye. This element should be investigated when more specimens become available.

Upper Jaw—The external surface of the maxilla and the supramaxillae is covered by a thick layer of ganoine that is weakly ornamented, with few longitudinal ridges extending along the bones. In addition, tubercles of ganoine are scattered on the maxillary blade close to its oral margin.

The premaxilla (Figs. 31, 32) is a small, triangular bone, with a very short and acute ascending process. One row of conical teeth is placed in the oral margin of the bone. Although the teeth are small, they are comparatively larger than the tiny teeth present in †*Pholidophorus* and †*Parapholidophorus*. A rostrodermethylid is not present.

The broad and slightly curved maxilla (Figs. 31, 32) is short. Its maxillary blade is oriented nearly perpendicular to the skull roof plate. The maxilla has a very short articular region anteriorly. The maxillary blade is slightly shallow anteriorly, but its broadness increases distally. The dorsal margin of the bone is slightly concave, whereas its ventral margin is markedly convex. The dorsal margin does not possess a well-defined supramaxillary process. The pos-

terior margin of the maxilla is gently rounded, without a notch. A single row of small conical teeth is present on the whole oral margin of the blade, apparently forming almost a continuous toothed surface including both the premaxilla and maxilla.

Two broad supramaxillary bones (Figs. 31, 32) cover almost the whole dorsal margin of the maxilla, just posterior to the maxillary articular region. Supramaxilla 1 is a moderately small, slightly triangular bone. In contrast, supramaxilla 2 is comparatively a longer and larger bone that extends forward, overlapping the tip of supramaxilla 1 with its rudimentary anterodorsal process.

Lower Jaw—The lower jaw (Figs. 31–33) is partially preserved in MCSNB 11282b. The lower jaw is short, and its articulation with the quadrate (Figs. 31, 32) is positioned inferior to the anterior half of the orbit. The jaw (Fig. 33) is broken, showing its external part anteriorly, but its medial region posteriorly. Additionally, the surangular region is preserved in between the infraorbitals and dorsal margin of supramaxillae 1 and 2 in MCSNB 11282a. The main element of the jaw is the dentary, which unfortunately has a broken dorsal margin in MCSNB 11282b. A prominent ridge separates the dorsal (dental) and ventral (splenial) regions of the dentary from its anterior-most tip to the posterior end, as in all other species studied herein. The course of the mandibular canal and its pores is not observed. There are no traces of them at all along the jaw. The posterior part of the jaw consists of only one element, which probably represents the ontogenetic fusion among the angular, articular, and retroarticular. This feature is present in other fossil basal teleosts such as †*Pholidophorus* †*bechei* and †*Leptolepis coryphaenoides* (Arratia, 1997, 1999, 2010; Patterson and Rosen, 1977) and partial fusion is present in some extant basal teleosts (Arratia, 2010). In front of this complex element, remains of Meckel's cartilage are present. A surangular, partially preserved, forms the posterodorsal corner of the jaw. The profile of the posterior part of the jaw, unlike all other species studied here, is not truncated, but ascends gently from the posterior tip of the jaw to the surangular. A rudimentary posterior process extends posteriorly to the articular facet of the jaw.

Palatoquadrate and Suspensorium—Most bones of the palatoquadrate and the suspensorium are hidden by other bones. The anterodorsal part of the quadrate is preserved (Figs. 32, 33) and is mainly cartilaginous, as in all other taxa examined here. Most of the bone is covered laterally by the anterior expansion of the preopercle. A piece of the articular region of the quadrate is preserved in specimen MCSNB 11282b. It is unknown whether only the quadrate articulated with the jaw or if the symplectic was also part of the articulation. Dorsal to the quadrate is another chondral element that has a small amount of ossification, here interpreted to be the metapterygoid. The metapterygoid (Fig. 32) seems to be large, projecting anterodorsally in front of the quadrate. An entopterygoid is not preserved.

Opercular, Branchiostegal Series, and Gular Plate—The opercular bones are represented by the preopercle, opercle, subopercle, and interopercle. A median gular plate is not preserved. All opercular bones, as well as the branchiostegal rays, are covered by a layer of ganoine with a variable number of large tubercles. The posterior margins of the opercle and subopercle, plus the ventral margin of the interopercle, produce a profile of about 90 degrees.

The preopercle (Figs. 31, 32) has its anteroventral region expanded and marked by a deep notch, giving the bone the shape of an inverted heart, whereas the dorsal region is narrower. Consequently, the preopercle lacks well-defined dorsal and ventral arms. Its posteroventral margin is smooth, and a notch is absent. The larger suborbital bone covers the dorsal part of the preopercle. The anterodorsal region of the preopercle is expanded anteriorly, covering part of the hyosymplectic and posterior region of quadrate. The pathway of the preopercular sensory canal is

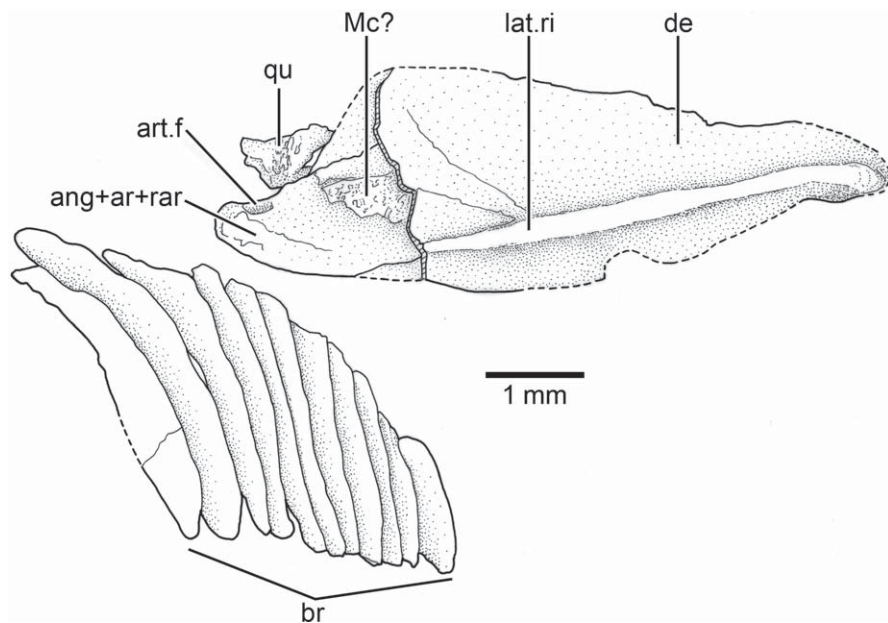


FIGURE 33. *†Annaichthys pontegiurinensis*, gen. et sp. nov. Drawing of broken right lower jaw in lateral and partially preserved medial views and branchiostegal rays of the opposite side of the body (MCSNB 18282b).

visible through vestiges of incomplete tubules and lies closer to the posteroventral and ventral margins of the bone.

The opercle (Figs. 31, 32) is a moderately large bone, approximately square-shaped dorsally. Its dorsal margin is partially hidden by the lateral margin of the skull roof plate and by displaced scales. The anterior margin of the opercle is slightly wavy, and the posterior margin is almost straight. The ventral margin of the opercle is markedly oblique. The external surface of the bone is covered with tubercles of ganoine of different sizes, with some being very prominent.

The subopercle (Figs. 31, 32) is almost as deep as the opercle. It is interesting to remark that its posterior margin is slightly deeper than its anterior one, contrary to the situation found in other pholidophorids. Its ventral margin is almost straight. The exposed anterodorsal process is short and blunt and projects dorsally in front of the anterior margin of the opercle.

The well-developed, roughly triangular interopercle (Figs. 31, 32) is displaced below the preopercle in the holotype. Its exact size cannot be determined, because the interopercle is laterally covered by the preopercle. The external surface of the bone is covered with tubercles of various sizes.

There are 11 branchiostegal rays (Fig. 33) in MCSNB 11282b, but it is possible that a few anterior-most rays are missing. The anterior branchiostegals are relatively narrow and elongate. The last branchiostegal rays are the longest and broadest.

Vertebral Column and Intermuscular Bones—A few incomplete and displaced chordacentra (Fig. 34) are preserved in the holotype, just behind the head. A few more chordacentra (Fig. 30B) are observed between the scales covering the middle region of the body in the paratype, in the transition between the abdominal and caudal regions. The displaced centra are ring-like chordacentra, with thin walls and bear unpaired neural spines in the caudal region and the last abdominal centrum. The last abdominal centrum has a narrow neural arch (lacking an epineural process) and a well-developed parapophysis articulating with a thin, small rib. The caudal vertebrae have large neural and hemal arches.

Paired Fins—The pectoral girdle and fin are poorly preserved in both the holotype and paratype. The posttemporal has not been

identified among the broken bones and scales positioned at the posterior part of the skull roof. An incomplete supracleithrum (Figs. 31, 32) is preserved just posterior to the opercle and dorsal to the cleithrum. The supracleithrum appears to be a broad bone, with a smooth posterior margin and a series of elongate ridges of ganoine covering its anterior region. Only a portion of an almost straight cleithrum (Fig. 32) is preserved; the bone is moderately inflected ventrally so that well-developed dorsal and ventral arms are not present. The external surface preserved close to the medial margin is covered with a series of long ridges of ganoine, forming one long serrated appendage. No other bones can be identified.

The pectoral fins are positioned low on the flank, close to the ventral margin of the body. There are about 12 poorly preserved lepidotrichia in the counterpart.

The pelvic fins are incompletely preserved in the holotype and paratypes so that an accurate count of rays cannot be provided. A triangular, elongate axillary process (Fig. 34) is preserved in the paratype.

Dorsal and Anal Fins—The unpaired dorsal and anal fins are incompletely preserved or not preserved (anal fin lacking in the paratype) so that no information can be provided.

Caudal Fin—Although some of the distal tips of the caudal fin rays are broken, the tail is almost completely preserved in the holotype and paratype. The hemi-heterocercal caudal fin (Figs. 30B, 35) is moderately forked, with moderately short middle principal rays in comparison with the long leading margins of the epaxial and hypaxial lobes of the fin. The area covered by ganoid scales at the base of the caudal fin ends in a slightly triangular area in the epaxial lobe. The area of ganoid scales covering the base of the caudal fin in front of the hypaxial lobe is markedly shorter and slightly rounded in comparison with the condition of the epaxial lobe.

The caudal fin consists of nine epaxial basal fulcra, a series of elongate epaxial fringing fulcra, one epaxial rudimentary ray, 20 to 22 principal rays, and a series of elongate hypaxial fringing fulcra. It is unclear how many hypaxial procurent rays and hypaxial basal fulcra are present because of poor preservation of the ventral margin of the fin.

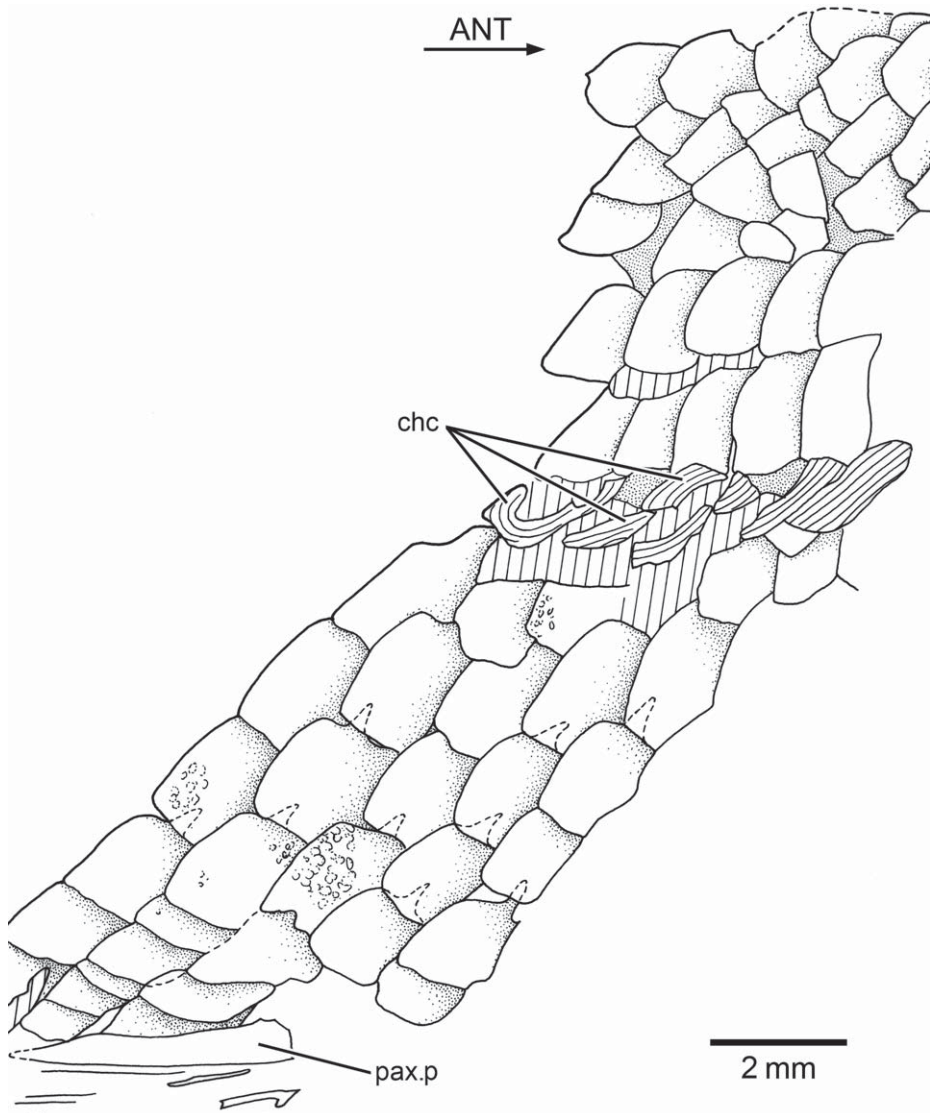


FIGURE 34. *†Annaichthys pontegiurinensis*, gen. et sp. nov. Drawing of squamation, broken chordacentra, and incomplete right pelvic fin (MCSNB 11283). Hatched lines indicate broken bone surface.

The rudimentary ray is a very thin, delicate element. The epaxial basal fulcra (Figs. 30B, 35) are elongate, leaf-like elements that expand laterally, partially covering the next fulcrum. It is not possible to confirm if the basal fulcra are paired or not because only their lateral surfaces are preserved.

The epaxial rudimentary ray and first principal ray (segmented and unbranched) are short so that the second principal ray forms part of the epaxial leading margin of the fin. It is unclear whether the last principal ray alone forms the ventral leading margin of the fin or the antepenultimate ray also takes part. The bases of the principal rays are short and thin. The articulation between segments of all principal rays is straight (Fig. 35). As far as preservation permits, no dorsal processes associated with the bases of the middle principal rays have been observed.

Fringing fulcra (Fig. 35) lie at least on the dorsal margin of the epaxial rudimentary ray, the exposed dorsal margin of the first principal ray, the exposed ventral margin of

the last hypaxial procurent, and the ventral-most principal rays.

Part of the dorsal scute is exposed between the scales and first epaxial basal fulcrum. Its posterior tip is bifurcated. An elongate ventral scute lies between the scales and first hypaxial basal fulcrum.

Scales—The body is covered by thick ganoid scales (Figs. 30A, B, 34, 35), most of which are square or slightly deeper than long and with smooth posterior margins. Posteriorly, the scales become rhomboidal and smaller. The scales of the three horizontal rows covering the mid-region of the flank are slightly deeper than the dorsal and ventral scales. The main horizontal row carrying the lateral line canal cannot be followed because these scales are partially damaged or displaced so that part of the vertebral centra are observed. There is no obvious difference in shape among scales of the caudal region of the body, but the scales become progressively smaller posteriorly.

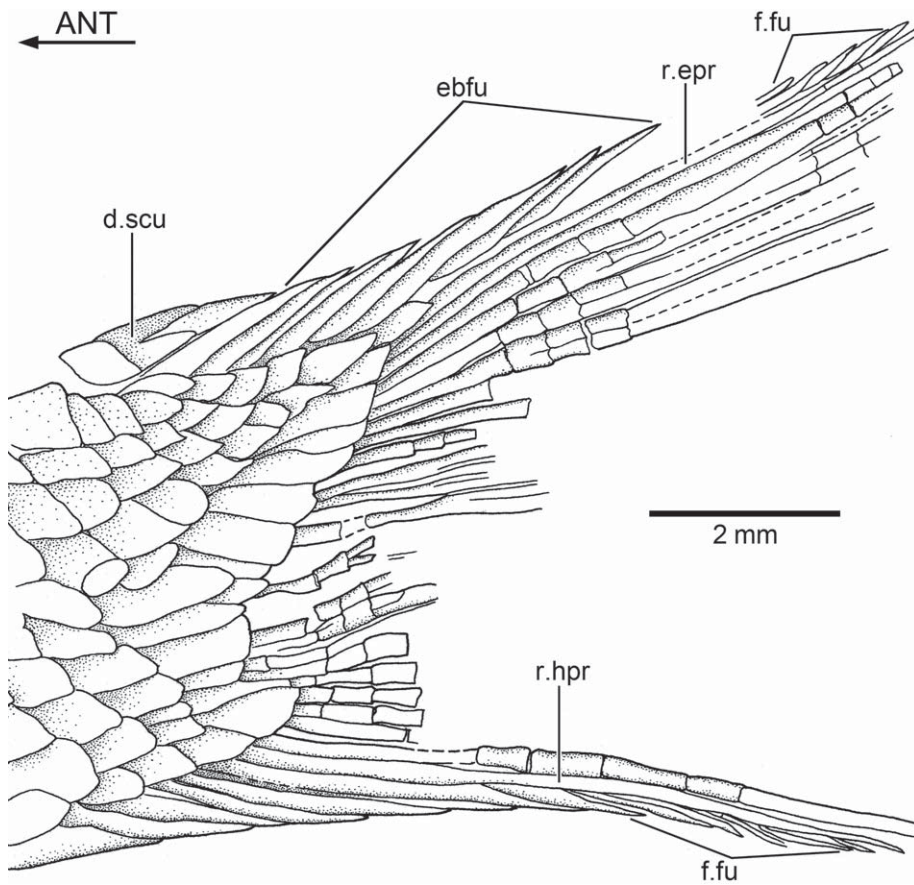


FIGURE 35. *†Annaichthys pontegiurinensis*, gen. et sp. nov. Drawing of caudal fin in left lateral view (holotype; MCSNB 18282b).

The surface of most scales is weathered away, but some show their external surfaces covered with scattered, large and rounded tubercles of ganoine, similar to those present on the head.

Lateral Line—I counted 36 to 38 vertical rows of scales from the posterior margin of the postleithral region to the last scale that would carry the lateral line canal. This number is within the range of scale rows found in other pholidophorids described here.

†KNERICHTHYS, gen. nov.

Diagnosis—Based on a unique combination of characters. Autapomorphies are identified with an asterisk [*]. Moderately large pholidophorid reaching about 140 mm total length. Cranial bones and scales are covered with ganoine. Characteristically paved ornamentation composed by small, rectangular ornaments of ganoine placed on postorbital region of skull roof plate [*]. Parietal bones ending anteriorly in a broad, almost straight margin [*]. Nasal bones broadly separated from each other by parietals [=frontal] bones. Infraorbital 3 extending posteriorly below suborbitals and extending to anterior margin of preopercle. One elongate supramaxilla, about half the length of maxilla [*]. Lower jaw elongated; quadrate-mandibular articulation behind posterior margin of orbit. Small preopercle, roughly rhomboidal [*], moderately expanded at its anteroventral region and moderately narrow dorsally. Straight anteroventral preopercular margin. Preopercle without a notch at its posterior margin. Caudal fin with many principal rays (28 or 29) [*]. Body covered by rhombic, square, and slightly triangular ganoid scales. Scale surfaces with characteristic

ornamentation of thick, straight, and concentric ridges of ganoine [*]. Scales with slightly serrated posterior margin.

Type Species—†*Knerichthys bronni* (Kner, 1866).

Content—Type species only.

†*KNERICHTHYS BRONNI* (Kner, 1866)
(Figs. 36–43)

†*Pholidophorus bronni* Kner, 1866:185, pl. 5, fig. 1.

†*Pholidophorus bronni* Schultze, 1966:fig. 21c₁, c₂.

Holotype—GBA 1866/004/0009 (Figs. 36, 37). An almost complete, but poorly preserved specimen with its body bent. With the exception of the caudal fin, all other fins are missing. Kner (1866:pl. 5, fig. 1) did not assign a type for his new species, †*Pholidophorus bronni*, but he illustrated one specimen that is currently cataloged in the GBA as the neotype. In contrast, Schultze (1966:251) interpreted it as the holotype, because it is the same specimen illustrated by Kner (1866) and the main source of his assignment as a new species. I interpret this specimen as the holotype.

Additional Material Examined—Innsb. 6b, 6c; GBA 2006/096/0024, GBA 2006/098/0150, GBA 2006/087/0055. Peels of scales from different parts of the body were studied. The peels were done by Hans-Peter Schultze using the methods described in Schultze (1966).

Type Locality, Age, and Distribution—The holotype and other specimens studied here were recovered in Raild (= Cave del Predil), Friaul, 15 km south of Tarvisio, province of Udine in Italy; Tarvisio is located at the borders of Austria and Slovenia.



FIGURE 36. †*Knerichthys bronni*, gen. nov. (GBA 1866/004/0009). Photograph of holotype in right lateral view. Scale bar equals 5 mm.

The rocks are Upper Triassic; Raibler Schiefer, Carnian, about 228–216 Ma.

Diagnosis—As for genus.

Etymology—*Knerichthys*, honoring the contribution of T. Kner to the knowledge of Late Triassic pholidophorids, and *ichthys* (Greek, fish).

Comments—Among the species presented here, †*Knerichthys bronni* is one of the most incompletely known; however, it is one of the species most easily identifiable due to its combination of unique features.

Description

With the exception of certain bones of the head and squamation, the anatomical description of certain regions of the body, as well as morphometric and meristic traits, is almost impossible due to conditions of preservation. Most specimens are markedly bent, so that fins are usually destroyed (Figs. 36, 38, 40). The vertebral column, ribs, supraneurals, and dorsal and anal pterygiophores are obscured by the presence of the squamation covering the postcranial skeleton.

Braincase—The braincase seems to be short; its posterior margin is positioned at the level of the anterior margin of the opercle. Except for the skull roof bones and pieces of the parasphenoid, no other elements of the braincase are observed.

Skull Roof—The skull roof is incompletely preserved in the holotype (Fig. 37), especially posteriorly. As far as the preservation permits, there are no crestae or fontanelles in the skull

roof, and all bones (parietals, postparietals, autosphenotics, and dermopterotics) are fused into a bony plate. Sutures are not observed, with the exception of an incomplete suture between the parietal bones anteriorly. The paired extrascapula and posttemporal bones are not preserved in the holotype. The skull roof is broad anteriorly, ending in an irregular margin that sutures anteriorly with the rostral bone and laterally with the nasal bones, which are separated medially. The skull roof plate maintains its breadth in the orbital region, which increases progressively posteriorly and becomes very broad at the level of the posterior corner of the orbital margin and throughout the postorbital region. The breadth of the skull roof at the level of the posterior tip of the nasal bones is about one-third of the postorbital region; this is a very different pattern from that in †*Pholidophorus latiusculus* (narrow: one-fifth), †*Pholidophorus gervasutii* (narrow: one-fifth or one-sixth the width of the postorbital region), and other species described here. There is no evidence of cephalic sensory canals or their pores in the skull roof plate. A well-developed, distinct middle pit-line groove is framed by thickened margins, nearly extending to the lateral margin of the skull roof plate. Only the right middle pit-line groove is preserved in the holotype. Anterior and posterior pit-line grooves have not been observed.

A piece of the rostral bone, positioned between both nasal bones, is present in the holotype. The nasal bones (Fig. 37) are incompletely preserved; they lack the round foramen that it is found in some pholidophorids; the right bone is covered with tubercles of ganoine. However, the preserved rostral and nasal bones are not informative.

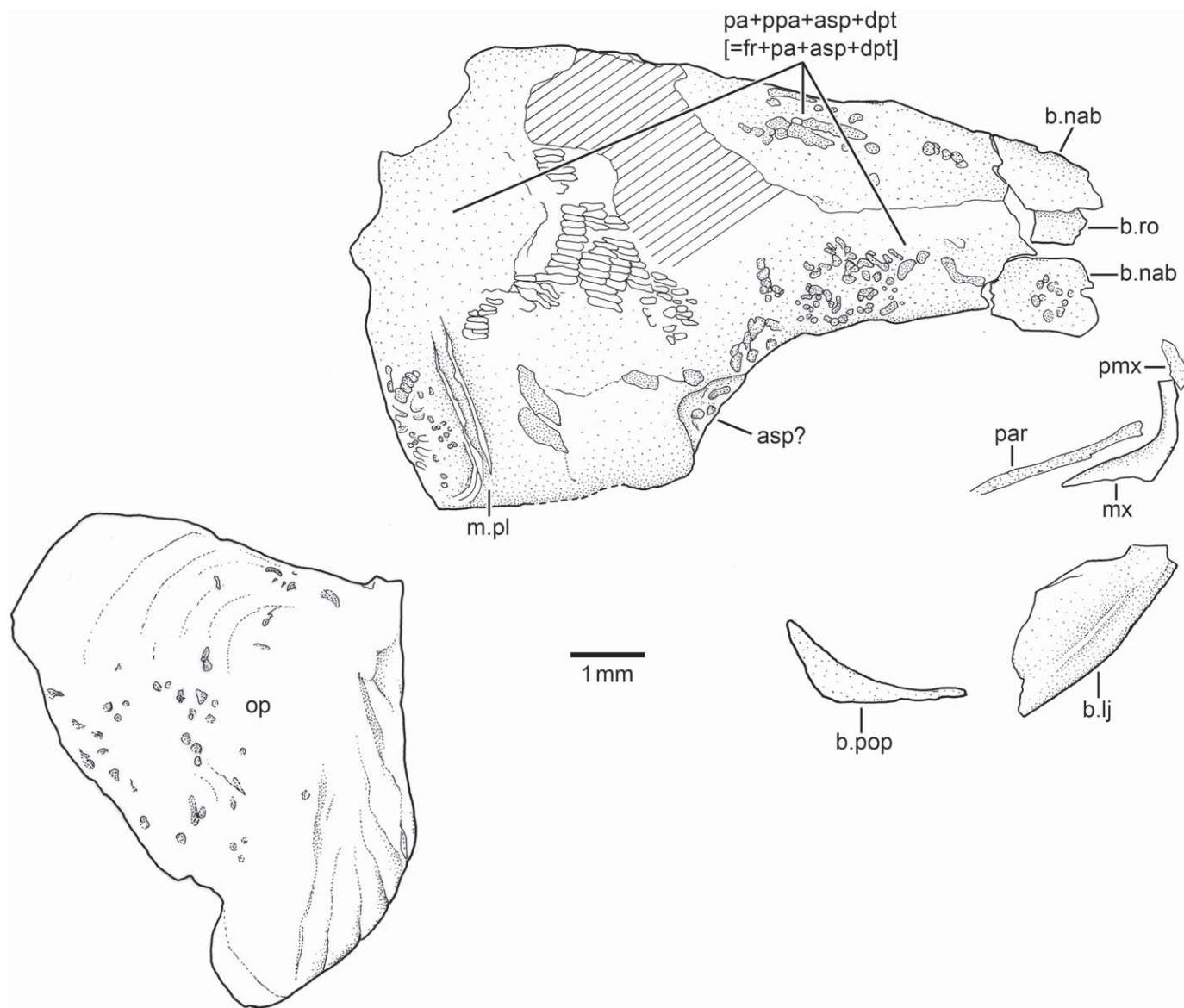


FIGURE 37. *†Knerichthys bronni*, gen. nov. (holotype; GBA 1866/004/0009). Drawing of skull roof bones and a few broken cheekbones in right lateral view. Noted the paved ornamentation of ganoine in the skull roof. The opercle is shown in approximately its normal position, but in the fossil, the bone is displaced and lying at the posterodorsal region of the cranium. Hatched lines indicate broken bone surface.

A large bone, preserved dorsal to the opercle, is interpreted here as the posttemporal (Figs. 39, 40). The bone does not appear to have processes to articulate with the posterior face of the braincase. The bone is expanded anteriorly, and its ventral portion is thickened where it carries the postotic canal or lateral line.

The surface of the skull roof plate (Fig. 37) is covered with tubercles of ganoine of different sizes; some large tubercles are observed close to the margin of the skull roof plate, in front and behind the deep and well-developed middle pit-line. The postorbital region of the skull roof plate is covered with characteristic elongate, rectangular plates of ganoine, arranged closely together in a kind of pavement (Fig. 37). This kind of ornamentation is concentrated at the middle of the postorbital region and is unique to this species among all taxa studied here.

Circumorbital Series—The circumorbital ring (Figs. 39, 40) is incompletely preserved and is represented by infraorbitals 1, 3, 4,

and 5 and the dermosphenotic. The antorbital and supraorbital are not preserved in the available material. In addition, several suborbitals and remnants of sclerotic bones are preserved.

An incomplete infraorbital 1 (Fig. 39) is observed in GBA 2006/097/0055. The bone is represented mainly by its anterior part. The infraorbital sensory canal apparently is positioned along the mid-section of infraorbital 1.

Although infraorbitals 3 to 5 are poorly preserved, it is possible to restore the area occupied by them and the suborbitals in BGA 2006/098/0150. It appears that the area between the posterior margin of the orbit and the anterior margin of both the opercle and preopercle is especially enlarged, a condition not observed in other pholidophorids. Infraorbital 3, as far its preservation permits, extends posteriorly, contacting the anterior margin of an elongate suborbital and the anterior margin of the preopercle. Infraorbitals 4 and 5 are slightly rectangular and small

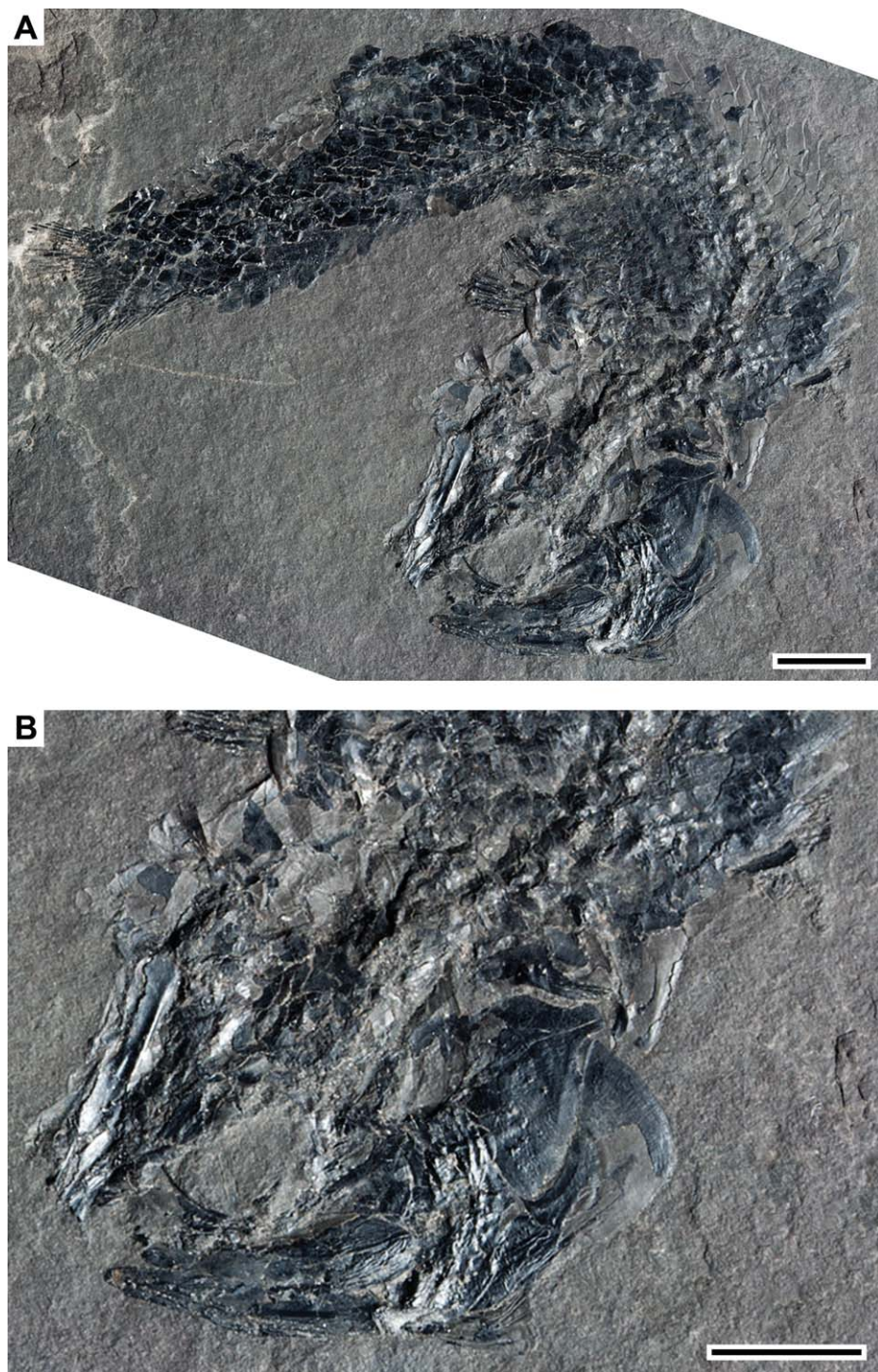


FIGURE 38. †*Knerichthys bronni*, gen. nov. **A**, photograph of specimen GBA 2006/097/0055. **B**, enlargement of the head. Scale bars equal 5 mm.

bones (about half the length of infraorbital 1). A slightly triangular, relatively small dermosphenotic is preserved at the posterodorsal corner of the orbit. The surface of this bone is covered by a thick layer of ganoine with a few tubercles of different sizes.

The space between the infraorbitals 3, 4, and 5, and the opercle is occupied by at least four suborbitals in BGA 2006/098/0150. Three of them are mainly rectangular, but the posterior one is long and positioned between the anterior suborbitals, posterior margin of infraorbital 3, and opercle. Because this region is damaged in

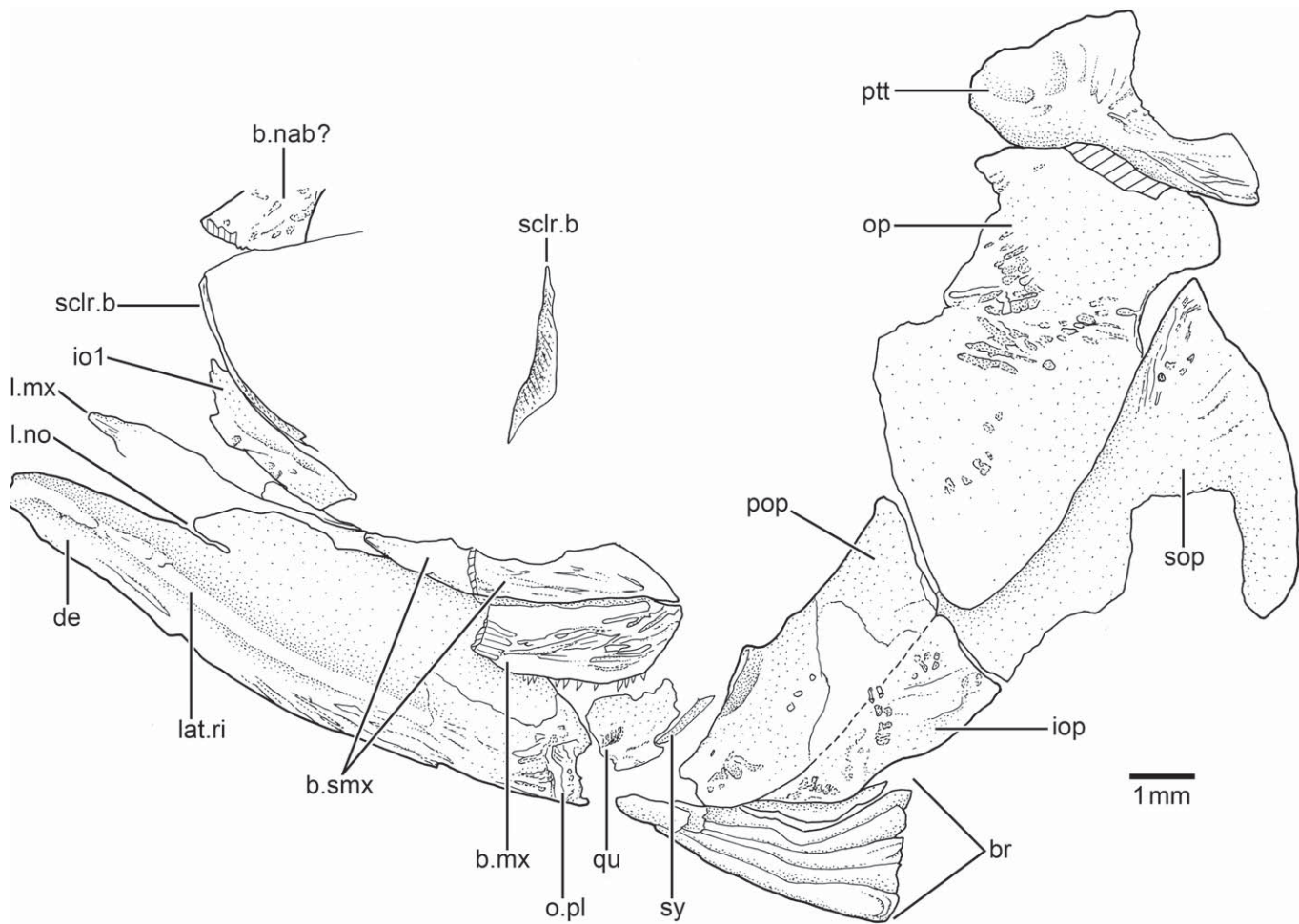


FIGURE 39. *†Knerichthys bronni*, gen. nov. Drawing of head in left lateral view (GBA 2006/097/0055). Note the shape and size of the preopercle and posttemporal. Hatched lines indicate broken bone surface.

other specimens, I refrain from making any conclusions about the presence of the suborbitals.

Upper Jaw—The upper jaw is represented by a small piece of the premaxilla, which is not informative, and the maxilla and a single supramaxilla.

The maxilla (Fig. 39) is incompletely preserved in the holotype and only represented by a long and curved anterior articular region. In other specimens, the maxilla is only known from its incompletely preserved blade. The posterior margin of the maxilla is slightly oblique (Fig. 39) in one specimen, but slightly notched in another. As far as can be observed, small conical teeth, ordered in one row, are carried by the oral margin up to its posterior corner. The exposed surface of the maxilla is densely covered by thick, short ridges of ganoine. A similar pattern of longitudinal ridges is observed on the surface of the supramaxilla.

Only one supramaxillary bone (Fig. 39) is present. Although the bone is broken in BGA 2006/097/0055, the two parts (*in situ*) show that the bone was about half the length of the maxillary blade. The supramaxilla is slightly fusiform, with its maximum depth close to the posterior margin.

Lower Jaw—The lower jaw (Fig. 39) is almost complete, but poorly preserved in BGA 2006/097/0055. The dentary (Figs. 39, 40) forms most of the lower jaw length, but the position of its suture with the angular is unclear due to the ornamented

layer of ganoine covering the region. Part of its dorsal margin is unknown because it is hidden by the maxilla and supramaxilla. The dentary has a region lacking ganoine, which is close to the oral margin above the strong longitudinal ridge that protrudes along its length. Because of the damage to the oral margin, it is unclear whether teeth were present or not. The posterior-most part of the jaw is broken in BGA 2006/097/0055 and is poorly preserved in BGA 2006/098/0150. The posterior region does not form a postarticular process. There is a narrow notch (in the position of the ‘leptolepid’ notch) in the oral margin of the dentary, at about the anterior third of the length of the jaw. Dorsal to the notch, the margin of the bone ascends abruptly, and its deepest point posterior. The ventral regions of the angular and dentary are ornamented with ridges of ganoine and a few tubercles.

Palatoquadrate, Suspensorium, and Hyoid Arch—With the exception of the quadrate and the ventral part of the symplectic, all other bones of the palatoquadrate and hyoid arch are hidden by other bones or are not preserved.

The quadrate (Fig. 39) is incompletely preserved, but it seems to be a small bone, with a well-ossified articular region for the lower jaw and posterior margin. However, the articular region for the jaw is narrow and not expanded laterally, and the posterior margin of the bone is short. Only the ventral tip of the symplectic is preserved.

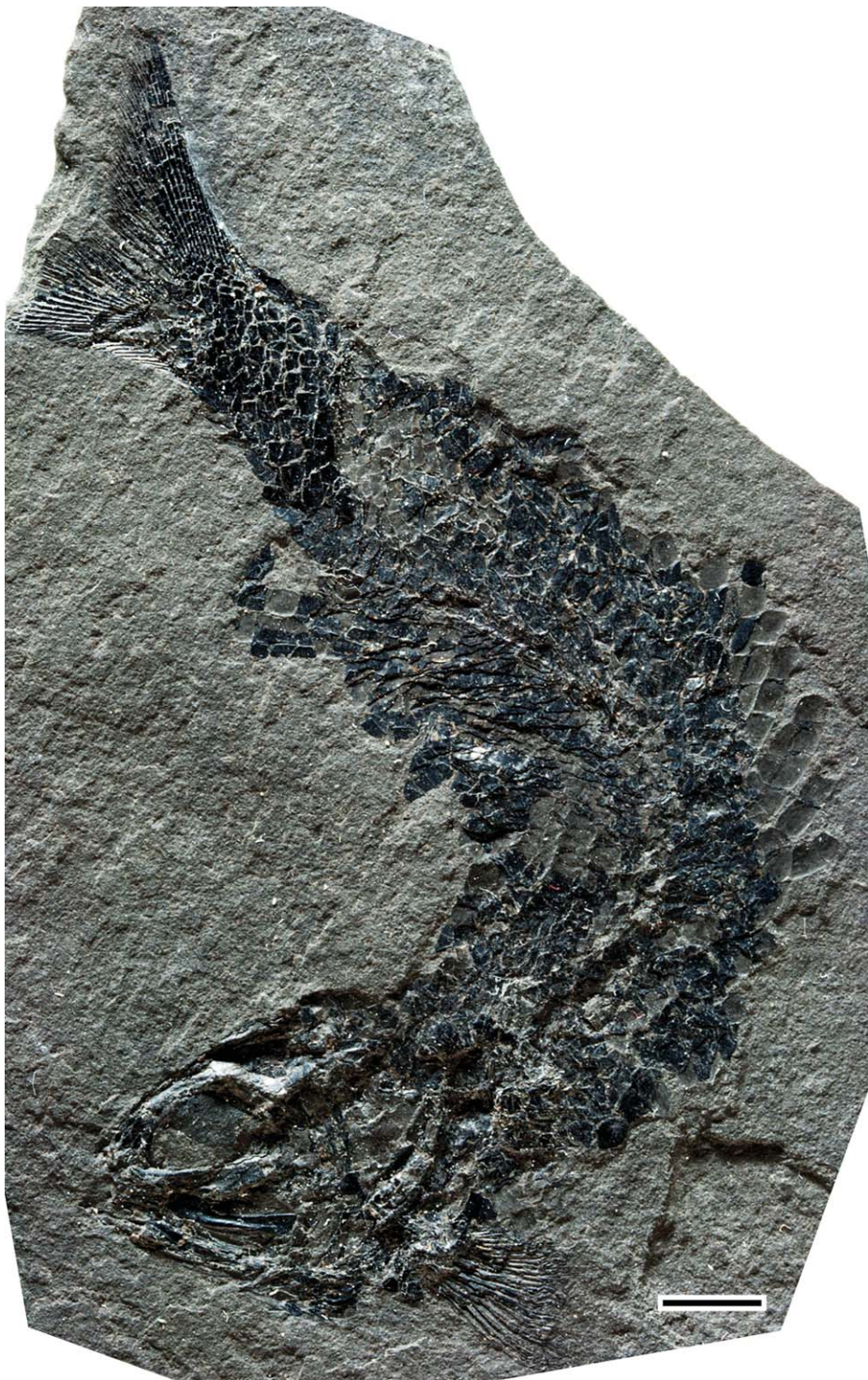


FIGURE 40. †*Knerichthys bronni*, gen. nov. Photograph of specimen GBA 2006/098/0150 in left lateral view. Scale bar equals 5 mm.

Opercular, Branchiostegal Series, and Gular Plate—The opercular bones and branchiostegal rays are incompletely preserved in the available material. The gular plate is not preserved. All opercular bones are almost completely covered by a combination of tubercles and ridges of ganoine. In addition,

the opercle of the holotype has concentric ridges close to its dorsal margin and a series of ridges close to its anteroventral margin.

The preopercle (Fig. 39) has a curious, slightly rhomboidal shape. It is not expanded ventrally and only narrows dorsally, end-

ing in an acute tip. There is no distinction between dorsal and ventral arms, and a notch is absent at the posterior margin of the preopercle. The anterior margin of the preopercle presents a narrow articular surface where the posterior margin of infraorbital 3 abuts. The anteroventral margin may have a tiny notch or the notch may be absent. The posterior margin of the preopercle joins the large interopercle. The course of the preopercular canal is unknown.

The opercle (Figs. 37, 39, 40) is a large, roughly triangular bone. The anterior margin of the opercle is partially straight, but becomes rounded ventrally. The ventral margin of the opercle is gently oblique and long.

The subopercle (Fig. 39) seems to be a large bone. Its posteroventral margin is somewhat rounded. Its anterior margin seems to be oblique. The anterodorsal process of the subopercle is well developed and sharp.

The interopercle (Figs. 37, 39, 40), displaced and partially exposed in BGA 2006/097/0055, is large and triangular. It is positioned between the posterior margin of the preopercle and anterior margin of the subopercle.

Vertebral Column and Intermuscular Bones—No information is available yet.

Paired Girdles and Fins—Very little can be said about the paired girdles and fins, because they are incompletely preserved

or are not exposed in the available material. Only one pectoral fin (Fig. 40) is moderately well preserved. The fin has about 22 rays; the most lateral rays are longer than those medially placed. The rays have long bases and are segmented and bifurcated only close to their distal tips. The structure of the first ray remains unknown. Additionally, it is unclear whether axillary processes are associated with the paired fins as in other pholidophorids described here.

Dorsal and Anal Fins—The dorsal fin and anal fins are not preserved, so a description is not possible.

Caudal Fin—The caudal endoskeleton has not been observed because the squamation is in situ in the studied specimens. The hemi-heterocercal caudal fin (Figs. 36, 40, 41, 42) is forked, with middle principal rays that are not as short compared with other caudal fins described here. The area covered by ganoid scales at the base of the caudal fin ends in two lobes formed by scales, but many of the scales are displaced or removed so that the exact posterior margin of the body squamation is unknown (Figs. 41, 42).

The caudal fin is slightly damaged in the holotype (Fig. 41) and better preserved in the other two specimens (e.g., Fig. 42). There are nine epaxial basal fulcra, a series of elongate epaxial fringing fulcra, one thin and short epaxial rudimentary ray, 28 or 29 principal rays, a series of elongate hypaxial fringing fulcra, four or five hypaxial segmented procurent rays, and four hypaxial basal fulcra. Long and thin accessory fulcra are positioned between the tips

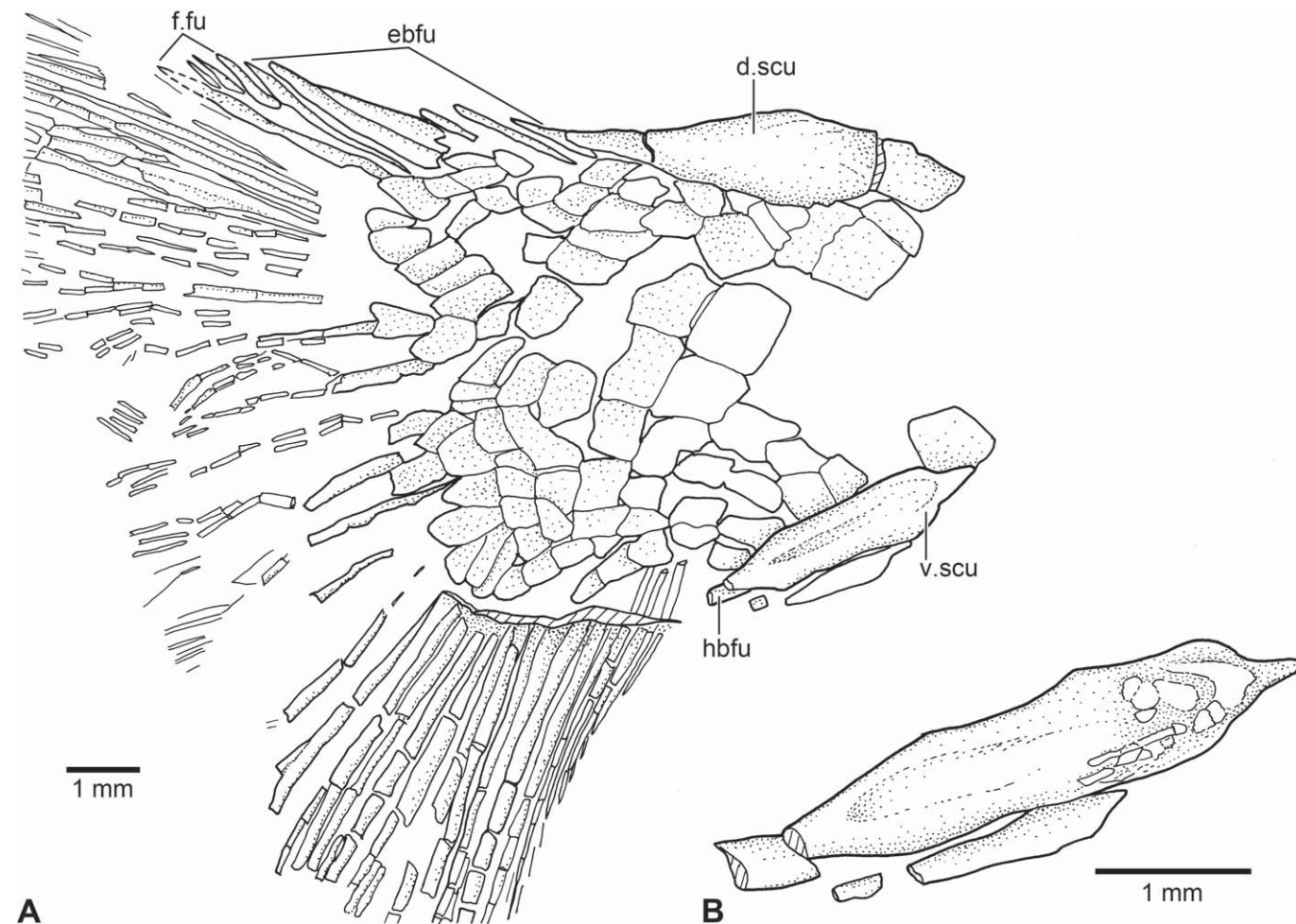


FIGURE 41. †*Knerichthys bronni*, gen. nov. (holotype; GBA 1866/004/0009). A, drawing of caudal fin and squamation in right lateral view. B, enlargement of ventral caudal scute and pieces of hypaxial basal fulcrum.

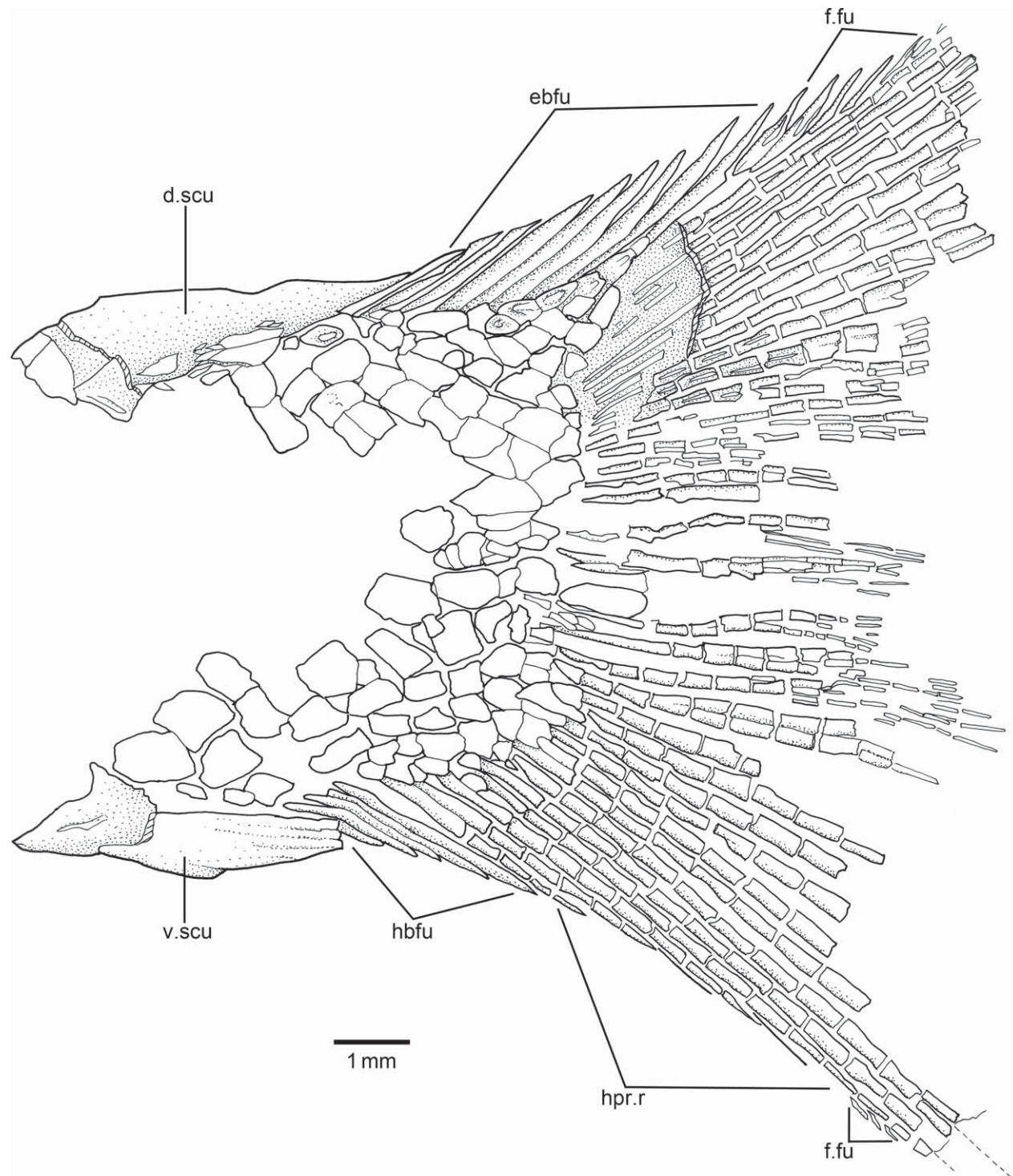


FIGURE 42. \dagger *Knerichthys bronni*, gen. nov. (GBA 2006/098/0150). Drawing of caudal fin and squamation in left lateral view.

of the procurent rays. The anterior-most epaxial basal fulcra are unpaired (also in GBA 2006/096/0024), and the hypaxial basal fulcra seem to be unpaired as well. The segmentation of the delicate, thinly ossified principal rays is straight.

The epaxial and hypaxial series of basal fulcra are preceded by well-developed scutes (Figs. 41, 42). The dorsal scute is longer and broader than the ventral one, and it ends in an acute tip posteriorly. The ventral scute is slightly protruding along its main axis

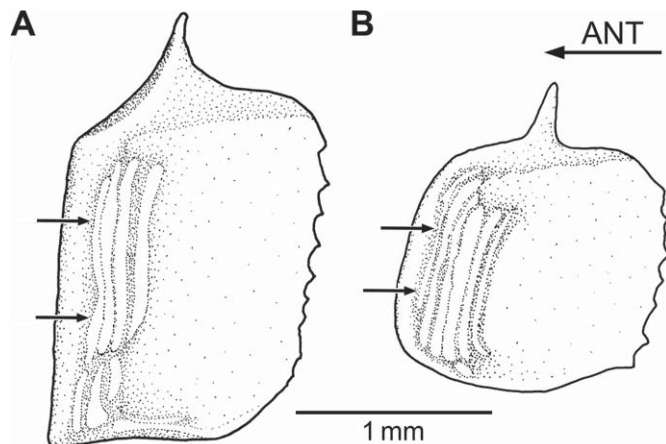


FIGURE 43. *†Knerichthys bronni*, gen. nov. (GBA 2006/098/0150). Scales from the middle (A) and ventral (B) regions of the body in front of pelvic fins; redrawn from Schultze (1966). Small arrows point to the thick ridges of ganoine.

and has preserved tubercles of ganoine of different sizes in the holotype.

Scales—*†Knerichthys* scales were first described and illustrated by Schultze (1966:fig. 21c). Ganoid rhombic scales (Fig. 43) of different sizes cover the body. The layer of ganoine covering the surface of the scales is characteristically ornamented with well-developed ridges of ganoine that may be straight or form a concentric pattern. The posterior margin of the scales is delicately serrated. The scales of the three main rows of the flank are deeper than broad and are slightly larger than those forming the dorsal and ventral horizontal rows. Most scales of the dorsal and ventral rows of the flank are rhombic or slightly rectangular or even square.

Lateral Line—Due to the curvature of the body of the available specimens, it is not possible to count the number of scales bearing the lateral line.

†PHOLIDORHYNCHODON Zambelli, 1980b

Diagnosis—Emended from Zambelli, 1980b, and based on a unique combination of characters. Autapomorphies are identified with an asterisk [*]. Moderately large pholidophorids reaching about 150 mm total length. Cranial bones and scales are covered by a thick layer of ganoine, ornamented with patches of intertwined tubercles and ridges producing a complex, distinct pattern [*]. Anterior tips of parietal bones unfused medially, commonly asymmetric, and joining rostral bone. Large nasal bones broadly expanded and separated from each other by anterior tips of parietal [= frontal] bones. Large, rounded foramen positioned near the lateral margin of nasal bone. Rostral bone with teeth moderately large and conical [*]. Dentate rostral and lateral rostrodermethmoid forming part of dorsal oral margin [*]. Premaxillaries laterally displaced by rostrodermethmoids [*]. Moderately small orbits, with a diameter of about 23% of the head length. A large plate-like and posteriorly expanded infraorbital 3. Large, squarish suborbital. Premaxilla, maxilla, and dentary with more than one row of strong conical teeth [*]. Jaws elongated; quadrate-mandibular articulation is posterior to orbit. Preopercle expanded at its anteroventral region with a small notch at its anterior margin (heart-like shaped) and a narrow dorsal region. Acute dorsal tip of cleithrum bent anteriorly [*]. Dorsal

fin insertion slightly anterior to pelvic fins [*]. Lateral line row comprising 38 to 40 scales. One or two additional lateral line canals extending between extrascapular bone and base of dorsal fin [*].

Content—*†Pholidorhynchodon malzannii* Zambelli, 1980b; only species known.

†PHOLIDORHYNCHODON MALZANNII Zambelli, 1980b (Figs. 44–56)

Holotype—MCSNB 3385 (Fig. 44A, B). Almost complete specimen missing part of the caudal fin. All fins are poorly preserved.

Material Examined—There are about 100 specimens cataloged in MCSNB. After checking all specimens, the following were selected for study because of the morphological information that they provide: MCSNB 3161, MCSNB 3164, MCSNB 3243, MCSNB 3244, MCSNB 3274, MCSNB 3276, MCSNB 3281, MCSNB 3284–3287, MCSNB 3335, MCSNB 3353, MCSNB 3381, MCSNB 3386, MCSNB 3392, MCSNB 3848, MCSNB 3859, MCSNB 3862, MCSNB 3887, and MCSNB 3914.

Type Locality, Age, and Distribution—Only known from the type locality Cene, about 17 km northeast of Bergamo, Lombardy, northern Italy; Late Triassic (Norian), about 210 Ma.

Diagnosis—As for the genus.

Description

Similar to all other species studied here, the anatomical description of certain regions of the body, such as the braincase and vertebral column and its associated elements, is difficult due to poor preservation. Internal structures, such as the vertebral column, ribs, and intermuscular bones, are obscured by the presence of squamation in most specimens. Due to this preservation, only sections of the vertebral column have been observed where the scales are damaged, removed, or displaced. Nevertheless, the preservation of some specimens provides new knowledge of some structures previously unknown in other Triassic pholidophorids, as will be shown below.

The members of this species are moderately large, reaching a total length of about 150 mm (MCSNB 3161). The fishes have slightly oblong bodies, with their maximum depth between the postcleithra and origin of the dorsal fin. The caudal peduncle is moderately narrower than the rest of the body. It is about one-third of the predorsal depth. The snout is short, measuring about 18% of head length. The head is moderately large, about 30% of the standard length. The head is almost triangular, with its deepest points at the posterior end of the cranial roof. The dorsal fin is positioned slightly anterior to the insertion of the pelvic fins, and the anal fin is closer to the pelvic fins than to the caudal fin. The pectoral fins are closer to the ventral margin of the body than to the middle region of the flanks. All fins are small, with very delicate and slender rays and bear elongate fringing fulcra associated with the leading margins.

The layer of ganoine covering the external cranial dermal bones, dermal bones of the pectoral girdle, and scales is often weathered away. However, where ganoine is preserved, it shows a curious pattern produced by a combination of corrugated ridges and tubercles (Figs. 44B, 45, 46) intertwined in such a way that the surface of bones and scales is uniquely ornamented among Triassic pholidophorids. The maxilla and supramaxillae bear mainly obliquely oriented ridges. The lower jaw, especially along the middle region where the prominent bony ridge protrudes laterally, is obscured by the dense ornamentation composed of peculiarly arranged ganoine ridges (Figs. 44B, 45B, 47). The thick ornamentation obscures the detection of pores of the cephalic sensory canals, as well as of pit-line grooves. Cephalic sensory canals,

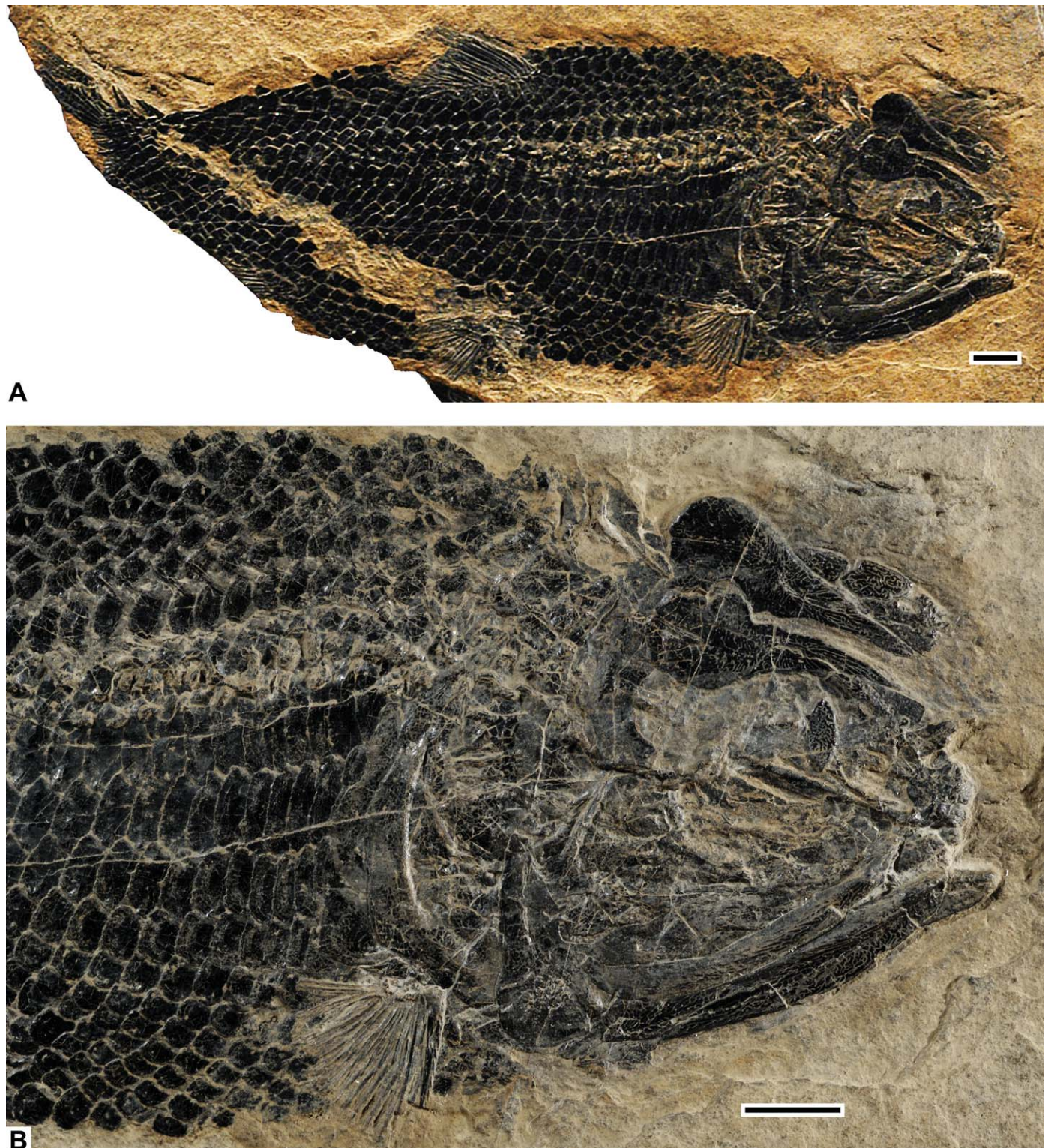


FIGURE 44. \dagger *Pholidorhynchodon malzannii* Zambelli (holotype; MCSNB 3385). **A**, photograph of holotype in right lateral view. **B**, enlargement of head. Scale bars equal 5 mm.

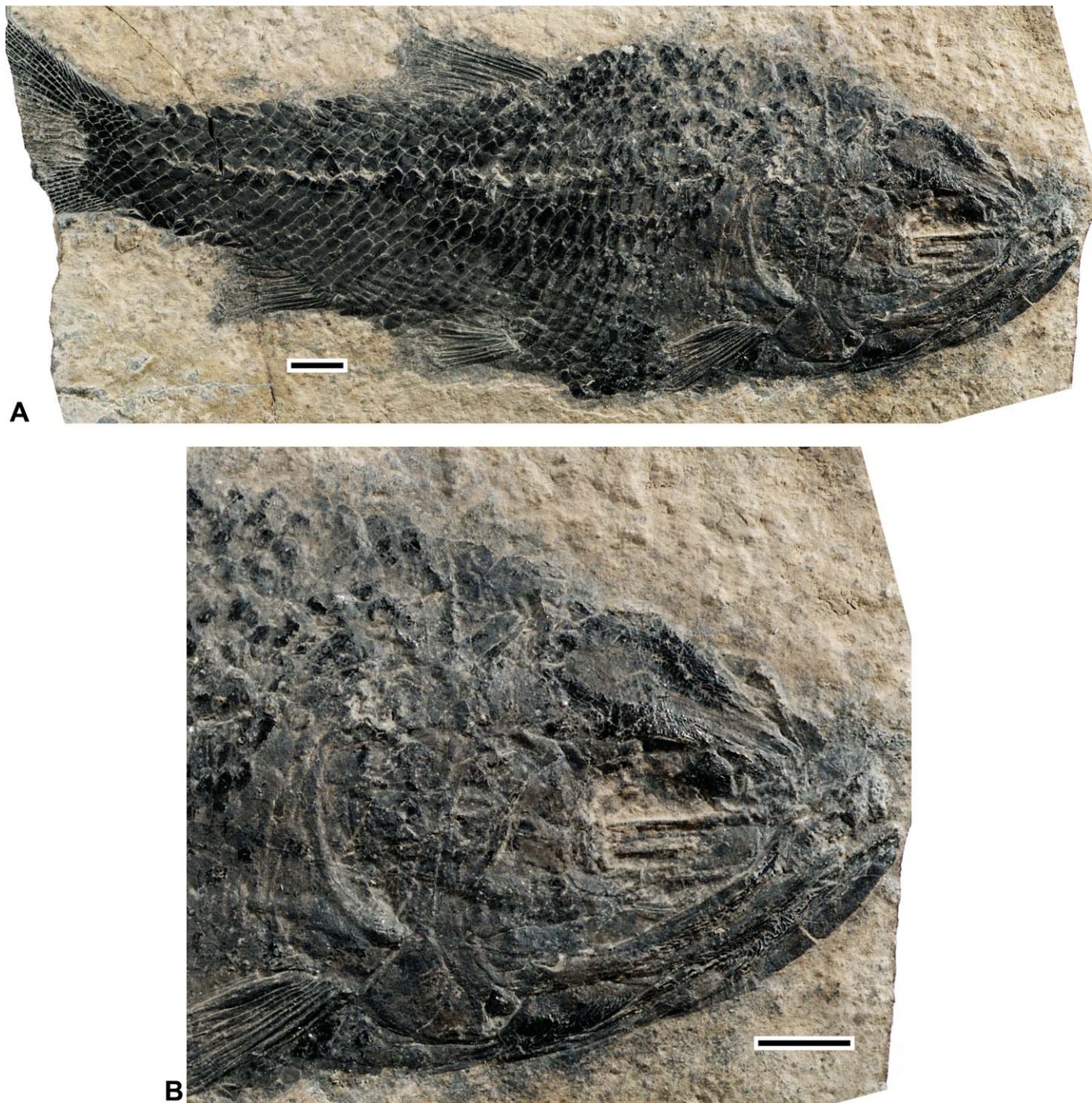


FIGURE 45. \dagger *Pholidorhynchodon malzannii* Zambelli (MCSNB 3164). A, photograph in right lateral view. B, enlargement of head. Scale bars equal 5 mm.

tubules, and/or pores are observed in specimens with the layer of ganoine weathered away.

Braincase—The braincase of the holotype (Fig. 44A, B) appears to be short, and in some specimens it is even shorter, so that the skull roof plate does not reach the level of the opercle (Fig. 47A). Except for the skull roof bones and parasphenoid, no other elements of the braincase are observed. The parasphenoid is shown

in ventral view in Figure 48A. The anterior part of the bone resembles an inverted 'V' in cross-section. The parasphenoid is slender; it is comparatively narrower than that of \dagger '*Pholidophorus*' *bechei* and \dagger '*Ph.*' *germanicus*, (Patterson, 1975:figs. 61–63, 142), but it is slightly broader than the parasphenoid in \dagger *Leptolepis coryphaenoides* (Patterson 1975:fig. 144; pers. observ.). In the anterior part of the orbit, the parasphenoid broadens, with its

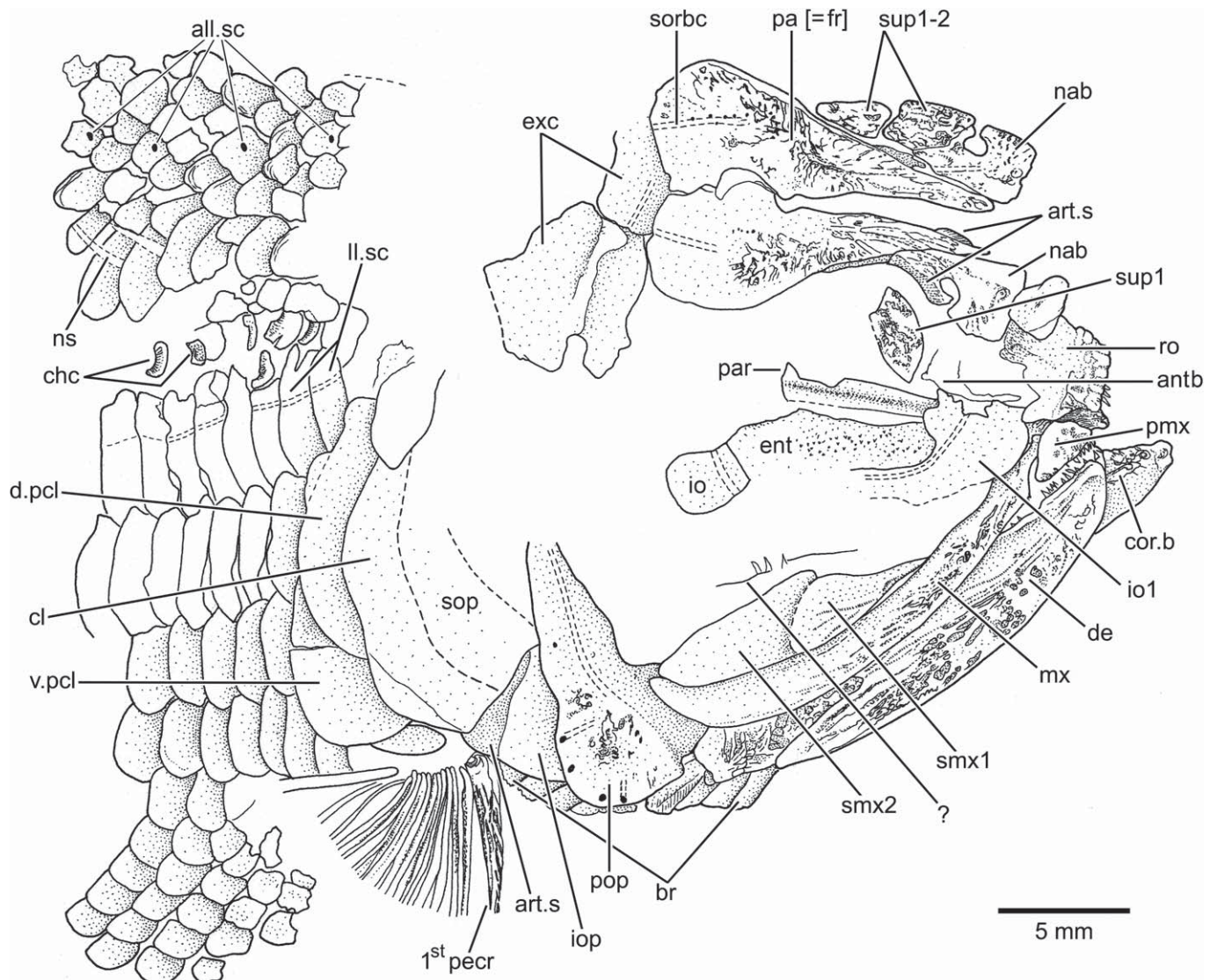


FIGURE 46. *†Pholidorhynchodon malzannii* Zambelli (holotype; MCSNB 3385). Drawing of head, pectoral girdle, and anterior body squamation in right lateral view.

breadth increasing progressively posteriorly to reach a maximum at the level of the basipterygoid processes. On the dorsal surface of the orbital part of the parasphenoid is a median groove, not a crest, for the insertion of the membranous interorbital septum. This crest is present in *†Pholidophorus bechei*, *†Ph. germanicus*, and *†L. coryphaenoides*. The basipterygoid process (Fig. 48A) is moderately large and seems to be entirely dermal. The root or base of the basipterygoid process is perforated by a large foramen for the efferent pseudobranchial artery (Fig. 48A). In the median region of the bone, between both basipterygoid processes, is the lower opening of the buccohypophysial canal (Fig. 48A). Behind the basipterygoid process is an almost acute ascending process; the two processes are not continuous as in *†Pholidophorus bechei* and *†Ph. germanicus*, but are separated by a deep notch. Both basipterygoid processes of the parasphenoid are also comparatively narrow and shorter than those in *†Ph. bechei* and *†Ph. germanicus*. The ascending processes are asymmetric; the right ascending process is formed by two portions separated by a notch

dorsally, but the left one is formed by one portion only. The internal carotid arteries pass through a pair of anterodorsally directed canals (Fig. 48A) entering the parasphenoid behind the base of the ascending process. Another notch separates the ascending process from the posterior section of the bone. The posterior section of the bone is less than one-third the length of the entire bone. The ventral surface of the bone is slightly convex, smooth, and framed anterolaterally by thick bony ridges. The pitted region at the base of the posterior part of the bone seems to be the place of attachment of some muscles and ligaments, which are placed more posteriorly in *†Ph. germanicus* and *†L. coryphaenoides*. Like the other pholidophorids described here, the parasphenoid has no teeth.

Skull Roof—The skull roof lacks crestae and fontanelles; however, its surface is uneven due to the dense ornamentation. The coossification of the skull roof (Figs. 46, 47A, 49A, B) is highly variable, unlike other species studied here. When comparing specimens of similar size, the skull roof may be (1) separated into individual skull roof bones; (2) separated only at the interparietal

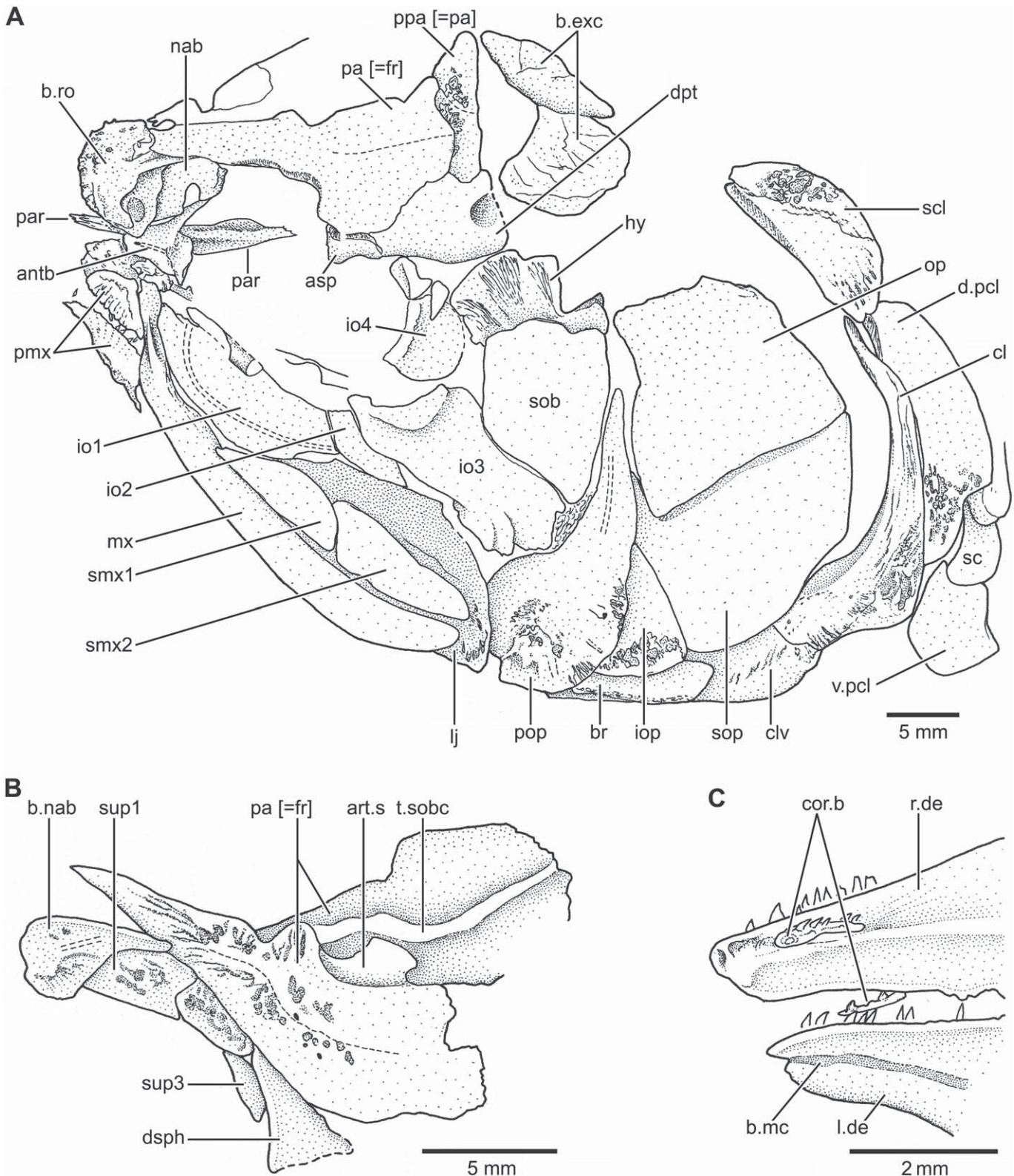


FIGURE 47. *†Pholidorhynchodon malzannii* Zambelli. **A**, drawing of head and pectoral girdle in left dorsolateral view (MCSNB 3335). **B**, displaced parietal and orbital bones (MCSNB 3838). **C**, anterior region of lower jaws (MCSNB 3848).

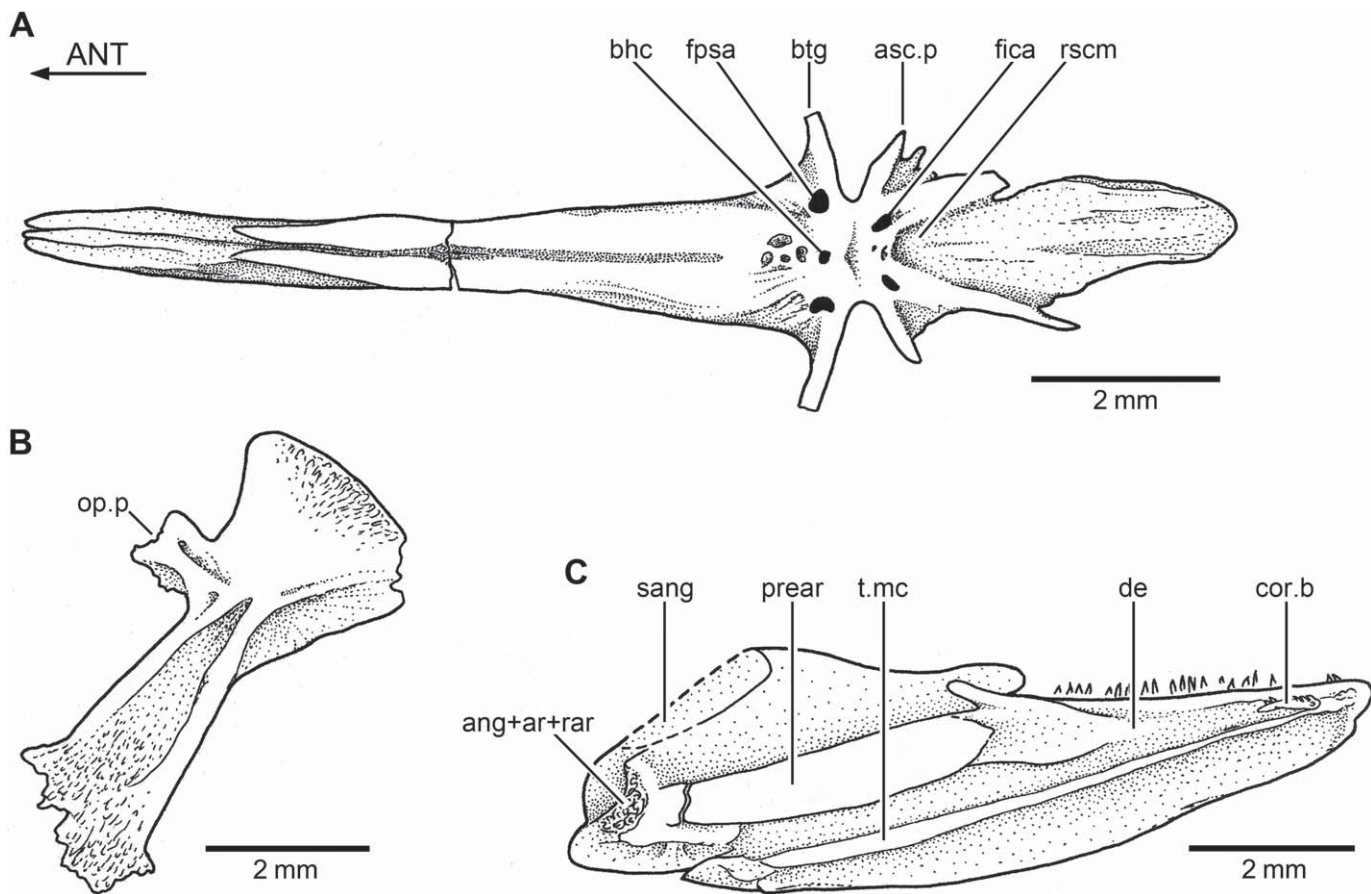


FIGURE 48. *†Pholidorhynchodon malzannii* Zambelli. A, drawing of parasphenoid in ventral view (MCSNB 3862). B, right hyomandibula in lateral view (MCSNB 3862). C, left lower jaw in medial view (MCSNB 3859).

suture; (3) completely fused into a skull roof plate; or (4) with incomplete sutures retained between bones. The most common state is parietals with their anterior tips asymmetrical. However, there is also additional variation of the anterior tip of each parietal, because in some specimens each parietal may end in just an acute tip or be irregular, ending in several projections, or even may be slightly straight. This means that in addition to the diversity of shapes, there is also diversity in the broadness of the anterior tip of each parietal.

Starting from the anterior tip of the parietals, the width of the skull roof increases progressively posteriorly, being very broad at the level of the posterior corner of the orbital margin in some specimens, whereas in others the maximum breadth is posterior to the autosphenotic region. The breadth of the postorbital region of the skull roof (Figs. 47A, 49A, B) is about four times wider than the anterior region.

In most specimens, there is no evidence of the trajectory of the supraorbital canal or its pores because the ornamentation obscures them, but where the layer of ganoine has been weathered away, the supraorbital canal and its pores are observed (e.g., Fig. 49A, B). The supraorbital canal is in the mid-region of each parietal bone, from the posterior margin of the bone (in those specimens with separated parietals) to about the first third of the bone close to the lateral margin where it enters the nasal bone (Fig. 49B). As far as can be observed, the supraorbital canal

does not continue into the postparietal region posteriorly. The pores are small and round and open directly above the canal. Their number is highly variable between the left and right sides of one specimen and among specimens. In contrast, Zambelli's (1980b) restoration shows the supraorbital canal nearer to the orbital margin of the skull roof than to the medial margin and with many more pores than I have been able to observe. A middle pit-line groove (Fig. 49A, B) is preserved in some specimens and ends near the lateral margin of the skull roof plate in the position where the dermopterotic would be. Both the anterior and posterior pit-line grooves are only occasionally observed.

A median, well-developed, heavily ossified, and slightly rhomboidal rostral bone (Figs. 46, 47A, 49A, B, 50A) is at the anterior-most region of the skull roof plate. When the bone is completely preserved, as in specimen MCSNB 3848, its anterior margin is obscured by the presence of a few conical teeth positioned on the anterodorsal margin of the rostral and by the presence of additional rows of teeth below the rostral that are interpreted here as belonging to the rostrodermethoids. There are two well-developed lateral processes that extend laterally to the anterior margin of the nasal bones. The lateral processes are usually damaged so that the complete size of the bone is unknown. A comparatively broad, triangular posterior region contacts the tips of the parietal bones medially and nasal bones laterally. The two lateral rostrodermethoids suture with each other medially and the rostral bone

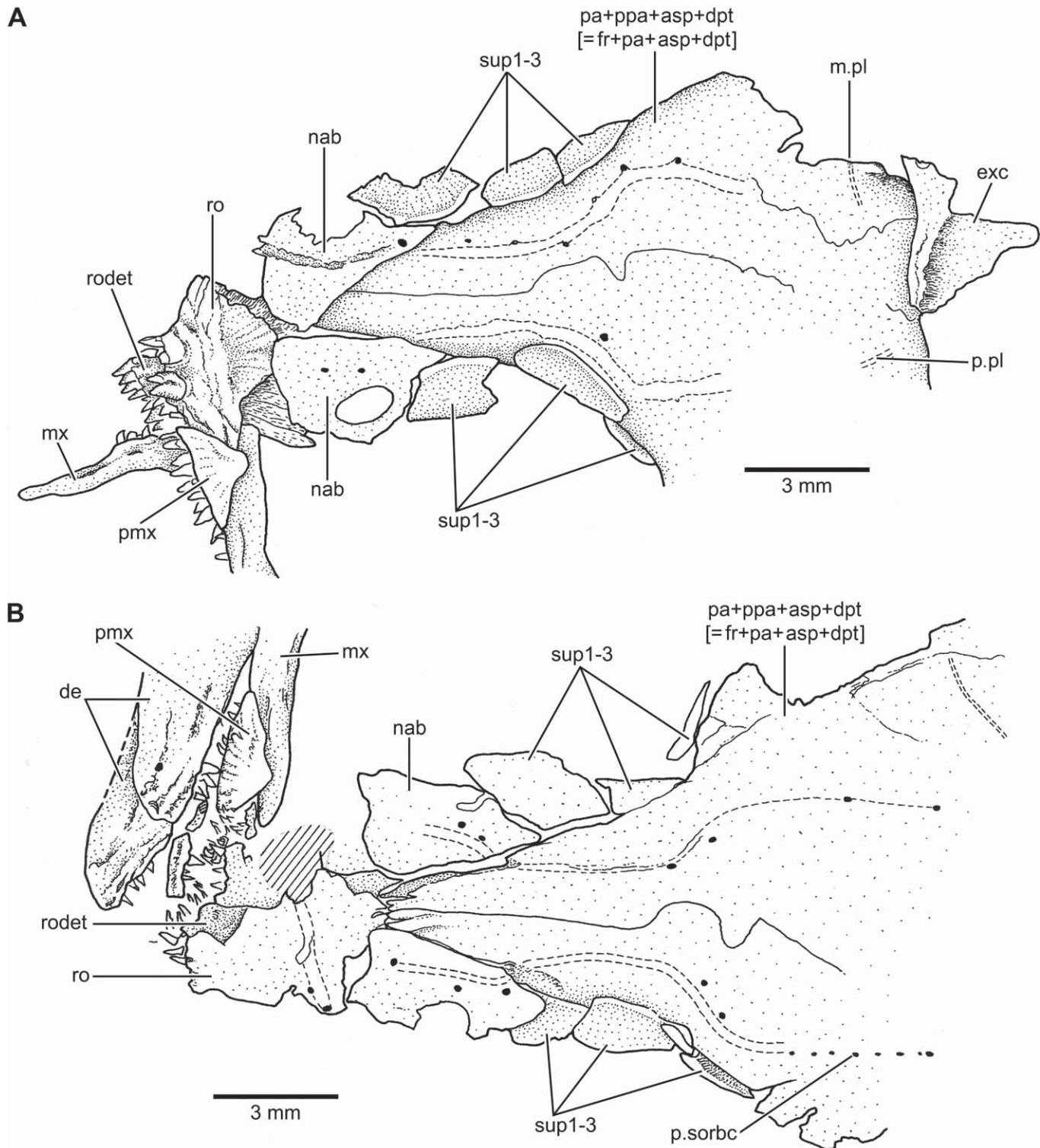


FIGURE 49. *†Pholidorhynchodon malzannii* Zambelli. Drawings of skull roof bones and associated bones. **A**, MCSNB 3848. **B**, MCSNB 11192. Hatched lines indicate broken bone surface.

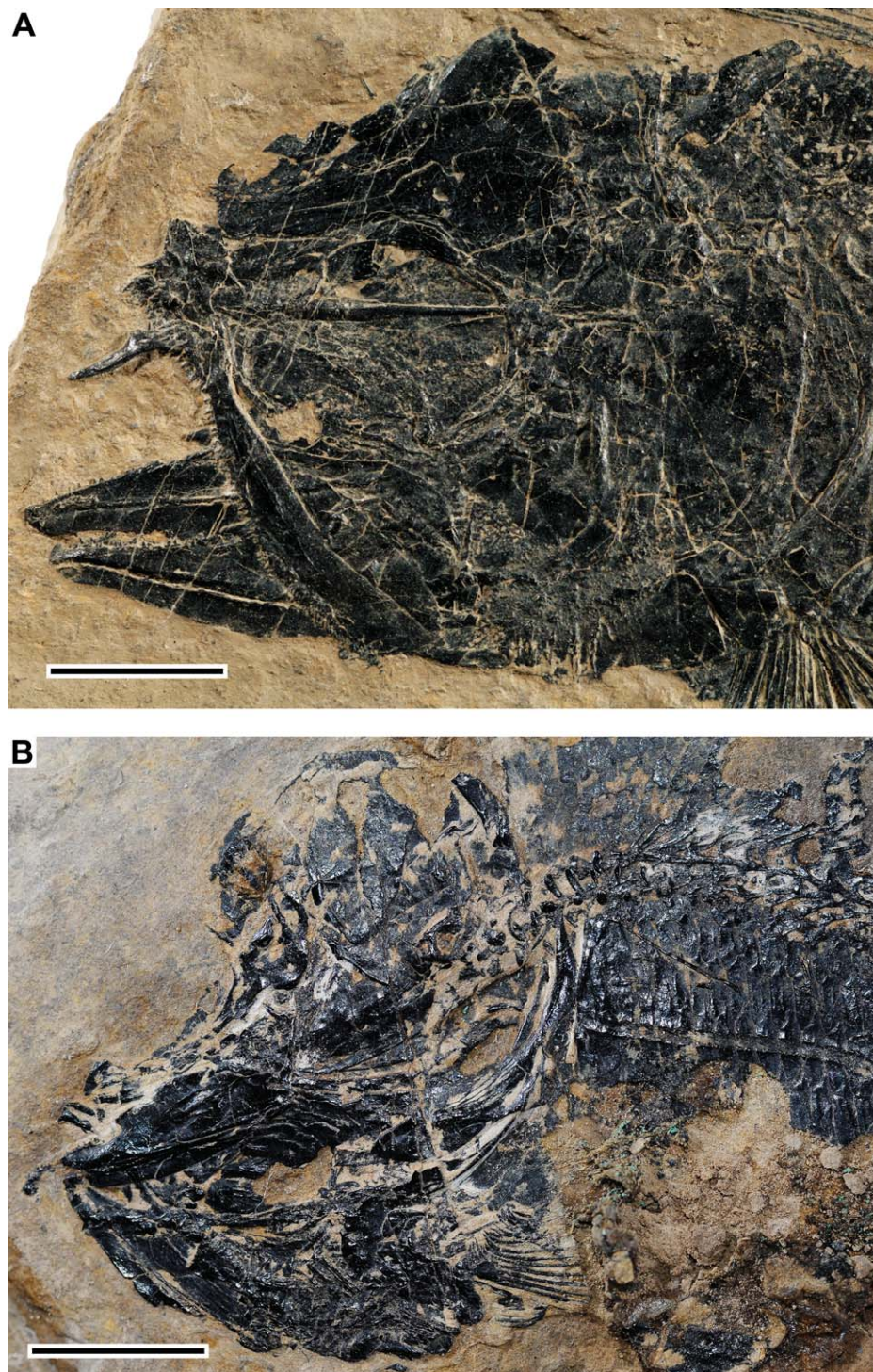


FIGURE 50. *†Pholidorhynchodon malzannii* Zambelli. Photographs of head and anterior part of body in lateral view. **A**, MCSNB 3848. **B**, MCSNB 11192. Scale bars equal 5 mm.

dorsally; each bone extends posteriorly in a lateral wing, which is partially covered by the nasal bone (Fig. 49A). A rostral and rostrodermethmoid such as these have not been observed in any of the other fishes studied here. As far as can be observed, the median oral margin is formed by the rostral and lateral rostroder-

methmoids, and the premaxillae are slightly laterally positioned. The rostral and rostrodermethmoid articulate bilaterally with the rudimentary ascending process of each premaxilla. Apparently, the posterior articulation between the rostral and nasal bones and anterior tips of the parietals is strong because of the additional

wings extending ventrally to the anterior margins of the nasal bones. Often the rostral bone is preserved in situ.

It is expected that the rostral or ethmoidal commissure is oriented transversely, extending from one lateral process to the other, but thickness of the bone makes it difficult to follow its course. Occasionally the ethmoidal commissure can be observed (Fig. 49B). According to the position of adjacent bones, it is expected that the ethmoidal commissure would join the anterior branch of the infraorbital sensory canal exiting the antorbital.

There are two large, slightly rectangular, plate-like nasal bones (Figs. 44B, 46, 47A, 48A, 49A, B, 51A) that project laterally to the anterior margin of the first supraorbital bone. The shape varies slightly among nasal bones, but often the nasal is remarkably broader anteriorly than posteriorly, ending in an acute tip or triangular region posteriorly. The anterior margin is usually straight or

notched. The medial margin is almost straight and is sutured to the anterolateral margin of the parietals or the skull roof plate. The anterolateral margin is laterally rounded, but is almost straight or concave posterolaterally. Each nasal has a rounded or oval foramen (posterior nostril opening) positioned close to the lateral margin in all specimens with a complete bone. In many specimens, the lateral margin is broken, giving the impression of a notched nasal, but this is an artifact of preservation. The nasals do not join each other medially and are narrowly separated by the anterior tips of the parietal bones. Each nasal medially joins the lateral margin of the parietal region of the skull roof plate and is sutured posterolaterally with supraorbital 1. The supraorbital sensory canal (Fig. 49A, B) is closer to the middle region of the bone than to the medial or lateral margins. Small rounded pores are observed where the ganoine is damaged or removed.

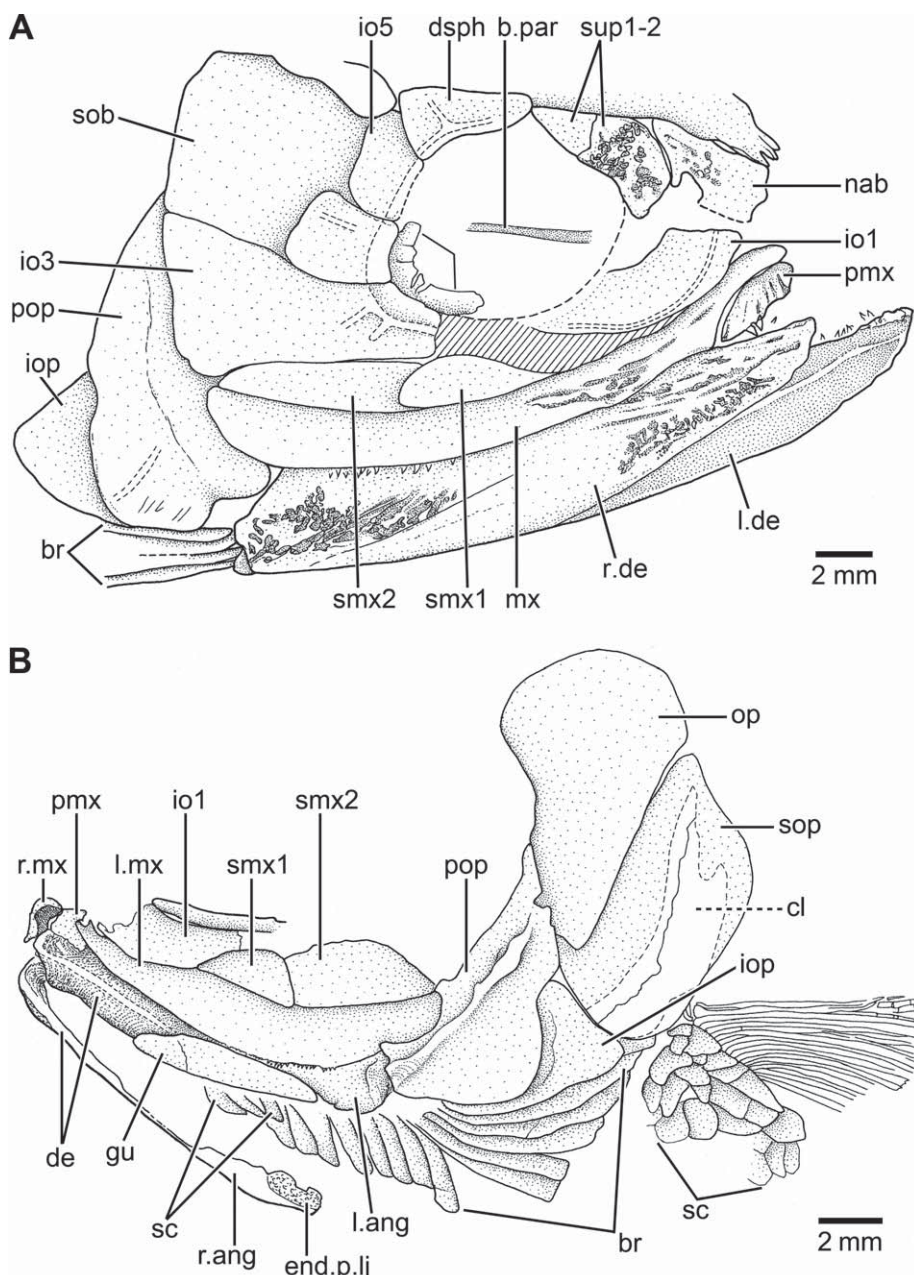


FIGURE 51. *†Pholidorhynchodon malzani* Zambelli. Drawings of heads in lateral view. **A**, MCSNB 3164. **B**, MCSNB 4446. Hatched lines indicate broken bone surface.

There is no evidence of a supraoccipital bone, which is the condition described here for all other Triassic species. There is no evidence either in a change of ossification in the most posterior region of the plate, as an indication of the possible presence of chondral portions. The dermal skull roof plate ends almost in a straight line at the posterior margins of the dermopterotic and postparietal regions. It is of interest that one specimen (Fig. 47A) has a small, but deep fossa close to the posterior margin of the dermopterotic region of the skull roof.

Two moderately large, triangular-shaped, paired extrascapular bones (Fig. 47) cover the posterior region of the skull roof plate, just overlapping the posterior margin where the postparietals and dermopterotics would end. The extrascapulae are comparatively smaller than those found in other species described here. The extrascapular canal or supratemporal commissure is difficult to discern in most specimens and commonly only segments of its trajectory are preserved. The commissure is closer to the anterior margin than to the middle region of the extrascapula, and usually no pores are observed.

Zambelli (1980b) recognized a tendency of the skull roof bones to fuse in *†Pholidorhynchodon* and in all Italian Triassic fishes studied by him. Although he identified and described the skull roof as the "fronto-parieto-dermopterotico," he illustrated them as three separate bones in his restoration of the skull roof (Zambelli, 1980b:138, fig. 2). In addition, he provided complete restorations of the supraorbital and otic canals, including pores and sensory tubules (Zambelli, 1980b:fig. 2), but I have been unable to observe the otic canal and its pores—not even in specimens with the ganoine weathered away.

Circumorbital Series—The circumorbital ring consists of two or three supraorbitals, one antorbital, five infraorbitals, and one or two dermosphenotics. Part of the lateral wall of the nasal bone forms part of the circumorbital ring in all but one specimen (Fig. 51A). In addition, *†Pholidorhynchodon malzannii* has one large suborbital, occasionally one accessory suborbital, and sclerotic bones.

Three thick bones are commonly present lateral to the orbital margin of the skull roof plate, in between the nasal bone anteriorly and the dermopterotic posteriorly (Fig. 49A, B). The two anterior-most elements are interpreted as supraorbitals 1 and 2, but it is unclear whether the last small bone is a third supraorbital or an additional dermosphenotic. Other specimens present only two bones in between the nasal and dermosphenotic (e.g., Fig. 51A).

Supraorbital 1 (Figs. 49A, B, 51A) is commonly a large rectangular or fusiform bone. It joins the posterior margin of the nasal bone anteriorly and supraorbital 2 posteriorly. Supraorbital 2 may be fusiform or rectangular. Its posterior margin joins supraorbital 3, the dermosphenotic, or an additional dermosphenotic when it is present. The dermosphenotic (Figs. 49A, B, 51A) is a large, triangular bone, almost forming half of the orbital margin dorsally. The bone lies on the autosphenotic region of the skull roof plate and sutures anteriorly with supraorbital 2 (or supraorbital 3) and posteroventrally with infraorbital 5. The dermosphenotic carries a section of the infraorbital canal that bifurcates inside the bone (see Fig. 51A). Some specimens have an additional element that is located lateral to the posterior tip of supraorbital 2 and the dermosphenotic. The bone is splint-like or fusiform, and it does not carry a section of the infraorbital canal. For these reasons, the bone can be interpreted as a supraorbital. Zambelli (1980b) reported the presence of one pore in two specimens, and he identified this additional bone as dermosphenotic 2. However, no evidence of an infraorbital canal has been observed in this bone, making this interpretation doubtful; see below, description of *†Parapholidophorus*, for comparison. Until a sensory canal is confirmed in more specimens, I sug-

gest referring to this element as a third supraorbital. According to Zambelli's (1980b) interpretation, the dermosphenotic would correspond to dermosphenotic 1 + 2, but in some specimens both parts are present as a separate dermosphenotic 1 (the larger element) and dermosphenotic 2 (the smaller element). This condition would differ from that of all advanced actinopterygians and the pholidophorids examined here.

The antorbital (Fig. 47) is a moderately large, triangular or comma-shaped bone carrying portions of the infraorbital canal.

Infraorbital 1 (Figs. 47A, 51A, B) is a large, slightly oval bone. The infraorbital sensory canal, parts of which are visible in a few specimens, is close to the ventral margin of the bone. Although the antorbital, infraorbital 1, and the infraorbital canal (pores and tubules) are completely restored in Zambelli's (1980a:fig. 1) work, I have been unable to find support for such a restoration in the material.

Infraorbital 2 (Fig. 47A) is a narrow, rectangular bone. The infraorbital sensory canal is enclosed within the bone, and no sensory pores are observed.

Infraorbital 3 (Figs. 47A, 51A) is a large, roughly rhomboidal bone, with a slightly concave anterior margin and a large plate-like extension extending posteriorly and covering the anterior margin of the preopercle. Infraorbital 3 has a straight dorsal margin that contacts infraorbital 4 and the suborbital. The infraorbital sensory canal—enclosed by bone—is close to the orbital margin. A few sensory tubules (two or three) are observed where the ganoine is weathered away. In contrast, Zambelli (1980b:fig. 1) restored infraorbital 3 with six sensory tubules. A pit-line groove (anterior division of the supramaxillary pit-line) has been observed in some specimens.

Infraorbitals 4 and 5 (Fig. 51A) are small in comparison with infraorbital 3. They are slightly square or rectangular bones carrying the infraorbital canal close to their orbital margin. Vestiges of sensory tubules are observed in a few specimens. Both infraorbitals contact the suborbital posteriorly, but infraorbital 5 in addition contacts the dermosphenotic dorsally and the accessory suborbital posteriorly (when the latter bone is present). One large suborbital (Fig. 51A) occupies the space between the posterior margins of infraorbitals 4 and 5 anteriorly, infraorbital 3 dorsally, mainly the opercle posteriorly, and the lateral wall of the dermopterotic region of the skull roof plate dorsally. When an accessory suborbital is present, the bone is small, triangular and narrow or oval-shaped. It lies usually on the dorsal region of the suborbital, close to its dorsal margin.

The anterior and posterior sclerotic bones, often poorly preserved, form a complete ring surrounding the eyeball.

Upper Jaw—The premaxilla (Figs. 46, 47A, 49A, B, 51A, 52A) is displaced in most specimens and commonly is preserved incompletely. However, and according to the position of the rostrodermethoids, the premaxillary bones are positioned lateral to the rostrodermethoids. The premaxilla is a small, triangular bone, with a very short ascending process. Moderately large, strong conical teeth are placed on the oral margin of the bone. More than one row of teeth is present.

The gently curved maxilla (Figs. 46, 47A, 49A, B, 51A, B, 52A, B) is a long bone, with a moderately long articular process anteriorly; apparently, the longest process among all species studied here. The maxillary blade is slightly shallow anteriorly and posteriorly, but its depth increases slightly in its middle region. The dorsal margin does not possess a well-defined supramaxillary process, but some specimens show a rudimentary broad process in front of supramaxilla 1. The posterior margin of the maxilla is oblique, ending in a sharp tip dorsally in most specimens, but is gently convex in others. Two rows of strong conical teeth are present on the anterior half of the oral margin, but numerous rows of slightly

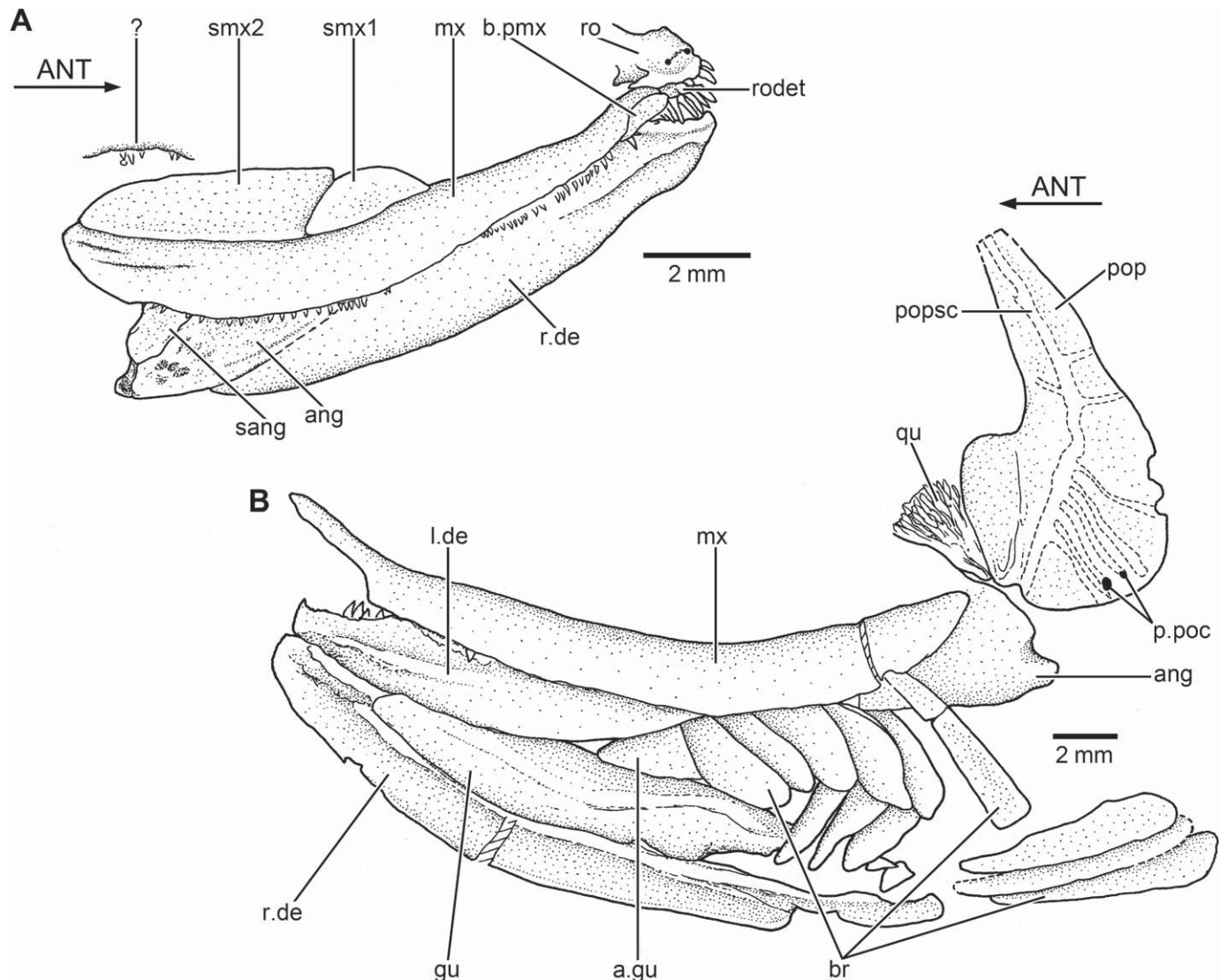


FIGURE 52. *†Pholidorhynchodon malzannii* Zambelli. **A**, drawing of jaws in right lateral view (MCSNB 3164). **B**, jaws, gular plate, and preopercle in left lateral view (MCSNB 3914).

smaller teeth can be observed close to the posterior margin of the maxilla.

Two supramaxillary bones (Figs. 46, 47A, 51A, B, 52A, B) cover the posterodorsal margin of the maxilla. Both bones together represent about 50% of the length of the maxilla. Supramaxilla 1 is a slightly oval or fusiform bone and varies in size, being much shorter than supramaxilla 2 or almost equal in size. Supramaxilla 2 is usually as deep as the maxilla and supramaxilla 1. Its anterodorsal process is rudimentary and slightly overlaps the dorsal region of supramaxilla 1. Its posterior tip may be slightly acute or rounded, giving an unusual smooth, curved profile to the posterior border of the upper jaw.

Lower Jaw—The lower jaw (Figs. 46, 51A, 52A, B) is often obscured by the long maxilla. However, complete jaws (Fig. 48C) are observed in a few specimens. The dorsal margin of the jaw is almost straight in its anterior half, ending in the ‘leptolepid’ notch. Then, the depth of the bone increases abruptly just posterior to the notch, reaching its greatest depth (coronoid process) closer to

the posterior margin of the jaw than to its middle region. The ventral margin of the jaw is gently convex. Dorsal and ventral regions are separated by a well-developed, distinct, lateral bony ridge that protrudes along the jaw, becoming inconspicuous in the anterior region of the angular.

The dentary, surangular, and angular form the lateral wall of each jaw. Because the sutures among the dentary, angular, and surangular are not visible in most specimens, the relative sizes of these three bones is unknown. The dentary (Figs. 46, 48C, 51A, 52A, B) apparently forms most of the lower jaw, extending below the lateral protruding bony ridge. It bears small conical teeth on the oral margin, which seem to be smaller than the premaxillary and maxillary teeth. At least two rows of teeth have been observed. The angular (Figs. 51A, 52A, B) forms the posteroventral lateral wall of the jaw. A thick layer of ganoin covers the angular. It is commonly ornamented with irregularly distributed tubercles of various sizes. An elongate surangular (Fig. 48C), sutured with the angular and dentary, forms the posterodorsal margin of the

lower jaw. Apparently, both the surangular and dentary form the coronoid process. The posterior margin of the jaw is truncated so that a postparticular process is lacking.

The medial view of the jaw (Fig. 48C) reveals important anatomical features. A chondral element is fused to the medial aspect of the angular, together forming the articular region for the quadrate. This chondral element has the position of the articular and retroarticular in other advanced actinopterygians. The posterior part of the jaw is interpreted here as comprising the fused angular, articular, and retroarticular. This complex ossification articulates with an elongate dermal bone, about half of the length of the jaw, the prearticular. Near the anterior tip of the dentary, in medial view, at least one elongate, slightly coronoid bone bearing small teeth has been observed in several specimens (e.g., Figs. 47C, 48C). It is unclear whether more than one coronoid bone is present in *†Pholidorhynchodon*.

The course of the mandibular sensory canal is below the lateral bony ridge of the lower jaw. However, its trajectory and its pores are difficult to discern due to the dense ornamentation of ganoine covering the jaw. I could not verify the complete mandibular canal bearing many tubules and small pores restored by Zambelli (1980b:fig. 1).

The lower jaw is long. The articulation between the lower jaw and quadrate is posterior to the orbit, about at the level of the posterior margin of the large infraorbital 3 and suborbital.

Palatoquadrate and Suspensorium—Commonly, all bones of the palatoquadrate and the suspensorium are hidden by cheekbones, so that the description is restricted here to a few bones. The quadrate (Fig. 52B) stays mainly as a partially ossified cartilaginous element that is laterally covered by the preopercle and infraorbital 3 so that its complete shape is unknown. The entopterygoid, as seen in some specimens, has a small dentition in its medial surface.

The hyomandibula (Fig. 48B) is a narrow element lacking membranous outgrowths, with the ventral portion being cartilaginous and the dorsal portion ossified. The element is strongly inclined posteroventrally. It articulates with the braincase at one facet. The short opercular process is heavily ossified. A preopercular process at the posterior margin of the hyomandibula is absent.

Hyoid Arch—No elements of the hyoid arch were observed due to preservation.

Opercular, Branchiostegal Series, and Gular Plate—The opercular bones are positioned posterior to the posterior margin of skull roof plate. All opercular bones, as well as the branchiostegals, are covered by a thick, heavily ornamented layer of ganoine. The posterior margins of the opercle and subopercle produce a gently rounded profile of the opercular apparatus.

Although the preopercle (Figs. 46, 47A, 51A, B, 52B) shows variation in its shape and size, commonly it is expanded anteroventrally, with a distinct notch that gives the bone the aspect of an inverted heart. The posterior margin is slightly notched in many specimens where the large interopercle abuts, whereas the notch is absent in others. The dorsal part of the preopercle is short so that the dorsal margin of the bone is distant from the lateral margin of the dermopterotic region of the skull roof plate. The anterior margin of the preopercle is partially covered by a small section of the suborbital and by the posterior margin of infraorbital 3. Zambelli (1980b:figs. 3, 4) illustrated the variation of shapes of the preopercle and of the notch at the posterior margin.

The anterior region of the preopercle is slightly expanded just anterior to the main course of the preopercular canal. The pathway of the preopercular sensory canal and its tubules is often not visible because of the thick layer of ganoine. When ganoine is not preserved, the preopercular canal can be observed. It ranges from absence of sensory tubules and pores to numerous tubules concentrated in the posteroventral region or to a variable number of

tubules in the posterior region of the preopercle. However, part of the observed variation may be related to the degree of preservation of the layer of ganoine and its ornamentation.

The opercle (Figs. 47A, 51A) is a large, roughly triangular bone, almost straight at its expanded dorsal margin. The anterior margin of the opercle is almost oblique and markedly thickened, and the posterior margin is short and rounded. The long ventral margin of the opercle is markedly oblique.

The subopercle (Fig. 47A, 51B) is a large bone, slightly smaller than the opercle. Its posteroventral margin is gently rounded. Its anterior margin is oblique and extends dorsally as part of the well-developed anterodorsal process of the subopercle. The anterior margin joins both the interopercle extensively and preopercle by a narrow portion. The well-developed anterodorsal process projects dorsally in front of the anteroventral margin of the opercle and posterior margin of the preopercle.

The interopercle (Figs. 47A, 51A, B) is a large bone, exposed between the posterior notch of the preopercle and anterior margin of the subopercle. Its complete size is unknown in most specimens, because the interopercle is covered anteriorly by the preopercle. Posteriorly, the bone has a broad articular surface for the anterior margin of the subopercle.

There are approximately 13 branchiostegal rays (Fig. 52B). The branchiostegals are relatively narrow bones, including the posterior-most one, and their lengths increase posteriorly. As far as can be observed, only their exposed surfaces are ornamented. Preceding each branchiostegal series is a rounded, small bone that I interpret as a lateral gular. Zambelli (1980b) interpreted it as the first branchiostegal, but the bone is not attached to the ceratohyal and lacks an articular process to join to the ceratohyal. A similar bone is well preserved in *†Parapholidophorus nybelini* (see description and illustration below).

As with the branchiostegals, the median gular plate (Fig. 52B) has not been observed in most specimens due to condition of preservation. The median gular plate is elongate, slightly oval, and about half of the length of the lower jaw. The thick layer of ganoine covering the exposed surface is ornamented with ridges and tubercles in a similar pattern to that found in the ventral part of the lower jaws.

Vertebral Column and Intermuscular Bones—Only a few segments of the vertebral column can be observed where the squamation is displaced or lost. All centra are chordacentra with a large notochordal space not constricting the notochord. The abdominal centra are formed by hemichordacentra that are arranged in a circular manner, producing a ring-like centrum. The neural spines are paired in the abdominal region, and the arches are slightly broader than the thin and slender spines. Apparently, the abdominal region is formed only by monospondylous centra. Only diplospondylous centra are observed in the caudal region, except for the last caudal centra. The diplospondylous centra are formed by moderately large basidorsal and interdorsal hemichordacentra and interdorsal and interventral hemichordacentra, which are smaller than the basidorsal and basiventral elements. The arcocentra, whose walls are formed by a large amount of cartilage, are present on the dorsal region of the basidorsal hemichordacentra. The thin neural spines of the caudal vertebrae are unpaired elements that are relatively short, not extending to the dorsal margin of the body. The ventral arcocentra are associated with the basiventral hemichordacentra, and their hemal spines are also thin and short as in the neural spines.

No other elements such as supraneurals, epineural processes, or epipleural bones have been observed.

Paired Fins—Bones of the pectoral girdle and fins are well preserved in several specimens. The following dermal elements of the pectoral girdle are preserved: posttemporal, supracleithrum, cleithrum, clavicle, and postcleithra. Among chondral elements,

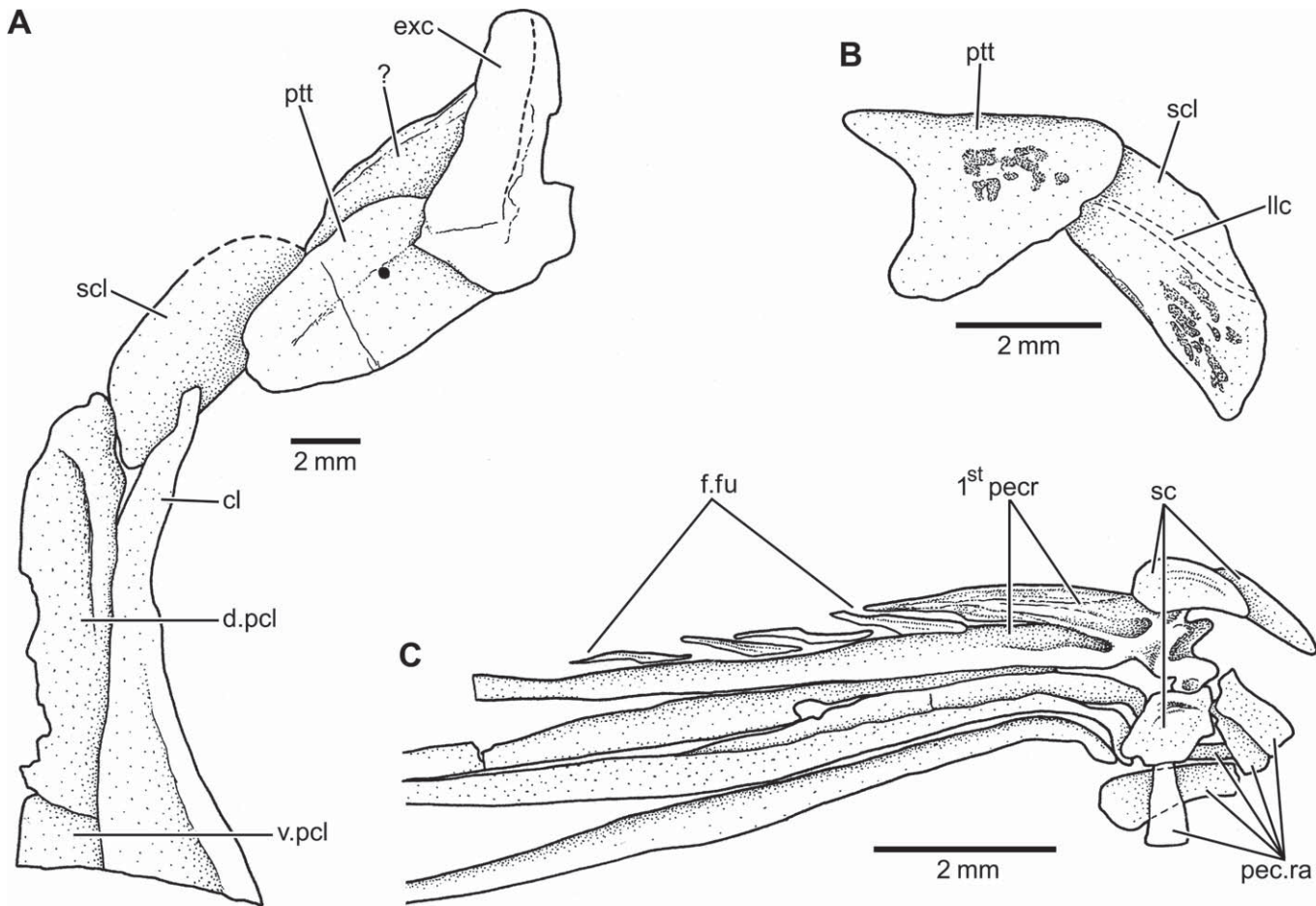


FIGURE 53. *†Pholidorhynchodon malzannii* Zambelli. A, drawing of dorsal portion of the right pectoral girdle in lateral view (MCSNB 3339). B, left posttemporal and supracleithrum in lateral view (MCSNB 3900). C, right first pectoral rays and radials in lateral view (MCSNB 3887).

only the radials are preserved. The bases of the rays are covered with a series of small rhombic or oval scales.

The posttemporal (Fig. 53A, B) is a small, plate-like bone. The bone lacks distinct, well-ossified processes to articulate with the braincase.

The supracleithrum (Figs. 47A, 53A, B) is a moderately broad, elongate bone, with its anterior part placed below the posttemporal and its posterior part overlying the dorsal region of the cleithrum and part of the dorsal postcleithrum posteriorly. The trajectory of the lateral line canal is visible along the upper part of the bone. The canal exits close to the middle region of the posterior margin. A thick layer of ganoine, ornamented with tubercles and ridges of different sizes, covers the supracleithrum.

The complete cleithrum (Fig. 47A) is exposed laterally in a few specimens. The elongate, slightly narrow dorsal region is almost vertically oriented and perpendicular to the moderately expanded, very short ventral region of the cleithrum. The cleithrum is slightly bent at its dorsal-most tip. Its anteromedial region is narrow, similar to the condition illustrated in Figure 20. One long-toothed element or serrated appendage extends along the medial surface of cleithrum. The serrated appendage is destroyed in several specimens that have the layer of ganoine weathered away. The anteroventral margin of the cleithrum joins an expanded clavicle

(Fig. 47A) that seems to be longer than in other species described here. However, the whole size and shape of the clavicle remain unknown because its external surface is partially covered by the subopercle and branchiostegal rays.

Two postcleithra (Figs. 46, 47A, 55A) are visible behind the cleithrum. The dorsal postcleithrum is the largest one and is located below the ventral region of the supracleithrum and posterior to the dorsal region of the cleithrum. The bone is broad, even broader than the dorsal region of the cleithrum. An almost straight junction is present between the dorsal postcleithrum and the smaller, slightly square-shaped ventral postcleithrum. Both bones are covered with a layer of ornamented ganoine. The shape and size of the ventral postcleithrum make it difficult to separate it from the surrounding scales, which may be as large as the ventral postcleithrum.

Five rectangular, plate-like pectoral radials (Fig. 53C) are preserved in MCSNB 3887. It is possible that a few more radials could be present. The radials are associated with the most lateral pectoral rays.

The pectoral fins are positioned low in the flank, close to the ventral margin of the body. Each pectoral fin consists of 20 or 21 lepidotrichia. The first ray (Figs. 53C, 54A), as in other species described here, is the thickest of all rays and is a compound element fused at least with one short, strong, and well-ossified

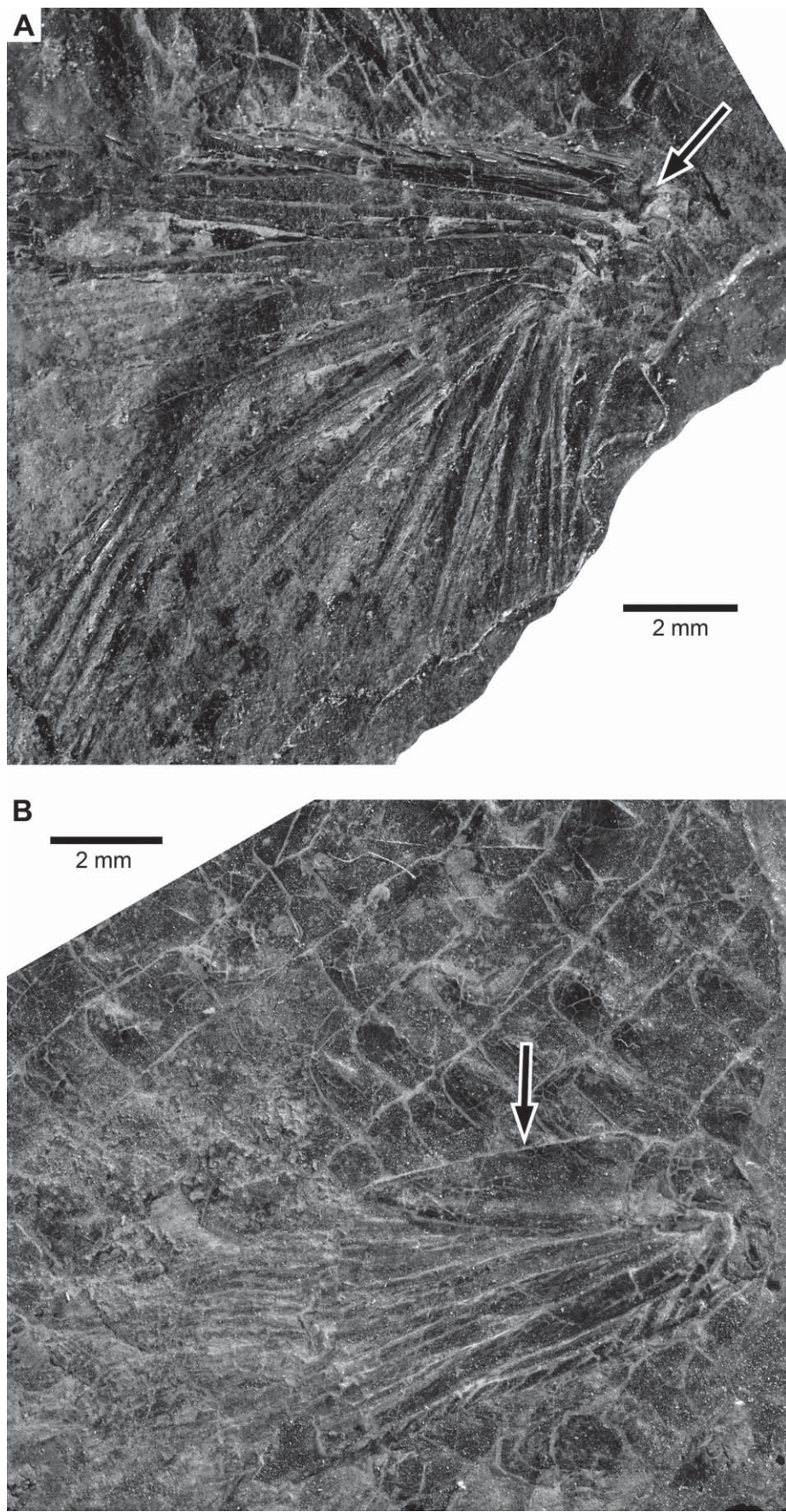


FIGURE 54. *†Pholidorhynchodon malzani* Zambelli. **A**, photograph of right pectoral fin with first fin ray indicated by an arrow (MCSNB 3887). **B**, right pelvic axillary process, rays, and scales (MCSNB 3399). Arrow points to the axillary process. See drawing in Fig. 55B. (Color figure available online).

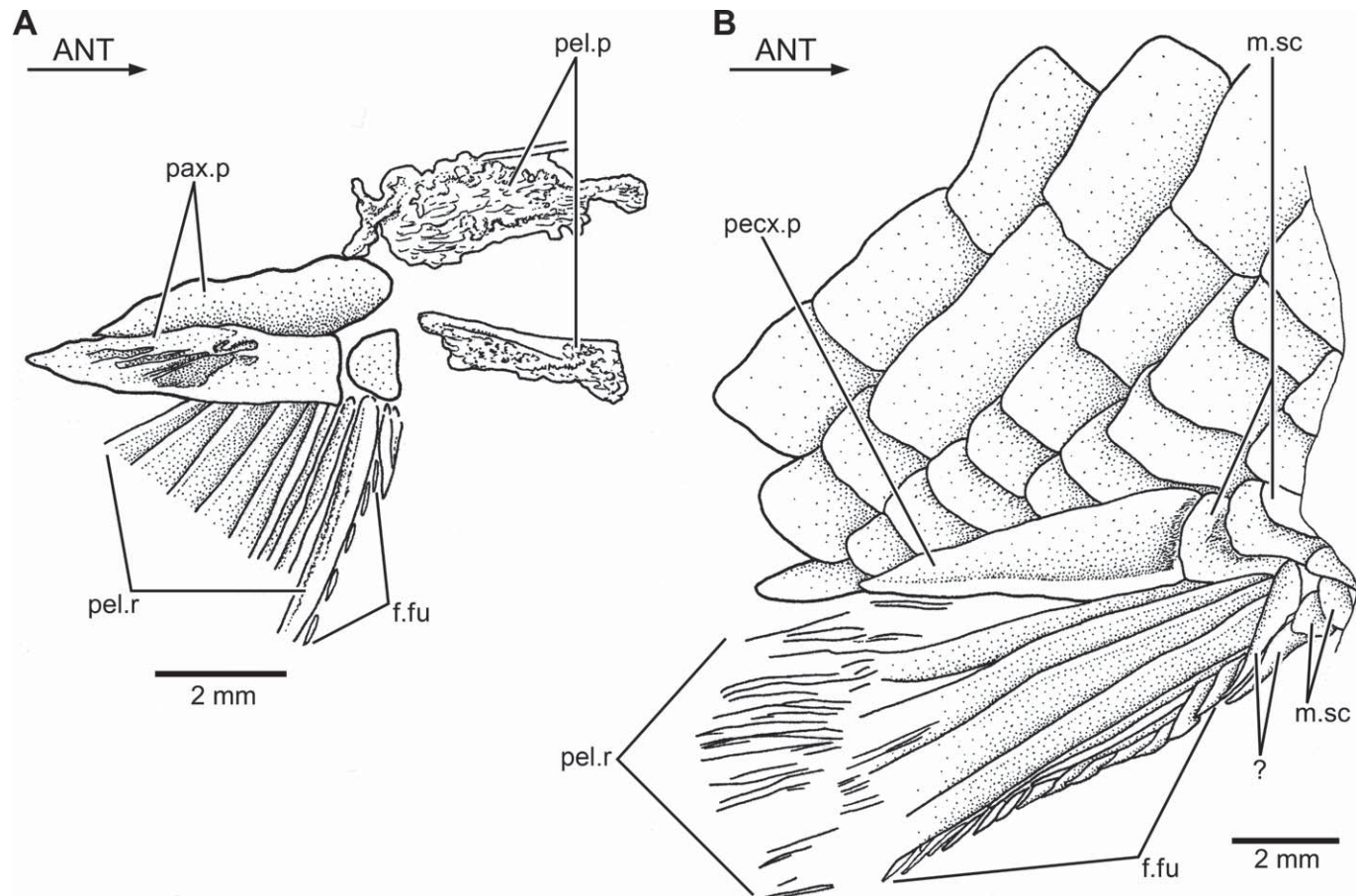


FIGURE 55. *†Pholidorhynchodon malzannii* Zambelli. **A**, drawing of right pelvic girdles and fin (MCSNB 3399). **B**, right pelvic fin, scales, and pelvic axillary process (MCSNB 3399).

basal fulcrum, which is followed by a series of elongate fringing fulcra. The proximal region of the first ray is massive and has an articular facet. A propterygium is not fused with the base of the first ray.

The pectoral rays have long bases; they are segmented and finely branched distally. When the fin and scales are in situ, a moderately long, leaf-like or triangular pectoral axillary process lies above the insertion of the pectoral fin.

The pelvic girdles or basipterygia (Fig. 55A) are incompletely preserved at least in one specimen. The basipterygia are formed mainly by cartilage partially ossified, and they are plate-like, slightly rectangular elements. The origin of the pelvic fin stands at the level of the 10th vertical row of scales. The pelvic fin consists of three to five leaf-like, elongate basal fulcra and about 14 rays. The lateral rays have very long, narrow bases and are only segmented and branched distally. The length of the rays becomes considerably shorter medially, and the most internal rays are very short and thin, as was described and illustrated above for *†Pholidophorus gervasutti* (Fig. 22). A series of small fringing fulcra are associated with the leading margin of the fin. A large, leaf-like (Fig. 54B), and well-ossified pelvic axillary process lies at the base of the fin, as has been described for other species.

Dorsal and Anal Fins—The origin of the dorsal fin is at about the level of the 18th vertical row of scales. The dorsal fin (Figs. 44A, 45A) is roughly triangular, with long first principal rays and very short posterior ones. The first pterygiophore (Fig. 56A)

seems to be simple. The pterygiophores are short and narrow, and it is unclear whether each one represents fusion of the proximal, middle, and distal radials.

The articular region of the dorsal rays (Fig. 56A) is small in comparison with the thicker appearance of the first rays. Five or six small basal fulcra precede the series of dorsal fin rays. The first fulcra are very small, unpaired elements that are followed by fulcra that are larger posteriorly. There are three or four procurent rays, and the first one is very small. There are about 10 or 11 principal rays, including the first segmented and unbranched ray. The principal rays (Fig. 56A) have long bases and are segmented and branched distally; the paired hemilepidotrichia forming each ray are asymmetric, with one much shorter than the other. A few fringing fulcra are positioned between the second and third procurent rays, but a combination of short fringing fulcra and elongate pieces of bone or incomplete rays stand between the third procurent ray and the first principal ray that is segmented distally. This is a curious pattern that I have not observed in any of other fish. The first and second principal rays form the leading margin of the fin. A series of small fringing fulcra are placed on the leading margin of the fin. Zambelli (1980b) described the dorsal fin with about seven simple (= procurent) rays and 11 segmented and branched rays. I have not been able to see as many procurent rays as Zambelli. It is possible that he interpreted some of the elongate pieces of bone or elongate fulcra as simple

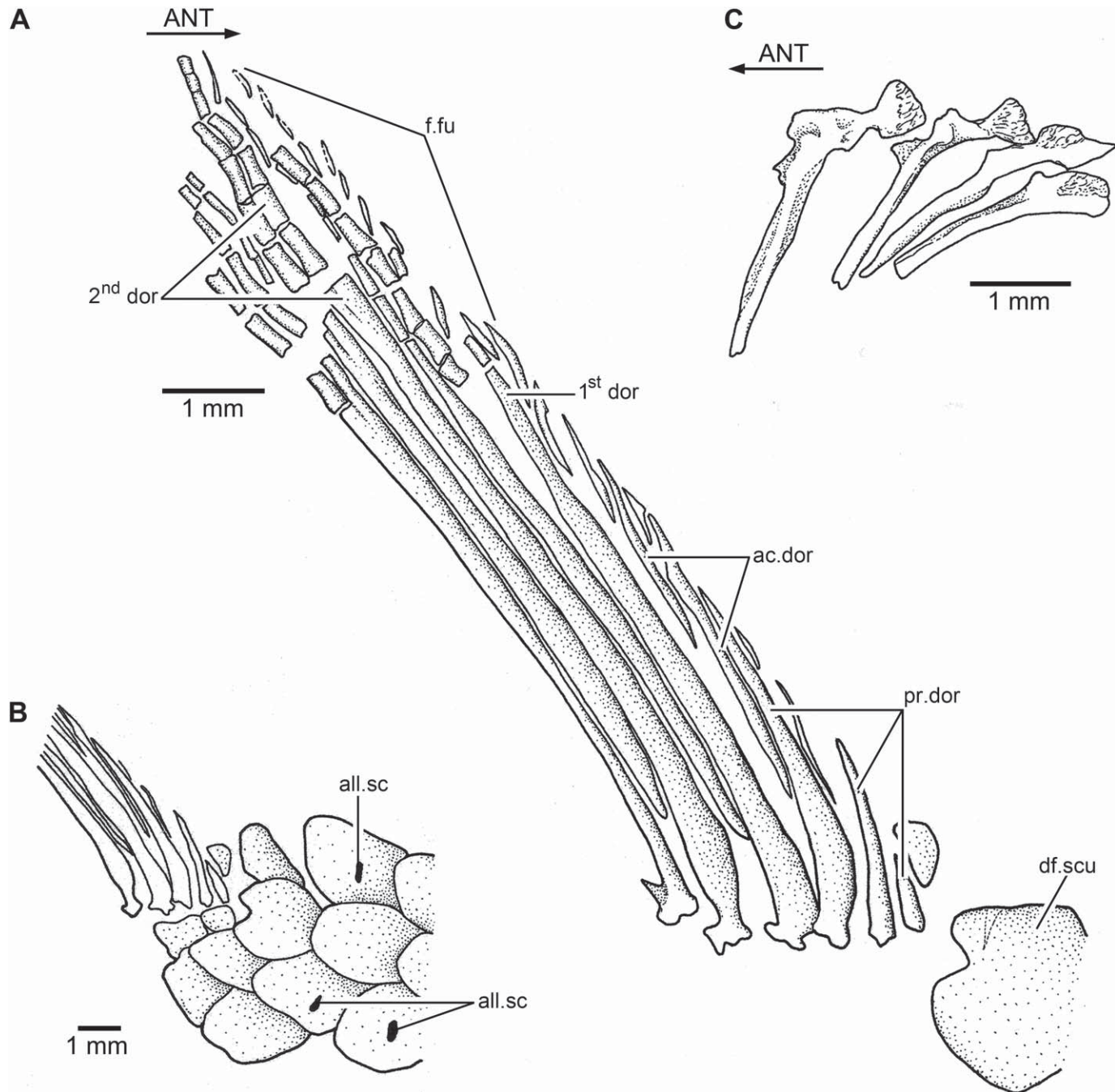


FIGURE 56. *†Pholidorhynchodon malzannii* Zambelli. A, drawing of anterior region of dorsal fin (MCSNB 3385) in lateral view. B, predorsal region of body showing pores of additional lateral line (MCSNB 3385). C, first dorsal pterygiophores (MCSNB 3914).

rays. Preceding the dorsal fin, a large, heart-like, and broad scute (Fig. 56A) is present.

The origin of the anal fin is about the level of the 19th vertical row of scales. The short anal fin (Fig. 45A) is posterior to the dorsal fin and closer to the pelvic fins than to the caudal fin. It consists of four or five small simple rays and eight or nine principal rays. The anal fin rays are also very delicate and thin and are frequently broken. Elongate fringing fulcra are associated with the leading margin of the fin.

Caudal Fin—The caudal endoskeleton is not preserved in any specimen so that its composition remains unknown.

Although some of the distal tips of the caudal fin rays are broken, the tail is almost completely preserved in a couple of specimens. The hemi-heterocercal caudal fin is deeply forked, with shorter middle principal rays in comparison with the long leading margins of the epaxial and hypaxial lobes of the fin. The terminal area covered by ganoid scales at the base of the caudal fin is divided into well-defined regions separated by a notch. Both

areas are slightly triangular-shaped. The dorsal region is formed by a series of rhombic and rectangular scales that reach to the level of the last epaxial basal fulcrum in the epaxial lobe of the caudal fin. The ventral region is shorter than the dorsal one, and the scales are distributed in an almost circular pattern. The scales framing the dorsal and ventral regions are usually rectangular or square. In some specimens, both scaly regions are of similar size.

The caudal fin has eight or nine epaxial basal fulcra, a series of elongate epaxial fringing fulcra (apparently an epaxial rudimentary ray is lacking), 20 or 21 principal rays, a series of elongate hypaxial fringing fulcra, three or four hypaxial segmented procurent rays, and two or three hypaxial basal fulcra. The epaxial basal fulcra are elongate, leaf-like elements that expand laterally, partially covering the next fulcrum. The first principal ray (only segmented) and the second principal ray (segmented and branched distally) apparently form the dorsal leading margin of the fin. The segmentation of the principal rays is straight. As far as preservation permits, no dorsal processes associated with the bases of the middle principal rays have been observed.

The hypaxial procurent rays are segmented, and the terminal segment usually resembles the shape of the fringing fulcra. Accessory fringing fulcra lie between the terminal segment of a procurent ray and the next one, as in other species described here.

The dorsal and ventral caudal scutes are often removed or covered by scales so that a description is not possible.

Scales—The body is covered by thick, rhombic ganoid scales (Figs. 45, 46), which have different sizes along the body. Although there is variation in the shape of the scales, the variation ranges mainly between rhombic and rectangular scales. The three main rows of the flank (the lateral line row and its bounding dorsal and ventral rows) are deeper than broad. Most scales of the dorsal and ventral rows of the body are smaller than the three main rows of the flank and have slightly rounded corners. The scales are covered by a thick layer of ganoine that is ornamented with tubercles of different sizes, which are unevenly distributed on the free field of the scales.

Lateral Line—Thirty-nine or 40 flank scales transmit the main lateral line canal. However, the trajectory of the lateral line is easily observed in the anterior-most scales, close to the pectoral girdle. Additionally, an accessory lateral line (Fig. 56B) is placed close to the dorsal margin of the body in the predorsal region. Apparently, the accessory lateral line branches off close to the dorsal fin, because there is more than one row of scales with pores opening on the surface.

†*PARAPHOLIDOPHORUS* Zambelli, 1975

Diagnosis—Emended from Zambelli, 1975, and based on a unique combination of characters. Autapomorphies are identified with an asterisk [*]. Small pholidophorid reaching about 70 mm total length. Cranial bones covered with a smooth layer of ganoine. Additional rostral bone extending onto skull roof plate [*]. Rostral bone relatively small, rhomboidal, with rudimentary lateral processes, not projecting over lateral margins of nasal bones [*]. Nasal bones separated medially. Lateral wall of nasal bone with a large, deep notch. Infraorbital 3 extending below suborbital. Infraorbitals 4 and 5 moderately large, deeper than long [*]. Accessory dermosphenotic containing a section of infraorbital canal [*]. One small accessory suborbital. Jaws moderately short; quadrate-mandibular articulation below middle of orbit or posterior half of orbit [*]. Suspensorium of lower jaw (quadrate and hyosymplectic) strongly inclined anteroventrally [*]. Preopercle expanded anteroventrally, with a notch at its anterior margin, and heart-shaped. Preopercle inclined anteroventrally. Course of preopercular canal closer to posterior margin than to middle region of bone. Posterior margin of preoper-

cle lacking distinct, well-pronounced notch. All cephalic sensory pores conspicuous, rounded or button-like. Lateral line row comprising 35 to 38 scales. An additional lateral line canal extending between extrascapula and base of dorsal fin. Scales with straight posterior margin. Scales covered with a smooth layer of ganoine.

Content—†*Parapholidophorus nybelini* Zambelli, 1975 (type species), and †*P. caffii* (Airaghi, 1908).

†*PARAPHOLIDOPHORUS NYBELINI* Zambelli, 1975 (Figs. 57–70)

Holotype—Specimen MCSNB 3013 (Figs. 57A, 58A, B) has been selected as the neotype, given its preservation and that it closely represents the original description of Zambelli (1975). This specimen replaces specimen MCSNB 3200 (Fig. 58B), which was assigned as the holotype by Zambelli, because the specimen has been lost, at least for the last 30 years.

Material Examined—There are more than 100 specimens catalogued in MCSNB. After checking all specimens, the following were selected for study because of the morphological information that they provide: MCSNB 431, MCSNB 2889–2897, MCSNB 2898, MCSNB 2900, MCSNB 2920, MCSNB 2938, MCSNB 2959, MCSNB 2962, MCSNB 2963, MCSNB 2966, MCSNB 2978, MCSNB 2982, MCSNB 2985, MCSNB 2992, MCSNB 3001, MCSNB 3005, MCSNB 3011, MCSNB 3072, MCSNB 3090, MCSNB 3213, MCSNB 3220, and MCSNB 4797g. The following specimens, included in the original study of Zambelli (1975), are not included here because they do not show the diagnostic characters of the species due to incomplete preservation: MCSNB 2967, MCSNB 2970 to MCSNB 2972, MCSNB 2974 to MCSNB 2977, MCSNB 2981, MCSNB 2986, and MCSNB 2988 to MCSNB 2990.

Type Locality, Age, and Distribution—Only known from the type locality Cene, about 17 km northeast of Bergamo, Lombardy, northern Italy; Late Triassic (Norian), about 210 Ma.

Diagnosis—Emended from Zambelli, 1975, and based on a unique combination of characters. Autapomorphies are identified with an asterisk [*]. Small fishes reaching about 70 mm total length. Large head, about 25–28% of head length. Large eyes, about 34–43% of head length [*]. Maxilla with rounded posterior margin. Supramaxilla 1 short, about one-third of the length of supramaxilla 2. Supramaxilla 2 with well-developed anterodorsal process extending over half of the dorsal margin of supramaxilla 1. Opercle larger than subopercle. Eighteen or 19 pectoral rays. About 10 anal rays. With 21 to 23 principal caudal rays. Lateral line row comprising 37 or 38 scales.

Description

The anatomical description of certain regions of the body, such as the braincase and the axial skeleton, is difficult due to conditions of preservation. The vertebral column, ribs, supraneurals, and dorsal and anal pterygiophores are commonly obscured by the squamation in most specimens. However, and in contrast to other species, I have been able to gather considerable information on some cranial bones that are usually hidden by other bones, as well as data about the vertebral column.

The members of this species are small and slender, reaching about 70 mm maximum length and with a maximum depth of the body (at the predorsal region) about 25% body length. Peduncular length is about 11–12% standard length. The snout length is short, only 14–17% head length. The pectoral fins are positioned nearer to the ventral margin of the body than to the middle region of the flanks. The pelvic and dorsal fins are positioned slightly posterior to the midpoint of the length of the fish, at about 51–55% of standard length; in some specimens the insertion of the dorsal fin is opposite to that of the pelvic fin, but in others the dorsal fin origin

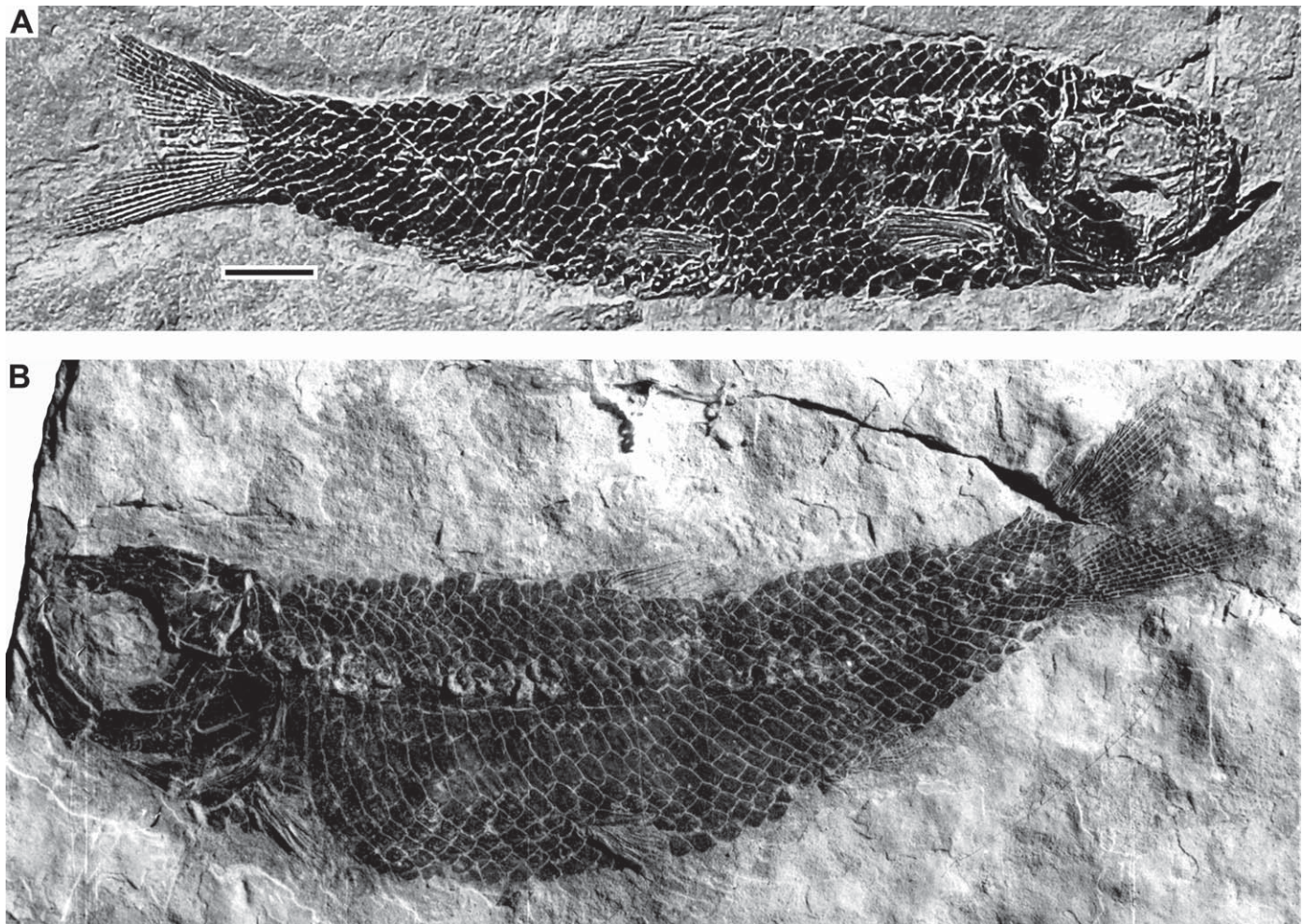


FIGURE 57. *†Parapholidophorus nybelini* Zambelli. **A**, photograph of neotype (MCSNB 3013) in right lateral view. Scale bar equals 5 mm. **B**, photograph of lost holotype in left lateral view. Scale bar is not available, but the specimen is of similar size to the neotype.

is slightly in front of the pelvic fin origin. The anal fin is posterior to the base of the dorsal fin and closer to the pelvic than to the caudal fin. All fins are small, with very delicate and slender rays, bearing elongate fringing fulcra associated with the leading margins.

External cranial dermal bones, dermal bones of the pectoral girdle, and scales are covered with a moderately thick layer of smooth ganoine, with a few exceptions, such as the rostral (ornamented with a few small tubercles) and the maxilla and supramaxillae, which are ornamented with characteristic longitudinal ridges of ganoine.

Braincase—The braincase, like that of other species described here, is short; its posterior margin is positioned at about the level of the anterior margin of the opercle, and its anterior margin is at the level of the suborbital bone. Except for the skull roof bones (Fig. 59A), no elements of the lateral and ventral walls of the braincase are observed. The remains of the parasphenoid are uninformative.

Skull Roof—The skull roof plate lacks crestae or fontanelles, and its surface is smooth. The skull roof (Figs. 60A, 61) is narrow anteriorly, ending in an acute tip. From this point the breadth of the skull roof increases posteriorly, being very broad at the level of the posterior corner of the orbital margin and maintaining this

breadth through the postorbital region. The breadth of the skull roof in the postorbital region is 3.5 to 4 times greater than the anterior nasal bones.

All bones of the skull roof (Figs. 59A, 60, 61) are fused into one large skull roof plate that includes the parietals, postparietals, autostophotic, and dermopterotics. Unlike other species described here that have different degrees of fusion among specimens, *†Parapholidophorus nybelini* consistently presents a uniform plate without sutures. This condition was noted first by Zambelli (1975). The trajectory of the supraorbital canal can be traced following the openings of the pores into the surface. Left and right series of pores are asymmetrical in number and position on either side of the head. The middle pit-line groove shows variation in length and in placement. There is no evidence of a postparietal branch or pit-lines, but Zambelli (1975:fig. 1) reconstructed long postparietal branches in continuation with anterior pit-lines, middle, and posterior pit-line grooves.

A median, slightly rhomboidal rostral bone (Figs. 59A, 61, 62) lies at the anterior-most region of the skull roof plate. In well-preserved specimens, the surface of the bone shows some small tubercles of ganoine (Fig. 62). Both the anterior and posterior margins of the rostral are slightly rounded. The lateral processes are

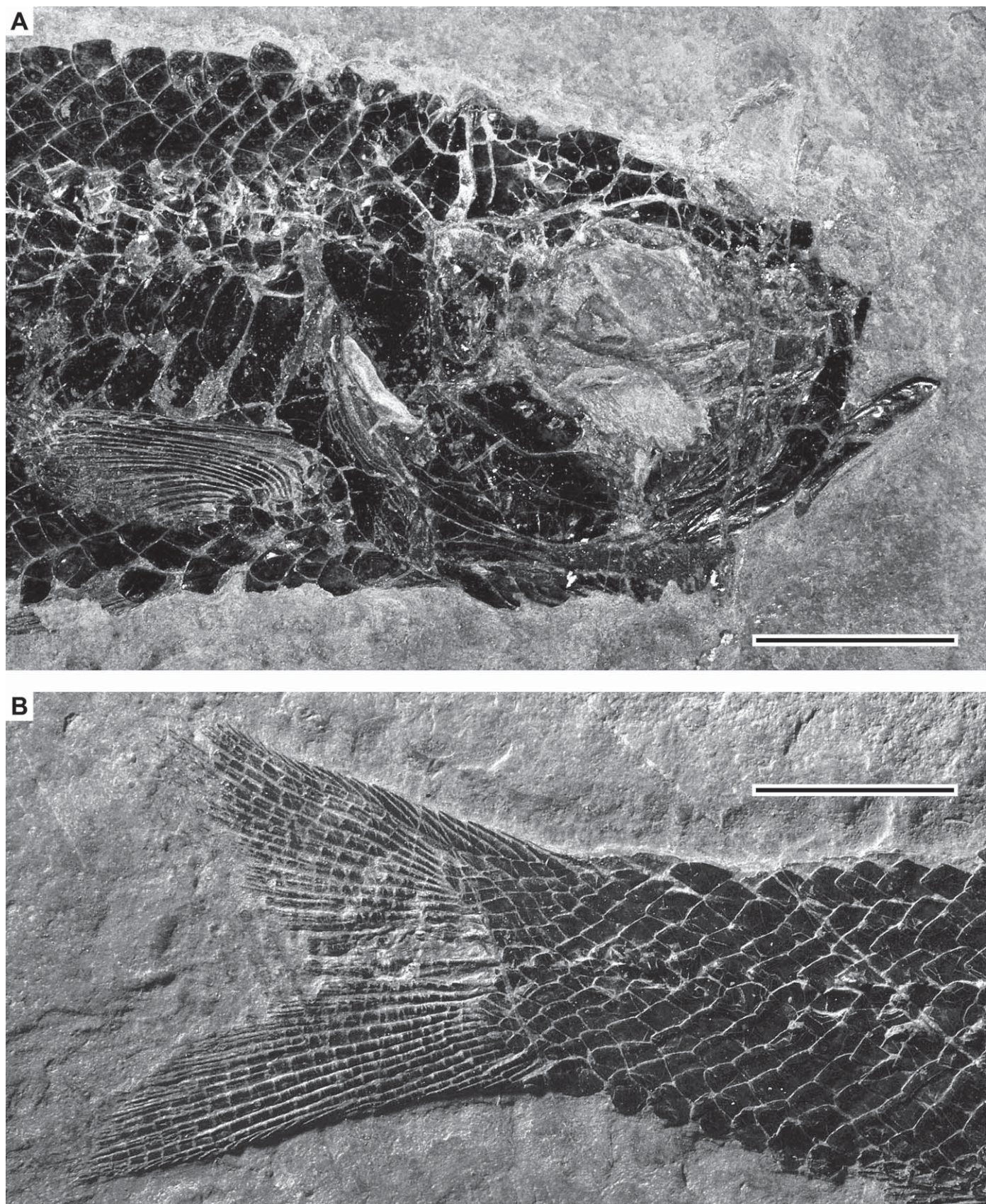


FIGURE 58. \dagger *Parapholidophorus nybelini* Zambelli. Photograph of the head (A) of the neotype (MCSNB 3013), and its caudal fin (B) in right lateral view. Scale bars equal 5 mm. (Color figure available online.)

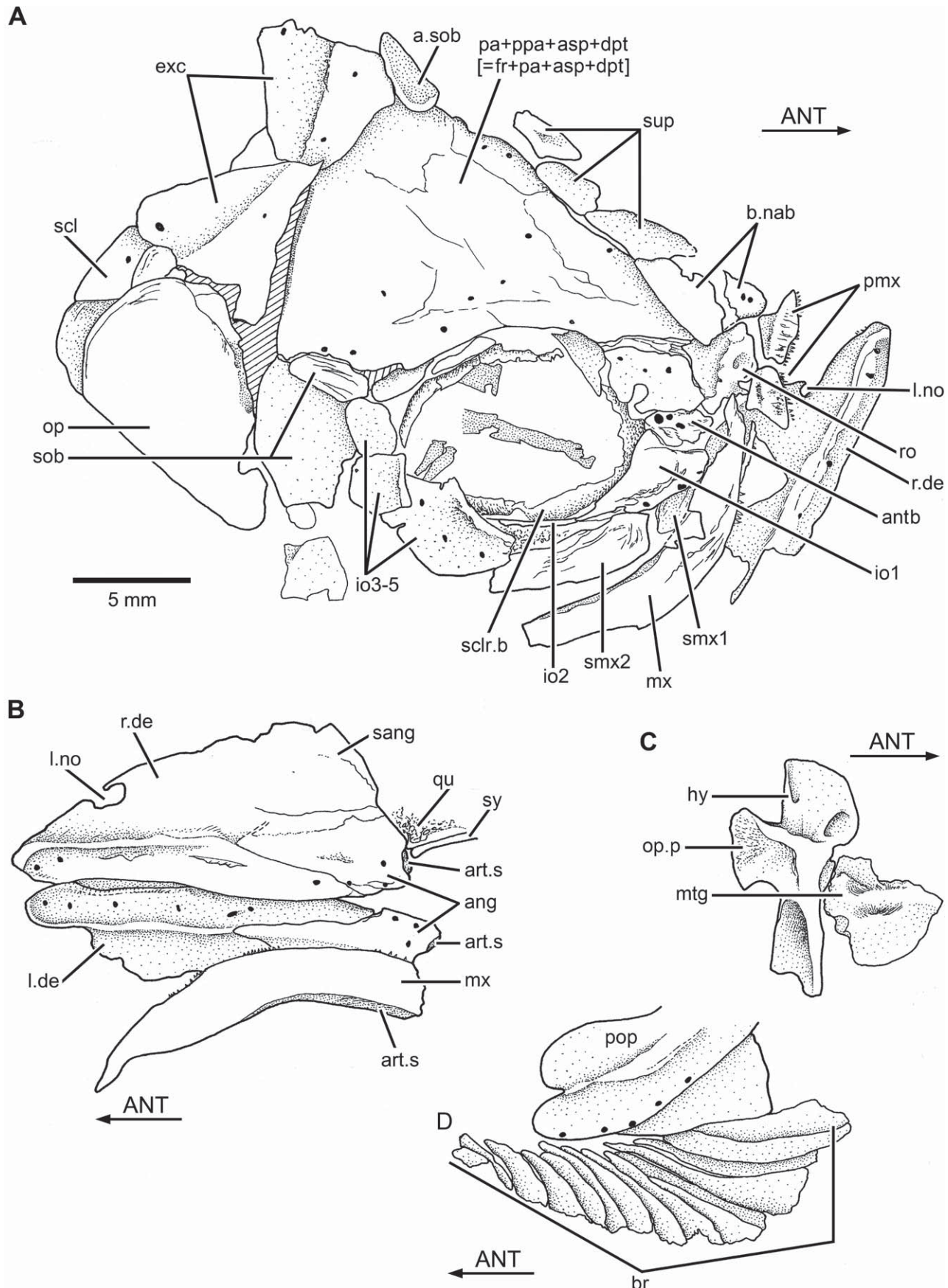


FIGURE 59. *†Parapholidophorus nybelini* Zambelli. **A**, drawing of cranium in a slightly oblique right dorsolateral view (MCSNB 2938). **B**, lower jaws in ventral view (MCSNB 2900). **C**, right hyomandibula and metapterygoid in lateral view (MCSNB 4797g). **D**, left opercular bones and branchiostegal rays in lateral view (MCSNB 3090). Hatched lines indicate broken bone surface. Scale bar applies to **A–D**.

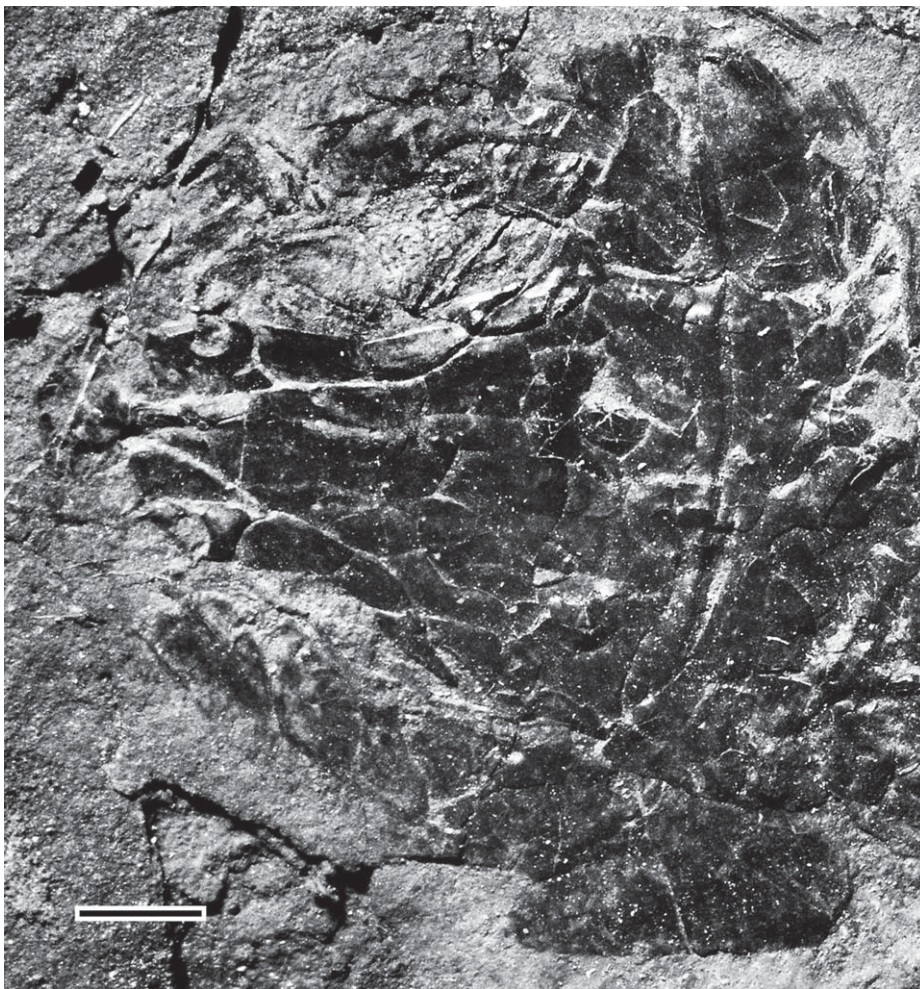


FIGURE 60. †*Parapholidophorus nybelini* Zambelli. Photograph of the dorsal view of skull roof of specimen MCSNB 2897. Scale bar equals 2 mm.

rudimentary and do not extend laterally to the anterior margin of the nasal bones. The ethmoidal or rostral commissure crosses the rostral from one side to the other. No pores are observed on the surface of the rostral that could belong to the commissure. It is unclear whether the ethmoidal commissure joins the anterior branch of the infraorbital sensory canal that exits the antorbital or not, because the few preserved antorbital bones are displaced. The surface anterior to the trajectory of the ethmoidal commissure shows small tubercles of ganoine, which are apparently lacking in the posterior surface of the bone. Anteriorly, the rostral bone overlies the rudimentary ascending process of the small premaxillae. The posterior contact between the rostral and the anterior tip of the skull roof plate includes an intermediate plate-like bone that it is identified here as an additional rostral bone (Fig. 62) to avoid confusion with the postrostral bone present in primitive actinopterygians (e.g., †*Cheirolepis*; see a discussion on rostral bones in Arratia and Cloutier, 1996).

The additional rostral is a small, slightly rectangular bone covering the contact margins of the rostral and skull roof plate. The additional rostral seems to be fused with the rostral bone in specimen MCSNB 2938, because the posterior projection resembles this separate bone found in other specimens.

There are two large, rectangular nasal bones (Figs. 59A, 60, 61, 62). The shape varies slightly between nasals, but the bone com-

monly has very well-defined margins. The anterodorsal margin is straight close to the medial wall of the nasal bone and is weakly sutured to the rostral bone, but it is markedly notched laterally, framing the anterior nostril. The medial margin is straight and sutures with the skull roof plate. The posterior margin may be straight or slightly irregular and has a weak contact with supraorbital 1. The supraorbital sensory canal (Fig. 62) is in the middle region of the nasal, but curves anterolaterally to exit the bone. One or two pores (or no pores) of the supraorbital canal are present in different specimens. Although most specimens have nasal bones with completely smooth surfaces, a few tubercles or ridges of ganoine are present in some specimens.

There is no evidence of a supraoccipital bone. The dermal skull roof plate ends almost in a straight line at the posterior margins of the dermopterotic and postparietal regions.

Two large, triangular, paired extrascapular bones (Figs. 58A, 59A, 61) cover the posterior region of the skull roof plate, just overlapping the posterior margin where the postparietals and dermopterotic would end. The extrascapulae are broken in most specimens, but each extrascapula has an almost straight anterior margin, whereas its posterior margin is roughly triangular. The extrascapular canal or supratemporal commissure runs transversely, about the mid-region of the bone, as indicated by the presence of a few rounded pores.

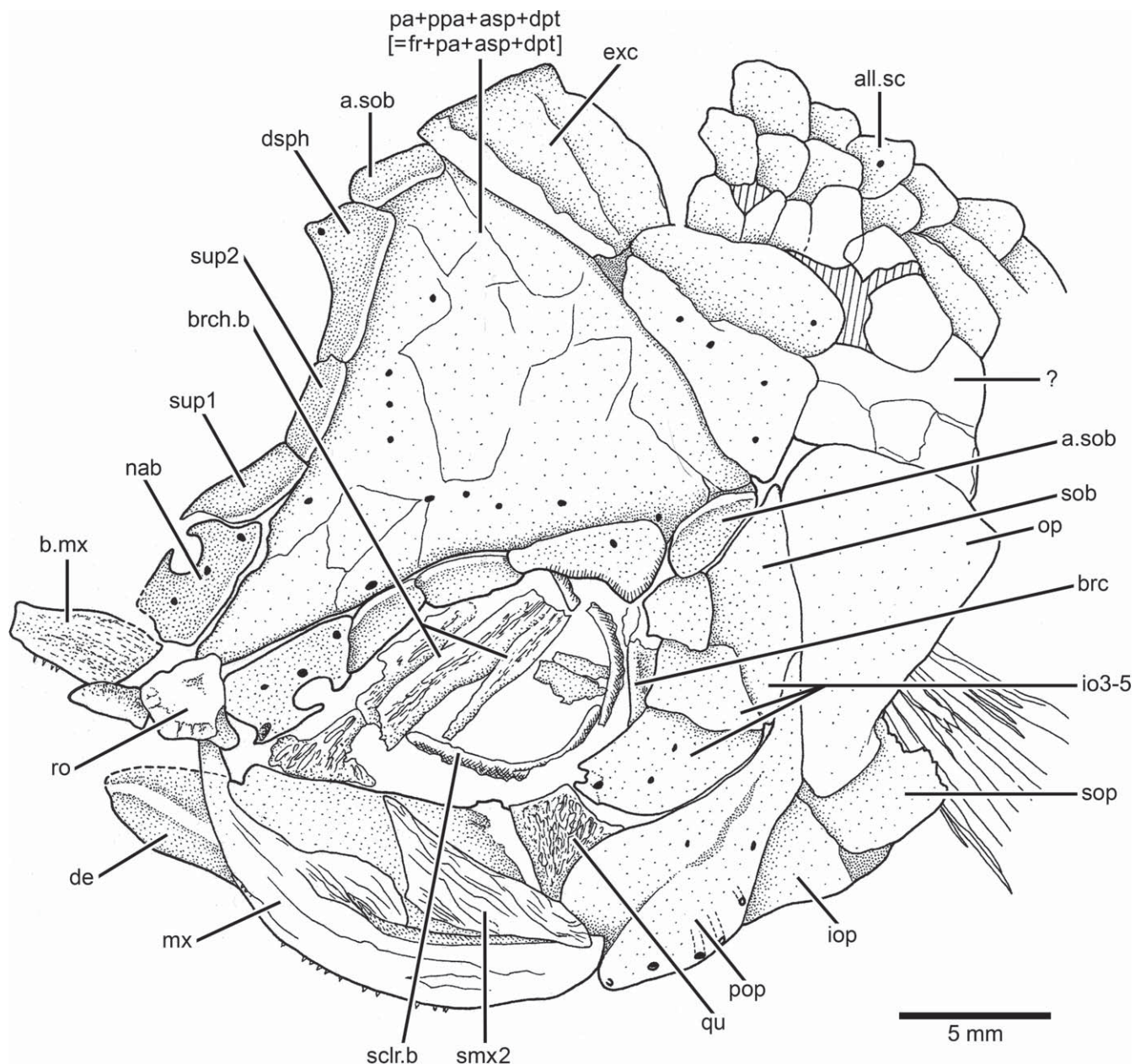


FIGURE 61. *†Parapholidophorus nybelini* Zambelli (MCSNB 3220). Drawing of cranium and anterior part of body in slightly oblique left dorsolateral view.

Circumorbital Series—The circumorbital ring consists of two or three supraorbitals, one antorbital, five infraorbitals, one dermosphenotic, and occasionally an additional dermosphenotic. The orbital margin is closed by the contribution of a skull roof element, the nasal bone, which forms the anterodorsal corner of the orbit between supraorbital 1 and the antorbital. One large suborbital and one accessory suborbital are other elements of the circumorbital series. All these bones, with the exception of the accessory dermosphenotic and accessory suborbital, are consistently present. In addition, sclerotic bones are present.

Commonly, two or three elongate, thick supraorbital bones are lateral to the orbital margin of the skull roof plate and

in between the nasal bone anteriorly and the dermosphenotic posteriorly. But this pattern is variable because some specimens have only two elongate supraorbitals, whereas others have three. The shapes and sizes of the elements vary between left and right sides of the cranium in some specimens.

Supraorbital 1 (Figs. 59A, 61, 62) is commonly slightly rectangular. It joins the posterior margin of the nasal bone anteriorly and supraorbital 2 posteriorly; the posterior margin of the latter joins the anterior tip of supraorbital 3 when it is present or the dermosphenotic laterally. When three supraorbitals are present, the three bones are slightly smaller than when two supraorbitals are present.

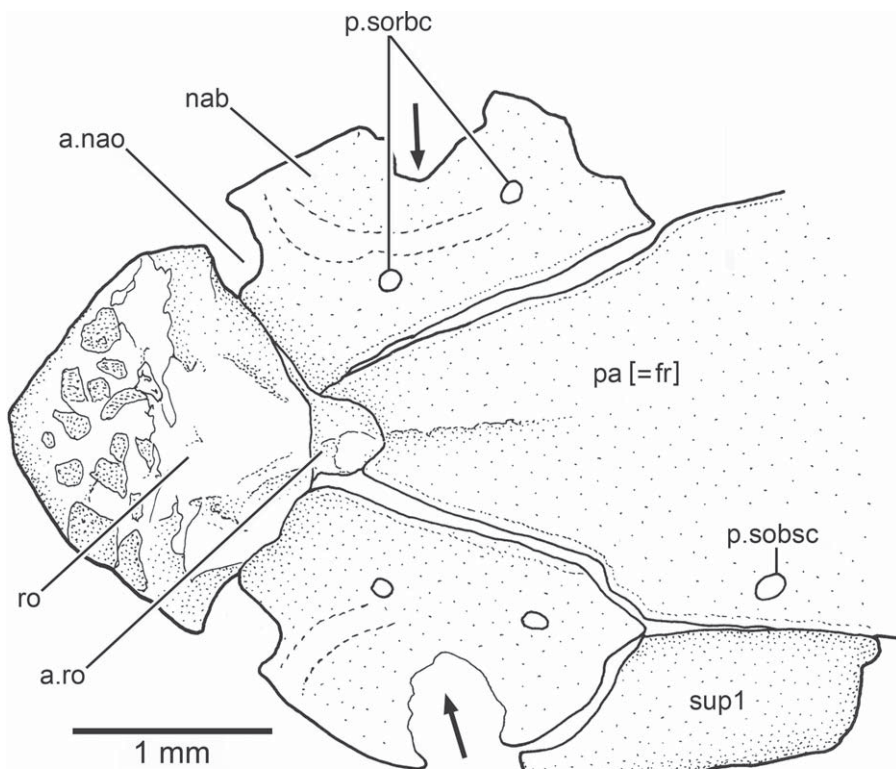


FIGURE 62. *†Parapholidophorus nybelini* Zambelli (MCSNB 3001). Drawing of anterior part of skull roof bones in dorsal view showing their relationships. Arrows point to a notch or posterior nasal openings.

The antorbital (Fig. 59A) has different shapes and sizes in the few specimens where it is preserved. Thus, I am not able to provide a complete description of this bone that varies in shape from an elongate, roughly triangular bone, a teardrop-like bone, to an irregularly shaped bone. Independent of the shape, the bone consistently carries the infraorbital canal, and one to three pores are observed on its lateral side.

Infraorbital 1 (Fig. 59A) is a large bone, but comparatively not as large as that in *†Pholidophorus gervasutti*. Its shape may be almost oval in some specimens, but triangular in others. It commonly has a small projection extending ventral to infraorbital 2. The infraorbital sensory canal is close to the ventral margin of the bone, as revealed by the tube-like aspect of this region and the series of small pores opening close to the ventral margin.

Infraorbital 2 is an elongate, tube-like bone that transmits the infraorbital sensory canal (e.g., MCSNB 4311). Occasionally one sensory pore can be observed.

Infraorbital 3 (Figs. 59A, 61, 63) is almost rhomboidal-shaped, with a concave anterior margin. In some specimens, infraorbital 3 has an almost straight dorsal margin, whereas the posterior margin is almost rounded. Infraorbital 3 projects posteriorly and extends below the suborbital bone, contacting the anterior margin of the preopercle. This is the condition present in the lost holotype and in the newly assigned neotype. However, a few specimens identified as *†Parapholidophorus nybelini* by Zambelli (1975) present a short infraorbital 3 (e.g., MCSNB 2955). Infraorbital 3 contacts infraorbital 2 anteriorly, the preopercle posteriorly, and infraorbital 4 and suborbital dorsally. The infraorbital sensory canal is close to the orbital margin and has a variable number (two to five) of short sensory tubules and pores. A pit-line groove (anterior division of the supramaxillary pit-line) has been observed in some specimens.

Infraorbitals 4 and 5 (Figs. 59A, 61, 63) are small, slightly rectangular bones, deeper than broad, carrying the infraorbital canal close to their orbital margin. Both infraorbitals may present variability in their shape and size. Both infraorbitals contact the suborbital posteriorly, but infraorbital 5 contacts the dermosphenotic dorsally and may contact the accessory suborbital posteriorly.

The moderately large and triangular dermosphenotic (Figs. 59A, 61) is positioned posterior to supraorbital 2 (or supraorbital 3 when it is present), anterolateral to the posterior corner of the dorsal orbital margin, and dorsal to infraorbital 5. The dermosphenotic does not fuse to the underlying autosphenotic region of the skull roof plate and narrowly extends over the dermopterotic region of the skull roof plate posteriorly. The dermosphenotic lacks well-defined processes, and it can be interpreted as type Ib in Poplin's (2004) classification of dermosphenotics. The infraorbital and otic canals join in the dermosphenotic; one sensory pore is commonly present close to the posterior margin of the bone. An additional dermosphenotic is present in some specimens. The bone is roughly triangular, and it lies at the anteroventral border of the dermosphenotic. This bone is interpreted here as an additional dermosphenotic, because it contains part of the infraorbital canal and has a pore near the dorsal margin of the bone.

The anterior and posterior sclerotic bones (Fig. 59A, 61, 64) form a complete ring surrounding the eyeball. The bones, which are completely preserved in a few very well-preserved specimens, are thin and broad.

One large suborbital (Figs. 59A, 61) occupies the space defined by the posterior margins of infraorbitals 3, 4, and 5 anteriorly, and the opercle and preopercle posteriorly. The suborbital is roughly rectangular in the neotype (as well as in the lost holotype). Its straight ventral margin has a conspicuous articulation with the

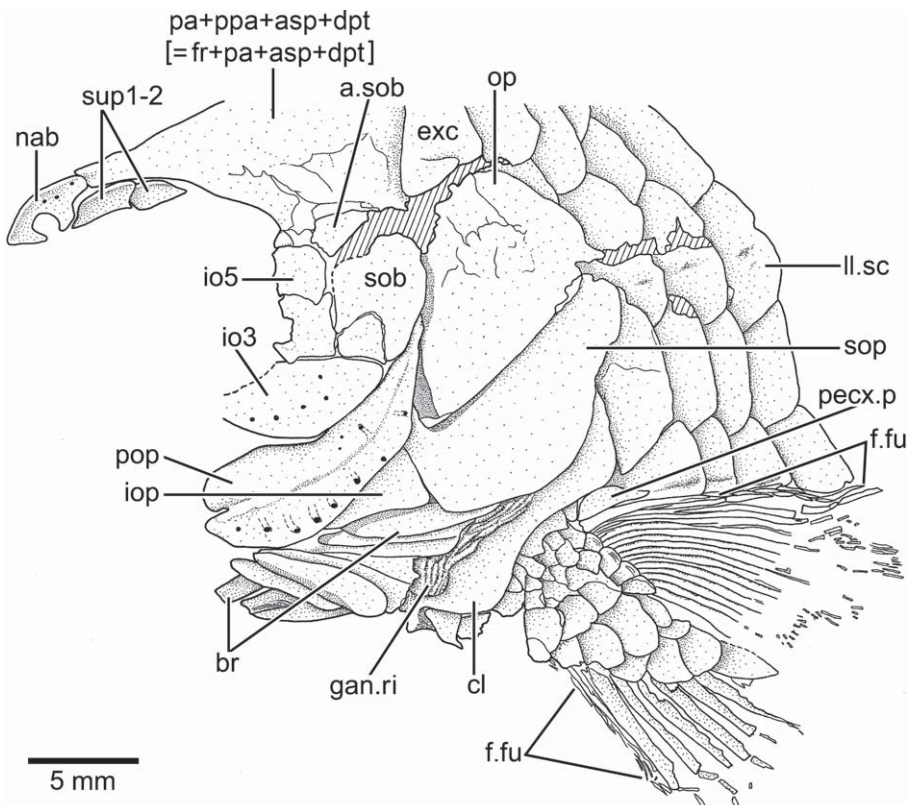


FIGURE 63. *†Parapholidophorus nybelini* Zambelli (MCSNB 2897). Drawing of posterior part of cranium and anterior region of body in left lateral view. Hatched lines indicate broken bone surface.

dorsal margin of infraorbital 3. However, in other specimens, the ventral margin ends in an acute tip that is narrowly in contact with infraorbital 3.

A small triangular or ovoid accessory suborbital bone (Fig. 61) is commonly present, lying on the large suborbital bone and lateral to the dermopterotic region of the skull roof plate. It may extend posteriorly onto the opercle. The suborbital and the additional suborbital have their surfaces covered with a smooth layer of ganoine.

Upper Jaw—The upper jaw is composed of the paired premaxillae and maxillae and two supramaxillae on each side of the skull. Occasionally only one supramaxilla is present. The external surface of the maxilla and supramaxillae are covered by a thick layer

of ganoine, which is ornamented with irregular, longitudinal ridges of ganoine of different lengths and tubercles of different sizes. Premaxillae are covered with tubercles of ganoine.

The premaxilla (Figs. 59A, 65) is displaced in most specimens and is incompletely preserved. The bone is small, roughly triangular with a short ascending process. Tiny conical teeth are on the oral margin of the bone. A rostrodermethmoid has not been observed in any specimen.

The gently curved maxilla (Figs. 59A, 61) is as long as or longer than the lower jaw. It has a moderately long articular process anteriorly. The maxillary blade is slightly deeper anteriorly, but its depth decreases slightly posteriorly. The dorsal margin of the bone is slightly concave and has a narrow articular surface, without ganoine, for the supramaxillae. The dorsal margin does not possess a well-defined supramaxillary process, but a bump is present. The posterior margin of the maxilla is rounded (see Fig. 61). A single row of very small conical teeth is present along the oral margin of the blade, extending almost to the posterior margin of the bone.

Two supramaxillary bones (Figs. 59A, 61) are positioned on the posterodorsal margin of the maxilla. Together they represent about 70–80% the length of the maxillary blade, and supramaxilla 2 alone is about half of the length. Supramaxilla 1 is a slightly oval or triangular bone and is considerably smaller than supramaxilla 2. Supramaxilla 2 is a large and deep bone, with its maximum depth equal or even deeper than that of the maxilla. Its well-developed anterodorsal process overlaps completely the dorsal margin of supramaxilla 1, even extending further anteriorly in some individuals. Its posterior tip may be slightly acute or rounded, producing a gentle profile to both posterior tips of supramaxilla 2 and the maxilla. A few specimens (e.g., MCSNB 3090) have a single long supramaxilla that apparently is the result of fusion of the two supramaxillae (see Fig. 66). This conclusion is based on the

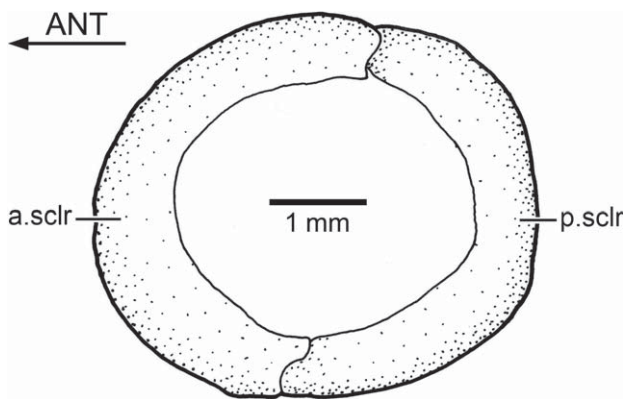


FIGURE 64. *†Parapholidophorus nybelini* Zambelli (MCSNB 2962). Drawing of sclerotic bones of left eye in lateral view.

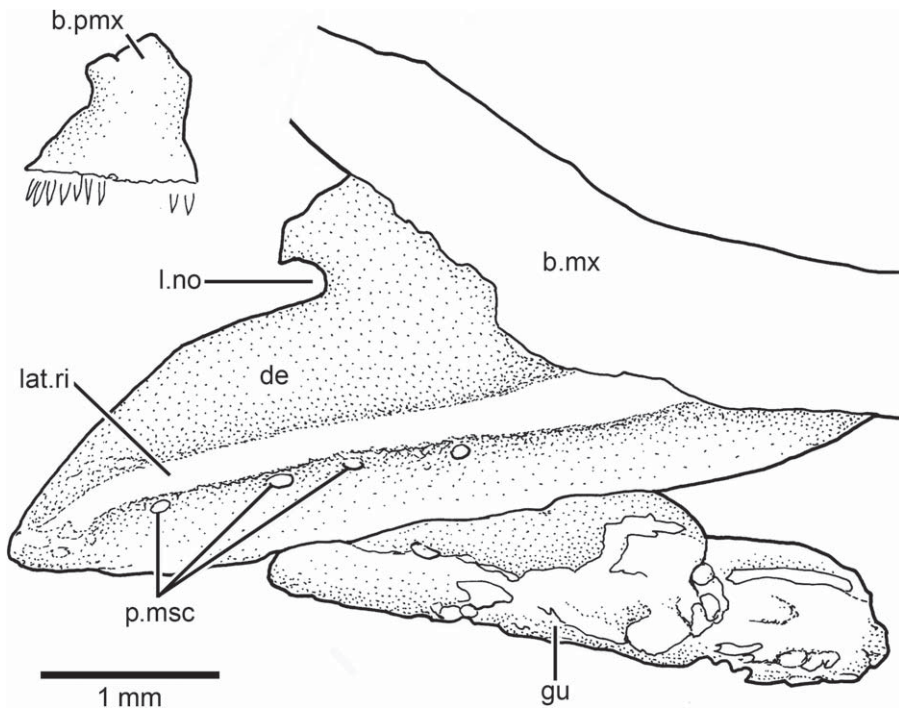


FIGURE 65. *†Parapholidophorus nybelini* Zambelli (MCSNB 3211). Drawing of anterior part of left jaws in lateral view and gular plate in ventral view.

morphology of the anterodorsal part of the bone, which corresponds to the anterodorsal process of supramaxilla 2 in other specimens.

Lower Jaw—The lower jaw (Figs. 59A, B, 61, 65) is often damaged or covered by the maxilla and supramaxilla so that only the anterior part of the jaw and its ventral region are visible. However, a few complete jaws (Fig. 59B) are observed in some specimens. Laterally, each jaw is composed by the dentary, surangular, and angular. The dorsal margin of the jaw ascends in an almost oblique line, with its highest point at the level of the surangular, and then decreases abruptly posteriorly. A deep, almost rounded ‘leptolepid’ notch is located at about the first third of the jaw length. A well-developed, distinct lateral ridge protrudes along the jaw and becomes inconspicuous in the anterior region of the angular. It separates dorsal and ventral regions of the jaw.

The dentary (Figs. 59B) extends below the angular posteroventrally and forms most of the lower jaw. The limit between both bones is usually unclear, as is the limit between the surangular and dentary. The dentary bears very small conical teeth on the oral margin; in most specimens they are damaged. The angular

(Fig. 59B) forms the posteroventral lateral wall of the jaw. An elongate surangular, which is sutured with the angular and dentary, forms the posterodorsal margin of the lower jaw and is the main element forming the coronoid process of the jaw. The jaw illustrated in Figure 59B shows incomplete sutures due to poor preservation of this region.

The posterior margin of the jaw (Figs. 59B, 67) is truncated, because a postarticular process is lacking. A chondral element, which I interpret (because of its position and comparison with other jaws) as the posterior portions of the articular-retroarticular, is medial to the angular.

A series of rounded pores belonging to the mandibular sensory canal are positioned below the lateral, protruding bony ridge of the jaw. The number of pores is variable (six to 10). A short, vertical oral pit-line groove is observed near the posterior corner of the angular. The posterior opening of the mandibular sensory canal is positioned medially.

The articulation between the lower jaw and quadrate (Fig. 58A) is below mid-orbit or slightly anterior.

Palatoquadrate and Suspensorium—Only a few bones of the palatoquadrate and the suspensorium are observed because other bones of the cheek obscure them. The quadrate (Figs. 59B, 67) is observed as a partially ossified cartilaginous element. A well-developed posteroventral process is not present at the posterior margin of the quadrate, although the margin is well ossified. An elongated, rod-like symplectic (Fig. 59B) is posterior to the quadrate, and both bones extend ventrally to the articulation with the lower jaw, a condition also observed in some specimens of *†Pholidophorus gervasutti*. The complete symplectic is unknown because its posterodorsal region is covered by the preopercle. However, it is expected that the symplectic would be long due to the position of the articulation of the lower jaw, which is slightly anterior in comparison with *†Pholidophorus latiusculus* and *†Ph. gervasutti*. These fishes have longer jaws than *†Parapholidophorus*. There is no evidence of a quadratojugal.

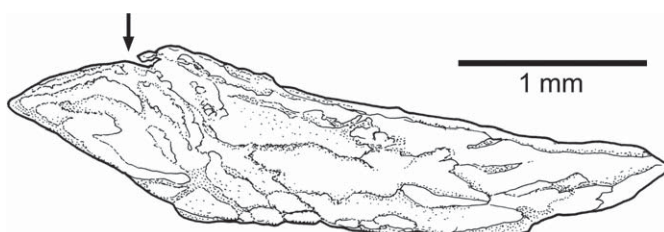


FIGURE 66. *†Parapholidophorus nybelini* Zambelli (MCSNB 3090). Drawing of left supramaxilla in lateral view. Note that the layer of ganoine and ornamentation obscure the region (indicated by an arrow) where the articulation between supramaxillae 1 and 2 should be.

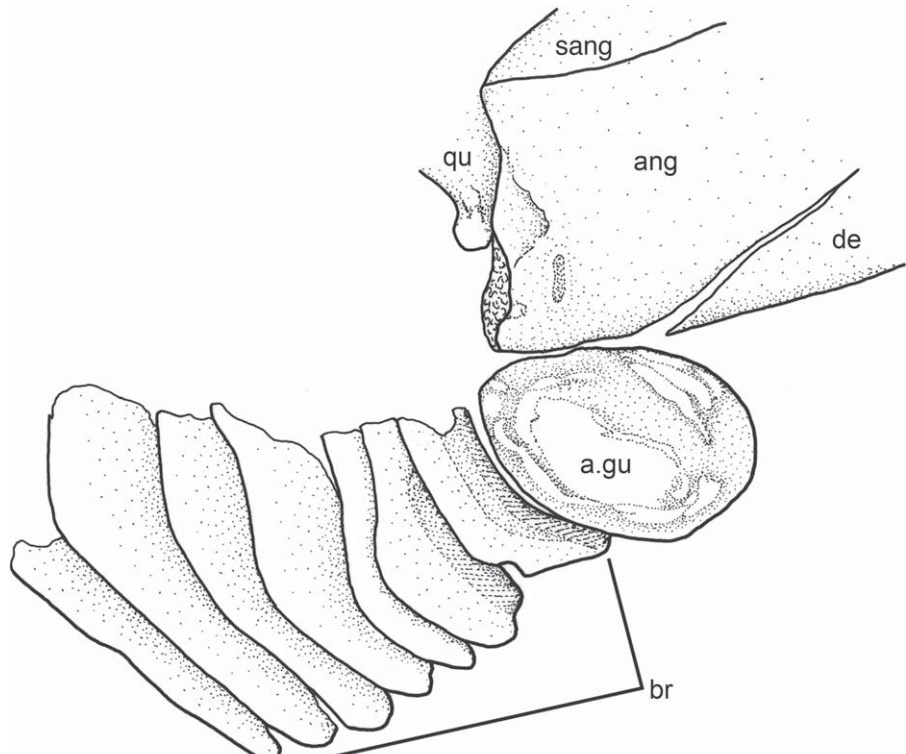


FIGURE 67. *†Parapholidophorus nybelini* Zambelli (MCSNB 3072). Drawing of posterior part of right lower jaw, additional gular plate, and branchiostegal rays in lateral view.

The metapterygoid (Fig. 59C) is an irregularly shaped bone in front of the hyomandibula. The metapterygoid is well ossified in the region of the levator autoplatini crest, but dorsal and ventral to the crest, the bone is thin and formed by cartilage, as in the quadrate. It is notable that both the entopterygoid and ectopterygoid have not been observed in any specimen. Likely, they were very small, thin bones.

Although the suborbital and part of the preopercle cover the hyomandibula laterally, it is possible to observe part of the hyomandibula when the suborbital is displaced or not preserved. The hyomandibula (Fig. 59C) is a moderately narrow and short bone that lacks membranous expansions at its anterior border; its main shaft is heavily ossified. Its dorsal margin, apparently, has only one facet to articulate with the braincase. A well-developed, moderately short and broad process to articulate with the opercle is near the posterodorsal margin of the bone. A preopercular process is absent at its posterior margin.

Hyoid Arch and Branchial Arches—With the exception of an elongate and narrow anterior ceratohyal (MCSNB 2992), no other elements of this arch have been observed. A few pieces of branchial arches, probably ceratobranchials, are observed in one specimen (Fig. 62). Tooth plates or gill rakers seem to be lacking.

Opercular, Branchiostegal Series, and Gular Plate—The opercular bones are positioned posterior to the posterior margin of the skull roof plate. All opercular bones, as well as the branchiostegals, are covered by a smooth layer of ganoine, with the exception of a few fine ridges of ganoine that are occasionally present at the dorsal margin of the opercle and interopercle.

The shape and size of the preopercle (Figs. 61, 63) are consistent in the available exemplars. The bone is expanded anteroventrally in an inverted heart shape, narrowing progressively dorsally to end in an acute tip. No distinct ventral and dorsal arms are present, but there is a slight inclination of the anterior margin from the dorsal

to ventral direction. The bone presents a well-developed expansion that is anterior to the main course of the preopercular canal, which is slightly closer to the posterior margin than to the anterior one. Anteriorly, the preopercle presents a deep, acute notch where the preopercular canal exits. This notch can have different sizes, but it is consistently present. The posterior preopercular margin is generally smooth, similar to the condition observed in *†Parapholidophorus caffii* (see below). The dorsal part of the preopercle, exposed in several specimens, is short so that the dorsal margin of the bone is distant from the lateral margin of the dermopterotic region of the skull roof plate. The anterior margin of the preopercle is narrowly covered by the posterior margins of the suborbital and infraorbital 3.

The pathway of the preopercular sensory canal and its tubules is not visible because of the layer of ganoine. However, its trajectory can be assumed based on a series of six to 10 large, rounded pores opening close to the posteroventral margin of the preopercle.

The opercle (Figs. 59A, 61, 63) is a large, roughly triangular bone, with an almost rounded dorsal margin. The anterior margin of the opercle is markedly thickened and almost vertically oriented, but ventrally, in front of the anterodorsal process of the subopercle, it is gently rounded. The long ventral margin of the opercle is markedly oblique.

The subopercle (Fig. 63) is a large bone, but slightly smaller than the opercle. Its posteroventral margin is gently rounded. Its anterior margin is slightly notched in front of the interopercle and extends dorsally as part of the well-developed anterodorsal process of the subopercle.

The interopercle (Figs. 61, 63) is large and well exposed between the posterior margin of the preopercle and anterior margin of the subopercle. The bone extends anteriorly and is medial to the preopercle. The exposed portion of the interopercle is triangular, with

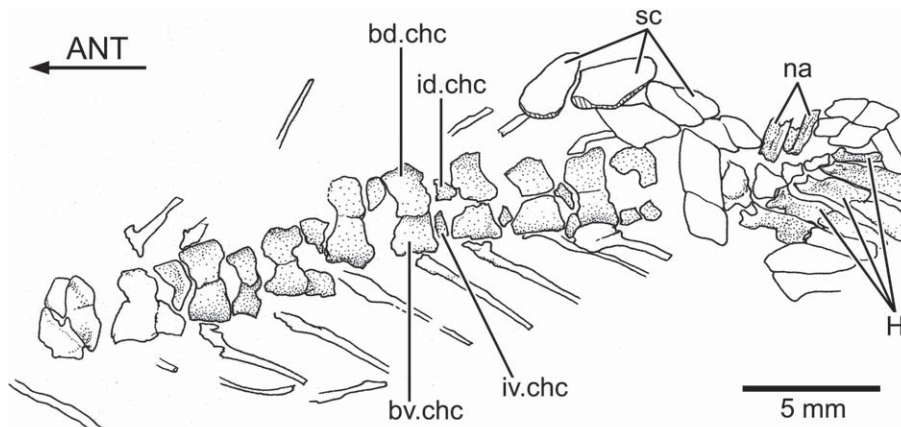


FIGURE 68. *†Parapholidophorus nybelini* Zambelli (MCSNB 2898). Drawing of caudal vertebrae and endoskeleton in left lateral view.

a slightly straight posterior margin and a slightly concave posterior one.

There are 15 branchiostegal rays (Fig. 59D) preserved in specimen MCSNB 3090. However, in most specimens the series is incompletely preserved, with the most anterior branchiostegals missing. The anterior branchiostegals are relatively short, broad bones, whereas the posterior-most ones are longer and slightly triangular. As far as can be observed, their exposed surfaces are covered with ganoine; in contrast, the areas of overlap between rays lack ganoine (Fig. 67).

As with the branchiostegals, the median gular plate is not seen in most specimens due to the condition of preservation. The median gular plate (Fig. 65) is elongate, slightly oval-shaped, and about half of the length of the lower jaw. The external surface of the gular plate is covered with a thick layer of ganoine roughly ornamented. Preceding the branchiostegal series is a round plate (Fig. 67) that is interpreted here as an additional gular that lacks an articulation with the hyoid arch. The additional, paired gulars are lateral to the median elongate gular. It is unclear whether this additional gular is consistently present in this species or is a variable feature. The surface of the additional gular is covered with a thick layer of ganoine that is ornamented with concentric ridges. A similar element has occasionally been observed in other pholidophorids, e.g., *†Pholidophorus gervasutii* and *†Pholidorhynchodon*.

Vertebral Column and Intermuscular Bones—Only a few elements of the vertebral column can be observed where some scales are displaced or lost. The vertebral abdominal region is formed by monospondylous centra, whereas diplospondylous centra (Fig. 68) are observed in the caudal region. Each monospondylous abdominal centrum is formed by one basidorsal and one basiventral hemichordacentrum, which may fuse to form a thin-walled, ring-like chordacentrum. No supraneural bones are observed, and this could be due to the fact that these thin, delicate elements are commonly weakly ossified. So far as can be observed, no epineural or epipleural bones are associated with any vertebra.

The last caudal vertebrae can be observed in MCSNB 2898, because the scales are displaced. All centra, except the last ones, are diplospondylous. Each centrum (Fig. 68) is formed by basidorsal and basiventral hemichordacentra and interdorsal and interventral hemichordacentra. The basidorsal and basiventral hemichordacentra are larger than their corresponding interdorsal and basiventral elements, and they may join at mid-height. In contrast, the smaller interdorsal and interventral commonly do not meet in

this region. The interdorsal and interventral are smaller in the last caudal vertebrae, and they are absent in front of the hypurals.

Paired Fins—Bones of the pectoral girdle and fins are preserved in many specimens. The following dermal elements of the pectoral girdle are preserved: supracleithrum, cleithrum, clavicle, and postcleithra. The structure of the posttemporal remains unknown. The chondral bones are not preserved so that the number of radials is unknown.

The supracleithrum is a moderately broad, elongate bone that overlies the dorsal region of the cleithrum ventrally and part of the dorsal postcleithrum posteriorly. The posterior margin has a small notch where the lateral line exits. This notch is positioned almost in front of the series of lateral line scales. The lateral line may lie at the upper half or middle region of the supracleithrum.

The cleithrum (Fig. 69) is exposed laterally in a few specimens. The elongate cleithrum is slightly vertically oriented, and dorsal and ventral arms are not clearly discernible. The dorsal-most tip of the cleithrum is narrow, and the bone expands ventrally, producing a slightly sigmoid posterior margin, and continues in a narrow and short ventral arm that ends in a vertical anteroventral margin. This margin articulates with a narrow triangular element, the clavicle. The clavicle (Fig. 69) has posteriorly a well-defined articular surface for the cleithrum. The anterior margin of the clavicle together with the cleithrum produce a slightly rounded anteroventral region of the dermal pectoral girdle, as already described for *†Pholidophorus gervasutii*.

The whole anterior surface of the cleithrum is covered with a series of long, toothed ridges that form the serrated appendage or clavicular element (Fig. 69). The ridges are firmly attached to the cleithrum. Medial to the serrated appendage, the cleithrum expands in a slightly broad region that lacks ganoine.

Two postcleithra are present posterior to the cleithrum. The dorsal postcleithrum is the largest one, and it is slightly deeper than the scales of the lateral line. The dorsal postcleithrum is located posterior to the ventral region of the supracleithrum and posterior to the cleithrum. An almost oblique junction is present between the dorsal postcleithrum and the small, slightly square-shaped ventral postcleithrum. Both bones are covered with a smooth layer of ganoine and are difficult to differentiate from the surrounding scales.

The pectoral fins are positioned low in the flank, close to the ventral margin of the body. Each pectoral fin consists of 18 or 19 lepidotrichia. The first ray is the thickest of all rays and is a compound element, fused at least with two elongate basal fulcra and elongate fringing fulcra, as in the condition described above

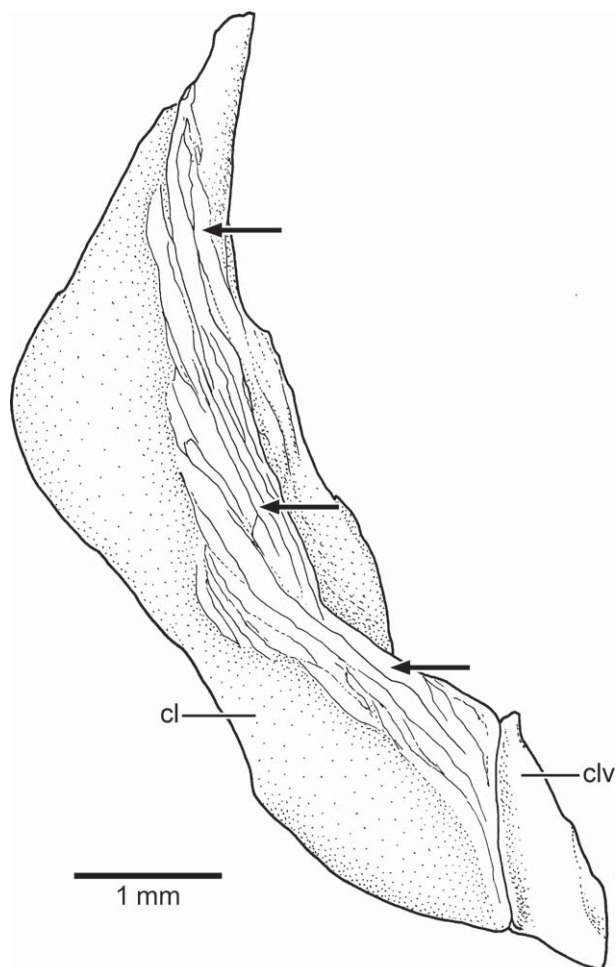


FIGURE 69. *†Parapholidophorus nybelini* Zambelli (MCSNB 2962). Drawing of right cleithrum and clavicle in lateral view. Arrows point to the serrated appendage.

for *†Pholidophorus gervasutii* and *†Pholidorhynchodon malzani*. The proximal region of the first ray is massive and has an articular fossa, as in other species described here. A pterygium is not fused with the base of the first ray. The pectoral rays have long bases; they are segmented and finely branched distally. A series of elongate fringing fulcra is associated with the leading margin of the fin. A moderately long, leaf-like pectoral axillary process lies above the insertion of the pectoral fin.

The pelvic girdles or basipterygia have not been observed in any specimens due to the fact that the ganoid scales cover them. The origin of the pelvic fin is at the level of the eighth or ninth vertical row of scales. The pelvic fin consists of three to five leaf-like, elongate basal fulcra and 10 or 11 rays. The lateral rays have very long, narrow bases; they are segmented and branched at their distal tips. In contrast, the inner rays become considerably shorter medially, and the most internal rays are very short and thin. A series of small, elongate fringing fulcra are associated with the leading margin of the fin. A large, leaf-like, and well-ossified pelvic axillary process lies at the base of the fin.

Dorsal and Anal Fins—The origin of the dorsal fin is at the level of the 17th, 18th, or 19th vertical row of scales. The dorsal fin (Fig. 57A, B) is roughly triangular, with long first principal rays

and very short posterior ones. Four or five small basal fulcra precede the series of dorsal fin rays. The first fulcra are very small, unpaired elements that are followed by fulcra that become larger posteriorly. There are 11 or 12 principal rays, including the first segmented but unbranched ray; all rays have a very fragile aspect and are usually broken. The principal rays have long bases with only a little segmentation and branching distally. It is unclear if only the first principal ray forms the leading margin of the fin or whether the second principal ray is included. Small, elongate fringing fulcra lie between the last basal fulcrum and the leading margin of the fin.

The origin of the anal fin is about the level of the 18th, 19th, or 20th vertical row of scales. The short anal fin (Fig. 57A) is posterior to the dorsal fin and is closer to the caudal fin than to the pelvic fins. The anal fin consists of three or four small basal fulcra and about 10 principal rays. The anal fin rays, as in the dorsal rays, are very delicate and thin, and so are frequently broken in most specimens. Elongate fringing fulcra are associated with the leading margin of the fin.

Caudal Fin—The caudal endoskeleton (Fig. 68) is partially preserved in specimen MCSNB 2898. The last hemal spine and hypurals are broadly expanded in comparison with the preceding hemal spines. At least four hypurals are preserved. They are perichondrally ossified. Each hypural is associated with one ventral hemichordacentrum, producing a polyural type of caudal skeleton. Two expanded neural arches are observed above the hypural region. Epurals and uroneurals have not been observed.

Although the distal tips of the caudal fin rays (Fig. 58) are often broken, the tail is almost completely preserved in a few specimens (Fig. 58B). The hemi-heterocercal caudal fin is deeply forked, with long leading margins of the epaxial and hypaxial lobes of the fin. All rays are very thin, and their segments are weakly articulated. The terminal area covered by ganoid scales at the base of the caudal is divided in two well-defined regions formed by scales of different sizes and shapes, but ordered in a precise pattern. The dorsal area is longer than the ventral one and is formed by a series of rhombic, rectangular, and even fusiform scales that extend to the level of the last epaxial basal fulcrum in the epaxial lobe of the caudal fin. The ventral area is shorter than the dorsal one, and the scales are distributed in an almost circular pattern. The posterior margins of the scales framing the dorsal and ventral regions are usually rectangular. Posterior scales are slightly more elongate than anterior ones.

The caudal fin (Figs. 58B, 70) has eight or occasionally nine epaxial basal fulcra, a series of elongate epaxial fringing fulcra, 21 to 23 principal rays, a series of elongate hypaxial fringing fulcra, three or four segmented procurent rays, and two or three hypaxial basal fulcra. The epaxial basal fulcra are elongate, leaf-like elements that expand laterally, partially covering the next fulcrum. The anterior basal fulcra are unpaired, but the most posterior ones are paired. The first principal ray (only segmented) and the second principal ray (segmented and branched distally) form the dorsal leading margin of the fin. The series of epaxial fringing fulcra is on the dorsal margin of the first and second principal rays. The segmentation of the principal rays is straight. Dorsal processes of the bases of the middle principal rays are absent. The hypaxial procurent rays are segmented, and the terminal segment usually resembles the shape of the fringing fulcra. Accessory fringing fulcra are between the terminal segment of a procurent ray and the next one. A series of elongate fringing fulcra are positioned along the ventral margins of the last (only segmented) and penultimate (segmented and branched distally) principal caudal rays.

One slightly rhomboidal dorsal scute and another rhomboidal ventral one (Fig. 70) precede the epaxial and hypaxial series of basal fulcra. The dorsal scute usually presents a middle ridge and is covered by a smooth layer of ganoine. However, a few tubercles

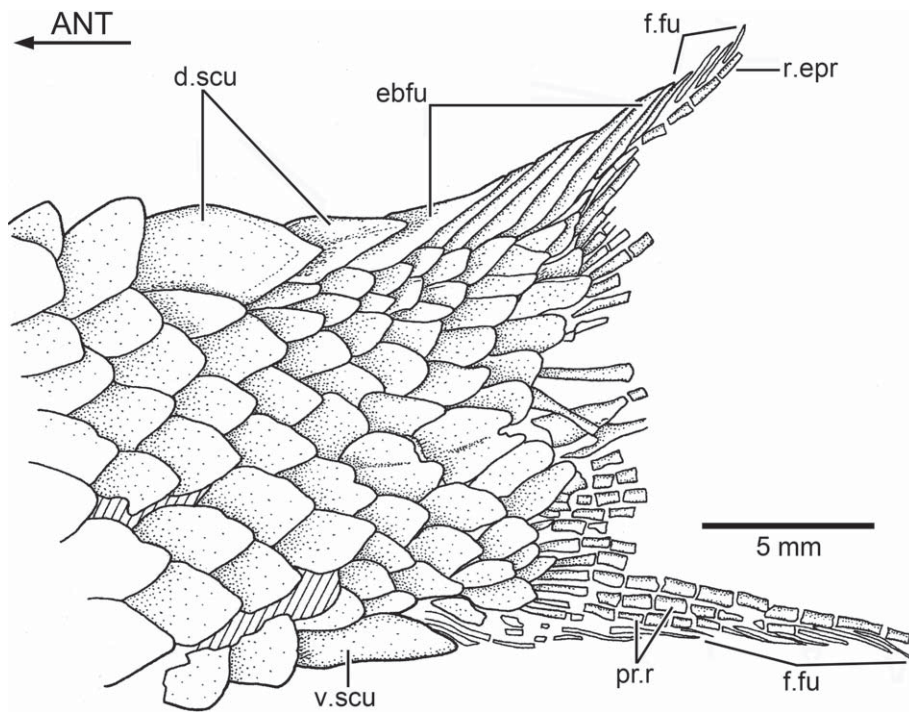


FIGURE 70. *†Parapholidophorus nybelini* Zambelli (MCSNB 3012). Drawing of caudal fin in left lateral view. Hatched lines indicate broken bone surface.

of ganoine were observed in specimen MCSNB 3005. The ventral scute is smaller than the dorsal one.

Scales—The body is covered by thick ganoid scales (Figs. 57A, B, 58A, B). The scales have different sizes and shapes along the body. Most scales of the dorsal and ventral rows of the body are rhombic, slightly rectangular, or even square-shaped. However, the three main rows of the flank (the lateral line row and its bounding dorsal and ventral rows) are deeper than broad. The scales of the flank become progressively smaller in the caudal peduncle. In the caudal region, the scales are more uniform in size, but they have different shapes; some are rhombic, others are rectangular, and some have slightly rounded posterior margins.

Lateral Line—Thirty-seven or 38 scales carry the main lateral line canal along the flank. However, the trajectory of the lateral line is observed only in a few scales, with an oval foramen more or less in the mid-region of the scale.

†*PARAPHOLIDOPHORUS CAFFII* (Airaghi, 1908) (Figs. 71–73)

Pholidophorus Caffii: Airaghi, 1908:3, text-fig. 2.

Pholidophorus latiusculus: Bassani, 1914:379 (in part).

Pholidophorus latiusculus: Alessandri, 1920:96 (in part).

Pholidophorus latiusculus: Boni, 1937:132, pl. 4, fig. 4, pl. 5, fig. 3, text-figs. 9, 10.

Pholidophorus (?) *caffii*: Nybelin, 1966:376–382, fig. 5, pl. 6, fig. 1.

Parapholidophorus caffii (Airaghi): Zambelli, 1975:14.

Parapholidophorus caffii: Arratia and Herzog, 2007:fig. 5.

Holotype and Only Specimen—MCSNB 563 (Fig. 71A, B). Almost complete specimen, with the skull roof bones destroyed.

Type locality, Age, and Distribution—Viciarola near Saint Pellegrino, about 23 km north of Bergamo, Lombardy, northern Italy; Late Triassic (Rhaetian), about 204 to 200 Ma.

Diagnosis—Emended from Nybelin, 1966, and based on a unique combination of characters. Autapomorphies are identified

with an asterisk [*]. Head about 25% of standard length. Eyes moderately large, about 33% of head length. Depth of caudal peduncle about 10% of standard length. Acute posterior margin of maxilla. Supramaxilla 2 with rudimentary anterodorsal process. Preopercle broad, with large anterior expansion extending below infraorbital 3 and maxilla [*]. With about 35 lateral line row scales. Caudal fin with 20 principal caudal rays.

Description

The holotype is small, reaching about 58 mm total length and about 49 mm from the tip of the snout to the posterior-most lateral line scale. The fish is slightly fusiform, with its maximum depth in the predorsal region. The head is almost triangular in shape, with its deepest points at the posterior end of the cranial roof. The caudal peduncle is slightly narrower than the rest of the body. The pectoral fins are positioned nearer the ventral margin of the body than to the middle region of the flanks. The origin of the dorsal and pelvic fins is at mid-length. The anal fin is placed posterior to the base of the dorsal fin. All fins are small, with very delicate and slender rays, and elongate fringing fulcra.

The cranial bones and scales are covered with a smooth layer of ganoine, with the exception of the maxilla and supramaxillae, which are ornamented with longitudinal ridges of ganoine.

Braincase—The braincase is mostly destroyed. Pieces of bones that belong to the posterior part of the skull roof are preserved, but nothing can be said about them. For example, the parietal and extrascapular bones tentatively illustrated by Nybelin (1966:pl. 6, fig. 1) cannot be identified with certainty. A thin portion of the parasphenoid can be observed (Fig. 72). No teeth are associated with the parasphenoid or scattered where the entopterygoid would be visible.

Circumorbital Series—The antorbital, five infraorbitals, and a piece of the dermosphenotic are preserved (Figs. 71B, 72). In addition *†Parapholidophorus caffii* presents one large suborbital that is broken into two pieces.

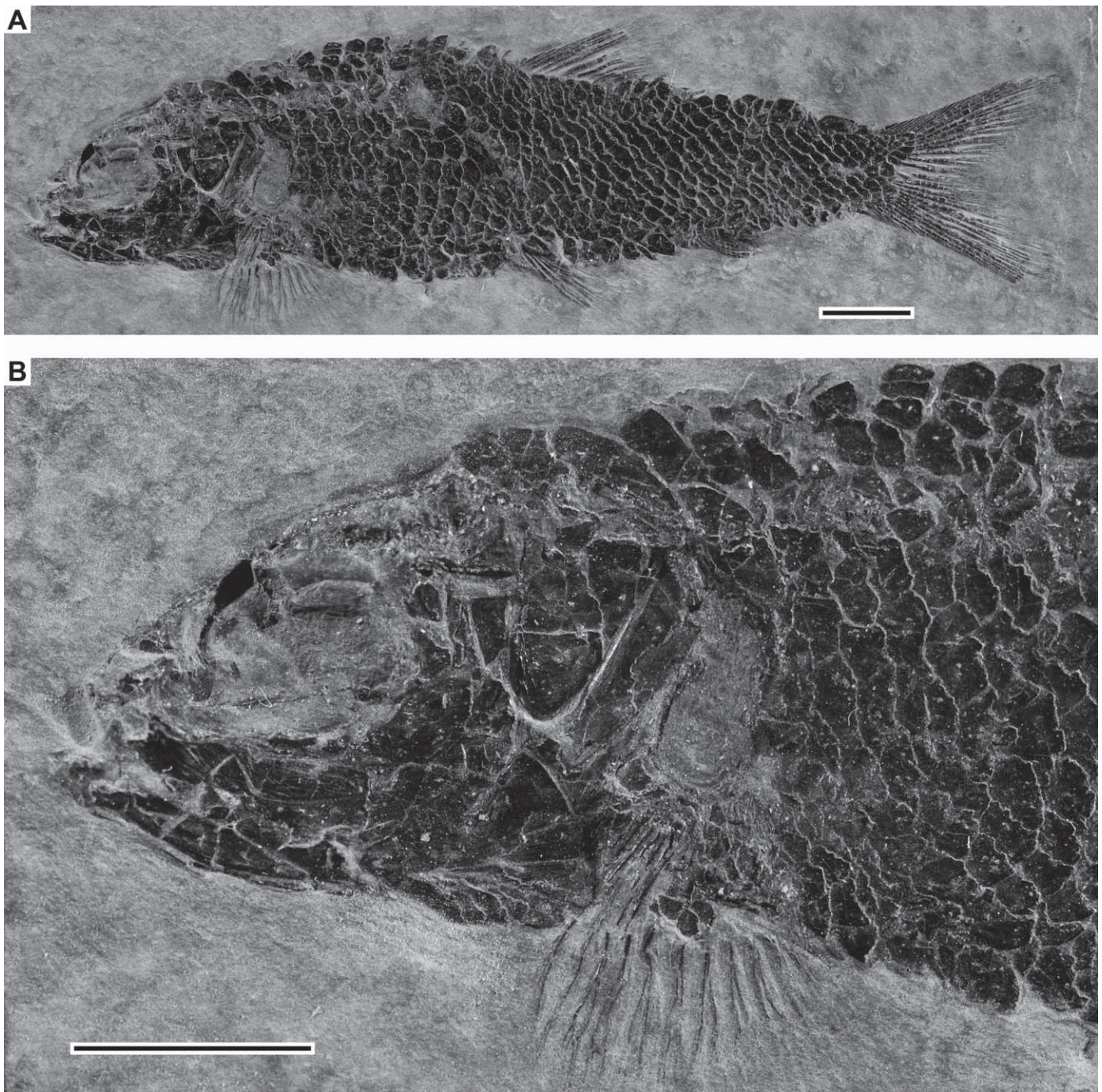


FIGURE 71. *†Parapholidophorus caffii* (Airaghi; MCSNB 563). **A**, photograph of the holotype and only known specimen in left lateral view. **B**, enlargement of the head. Scale bars equal 5 mm.

The antorbital (Figs. 72) is a relatively large, thick, teardrop-like bone positioned dorsal to the anterodorsal margin of infraorbital 1. It forms the anteroventral margin of the orbit. This small bone was covered with ganoine that now is almost weathered away. Although I have not been able to see the complete trajectory of the infraorbital canal, an extension of this canal is enclosed in bone. The antorbital carries part of the anterior section of the infraor-

bital canal, as shown by the path of the canal and the presence of a large pore at the posterodorsal tip of the bone.

Infraorbital 1 (Fig. 72) is incompletely preserved, and it probably was the largest bone of the infraorbital series. No pores of the infraorbital canal are observed.

The broken infraorbital 2 (Fig. 72) appears to be a narrow, tube-like bone, with a large pore close to its joint with infraorbital 3.

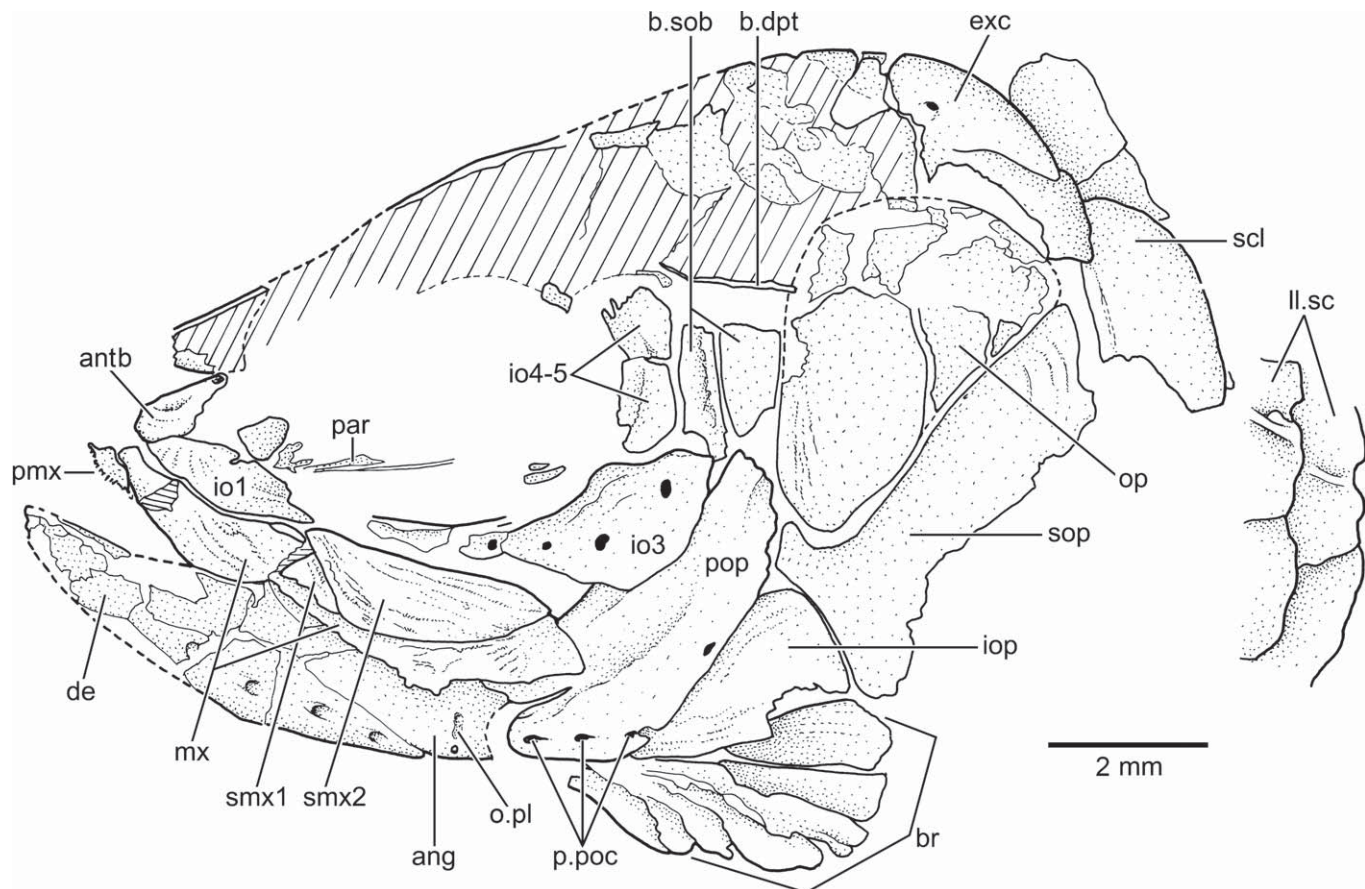


FIGURE 72. *†Parapholidophorus caffii* (Airaghi; MCSNB 563). Drawing of head in left lateral view. Hatched lines indicate broken bone surface.

Infraorbital 3 (Fig. 72) has a slightly concave anterior margin, a slightly concave dorsal margin, and a straight ventral one. Infraorbital 3 is positioned at the posteroventral corner of the orbit. It contacts infraorbital 2 anteriorly, the preopercle posteriorly, and infraorbital 4 and the suborbital dorsally. Infraorbital 3 broadly overlaps the anterior margin of the preopercle. The posterior margin is smooth and slightly rounded. The infraorbital sensory canal is close to the orbital margin and produces three short tubules that open to the surface by three relatively large, rounded pores. A groove for a pit-line (anterior division of the supramaxillary pit-line) is not observed on the middle region of the bone.

Infraorbitals 4 and 5 are small, rectangular bones, slightly deeper than broad. They carry the infraorbital canal close to their orbital margin. No sensory pores have been observed.

The suborbital is broken into two pieces, and its dorsal and ventral margins are incomplete. When its margins are restored, the suborbital appears as a slightly square bone (Fig. 72) that occupies the space outlined by infraorbitals 4 and 5 anteriorly, the lateral margin of the skull roof plate, the opercle posteriorly, and infraorbital 3 and preopercle ventrally.

Upper Jaw—The upper jaw (Figs. 71B, 72) is composed of the paired premaxillae and maxillae and two supramaxillae on each side (contra Nybelin, 1966; Zambelli, 1975). The external surface of the maxilla and supramaxillae is covered by a thick layer of ganoine, which is ornamented with longitudinal ridges extending along the bones. The orientation of the ridges differs between bones, making their individual outlines clear.

The premaxilla (Fig. 72) is a small, slightly triangular bone that is incompletely preserved. A row of small sockets for teeth is on its oral margin.

The maxilla (Fig. 72) is as long as or slightly longer than the lower jaw. The complete length of the bone is unclear because the maxilla is broken into two pieces, displaced from each other, and part of the ventral margin of the bone is missing. The maxilla has a short articular region anteriorly. The maxillary blade is slightly shallow anteriorly, but its depth increases slightly distally, but then ends in an acute tip. The posterior region of the maxillary blade overlaps the anterior margin of the preopercle. The oral margin of the maxilla is broken so no teeth have been observed.

Two supramaxillary bones (Fig. 72) cover the posterodorsal margin of the maxilla, just posterior to the supramaxillary process. Both bones together occupy most of the length of the maxillary blade. Supramaxilla 1 is a very small bone, missing its anterior part. In contrast, supramaxilla 2 is comparatively a long and large bone that extends forward, overlapping part of supramaxilla 1 with its broad and rudimentary anterodorsal process. The external surface of both supramaxillae is covered with ridges of ganoine, and the direction of the ridges differs so that it is possible to identify the presence of the broken supramaxilla 1 in front and below the anterodorsal process of supramaxilla 2. Boni (1937:text-fig. 6) and Nybelin (1966:fig. 5) identified only one supramaxilla. According to Nybelin (1966:378), the maxilla has “a roughly triangular or semicircular elevation on the dorsal margin of the maxillary, corresponding to supramaxillary 1 in other forms.”

Apparently, Nybelin did not realize that the maxilla is broken into two parts that sit at different angles at the point that he interpreted as “triangular or semicircular elevation.” For this reason, Nybelin interpreted the maxilla as fused with supramaxilla 1 (but see Fig. 72), a condition that I have not observed in any specimen in this study.

Lower Jaw—The lower jaw is poorly preserved, and its posterior margin is destroyed. The oral margin of the jaw is almost straight in the first third of its length, and it is covered by the displaced maxilla and supramaxillae posteriorly. The ventral margin of the jaw is gently convex and ends anteriorly in a narrow symphysis.

The dentary (Fig. 72) forms most of the length of the lower jaw and extends below the angular posteroventrally. Both bones are sutured to each other, and no space is left between them at their ventral margins. The oral margin of the dentary is damaged, and no teeth are preserved. The mandibular sensory canal is below the longitudinal, protruding bony ridge, close to the ventral margin of the bone. Five large pores open in the surface of the dentary and are an indication of the trajectory of the canal.

The angular (Fig. 72) forms the posteroventral lateral wall of the jaw, but its posterior border is broken. It is a thin bone covered by a thin, smooth layer of ganoine. One small, round foramen opens close to the ventral margin of the bone. It is unclear if this foramen is part of the short oral pit-line groove positioned just above it.

The articulation between the lower jaw and quadrate is positioned in front of the posterior half of the orbit.

Palatoquadrate and Suspensorium—All bones of the palatoquadrate and the suspensorium are hidden by other bones.

Opercular, Branchiostegal Series, and Gular Plate—The opercular bones (Figs. 71B, 72) are placed posterior to the skull roof plate. All opercular bones are covered by a smooth layer of ganoine.

The preopercle (Figs. 71B, 72) is a broad, crescent-shaped bone, with a large anterior expansion extending below infraorbital 3 and the posterior part of the maxilla. The preopercle lacks well-defined dorsal and ventral arms. Its posteroventral margin is straight. The pathway of the preopercular sensory canal, visible through its pores, is closer to the posteroventral margin, rather than to the middle region of the bone as illustrated by Nybelin (1966:fig. 5). I observe only three large oval pores in the ventral margin of the bone and another in its posterior margin, but Nybelin's (1966:fig. 5) restoration shows eight pores and tubules. Ventrally, the preopercular canal continues in the mandibular canal. Remnants of two pit-line grooves are present in the dorsal region in front of infraorbital 3. The dorsal groove corresponds to the anterior division of the supramaxillary pit-line, and the perpendicular groove corresponds to the oral pit-line.

The opercle (Figs. 71B, 72), subopercle, and interopercle are displaced dorsally. The opercle is a moderately large bone that is gently curved at its dorsal margin. The anteroventral margin of the opercle is markedly rounded, whereas its posterodorsal corner is acute. The external surface of the bone is smooth, with the exception of some growth lines close to the dorsal margin.

The subopercle (Fig. 72) is a large bone, although its ventral region is destroyed. Its anterodorsal process is short, blunt, and almost square and projects dorsally in front of the anteroventral margin of the opercle. When the subopercle is in situ, the anterodorsal process is mostly hidden by the posterior margin of the preopercle. The subopercle has a slightly concave anterior margin where the interopercle abuts.

The elongate, triangular interopercle (Fig. 72) is below the preopercle. Its dorsal tip is rounded and abuts the anterodorsal process of the subopercle. The anterior tip of the interopercle is covered by the preopercle.

Seven branchiostegal rays (Fig. 72) are preserved. The branchiostegals are relatively short and broad and are below the preopercle and interopercle. No remnants of branchiostegals are observed below the subopercle, so that I estimate that the last two branchiostegals, at least, were much longer. By comparison with *†Parapholidophorus nybelini*, I hypothesize that the series is incomplete, because the anterior-most rays are not preserved. A gular plate is not preserved.

Vertebral Column—Due to the preservation of a complete squamation, the vertebral column is not observed in the holotype, with the exception of a few ring-like chordacentra displaced among the scales.

Paired Fins—Some of the dermal elements of the pectoral girdle are poorly preserved, such as the supracleithrum and postcleithra. The posttemporal (Fig. 72) seems to be a large, plate-like bone, with an almost rounded posterior margin. One large, round sensory pore is observed. The anterior margin of the bone is destroyed, so it is not possible to elucidate whether the bone has processes or not.

Part of the supracleithrum (Fig. 72) is preserved. The bone carries the lateral line canal, but no pores are observed on the preserved surface. The cleithrum is partially represented by its imprint. Apparently, the cleithrum was broader than that of *†Parapholidophorus nybelini*.

A deep, bony plate posterior to the impression of the cleithrum was interpreted by Nybelin (1966) as a postcleithrum. Given the current preservation of the specimen, I am not able to discern such an element.

The pectoral fin (Fig. 71B) is positioned low in the flank, close to the ventral margin of the body. Eleven lepidotrichia are preserved, as first described by Boni (1937). However, Nybelin (1966) interpreted the fin as having about 18 rays based on the numbers of rays of *†Pholidophorus bechei* and *†Ph. latiusculus*. All pectoral rays are delicate, with long bases, and are branched and segmented distally. Only a few remnants of tiny, delicate fringing fulcra are preserved in association with the leading margin of the fin. A pectoral axillary process is not preserved.

The pelvic fin (Fig. 71A) is poorly preserved, but at least one or two basal fulcra and five or six rays are counted. The rays have long bases and are branched and segmented distally. A few remnants of fringing fulcra are preserved. A large, triangular pelvic axillary process is present.

Dorsal and Anal Fins—The dorsal fin (Figs. 71A, 73A) is triangular-shaped, with long first principal rays and very short posterior ones. The dorsal fin is preceded by three unpaired basal fulcra; the first one is very small. There are about 10 principal rays, including the first segmented but unbranched ray, and nine branched and segmented rays; all rays are very delicate and are usually broken. The principal rays have long bases and are segmented and slightly branched distally. The first principal ray has a long base and only one elongate segment that resembles a fringing fulcrum. The second principal ray is the main element forming the leading margin of the fin. Elongate and delicate fringing fulcra are between the last basal fulcrum and leading margin of the fin.

The short anal fin (Figs. 71A, 73A) is located posterior to the dorsal fin. Remnants of three incomplete basal fulcra and six rays are present. The anal fin rays are very delicate and are mostly broken. A series of tiny fringing fulcra is associated with the leading margin of the fin.

Caudal Fin—The hemi-heterocercal caudal fin (Fig. 73) is moderately forked, with the middle principal rays about half the length of the leading margins of the fin. The area covered by ganoid scales at the base of the caudal fin ends in a slightly triangular area in the epaxial lobe. The area of ganoid scales covering the base of the caudal fin in front of the hypaxial lobe is slightly shorter and rounded in comparison with the condition in the epaxial lobe. A

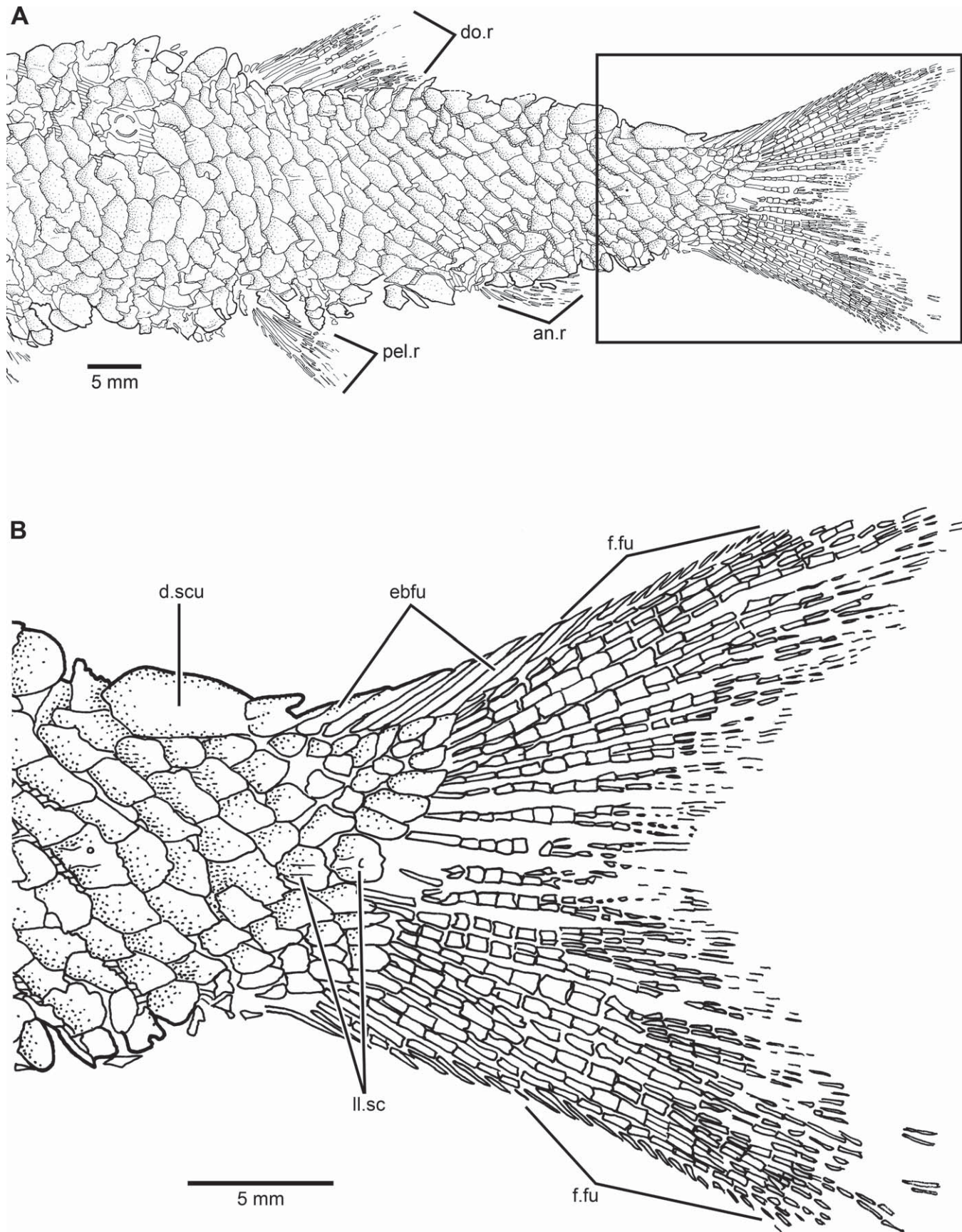


FIGURE 73. *†Parapholidophorus caffii* (Airaghi; MCSNB 563). **A**, drawing of posterior part of the body in left lateral view. **B**, enlargement of the caudal fin.

large, round scale bearing the last portion of the lateral line canal is in the middle of both lobes.

The caudal fin consists of seven epaxial basal fulcra, a series of epaxial fringing fulcra, 20 principal rays, a series of elongate hypaxial fringing fulcra, and three hypaxial, segmented procurent rays. Remnants of at least two hypaxial basal fulcra are present. It is not possible to confirm if all basal fulcra are paired or not. The hypaxial procurent rays each end on a fulcrum-like segment. Accessory fringing fulcra are inserted between the distal segments of the procurent rays.

As far as can be observed, fringing fulcra (Fig. 73) lie at least on the dorsal margin of the first and second principal rays. The distal tips of the leading principal rays are destroyed. The articulation between segments of all principal rays is straight. No dorsal processes associated with the bases of the middle principal rays have been observed. By comparison with other species studied here, I consider that the dorsal processes are absent.

One long dorsal scute (Fig. 73) is present. The scute is rounded anteriorly and becomes narrower posteriorly. A ventral scute is not preserved.

Scales—The body is covered by thick ganoid scales (Figs. 71A, 73) that strongly overlap each other. The scales lack ornamentation. Most scales are damaged, but it is possible to postulate that they have smooth posterior margins based on a few scales with complete margins located below the dorsal fin. Scale shape and size differ along the body. For instance, the scales of the mid-flank, between the posterior margin of the dorsal postcleithrum and the origin of the dorsal fin, are larger and slightly deeper than long than scales of the posterior half of the body, which are rhomboidal and smaller. The scales close to both the dorsal and ventral margins of the body are smaller than those of the mid-flank region. Each vertical row has about 11 or 12 scales in the predorsal region; a similar number of scales are found in the vertical rows between the dorsal and anal fins, and posterior to the anal fin. Although the number of scales remains unchanged, the size of the scales changes. There is a big change in the aspects of the scales posterior to vertical row 34 where the scales may be square, rectangular, or oval in outline.

Lateral Line—Thirty-five flank scales carry the main lateral line canal. I interpret the trajectory of the lateral line as continuous along the flank, although it is difficult to observe due to condition of preservation. The scales are rectangular with smooth posterior margins.

†*PHOLIDOCTENUS* Zambelli, 1977

Diagnosis—Emended from Zambelli, 1977, and based on a unique combination of characters. Autapomorphies are identified with an asterisk [*]. Most cranial bones covered with a layer of smooth ganoine, except the maxilla, supramaxillae, and median gular with thick ridges of ganoine. Extrascapulae, posterior infraorbitals, opercular bones, and dermal pectoral girdle bones with serrated posterior margins [*]. Large nasal bones joining each other medially and completely separating the anterior tips of the parietal [=frontal] bones from the rostral bone [*]. Large concave notch at the lateral border of nasal. Antorbital joining the nasal bone [*]. Supramaxilla 2 with long anterodorsal process. Narrow and short crescent-shaped preopercle with undistinguishable dorsal and ventral arms, not extending to lateral margin of skull roof. Preopercle lacking a notch at its posteroventral margin. A triangular, small additional preopercle positioned in front of anteroventral region of preopercle and lateral to quadrate [*]. Anterior extension of interopercle almost at the level of or extending slightly forward to anterior margin of preopercle [*]. Eighteen to 20 principal caudal rays present. Diplospondylous vertebrae present in both abdominal and caudal region [*]. Additional lateral line canal

extending between extrascapula and the base of dorsal fin. Scales covered with a smooth layer of ganoine. Posterior margin of scales with a few conspicuous acute projections or serrae.

Type Species—*Pholidoctenus serianus* Zambelli, 1977.

Content—Type species only.

†*PHOLIDOCTENUS SERIANUS* Zambelli, 1977 (Figs. 74–88)

Pholidoctenus serianus: Zambelli, 1977:1–2, figs. 1–2, pls. 1–3.

Holotype—MCSNB 3067 (Fig. 74). Almost complete specimen with pectoral, dorsal, and anal fins preserved; the pelvic fins are poorly preserved, and the caudal fin and anterior part of the snout are missing.

Material Examined—MCSNB 2875–2877, MCSNB 3012, MCSNB 3034–3063, MCSNB 3064a–m, MCSNB 3065, 3066, 3068–3070, MCSNB 3095, MCSNB 3097, MCSN 3099, MCSNB 3312–3315, MCSNB 3357, and MCSNB 3373–3378.

Type Locality, Age, and Distribution—Only known from the type locality Cene, about 17 km northeast of Bergamo, Lombardy, northern Italy; Late Triassic (Norian), about 210 Ma.

Diagnosis—As for the genus.

Description

The anatomical description of certain regions of the body, such as the lateral view of the braincase and the abdominal or precaudal vertebral region and its associated elements, is difficult due to conditions of preservation. The vertebral column, ribs, and intermuscular bones are obscured by the squamation covering the postcranial skeleton in most specimens. Due to this kind of preservation, only sections of the vertebral column have been observed where the scales are damaged, removed, or displaced, a condition observed in only a few specimens (Fig. 75A, B).

The members of this species are small, reaching about 55 mm standard length, with a total length of about 63 to 65 mm. The fishes have slightly fusiform or oval bodies, with their maximum depth in the predorsal region. The snout length is characteristically short; it is about 16% of head length. The head is about 25% of standard length, with relatively large orbits that have a diameter of about 30–32% of head length. The head is almost triangular, with its deepest points at the posterior end of the cranial roof. The caudal peduncle is moderately narrower than the rest of the body. The dorsal fin is positioned slightly posterior to the midpoint of the standard length, whereas the pelvic fins are positioned slightly more anterior. The pectoral fins are positioned nearer the ventral margin of the body than to the middle region of the flanks. The anal fin is posterior to the base of the dorsal fin. All fins are small, with very delicate and slender rays that have elongate fringing fulcra.

The external cranial bones and scales are covered by a layer of smooth ganoine. Weak ornamentation has been observed on some cranial bones, such as the rostral, premaxillae, maxilla, supramaxillae, anterior margin of opercle, gular plate, and anterior margin of supracleithrum.

Braincase—The braincase seems to be short; its posterior margin is located at the level of the opercle. With the exception of the skull roof bones and the parasphenoid, no other elements of the braincase are observed. A section of a moderately narrow parasphenoid is preserved only in a few specimens (Figs. 74, 76). No teeth are visible on or around the exposed section of the bone.

Skull Roof—The surface of the cranial roof is smooth, and its profile is gently convex. The smoothness of the surface is interrupted by the presence of a few, small, elongate pores for the cephalic sensory canals. As in other species described here, all dermal bones forming the skull roof are fused into a large plate,

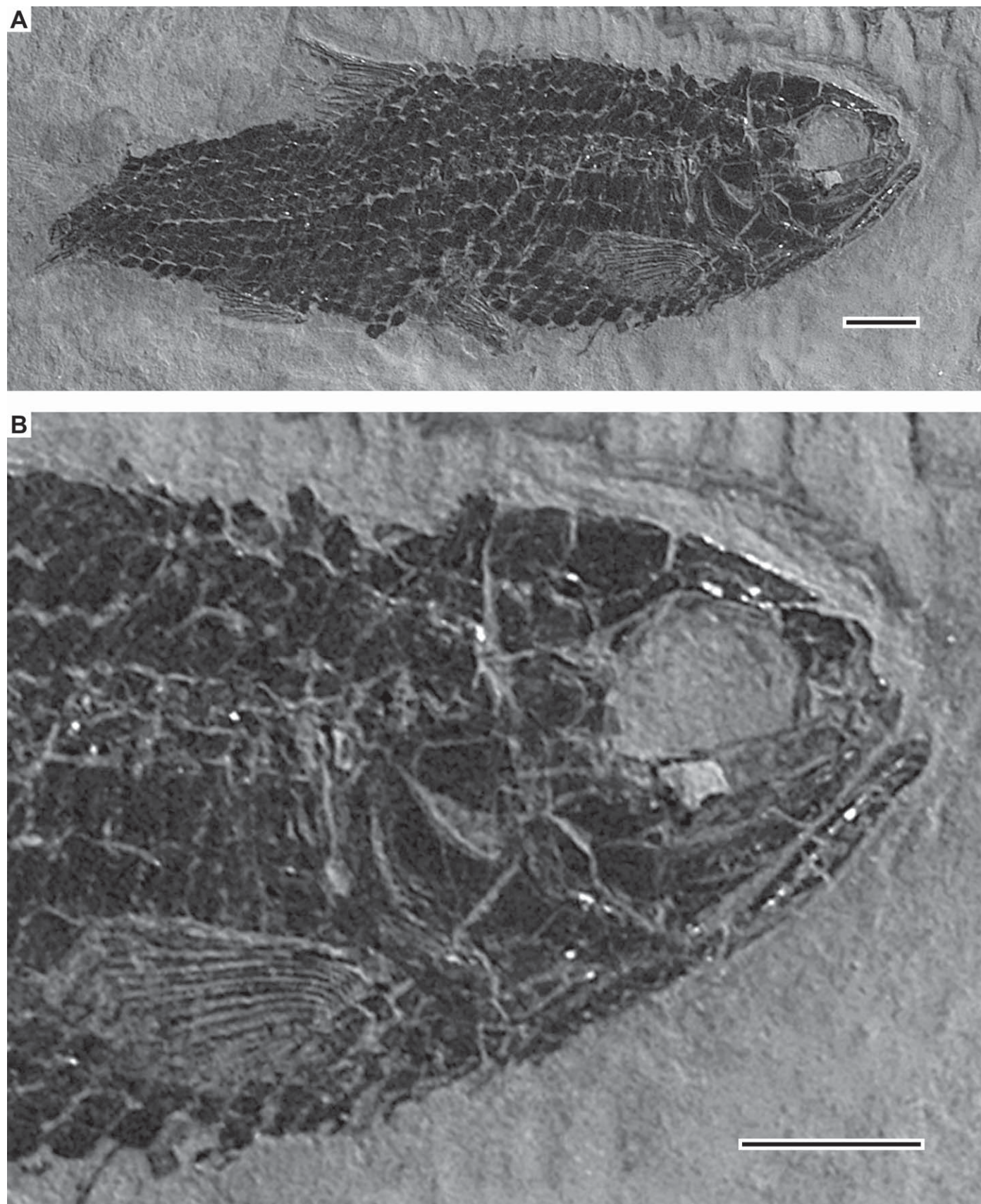


FIGURE 74. \dagger *Pholidocetus serianus* Zambelli (holotype; MCSNB 3067). **A**, photograph of the holotype in right lateral view. **B**, enlargement of the head and pectoral region. Scale bars equal 5 mm. (Color figure available online.)

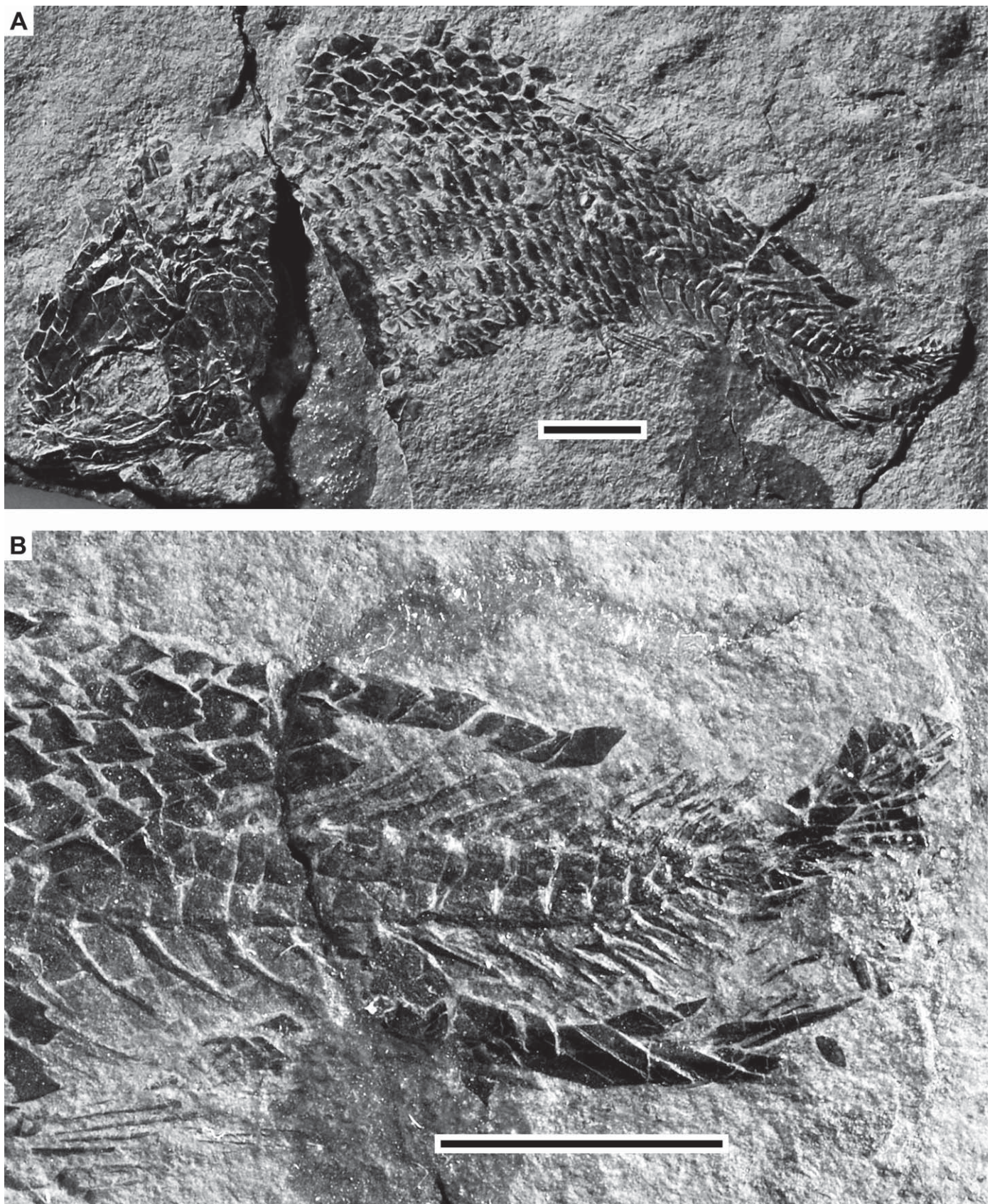


FIGURE 75. \dagger *Pholidoctenus serianus* Zambelli. **A**, photograph of MCSNB 3377 in left lateral view. **B**, enlargement of caudal region including caudal endoskeleton. See drawing in Figure 84. Scale bars equal 5 mm. (Color figure available online.)

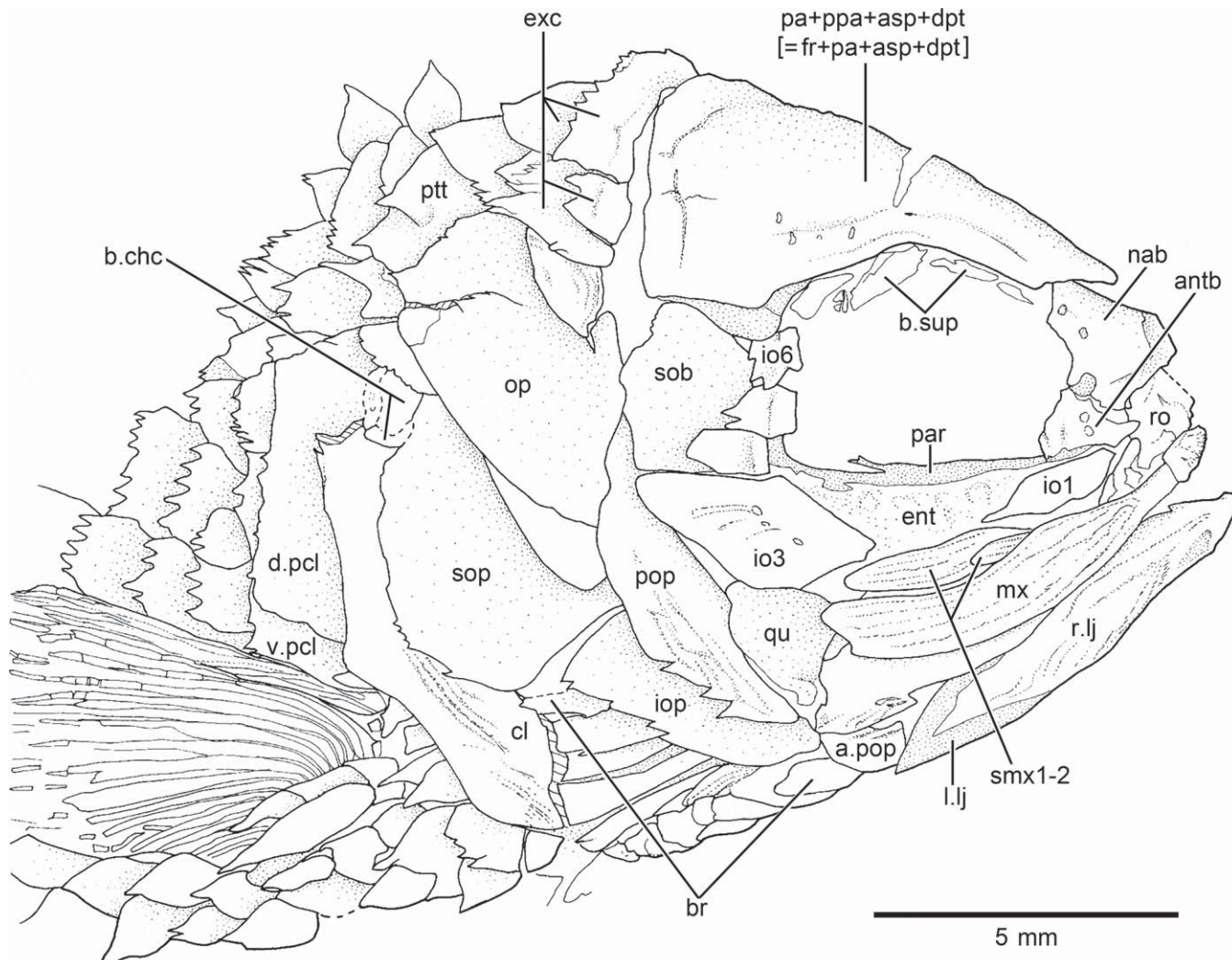


FIGURE 76. \dagger *Pholidoctenus serianus* Zambelli (holotype; MCSNB 3067). Drawing of head and anterior part of the body in right lateral view.

with the exception of the rostral and nasal bones. The skull roof plate (Figs. 76, 77A, B, 78A, B, 79) is almost triangular, being very narrow anteriorly and expanding posteriorly, reaching its maximum width at the dermopterotic level. The plate ends in an almost straight line at the posterior margin of the postorbital region. No traces of a supraoccipital or epiotics have been observed.

The main element of the skull roof is the large compound plate that is interpreted here as the result of ontogenetic fusion of the parietal bones [= frontals] with the postparietals [= parietals] posteriorly and the autosphenotics and dermopterotics laterally (Figs. 77A, B, 78A, B, 79, 80A, B). Incomplete lines of fusion still present in some skulls support this interpretation. Zambelli (1977) interpreted the skull roof as formed by the fronto-parieto-dermopterotic even though he illustrated all skull roof bones as separate elements.

The parietal [= frontal] region of the skull roof plate ends anteriorly in an acute border that is completely separated from the rostral bone (Figs. 78A, B, 79). Consequently, a joint between both bones is missing. The skull roof plate broadly expands laterally at the posteroventral corner of the orbit (in the region where the au-

tosphenotic and dermopterotic would be). The identifications of these skull roof regions can be corroborated partially with the assistance of the trajectory of the supraorbital and otic canals and the grooves for pit-lines.

All cephalic sensory canals are simple canals that apparently lack sensory tubules. If these tubules were present, they were very short, lying just next to or over the main canal. Following the position of the pores of the supraorbital sensory canal, the canal (Figs. 77B, 78A, 79, 80A, B) is relatively close to the orbital margin of the skull roof plate. I am unable to see a posterior branch of the supraorbital sensory canal as was illustrated in Zambelli's (1977:figs. 1–2) restorations of the lateral and dorsal views of the head of *Pholidoctenus*. The best specimen showing the pores of the supraorbital canal (Fig. 78A) presents seven pores. The last pore is in front of the region where the autosphenotic would be. A medial curvature of the canal (or parietal branch of the supraorbital canal) was observed in only one specimen. The canal ends at the level of the posterodorsal corner of the orbit and is distant from the anterior pit-line (Fig. 79). A supraorbital canal not extending posteriorly into a parietal branch resembles the

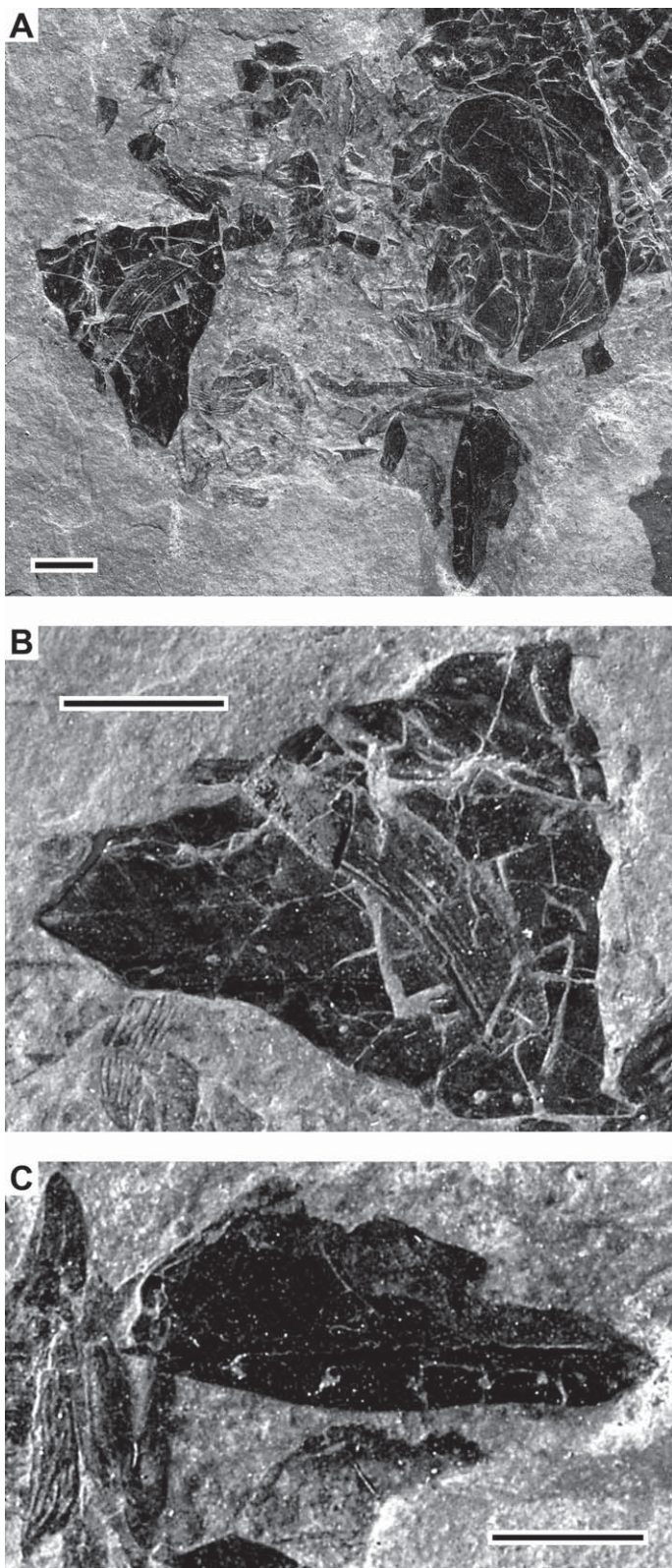


FIGURE 77. *†Pholidoctenus serianus* Zambelli. **A**, photograph of disarticulated cranial bones of MCSNB 3095. **B**, enlargement of the skull roof plate. **C**, enlargement of the right lower jaw. Scale bars equal 2 mm.

condition observed in all other pholidophorids described here. The otic canal is close to the posterolateral margin of the skull roof plate, where the dermopterotic would be. The trajectory of the otic canal (Figs. 77B, 80A, B) is marked by the presence of one to three pores, but some specimens have no pore. I was not able to observe the pore where the connection between the otic and preopercular sensory canals occurs. Any identification is difficult because the dorsal tip of the preopercle is separated from the lateral margin of the skull roof plate (region of the dermopterotic) by a considerable distance.

Three pairs of narrow but well-defined grooves containing pit-lines (Fig. 78B) are at the posterior region of the skull roof plate. The anterior and middle pit-line grooves are often present in the skull roofs examined, but the posterior pit-line is variably present. The groove for the middle pit-line (Figs. 78B, 79, 80A, B) is long and narrow, extending close to the lateral margin of the skull roof plate; in other words, it extends over most of the dermopterotic region of the skull roof. The middle pit-lines do not meet in the midline. The anterior pit-lines grooves (Fig. 79) are fairly consistent in position, contained mostly in the region of the post-parietals [= parietals], and are short. A very short groove for the posterior pit-line (Fig. 78B) is observed in a few specimens.

A small, median rostral bone (Figs. 79, 80A, B, 81) is at the anterior-most region of the skull roof. The bone has a slightly rounded anterior margin, with a slightly prominent median region, two short lateral processes, and a rounded posterior region. The ethmoidal or rostral commissure crosses the rostral from one lateral process to the other and continues with the anterior branch of the infraorbital sensory canal, exiting the antorbital. There are two small pores or openings of the commissure that are on the dorsal surface of the bone in some specimens, whereas in others the surface of the rostral is covered by small tubercles of ganoine. The rostral bone overlies anteriorly the dorsal tips of the small premaxillae. Each lateral process of the rostral is in contact with the antorbital for a short distance (Figs. 79, 81). The posterior region fuses with the anteromedial margin of the nasal bones.

There are two large, plate-like nasal bones (Figs. 78B, 79, 80A, B). Each nasal has an emarginated or notched anterolateral margin that forms the posterior edge of the anterior nasal opening, whereas its lateral margin has a lateral articular surface with the antorbital and a broad posterolateral notch for the posterior nasal opening. The lateral margin of the nasal is characteristically emarginated, and the notch forms a significant part of the margin. This broad notch is different from other species, which have a smaller, round notch (e.g., *†Parapholidophorus nybelini*). The nasals are sutured to each other medially by means of a straight suture ('sutura harmonica'). Laterally, the nasals are loosely articulated with the antorbitals. Posteriorly, the nasals are in contact with the anterior-most tip of the skull roof plate, the parietal region [= frontal]. The supraorbital sensory canal is along the mid-region or closer to the lateral margin of the bone than to the medial one. The canal opens to the surface by two or three small, rounded or oval pores. No sensory tubules are observed.

There is no evidence of a supraoccipital bone. The dermal skull roof plate ends in the postparietal and dermopterotic regions.

Two large, triangular, paired extrascapular bones (Figs. 79, 80A, B, 84, 81, 82A, 83B) cover the posterior region of the cranial roof, just overlapping the posterior margin where the postparietal and dermopterotic bones would end. Both extrascapulae broadly overlap each other medially. Each extrascapula has a straight anterior margin, whereas its acute posterior margin has one or a few serrae. The bone has a curious aspect anteriorly. Its anterior margin is rolled over to form a bony covering of

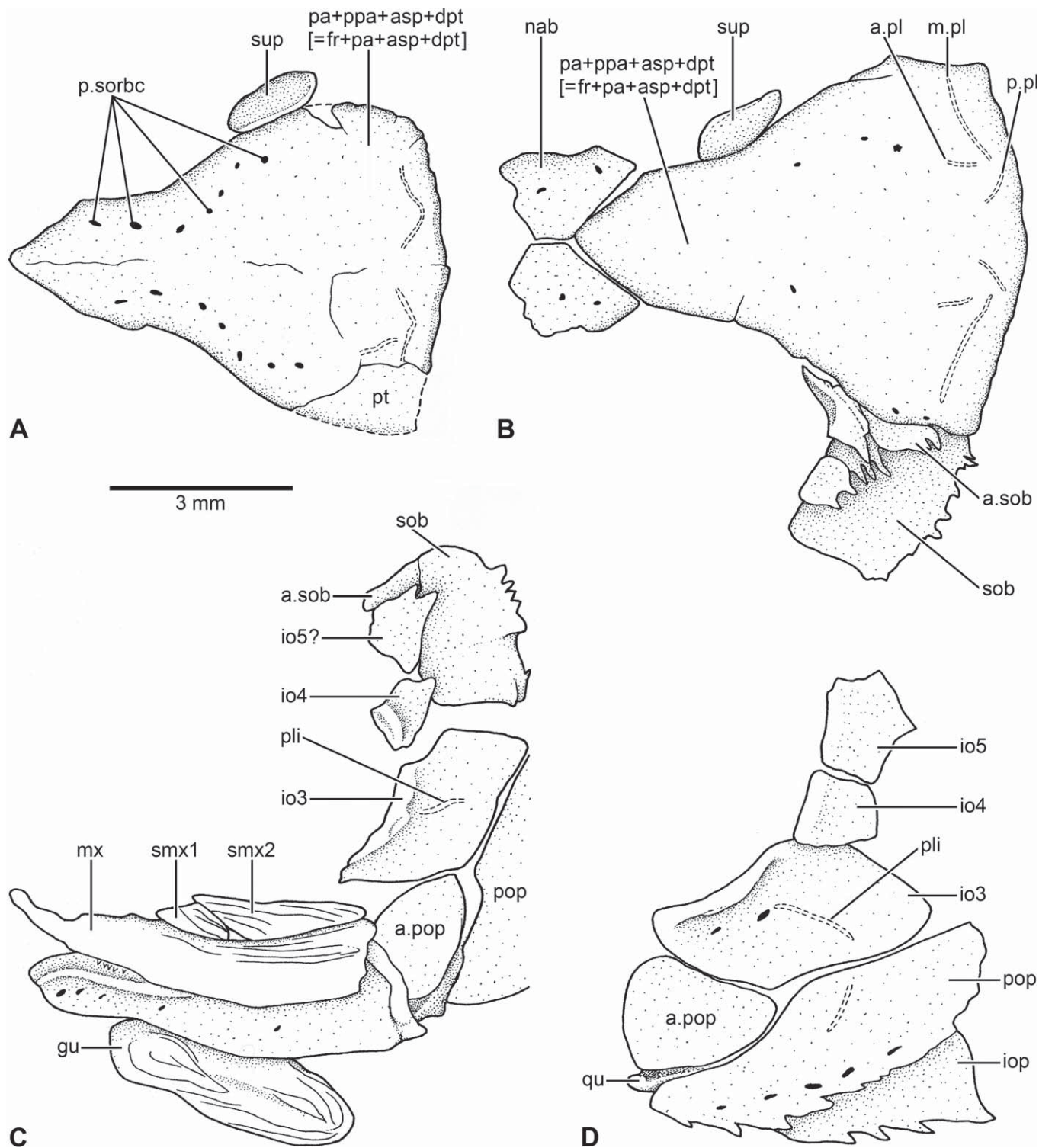


FIGURE 78. *†Pholidocetus serianus* Zambelli. **A**, drawing of skull roof plate in dorsal view (MCSNB 3048). **B**, skull roof plate and other cranial bones in dorsal view (MCSNB 3046). **C**, some orbital bones, jaws, and gular plate from the left side of the skull in lateral view (MCSNB 3041). **D**, some infraorbital and opercular bones from the left side of the skull in lateral view (MCSNB 3044). Anterior is to the right in all images. Scale bar applies to **A-D**.

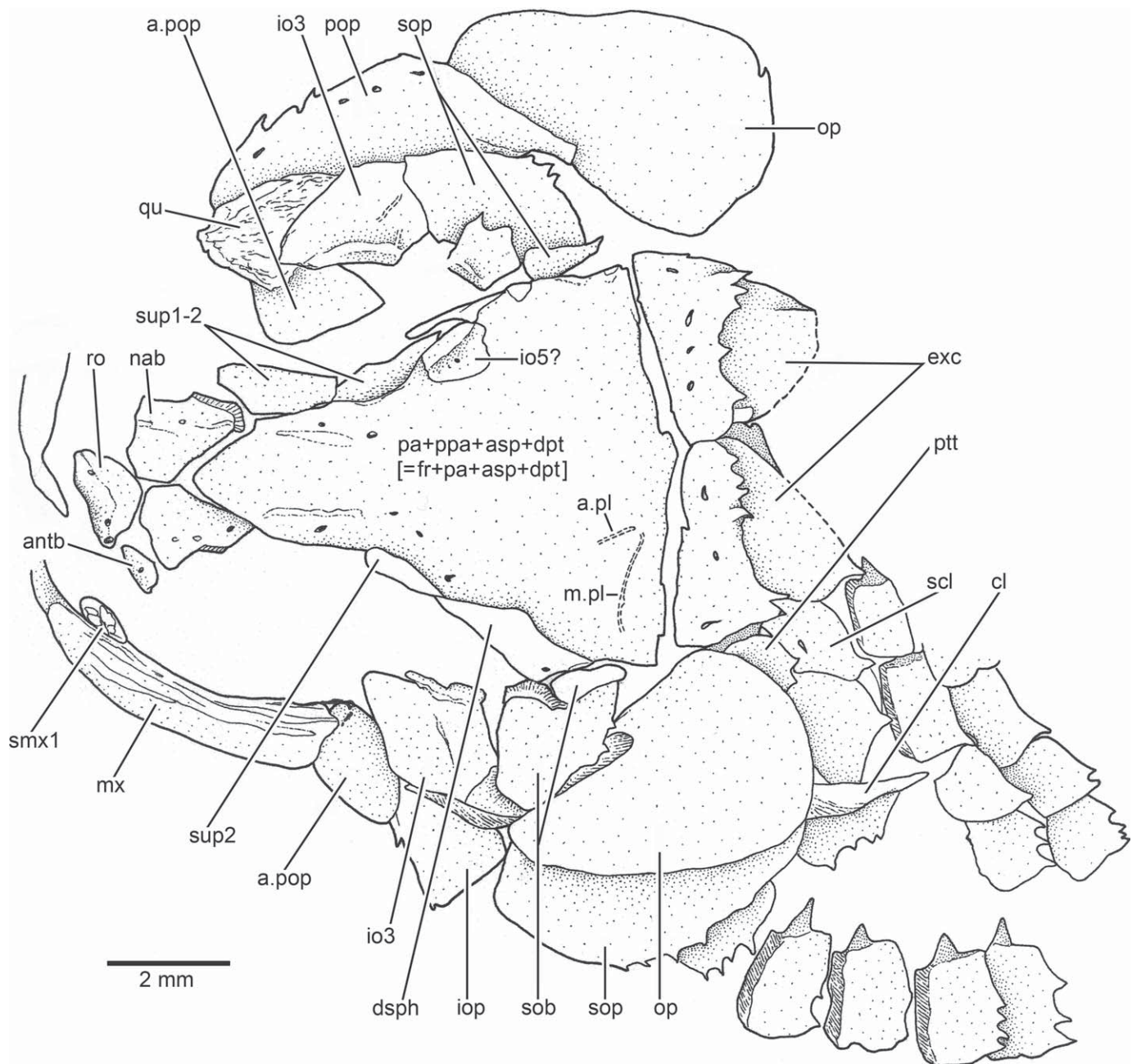


FIGURE 79. *†Pholidoctenus serianus* Zambelli. Drawing of cranial bones and anterior part of body in dorsal and left lateral views (MCSNB 2575).

the extrascapular canal or supratemporal commissure, so that the anterior half of the extrascapula is thicker than its posterior half. The posterior margin of this rolled-over bony plate has numerous acute serrations. The extrascapular canal or supratemporal commissure is in the middle region of the anterior, thicker region of the bone, as indicated by two to four oval pores. The canal does not produce sensory tubules, and the series of pores lies directly above the canal. Zambelli (1977:fig. 3) restored the large element placed posterior to the skull roof plate as an extrascapula (anterior thick part) and as a posttemporal (thin part). The lateral line was restored closer to the lateral margin of his extrascapula

and posttemporal, continuing in the supracleithrum posteriorly. I have not seen the lateral line canal in the lateral portion of the so called posttemporal. In specimens studied here, independent extrascapula and posttemporal are observed (Figs. 79, 81, 83). Consequently, I interpret this large bone as the extrascapula alone.

Circumorbital Series—The circumorbital ring consists of two supraorbitals, one antorbital, five infraorbitals (occasionally six), and one dermosphenotic. The circumorbital ring is closed by the contribution of the nasal bone. In addition, *†Pholidoctenus* presents one large suborbital and an accessory suborbital. All

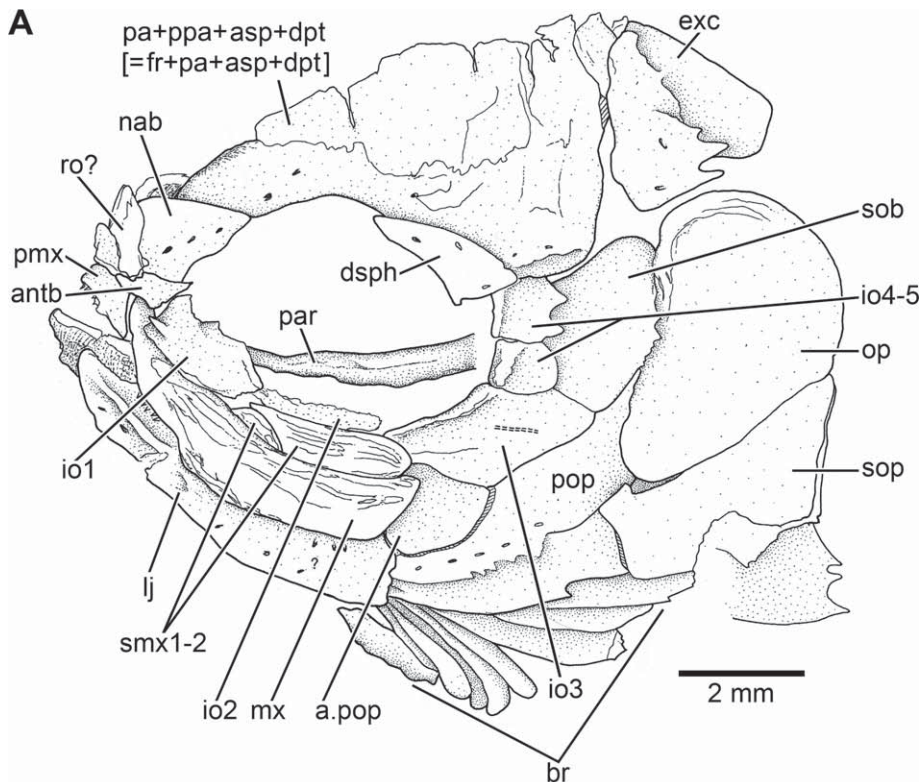
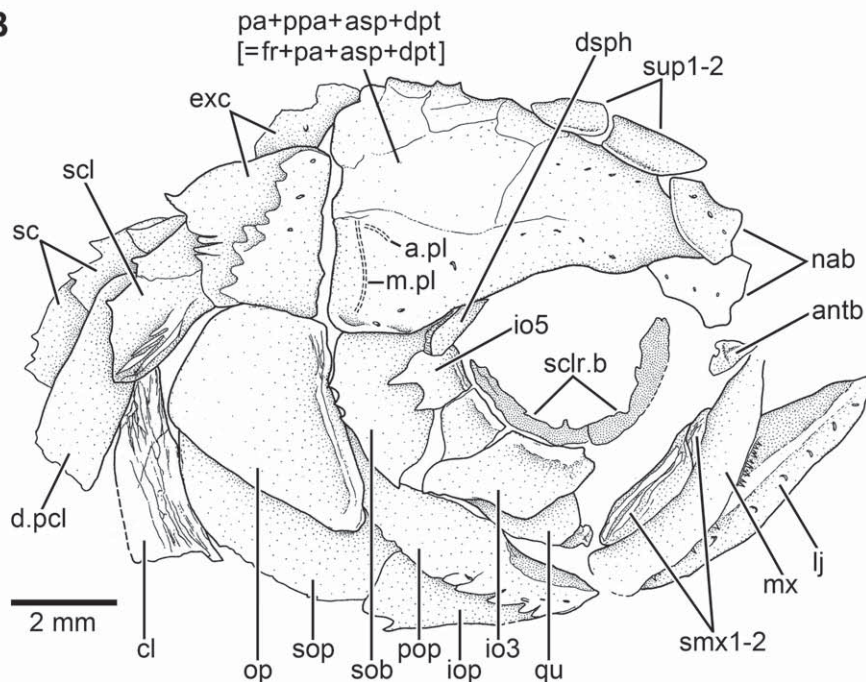
A**B**

FIGURE 80. *†Pholidothenus serianus* Zambelli. Drawings of crania in dorsolateral view. **A**, MCSNB 3035. **B**, MCSNB 3041.

these bones, with the exception of the accessory suborbital, are consistently present, but a certain degree of variation is observed for some of them (see description below). In addition, sclerotic bones are present.

Two elongate thick bones positioned lateral to the orbital margin of the skull roof plate are identified here as supraor-

bitals 1 and 2. Supraorbital 1 (Fig. 79) is commonly slightly rectangular. It joins the posterior margin of the nasal bone anteriorly and the supraorbital 2 posteriorly; the posterior end of the latter is covered by the anterior tip of the lateral dermosphenotic. No space is left between the dermosphenotic and supraorbitals.

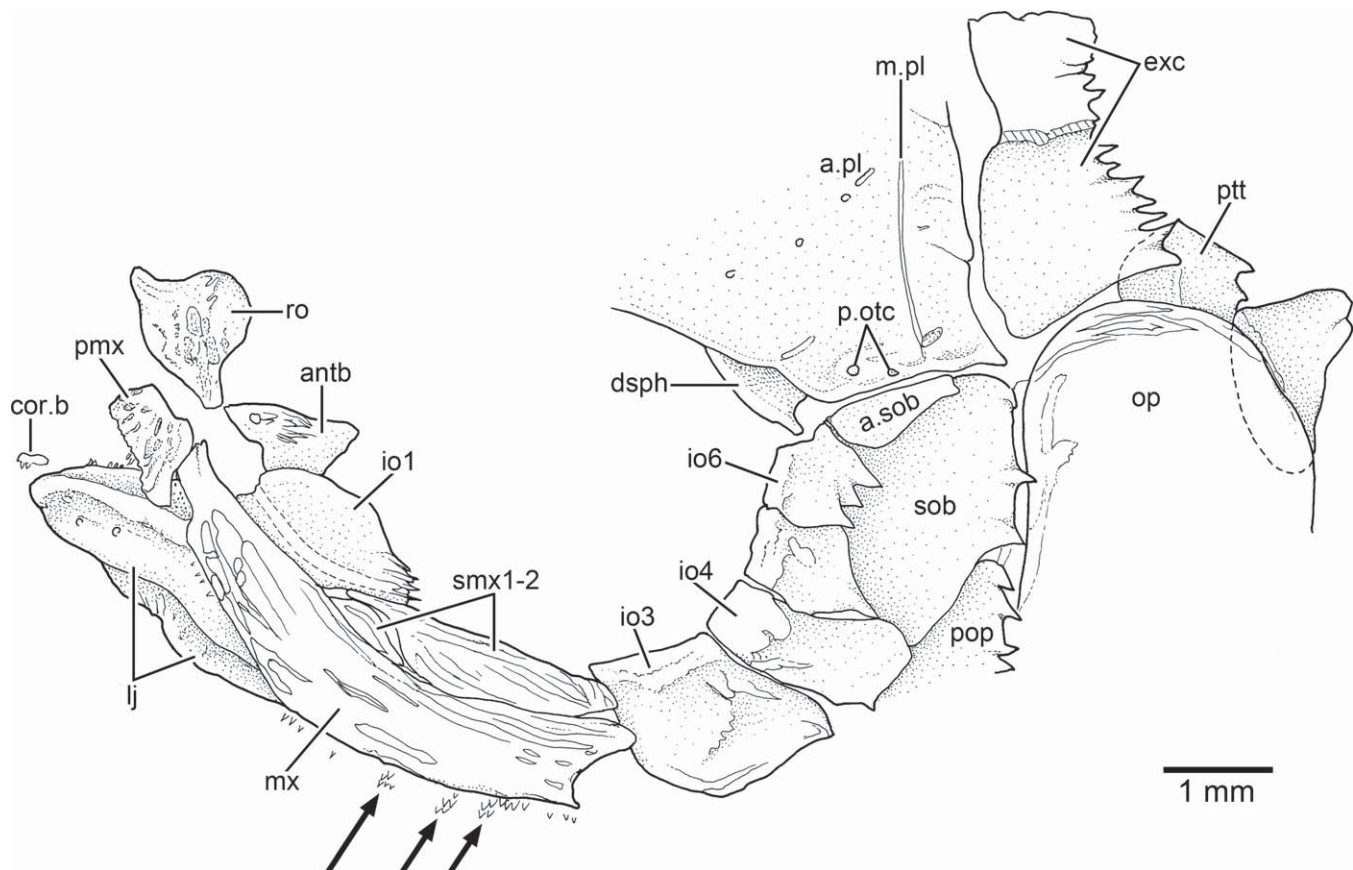


FIGURE 81. *†Pholidothenus serianus* Zambelli. Drawing showing the rostral bone, jaws, orbital bones, and their relationship to the skull roof and opercular bones in left dorsolateral view (MCSNB 3377). Arrows point to teeth.

The antorbital (Figs. 79, 80A, B, 81, 82A, 83) is a moderately large, thick, roughly triangular bone that is positioned dorsal to the anterodorsal margin of infraorbital 1, forming the anteroventral margin of the orbit. The antorbital, with a smooth surface covered with ganoine, is completely or almost completely preserved in only a few specimens. Although I have not been able to see the complete trajectory of the infraorbital canal, an extension of this canal is enclosed in the antorbital, as shown by a few small, round pores. The position of the lateral process of the rostral and antorbital suggests that there is a connection between the anterior branch of the infraorbital canal and rostral commissure.

Infraorbital 1 (Fig. 80A, 81, 83) is the anterior-most bone of the infraorbital series and is slightly oval or rectangular in shape. The shape is unclear because the bone is damaged in most specimens, including the holotype. However, a well-preserved infraorbital 1 is observed in MCSNB 3377. The bone (Fig. 81) is an almost oval shape, with the infraorbital sensory canal positioned close to the ventral margin, as shown in Zambelli's (1978:fig. 1) restoration.

Infraorbital 2 (Fig. 80A) is a narrow, elongate, tube-like bone carrying the infraorbital sensory canal. No sensory pores are observed.

Infraorbital 3 (Figs. 78C, D, 79, 80A, B, 81) is almost rhomboidal-shaped, with a slightly concave anterior margin. Some infraorbitals 3 have a slightly rhomboidal shape, with almost straight dorsal and ventral margins, or the dorsal margin may be slightly concave, as reported by Zambelli (1977). Infraor-

bital 3 is positioned at the posteroventral corner of the orbit. It contacts infraorbital 2 anteriorly, both the additional preopercle and the preopercle posteriorly, and infraorbital 4 and the suborbital dorsally. Infraorbital 3 overlaps the anterior margin of the preopercle in some specimens. The posterior margin of infraorbital 3 is smooth, lacking acute projections or serrations. The infraorbital sensory canal is close to the orbital margin and apparently does not produce sensory tubules, contrary to the restoration by Zambelli (1977:fig. 1). A groove for a pit-line (anterior division of the supramaxillary pit-line; Fig. 78C, D) is observed in the middle region of the bone. This pit-line groove is separated from a section of the supramaxillary pit-line present in the preopercle of some specimens. The surface of infraorbital 3 may be completely smooth, but in some specimens (e.g., the holotype) a few thin ridges of ganoine are close to the posterior margin. Ganoine ridges bearing small serrae are observed in a few specimens.

Infraorbitals 4 and 5 (Figs. 76, 78C, D, 83, 84) are small, square-shaped bones carrying the infraorbital canal close to their orbital margins. Occasionally, one pore may be present close to the orbital margin of infraorbital 4. Infraorbitals 4 and 5 are slightly triangular in a few specimens, but there is variation in the shape of both bones, especially infraorbital 4 (Zambelli, 1977:fig. 3). Both bones commonly have serrated posterior margins that overlap the suborbital.

A few specimens have six infraorbitals (Figs. 76, 81). The extra bone is apparently the result of a fragmentation of the dorsal

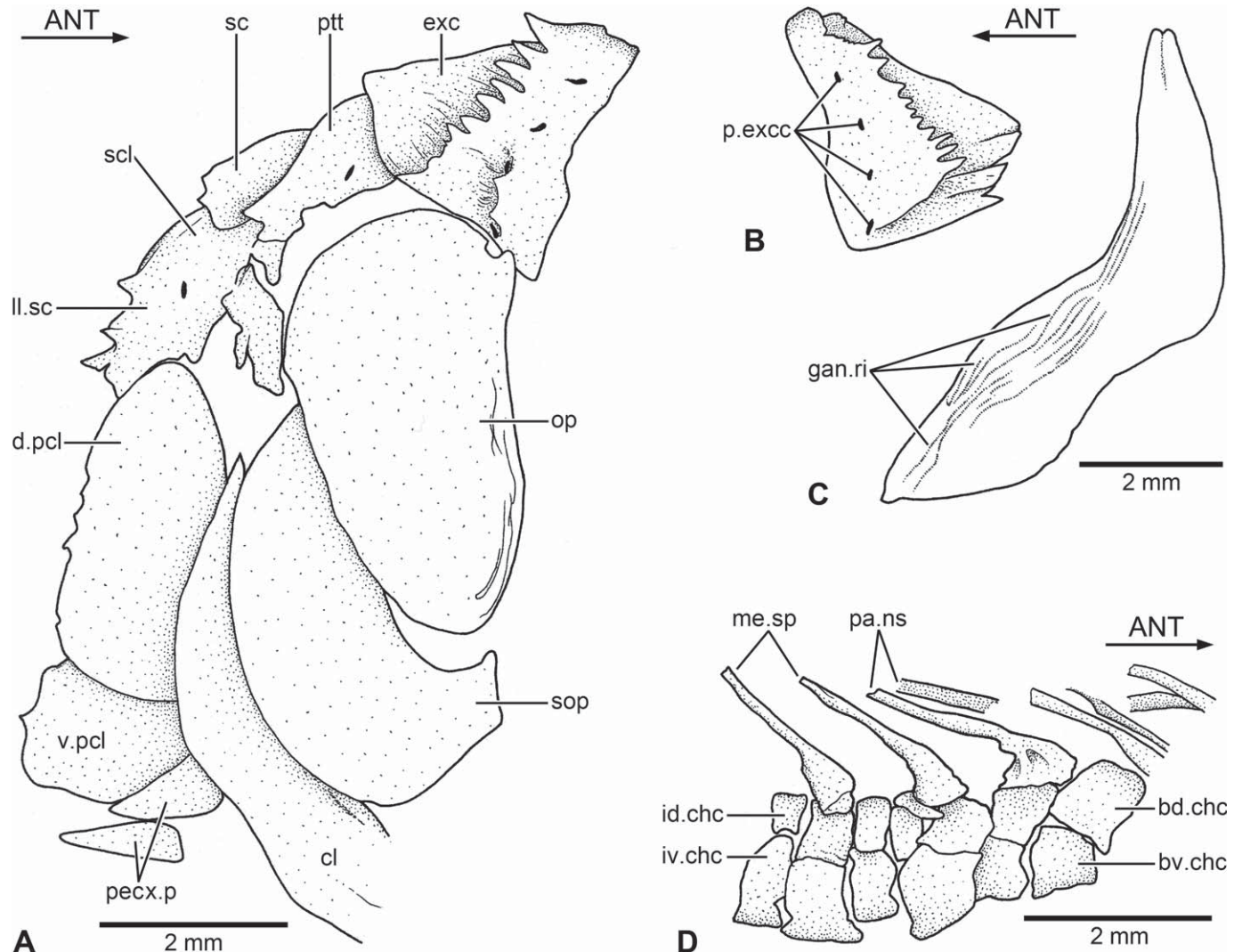


FIGURE 82. *†Pholidocetus serianus* Zambelli. **A**, drawing of posterior part of right opercular region and pectoral girdle in lateral view (MCSNB 3036). **B**, left extrascapular bone in dorsolateral view (MCSNB 3048). **C**, left cleithrum in lateral view (MCSNB 3048). **D**, portion of abdominal vertebral region in right lateral view (MCSNB 2879). Scale bar of **C** also applies to **B**.

region of infraorbital 3 (e.g., MCSNB 3040, MCSNB 3377) or simply is an additional element (e.g., Fig. 81). The uppermost infraorbital (fifth or sixth) contacts both the dermosphenotic anterodorsally and the accessory suborbital posteriorly.

The moderately large and triangular dermosphenotic (Figs. 80A, B, 81) is located posterior to supraorbital 2, anterolateral to the region of the autosphenotic in the skull roof plate, and dorsal to the uppermost infraorbital, commonly the fifth. The dermosphenotic does not fuse to the underlying autosphenotic and does not extend posteriorly over the dermopterotic region of the skull roof plate. The dermosphenotic lacks well-defined processes, and it can be interpreted as type Ib in Poplin's (2004) classification of dermosphenotics. Two or three pores open to the surface of the bone. The infraorbital and otic canals join in the dermosphenotic. However, there is no evidence that the supraorbital canal joins the other two canals in the dermosphenotic. The surface of the dermosphenotic is smooth

and usually lacks serrae at its posterior margin, although one or two serrae are occasionally present.

One large, slightly square or triangular suborbital (Figs. 76, 79C, 80A, B, 81) occupies the space defined by infraorbitals 4 and 5 (or 6 when it is present) anteriorly, the margin of the skull roof plate laterally (or with an additional suborbital when present dorsally), the opercle and preopercle posteriorly, and infraorbital 3 ventrally. The flat and thin bone is covered by a smooth layer of ganoin and presents a posterior margin with acute serrations extending over the opercle and preopercle.

A small, triangular and narrow additional suborbital bone (Figs. 79, 81) is often present dorsal to the large suborbital bone and lateral to the dermopterotic region of the skull roof plate. The posterior margin of the bone may present small acute projections and may extend posteriorly onto the opercle.

There are remnants of the anterior and posterior sclerotic bones (Fig. 80B), which formed a complete ring surrounding the eyeball.

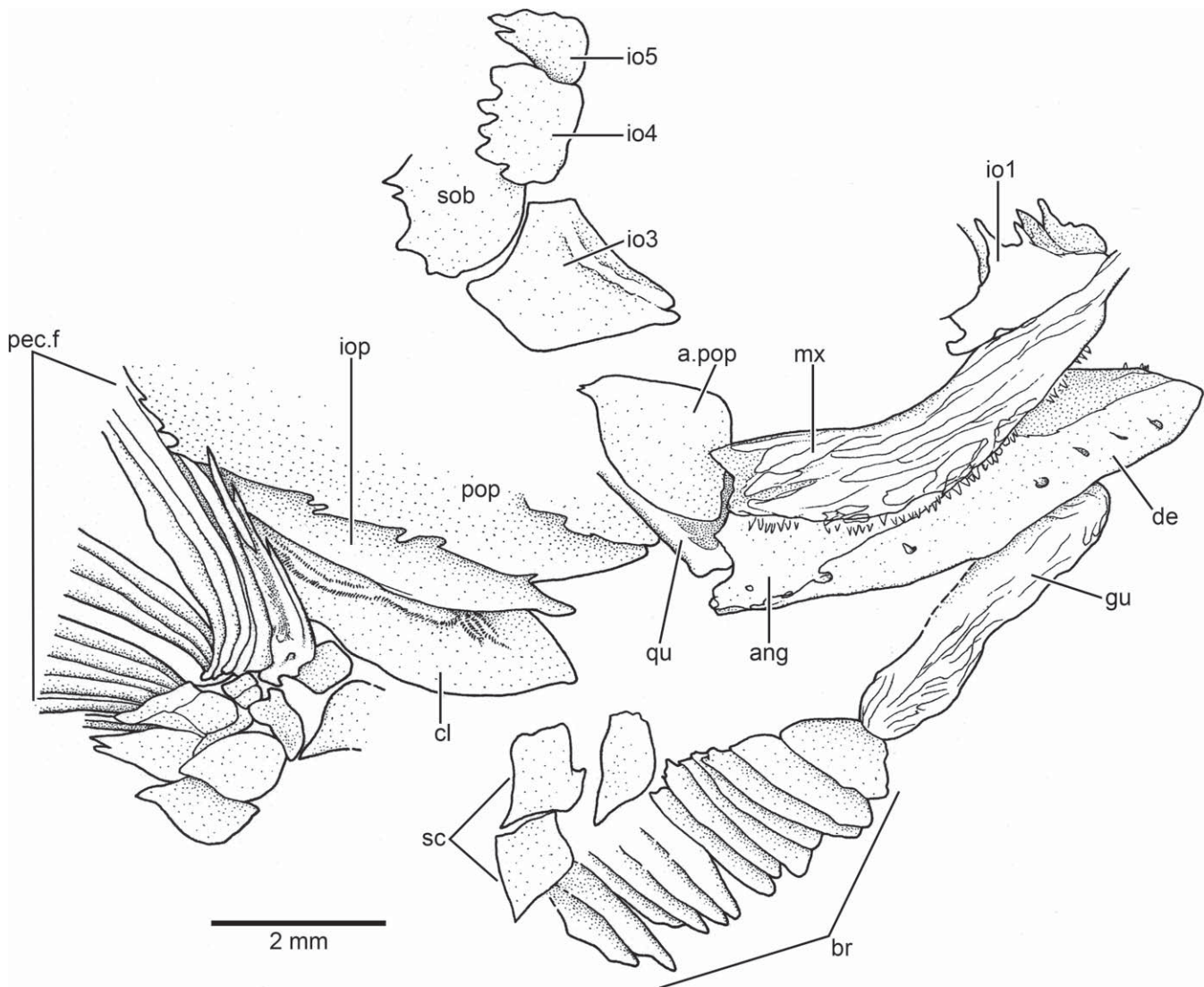


FIGURE 83. *†Pholidothenus serianus* Zambelli. Drawing of partially disarticulated cranial bones and pectoral fin in right lateral view (MCSNB 2876).

Upper Jaw—The premaxillae, maxillae, and two supramaxillae are part of the upper jaw. The premaxilla (Figs. 80A, 81) is a small, slightly triangular bone, with a very short ascending process; there is no evidence of a postprechmaxillary, nasal process, or rostrodermethmoid. Tiny conical teeth are present on the oral margin of the premaxilla.

The gently curved maxilla (Figs. 76, 80A, B, 81, 83) is as long as the lower jaw or slightly longer and has a moderately long articular region anteriorly. The maxillary blade is slightly shallow anteriorly, but its depth increases slightly posteriorly. The dorsal margin of the bone is slightly concave or almost straight, whereas its ventral margin is gently convex at mid-length. The dorsal margin does not possess a well-defined supramaxillary process, but it has a rudimentary process in some specimens. A narrow articular surface, where the supramaxillary bones lie, extends along the posterodorsal margin of the maxilla. The posterior margin of the maxilla (see Figs. 76, 81, 83) is characteristically notched; the posterior margin is round in a few specimens. The posterior tip of the blade may overlap the anterior margin of the additional preopercle. A

single row of very small conical teeth is present in the oral margin of the blade. It is uncertain if one single row of teeth is consistently present or more teeth are placed medially, because MCSNB 3377 (Fig. 84) presents more than one row of teeth scattered near the posterior region of the oral margin of the maxilla.

Two supramaxillary bones (Figs. 76, 80A, B, 81) cover the posterodorsal margin of the maxilla, just posterior to the supramaxillary process. Both bones together occupy most of the length of the maxillary blade. Supramaxilla 1 is a very small, slightly fusiform bone. In contrast, supramaxilla 2 is a longer and larger bone that extends forward, overlapping most of supramaxilla 1 with its anterodorsal process. A sigmoid contact region joins both supramaxillary bones.

The external surface of the maxilla and supramaxillae is covered with a thick layer of ganoine, which is ornamented with longitudinal ridges extending along the bones. A few small tubercles scattered between the ridges are present on the maxilla.

Lower Jaw—The lower jaw (Figs. 76, 77C, 80A, B, 81, 83) is composed laterally by three dermal bones: dentary, surangular,

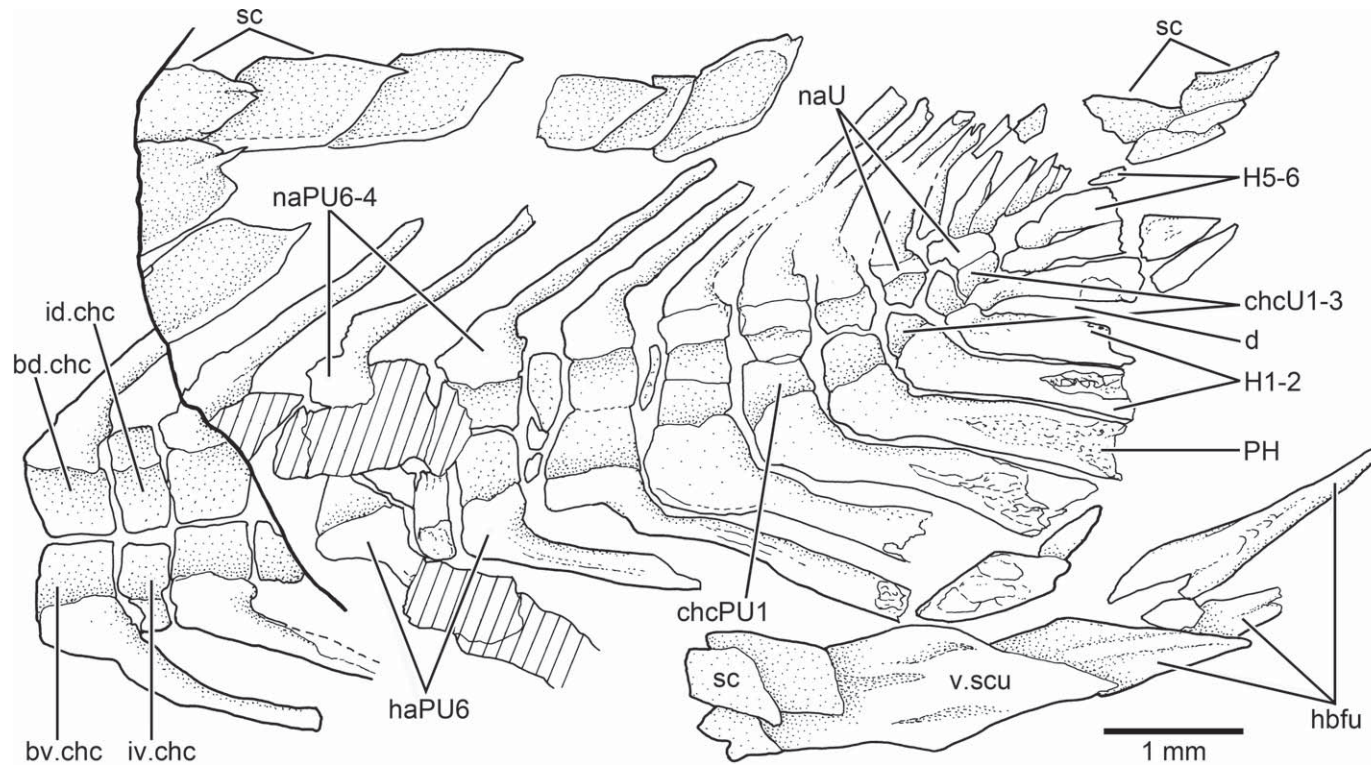


FIGURE 84. *†Pholidoctenus serianus* Zambelli. Drawing of posterior caudal vertebrae and caudal endoskeleton and scales in left lateral view (MCSNB 3377). Note the last ural neural elements are modified in shape, but still bear part of the dorsal arcocentra corresponding to ural centra 1–3. Hatched lines indicate broken bone surface.

and angular. A retroarticular is not exposed laterally in any of the studied specimens, but it may be fused to the articular and angular medially, as it is the condition present in *†Pholidophorus latiusculus* and *†Pholidorhynchodon malzani*. The oral margin of the jaw is almost straight along the first third of its length, and then forms a kind of notch (Fig. 77C) that does not resemble the ‘leptolepid’ notch found in *†Pholidophorus latiusculus* or any other species studied here. Posterior to this notch the margin projects abruptly in a high coronoid process. The coronoid process is formed mainly or only by the surangular. Its highest point is found at about the posterior third of the jaw.

The dentary (Fig. 83) forms most of the length of the lower jaw, extending below the angular posteroventrally. Both bones are sutured to each other, and no space is left between them at their ventral margins. The dentary bears very small conical teeth on the oral margin along the first third of the jaw length. The dentary has a region lacking ganoine close to the oral margin and above a well-exposed longitudinal ridge that runs along the length of the bone. The angular forms the posteroventral lateral wall of the jaw and is covered by a thin, smooth layer of ganoine. An elongate surangular sutured with the angular and dentary forms the posterodorsal margin of the lower jaw and is the main component of the tip of the coronoid process.

A postarticular process is lacking at the posterior margin of the jaw (Figs. 77C, 80B). There is no information available regarding the medial view of the lower jaw, consequently, it is unknown whether *†Pholidoctenus* has coronoid bones or not. The articulation between the lower jaw and quadrate is below the mid-region of the orbit.

The mandibular sensory canal (Fig. 80C) is below the bony ridge along the dentary and anterior part of the angular. A variable number of round or oval pores open on the surface of the dentary and are an indication of the trajectory of the canal. The posterior opening of the mandibular sensory canal is positioned medially. A vertical and short oral pit-line groove is present close to the posterior corner of the angular.

Palatoquadrate and Suspensorium—All bones of the palatoquadrate and suspensorium are hidden by other bones, so only rarely a small portion of the quadrate or the whole quadrate is observed (Figs. 76, 80). The quadrate is mainly a cartilaginous element, with the exception of an ossified articular condyle and posteroventral part of the bone. In specimen MCSNB 3041, a posteroventral process and quadratojugal are not present. There is no evidence that the symplectic forms part of the articulation of the lower jaw, and no evidence of an ossified symplectic either. Apparently, the metapterygoid remains as a cartilaginous element—an ossified bone has not been observed in the available specimens. The entopterygoid is preserved in the holotype. Under magnification, very tiny teeth are visible in MCSNB 3035 where the surface of the entopterygoid is broken.

Opercular, Branchiostegal Series, and Gular Plate—The opercular bones are located posterior to the posterior margin of skull roof plate. All opercular bones, as well as the branchiostegals, are covered by a layer of ganoine and present a variable number of acute projections or serrations on their posterior margins. The posterior margins of the opercle and subopercle, plus the ventral margin of the interopercle, produce a gently rounded profile of the opercular apparatus.

The preopercle (Figs. 76, 79, 80A, B) is a narrow, crescent-shaped bone overlying the hyosymplectic bones. Consequently, the preopercle lacks well-defined dorsal and ventral arms. Its posteroventral margin is serrated, and a notch at the posteroventral margin of the bone is absent. The dorsal part of the preopercle is covered by the suborbital and part of infraorbital 3. The anteroventral part of the preopercle projects anteriorly where the additional preopercle lies, and its bony surface lacks ganoine. The anterior margin of the preopercle is not expanded as in †*Pholidophorus latiusculus* and †*Parapholidophorus*. The pathway of the preopercular sensory canal is visible through its pores (four or five) that are positioned closer to the posteroventral margin, rather than to the central region of the bone. Although I have observed some pores, mainly concentrated close to the anteroventral margin of the preopercle, I have not observed the seven tubules with their respective pores positioned even closer to the dorsal tip of the bone, as reconstructed by Zambelli's (1977:fig. 1). In that same paper, Zambelli (1977:fig. 4) illustrated a preopercle without tubules and pores. I have observed variability in the number of pores, with the common condition being four or five pores. The dorsal connection between the preopercular and otic sensory canals has not been observed because the dorsal tip of the preopercle is hidden by the suborbital and opercle in all studied specimens. Ventrally, the preopercular canal continues in the mandibular canal. Up to two pit-line grooves are observed in the region just anterior to infraorbital 3. The dorsal one is the anterior division of the supramaxillary pit-line groove, and the ventral one, or oral pit-line, is almost perpendicular to the latter.

A bone identified here as an additional or accessory preopercle (= preopercle 2 of Zambelli, 1977; Figs. 76, 79, 80A, 83) is positioned in front of the anteroventral margin of the preopercle and below the ventral margin of infraorbital 3. The additional preopercle almost completely overlaps the quadrate. The additional preopercle sutures with a broad articular surface found on the anterior margin of the preopercle. The surface of the bone is smooth, and no pit-lines are observed. An accessory preopercle has not been observed in any of the other Triassic species studied here.

The opercle (Figs. 76, 79, 80A, B, 82A) is a moderately large bone, gently curved at its dorsal margin, which extends close to the lateral margin of the extrascapula. The anterior margin of the opercle is notched at the level of the articular facet for the hyomandibula and continues ventrally in a straight margin. The ventral margin of the opercle is markedly oblique. The external surface of the bone is smooth, with the exception of some growth lines, which are close to the dorsal margin (Fig. 81).

The subopercle (Fig. 76, 79, 80A, B, 82A) is a large bone. Its depth is about two times the opercular depth. Its ventral margin is gently rounded and in continuation with the rounded posteroventral corner of the opercle. The ventral margin possesses numerous serrations. The anterodorsal process is short and blunt, and it projects dorsally in front of the anterior margin of the opercle and is partially hidden by the posterior margin of the preopercle.

The elongate, narrow interopercle (Figs. 76, 79, 80A, B, 83) is below the preopercle. Its exact shape cannot be clarified because the interopercle is commonly partially covered by the preopercle. Its anterior tip extends below the anteroventral tip of the preopercle or even projects forward anteriorly, a different condition from other pholidophorids studied here. Its ventral margin has a variable number of serrations.

There are nine to 13 branchiostegal rays (Figs. 76, 80A, 83) preserved in the studied material. Zambelli (1977) reported the presence of 10 to 13 rays. The branchiostegals are relatively narrow, with their posterior margins bearing a variable number of small serrations. The last branchiostegal rays are the longest.

An elongate, oval-shaped gular plate (Figs. 78C, 83) is present. The gular plate is slightly shorter than the lower jaw and is ornamented with thick ridges of ganoine.

Vertebral Column and Intermuscular Bones—The vertebral column can be observed in those few specimens in which the squamation has been displaced or lost. The vertebrae of the abdominal region are formed by diplospondylous chordacentra in †*Pholidoctenus*. Each centrum is formed by basidorsal and basiventral hemichordacentra, and interdorsal and interventral hemichordacentra (Fig. 82D). Although they vary in shape, the four hemichordacentra are more or less square or rectangular. The four hemichordacentra do not constrict the notochord, because they form a thin-walled, ring-like centrum. The neural arches and their short spines are paired in the abdominal region and are fused medially in the caudal region. They retain cartilage covered by thin, perichondral bone. Parapophyses, as well as ribs, were not observed at the ventrolateral region of the centra. I expect that they are autogenous, so that they can be easily lost during fossilization. The caudal region (Fig. 84) shows the same morphology as the abdominal centra. However, the last caudal vertebrae are comparatively smaller, monospondylous, and formed only by dorsal and ventral chordacentra. The neural spines of the caudal region are simple, median elements.

Epineurial processes are not associated with the posterior margin or the lateral surface of the neural arches. Thus, epineurial, as well as epipleural, bones are absent in †*Pholidoctenus*.

Paired Fins—The pectoral girdle and fins are preserved in many specimens, occasionally as disarticulated elements, so that a satisfactory description can be produced. However, some bones are obscured by the presence of displaced scales. Only the dermal elements of the pectoral girdle are preserved. It is unclear if a clavicle articulating with the anterior region of the cleithrum is present or not because the region where a clavicle would be is covered by the subopercle and branchiostegal rays.

The posttemporal (Figs. 76, 81, 82A), a bone named 'postspiracle' by Zambelli (1977), is a small, plate-like element that is partially covered by the lateral margin of the large extrascapula. The anterior and lateral margins of the bone are thicker than the posterior one, and it appears that the bone has rolled over, covering the lateral line canal near the lateral margin. The posterior margin of the posttemporal presents one or two serrations. The lateral line canal is near the lateral margin; only one or two pores may be observed on the surface. Apparently, the bone lacks processes to connect with the braincase because I have not been able to see them in any of the disarticulated or displaced bones.

Underlying the posttemporal is the anterodorsal tip of the supracleithrum (Figs. 76, 82A). This slightly broad bone overlies the dorsal region of the cleithrum anteriorly and the upper part of the dorsal postcleithrum posteriorly. Its posterior margin possesses numerous serrations. The supracleithrum carries the lateral line canal, which exits about the middle region of the posterior margin. The cleithrum (Figs. 76, 82C, 83) is boomerang-shaped. The dorsal ramus is slightly shorter than the ventral one. Only a narrow portion of the cleithrum is exposed laterally, because most of its expanded anteromedial region is covered by the opercle and subopercle. The anterior surface of the cleithrum is covered with a series of long toothed ridges or a serrated appendage.

Two postcleithra (Fig. 72, 82A) are present posterior to the cleithrum. The dorsal postcleithrum is the largest and is located posterior to the cleithrum and ventral to the supracleithrum. An almost straight articulation is present between the dorsal postcleithrum and the small, slightly square ventral postcleithrum. Both bones present a few acute projections at their posterior margins.

The pectoral fins (Figs. 74, 76, 83) are positioned low on the flank, close to the ventral margin of the body. Each pectoral fin

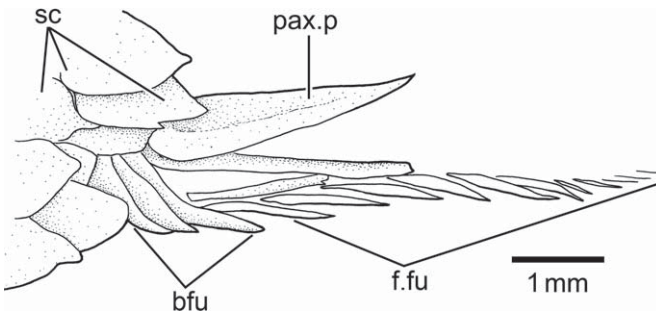


FIGURE 85. *†Pholidocetus serianus* Zambelli. Drawing of left pelvic axillary process and fulcra in lateral view (MCSNB 3035).

consists of 16 or 17 lepidotrichia. The first one is spine-like and slightly shorter than the following rays, which have long bases and are segmented and branched distally. The first pectoral ray (Fig. 83) is a compound bone that, in addition to a pair of moderately thin hemilepidotrichia, enlarges its size by fusion with a few basal fulcra, which alternate with fringing fulcra, a condition also described here for other taxa. A series of elongate fringing fulcra are associated with the leading margin of the fin. The propterygium does not fuse with the first pectoral ray as in other taxa described above.

A moderately long, leaf-like or triangular pectoral axillary process lies above the insertion of the pectoral fin. The pectoral axillary process is formed by one or two leaf-like bones (Fig. 82A) that are covered by a thin layer of ganoine.

The insertion of the pelvic fins (Fig. 74) is at the level of the eighth vertical row of scales. The pelvic fin consists of three to five leaf-like, elongate basal fulcra and about nine rays with elongate bases, which are distally segmented and branched. A series of elongate fringing fulcra are associated with the leading margin of the fin. A large, leaf-like, and well-ossified pelvic axillary process (Fig. 85) lies above the pelvic fin.

Dorsal and Anal Fins—The dorsal fin (Figs. 74) is roughly triangular, with long first principal rays and very short posterior ones. The anterior origin of the dorsal fin is at the level of the 18th, 19th, or 20th vertical row of scales. The dorsal fin is preceded by four or five basal fulcra. The first fulcrum is a very small, unpaired element that is followed by fulcra that increase in size posteriorly; all of them seem to be unpaired. There are about 10 principal rays,

all of which are branched and segmented, except that the first one is unbranched. The rays have a very fragile aspect and are usually broken. The principal rays have long bases and are segmented and scarcely branched distally. It is unclear whether only the first principal ray forms the leading margin of the fin or whether the second principal ray also forms the leading margin. Elongate fringing fulcra are between the last basal fulcrum and leading margin of the fin.

The beginning of the anal fin is at the level of the 17th or 18th vertical row of scales. The short anal fin (Figs. 74, 86) is posterior to the dorsal fin and is closer to the caudal fin than to the pelvic fins. It consists of three to five elongate and leaf-like basal fulcra and nine principal rays. The anal rays are also very delicate and thin and are frequently broken. At least the first and second principal rays form the leading margin of the fin. Elongate fringing fulcra are associated with the leading margin of the fin.

Caudal Fin—The caudal endoskeleton is observed in one specimen (MCSNB 3377) with scales removed in the posterior part of the body. The last vertebral centra (Fig. 84) are monospondylous chordacentra. Each centrum is formed by a dorsal and a ventral hemichordacentrum, even preural vertebra 1 and ural centrum 1. Ural centra 2 and 3 are formed only by a ventral hemichordacentrum. Ural centra 4 and 5 are not preserved. The chordacentra become very small posteriorly. The dorsal and ventral arcocentra also become smaller posteriorly. The neural spines are inclined to the body axis, and their lengths decrease posteriorly. It is unclear whether the elements above preural vertebrae 3 to 1 are broken spines or are epurals. Considering their preservation, they appear to be broken spines. The bones above the ural region are ural neural arches, but are not modified uroneurals; they maintain the same angle and same structure as the neural arches of preceding vertebrae.

The transition between hemal spines and hypurals is not obvious so that it is very difficult to separate them, but using hypural diastema as a landmark (see Schultz and Arratia, 1989, 2013) helps to identify hypurals 2 and 3. Five hypurals are preserved, but it is expected that more elements were present.

Although some of the distal tips of the caudal fin rays are broken, the tail is almost completely preserved in a few specimens. The hemi-heterocercal caudal fin is deeply forked, with very short middle principal rays in comparison with the long leading margins of the epaxial and hypaxial lobes of the fin. The area covered by ganoid scales at the base of the caudal fin (Fig. 87) is long and ends in an a slightly triangular area in the epaxial lobe; in contrast, the

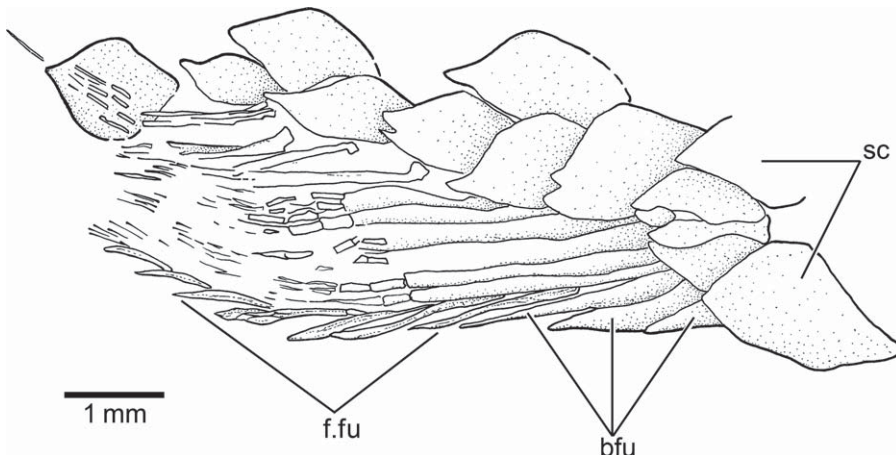


FIGURE 86. *†Pholidocetus serianus* Zambelli. Drawing of anal fin and scales in right lateral view (MCSNB 2876).

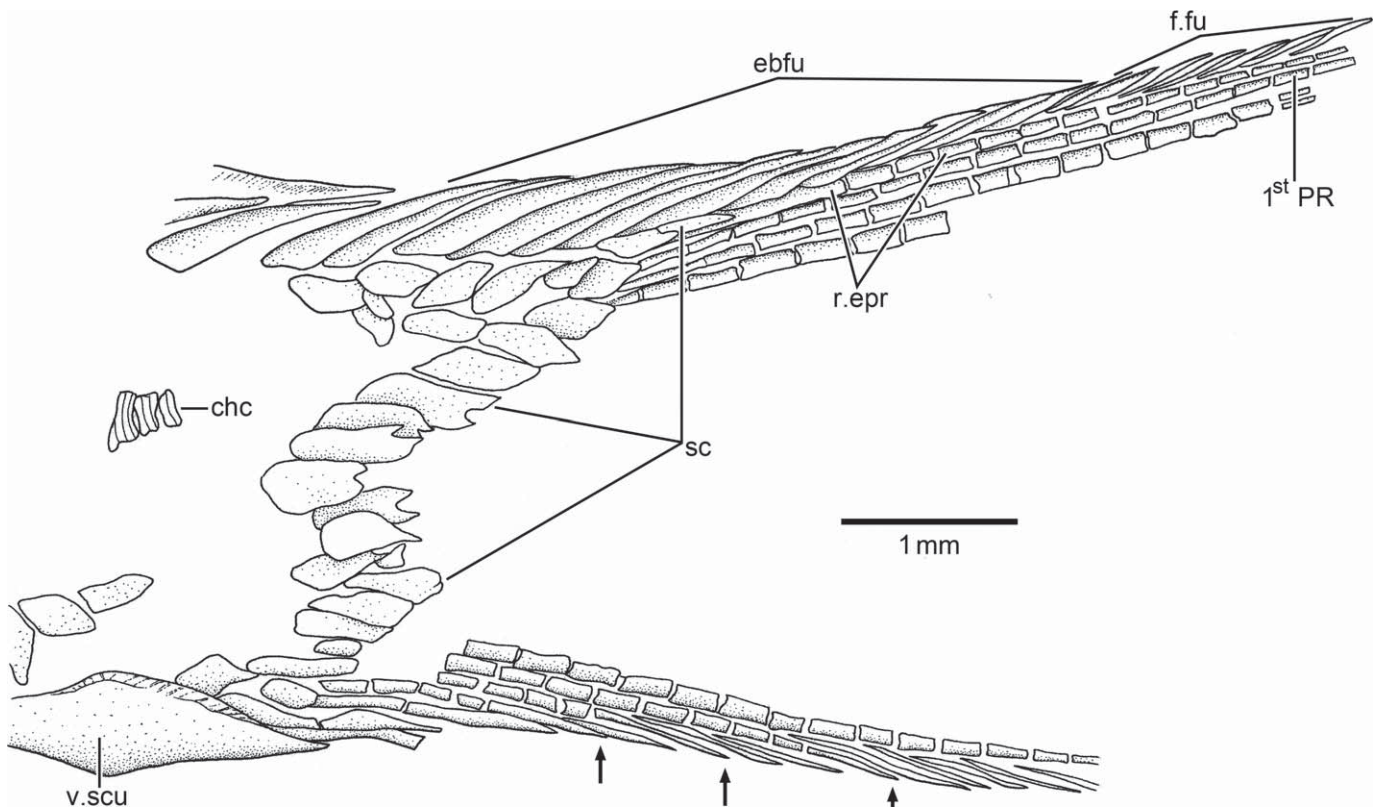


FIGURE 87. \dagger *Pholidoctenus serianus* Zambelli. Drawing of leading margins of the caudal fin and scales in left lateral view (MCSNB 3012). Arrows point to the terminal segment of procurent rays, which are intercalated between adjacent, additional fringing fulcra.

area of ganoid scales covering the base of the caudal fin in front of the hypaxial lobe is markedly shorter and slightly rounded.

The caudal fin has nine or 10 epaxial basal fulcra, a series of elongate epaxial fringing fulcra, one epaxial rudimentary ray, 18 to 20 principal rays (the lowest number among the species studied), a series of elongate hypaxial fringing fulcra, four hypaxial segmented procurent rays, and two elements interpreted as hypaxial basal fulcra. The epaxial basal fulcra (Fig. 87) are elongate, leaf-like elements that expand laterally, partially covering the next fulcrum. It is not possible to confirm if all basal fulcra are paired or not, but the most posterior ones are paired. The hypaxial procurent rays each end in a fulcrum-like segment; accessory fringing fulcra are inserted in between the distal segments of the procurent rays.

Fringing fulcra (Fig. 87) lie at least on the dorsal margin of the epaxial rudimentary ray and on the exposed dorsal margin of the first principal ray. The distal tips of the rays are usually damaged so that it is not possible to determine whether the second principal ray is part of the leading margin or not. The articulation between segments of all principal rays is straight. No dorsal processes associated with the bases of the middle principal rays have been observed.

One long or two rhomboidal dorsal scutes and another ventral one precede the epaxial and hypaxial series of basal fulcra.

Scales—The body is covered by thick ganoid scales (Figs. 74, 75A, B, 79, 81, 88) with peg-and-socket articulations. The pegs are well developed and acute. Most scales, with the exception of those covering the base of the caudal fin, have a few elongate, acute projections at their posterior margins or simply the scales

have leaf-like shapes. Scale shape differs according to body region. Although most specimens have three rows of larger scales, one of the best preserved specimens (MCSNB 3036) has two well-defined rows of larger, rectangular scales in the middle of the flank extending from just posterior to the dorsal postcleithrum until the insertion of the last principal dorsal rays. These two rows comprise

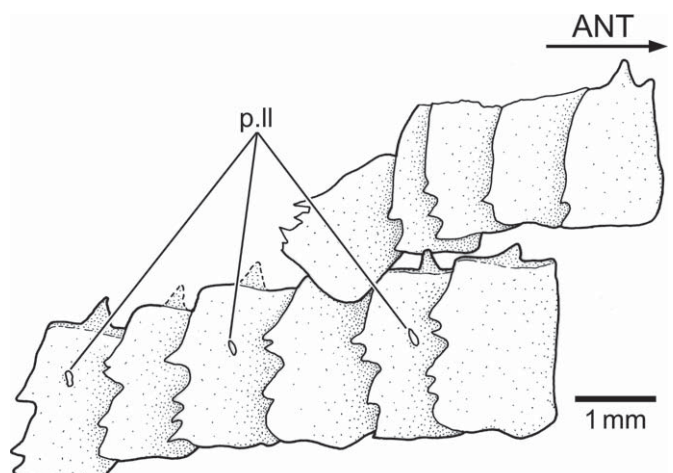


FIGURE 88. \dagger *Pholidoctenus serianus* Zambelli. Drawing of lateral line scales from right flank in lateral view (MCSNB 3041).

15 or 16 large scales, with a few acute serrations at their posterior margins. Dorsal to these two main rows, there are seven or eight vertical rows of smaller, slightly rhombic or leaf-like scales, usually with one or two acute serrations at their posterior margins. A similar number of vertical rows and scales are ventral to the two main rows and in front of the pelvic fins. There is a big change in the aspects of the scales posterior to vertical row 15 or 16, which become smaller and are more similar in shape, being leaf-like and with one acute projection posteriorly. The scales around the base of the fins have slightly modified shapes from neighboring scales; they are smaller and generally have smooth margins.

Lateral Lines—Thirty-five or 36 flank scales transmit the main lateral line canal. The scales are rectangular, with serrated posterior margins and superficial accessory pores of the lateral line that occur on every other scale (Fig. 88). A series of scales, extending close to the dorsal margin of the body up to the dorsal fin and showing pores, is interpreted as an accessory lateral line.

Comment—Serrated bones and serrated scales are known from at least *†Pholidoctenus* and the extinct family Archaeomaenidae Goodrich, 1909, which are ‘pholidophoriforms’ of unknown phylogenetic relationship. The archaeomaenids are Jurassic fishes known from Australia and Antarctica. Among archaeomaenids, the best-known species is *†Oreochima ellioti* Schaeffer, 1972, from Antarctica. Despite the fact that *†Pholidoctenus* shares with ar-

chaeomaenids the presence of serrated dermal bones, scales with serrated posterior margin, and nasal bones with extensive contact between them that separate the rostral bone from the anterior tips of the parietals, there are major differences between them. These include the presence of an additional preopercle in *†Pholidoctenus* (missing in archaeomaenids); an oblique opercular-subopercular suture in *†Pholidoctenus* (straight in archaeomaenids); skull roof bones fused into a plate in *†Pholidoctenus* (parietals, postparietals, autostrophonotics, and dermopterotics independent in archaeomaenids); five or six infraorbital bones in *†Pholidoctenus* (four in archaeomaenids); infraorbital 3 is positioned at the posteroventral corner of the orbit in *†Pholidoctenus* (infraorbital 2 occupies that position in archaeomaenids); and caudal fin with 18 to 20 principal rays in *†Pholidoctenus* (19 in archaeomaenids). I agree with Zambelli (1977) that the morphological differences between *†Pholidoctenus* and archaeomaenids are of such magnitude that they belong to separate families.

Among Triassic fishes previously interpreted as pholidophorids, *†Knerichthys bronni*, gen. nov. (Fig. 43), from the Carnian of Lunz, Austria (see above), and *†Jianligichthys serratus* Su, 1983 (Fig. 89), from the Upper Triassic of China share the presence of scales with serrated posterior margins. Serrations have not been observed in the cranial bones of the last two taxa. *†Jianligichthys* was included within the *†Pholidophoridae* by Su (1983). However, the preservation of the fish and its characters do not provide any solid evidence

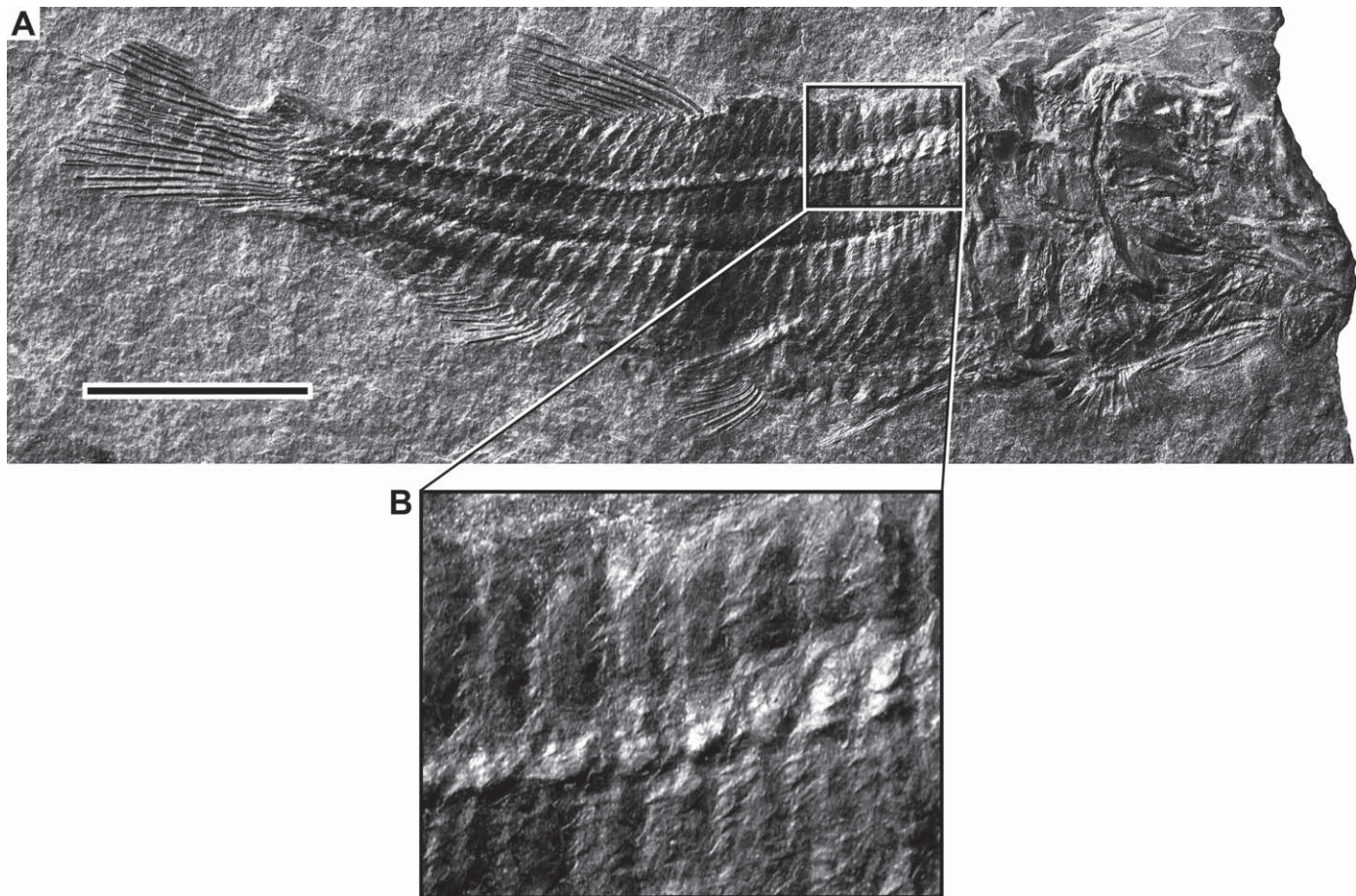


FIGURE 89. *†Jianligichthys serratus* Su (IVVP V6353-1.1b) from Sichuan Province, China. A, photograph in right lateral view. B, enlargement of portion within box. Scale bar equals 5 mm.

to support such an assignment. Thus, the taxonomic assignment of †*Jianlichthys* should be revised.

†PHOLIDOPHORETES Griffith, 1977

Diagnosis—Emended from Griffith, 1977. Pholidophorids of small to medium size, with small head, about 20–21% of standard length [*]. Ganoine ornamentation on dermal bones almost nonexistent. Nasals well developed, with extensive medial contact. Opercular roughly triangular, with strongly inclined lower edge. Preopercle with sensory canal nearer to posterior than anterior margin. A single suborbital; five infraorbitals; infraorbital 3 considerably enlarged and extending posteriorly, ventral to the suborbital. Maxilla of moderate size, not markedly deepened; posterior margin characteristically notched. Two supramaxillae; supramaxilla 1 very small; supramaxilla 2 large, slightly more than 50% of maxillary length. Dorsal fin positioned opposite to anal fin [*]; fringing fulcra present along anterior edges of all fins. Ganoid scales moderately thick; rhomboid-shaped with smooth posterior margins. Anterior scales of lateral line series twice as deep as broad.

Type Species—†*Pholidophoretes salvus* Griffith, 1977.

Content—Type species only.

†PHOLIDOPHORETES SALVUS Griffith, 1977 (Figs. 90–94)

Pholidophoretes Griffith, 1977:72, figs. 27–30, pl. 11C.

Holotype—NHMW 2007z170/0293a and b (Fig. 90). Head and anterior part of the body preserved in part and counterpart.

Paratype—NHMW 2007z0170/0094 (Fig. 91). Specimen showing the ventral surface of the head.

Additional Material Examined—The sample of †*Pholidophoretes salvus* deposited at the NHMW includes 45 incomplete, poorly preserved specimens (NHMW 2007z0170/0095, NHMW 2007z0170/0296–0339).

Type Locality, Geological Age, and Distribution—Polzberg bei Lunz, in the Northern Calcareous Alps, about 110 km southwest of Vienna, Austria; Upper Triassic Reingrabener Schiefer; Polzberggraben; Carnian (Julian Stage; Dalla Vecchia, 2006), about 228 to 216 Ma.

Diagnosis—Same as for genus.

Description

The fishes studied here correspond to the same material used by Griffith (1977) in the original description of †*Pholidophoretes salvus*. Except for certain bones of the head and scales, it is almost impossible to provide a description of certain body regions, as well as morphometric and meristic traits. My observations on particular cranial bones and their taxonomic and phylogenetic interpretations have some major differences with those of Griffith (1977), as explained below. The holotype and paratype present the best-preserved bones so that the descriptions are largely based on them, with the noted exceptions.

Although all specimens are incomplete, standard length can be obtained from a few. The longest specimen is 82 mm SL, but the average is smaller, about 70 mm SL. The head, apparently as wide as deep, is small, reaching about 21% of SL (Griffith, 1977). The fishes are elongate, with a maximum depth in the predorsal region, ranging from 26 to 32% of SL. The pectoral fins are positioned closer to the ventral margin of the body than to the middle region of the flanks. The pelvic fins are positioned in front of the origin of the dorsal fin, and the latter partially opposes the anal fin. All fins are small, with thin and slender rays that bear elongate fringing fulcra associated with leading margins.

Most external cranial bones and scales are covered by a thin layer of ganoine or the ganoine is missing completely. Certain elements such as the rostral, maxilla, supramaxillae, and gular are ornamented with tubercles or ganoine ridges and tubercles (see below). A few scattered small tubercles of ganoine are present on some cranial bones.

Braincase—The braincase seems to be short, with its posterior margin located at the level of the opercle. Except for the skull roof bones, no other elements of the braincase are observed in the holotype.

Skull Roof—The skull roof has a smooth surface lacking ridges, crestae, or fontanelles. All bones of the cranial roof, including the parietal, postparietal, autosphenotic, and dermopterotic, are fused into a single bony plate (Fig. 92A, B). Although numerous fractures are observed, they do not correspond to cranial sutures. Griffith (1977:figs. 27, 28), however, described and restored these bones as independent elements in what he named as his “composite reconstructions” of the head in dorsal and lateral views.

The skull roof (Fig. 92A, B) is narrow anteriorly, ending in a slightly rounded tip. The width of the skull roof increases progressively posteriorly, being very broad at the level of the posterior corner of the orbital margin, maintaining its breadth in the postorbital region. The posterior margin is straight and there is no evidence of a supraoccipital bone. The breadth of the skull roof at the level of the posterior margin of the nasal bones is about one-third of that of the postorbital region.

The smoothness of the surface of the cranial roof in the holotype is interrupted by a few wavy irregularities (Fig. 92A) in the region of the supraorbital canal pores and pit-line grooves and where the postparietal and dermopterotic would lie. The pores are only preserved on one side of the skull roof in the holotype, and it is unclear whether a parietal branch of the supraorbital canal is present. The long middle pit-line ends near the lateral border of the skull roof plate. A short anterior pit-line groove is preserved, but not the posterior one. There is bilateral variation in the length of the anterior pit-line, as well as its presence. Consequently, bilateral asymmetry is observed among individuals.

A median, moderately large, slightly rhomboidal rostral bone (Fig. 92B) is at the anterior-most region of the skull roof. The bone has a slightly rounded anterior region, lateral processes, and a large, broad posterior region. The slightly rounded posterior margin joins the anterior articular margin of both nasal bones. As far as can be observed in all examined specimens, there is no contact between the rostral and anterior part of the skull roof plate at its parietal tips. The anterior region of the rostral bone is incompletely preserved in the holotype; it is covered by thick tubercles of ganoine. The lateral processes are broken so that the complete size of the bone is unknown. The posterior region of the rostral is traversed by a smooth middle region where the ethmoidal or rostral commissure is positioned (Fig. 92B).

There are two large, characteristically shaped, plate-like nasal bones (Fig. 92A, B). The nasal is squarish anteriorly, but triangular posteriorly, ending in an acute tip. It has an anterior margin that is slightly notched (framing the anterior nostril opening), a straight medial margin that articulates with its opposite, and a lateral margin that may be straight or notched. The posterolateral margin joins supraorbital 1. The holotype poses a problem because one of the nasal bones has a foramen close to its lateral margin, whereas the other nasal lacks it. A foramen seems to be absent in the few specimens with preserved nasals. The supraorbital sensory canal (Fig. 92A) is closer to the lateral margin of the bone than to the medial one in the holotype.

The large, plate-like extrascapular bone (Fig. 92A, B), present at the posterior margin of the skull roof, extends posteriorly, almost completely covering the anterodorsal part of the body. Griffith (1977:fig. 27) erroneously restored two bones posterior to

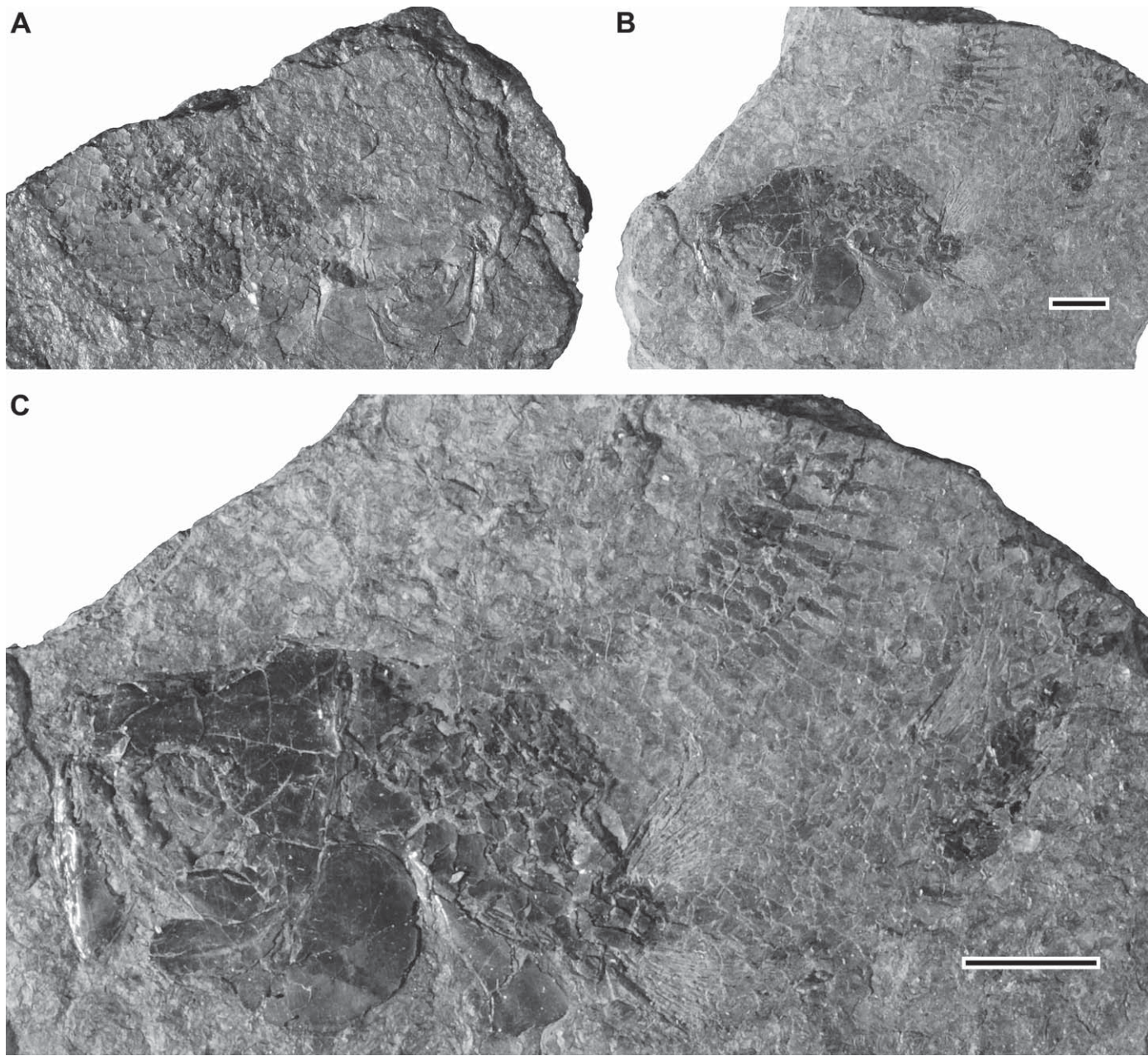


FIGURE 90. *†Pholidophoretes salvus* Griffith (holotype; NHMW 2007z170/0293a and b). **A, B**, photographs of part and counterpart. **C**, enlargement of holotype. Scale bars equal 5 mm. (Color figure available online.)

the skull roof plate—a narrow extrascapula and a large, roughly triangular suprascapula. The trajectory of the extrascapular commissure is partially visible, but its junction with the otic and lateral line canals is not preserved. A small bone, a possible posttemporal, is observed between the lateral margin of the extrascapula and supracleithrum in the holotype.

A composite restoration of the skull roof showing the trajectories of the cephalic sensory canals was presented by Griffith (1977:figs. 27, 28). According to him, “the arrangement of the sensory canals of the head is basically the same in all pholidophorids” (Griffith, 1977:76). This statement is not supported by the descriptions of other pholidophorids. For instance, the supraorbital canal is restored in continuation with the anterior pit-

line, a pattern that I have not observed (see Fig. 92A, B) and is not found in other fishes studied here. A posterior pit-line groove was erroneously restored in continuation with the middle pit-line, despite the statement (Griffith, 1977:76) that “there is no indication of a posterior pitline,” as my results also show. Additionally, Griffith restored the supraorbital sensory canal extending in front of the nasal bone, joining the ethmoidal commissure and the infraorbital canal. However, the incomplete preservation of the specimens, and especially of the sensory canals, does not support such a restoration.

Circumorbital Series—The circumorbital ring is incompletely preserved in most specimens. Two supraorbitals, five infraorbitals, and one dermosphenotic are preserved. An antorbital has not

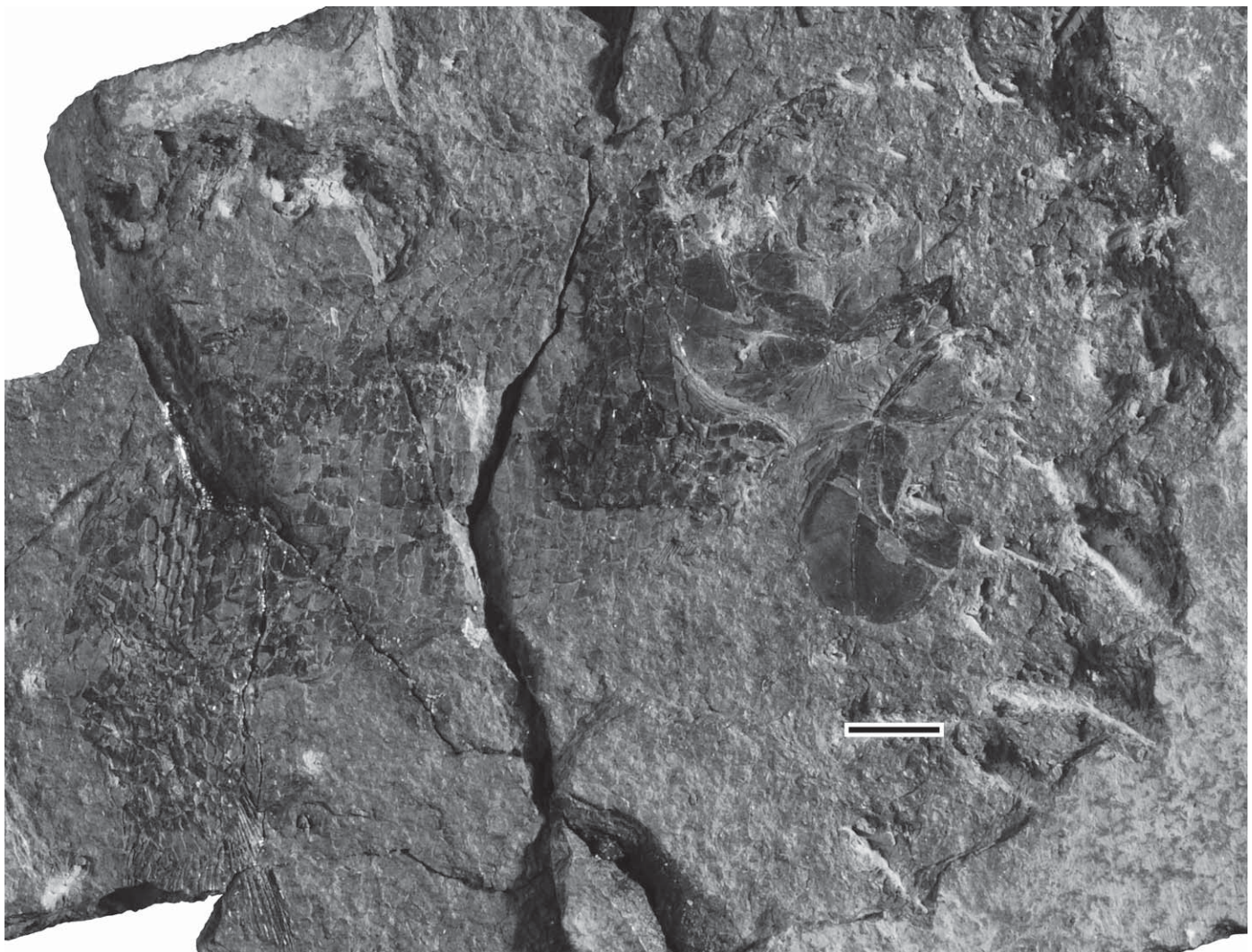


FIGURE 91. †*Pholidophoretes salvus* (paratype; NHMW 2007z0170/0094). Photograph in ventral view. Scale bar equals 5 mm. (Color figure available online.)

been observed. In addition, †*Pholidophoretes salvus* has one large suborbital.

Two elongate, thick supraorbital bones are lateral to the orbital margin of the skull roof plate, in between the posterolateral margin of the nasal bone and the dermosphenotic. Supraorbital 1 (Fig. 92B) seems to be smaller than supraorbital 2, which projects anterolaterally to supraorbital 1. Supraorbital 2 joins a small dermopterotic that is poorly preserved in all specimens (so a proper description cannot be presented). Three supraorbital bones were illustrated by Griffith (1977:fig. 28). The bone that he interpreted as supraorbital 3 is interpreted here as the dermosphenotic, and the bone that he interpreted as dermosphenotic is interpreted here as infraorbital 5 by comparison with other fishes studied here with complete circumorbital series.

Infraorbitals 1 and 2 are not preserved in the holotypic material. Infraorbital 3 (Figs. 92A, B, 93) is a large bone at the posteroventral corner of the orbit, extending posteriorly to the anterior margin of the preopercle. Infraorbital 3 contacts infraorbital 2 anteriorly, both preopercle and suborbital posteriorly, and infraorbital 4 dorsally. The infraorbital sensory canal is close to the orbital mar-

gin, and no tubules or pores are observed in the type material. A groove housing the anterior division of the supramaxillary pit-line is visible on the surface of the bone.

Infraorbitals 4 and 5 (Figs. 92B, 93) are squarish or rectangular bones carrying the infraorbital canal near to their orbital margins. They are shorter than infraorbital 3, but their size is variable among specimens. Both infraorbitals contact the suborbital posteriorly. Infraorbital 5, in addition, contacts the dermosphenotic dorsally.

A large suborbital (Fig. 92A, B) occupies the space defined by the posterodorsal margin of infraorbital 3, the posterior margins of infraorbitals 4 and 5 anteriorly, the opercle and preopercle posteriorly, and the lateral margin of the skull roof (dermopterotic region) dorsally. The suborbital is a squarish bone, with an almost straight dorsal margin and a slightly convex posterior margin. The suborbital may present a few concentric thin ridges of ganoine close to its posterodorsal corner.

Upper Jaw—The upper jaw (Figs. 92B, 94) is composed of paired dermal bones, the premaxillae, maxillae, and two supramaxillae. The premaxilla is displaced in a few specimens and

incompletely preserved. The bone is small, slightly triangular, and as far as can be observed, there is no evidence of a postpremaxillary or nasal process. Tiny conical teeth are present on the oral margin of the bone. A rostrodermethmoid seems to be absent, because it was not observed in any specimen (see also Griffith, 1977).

The maxilla is comparatively longer than in most species studied here, extending back as far as the posterior margin of the orbit and onto the anteroventral part of the preopercle. Its ventral margin is gently convex, and its posterior margin is distinctly notched (Figs. 92B, 94) in specimens with well-preserved maxillae. The articular process is moderately long, but narrower than the maxillary blade, which increases its depth slightly posteriorly. Due to the destruction of the ventral margin, teeth have not been observed in most specimens. A few small, conical teeth are preserved in the holotype. Almost the whole surface of the maxilla, with the exception of the anterior-most part of the articular process, is covered with a distinct pattern of longitudinal, thick ridges of ganoine.

One supramaxillary bone (Fig. 92B) is present in the holotype. However, two bones seem to be present in other specimens just posterior to the supramaxillary process of the maxilla. Supramax-

illa 1 is a small, triangular bone completely covered by thick ridges of ganoine characteristically arranged. Its length is about one-third the length of supramaxilla 2. In some specimens, the ornamentation makes it difficult to separate supramaxilla 1 from the maxilla (Fig. 94). Supramaxilla 2 is an elongate, fusiform or slightly fusiform bone, with its maximum depth about half that of the maxilla. It has a poorly developed anterodorsal process that barely overlaps the dorsal margin of supramaxilla 1, or the process is absent.

Lower Jaw—The lower jaw (Figs. 92A, 93) is only partially exposed in the holotype, as well as in a few other specimens. The lateral portions of the dentary and angular are visible. The deepest part of the jaw seems to be where an incompletely preserved surangular is, and the extent of the coronoid process is unknown, as well as the presence of a notch in the dorsal margin of the dentary. The suture between the dentary and angular is partially visible in a few specimens. A well-developed bony ridge protrudes laterally along the dentary and becomes weak as it crosses onto the angular and then disappears. The ridge separates the dorsal region, which usually lacks ornamentation, whereas the ventral

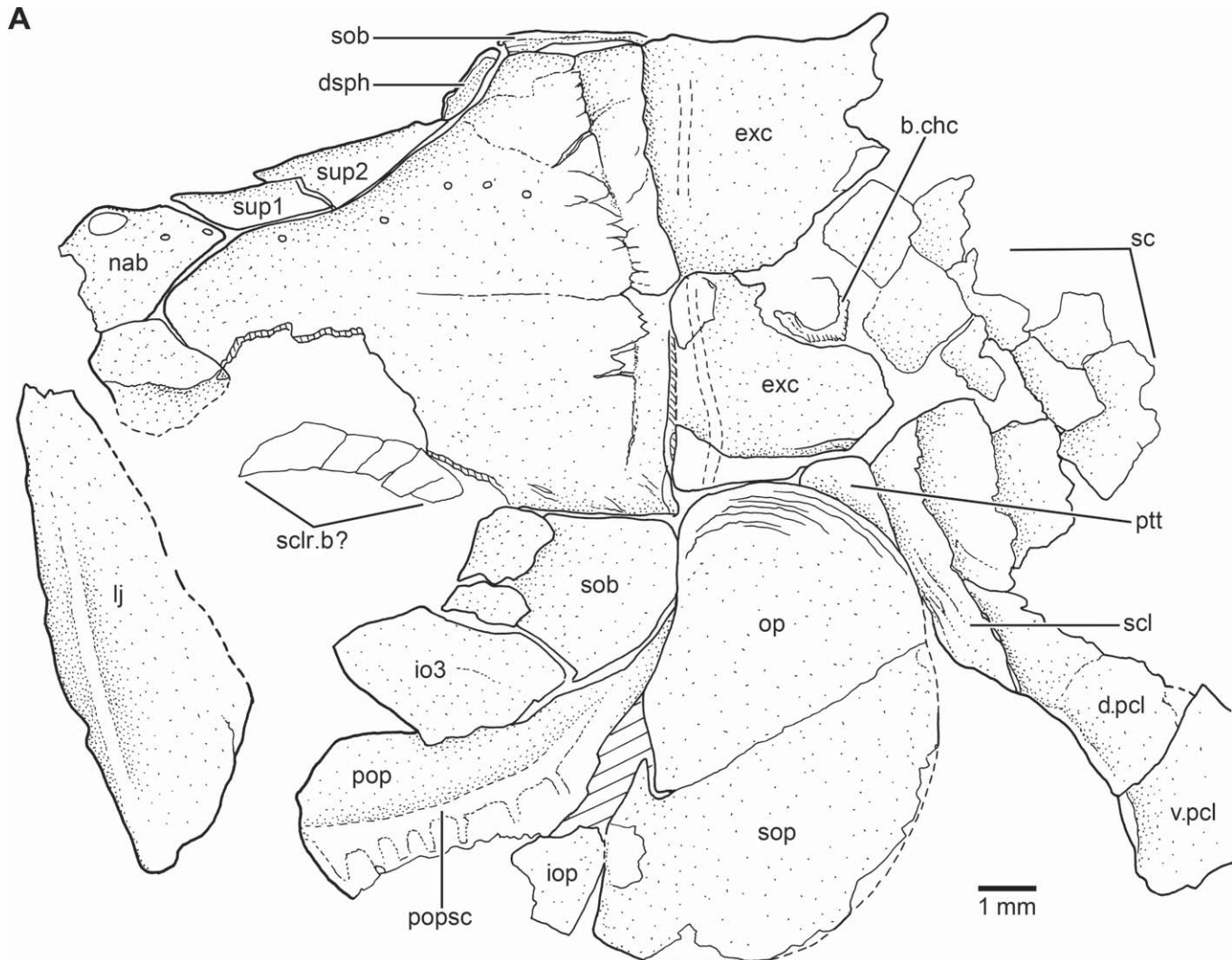


FIGURE 92. *†Pholidophoretes salvus* Griffith (holotype; NHMW 2007z170/0293a and b). Drawing of head and anterior part of body in part (A) and counterpart (B) in left lateral view. Hatched lines indicate broken bone surface.

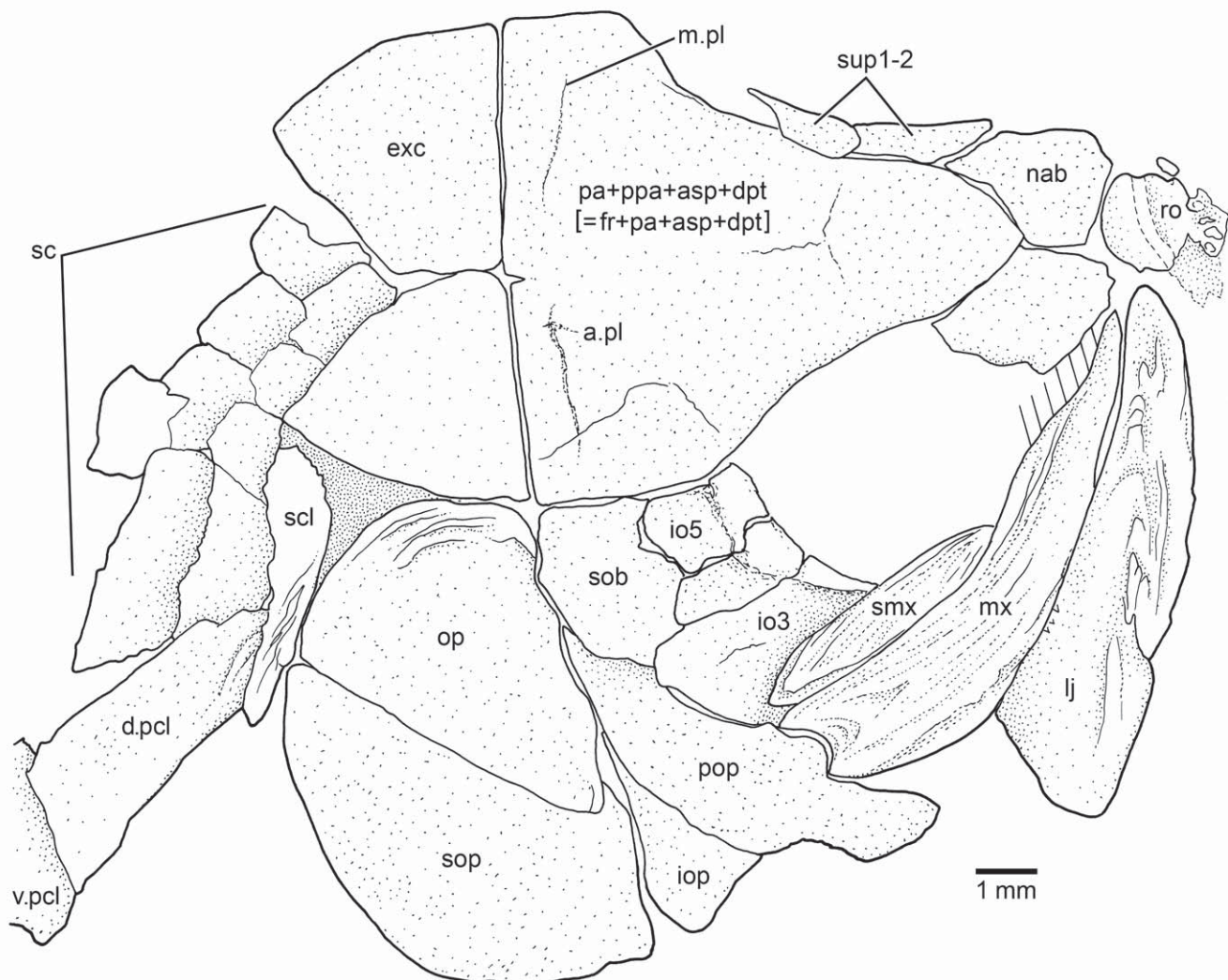
B

FIGURE 92. (Continued)

region is covered with longitudinal ridges of ganoine and elongate tubercles. Ornamentation obscures the trajectory of the mandibular canal. The dentary bears very small conical teeth, but the teeth are not preserved in the type material. Only a piece of the surangular sutured with the angular has been observed. A postarticular process is lacking at the posterior margin of the jaw.

The articulation between the lower jaw and quadrate is almost at the posterior margin of the orbit. The quadrate and symplectic are not observed in the available material, because the anterior expansion of the preopercle covers them.

Palatoquadrate, Suspensorium, and Hyoid Arch—All bones of the palatoquadrate, suspensorium, and hyoid arch are covered laterally by bones of the cheek so that a description is not possible.

Opercular, Branchiostegal Series, and Gular Plate—The opercular bones are relatively well preserved in the holotype and paratype. Branchiostegal rays and the gular plate are preserved in the paratype. The posterior margins of the opercle and subopercle, plus the ventral margin of the interopercle, produce a gently rounded profile of the opercular apparatus. All opercular bones are covered by a thin, smooth layer of ganoine.

The preopercle is moderately crescent-shaped without dorsal and ventral arms (see Figs. 92A, B, 93). A notch is not present on its posteroventral margin. Its anteroventral region is moderately expanded, being broader than the dorsal region of the bone. Its anteroventral margin is smooth, without a notch for the exit of the preopercular canal. The dorsal tip of the preopercle is covered by the suborbital, whereas the anterior margin of the preopercle is covered by the posterior projection of infraorbital 3 and posterior regions of the maxilla. The smooth anteroventral region of the preopercle is broadly expanded just anterior to the main course of the preopercular canal, which is closer to the posterior margin of the bone than to the anterior one. The course of the preopercular sensory canal bends through an angle of approximately 60 degrees at about two-thirds the depth of the bone, almost in front of the opercular/subopercular joint. Eight to 12 short, straight sensory tubules branch off from the main canal and open in round pores close to the margin of the bone. I count eight and 11 tubules in the left and right preopercles of the paratype (Fig. 93), but Griffith (1977:75) counted 10 and 12; the course of the preopercular sensory canal and its tubules

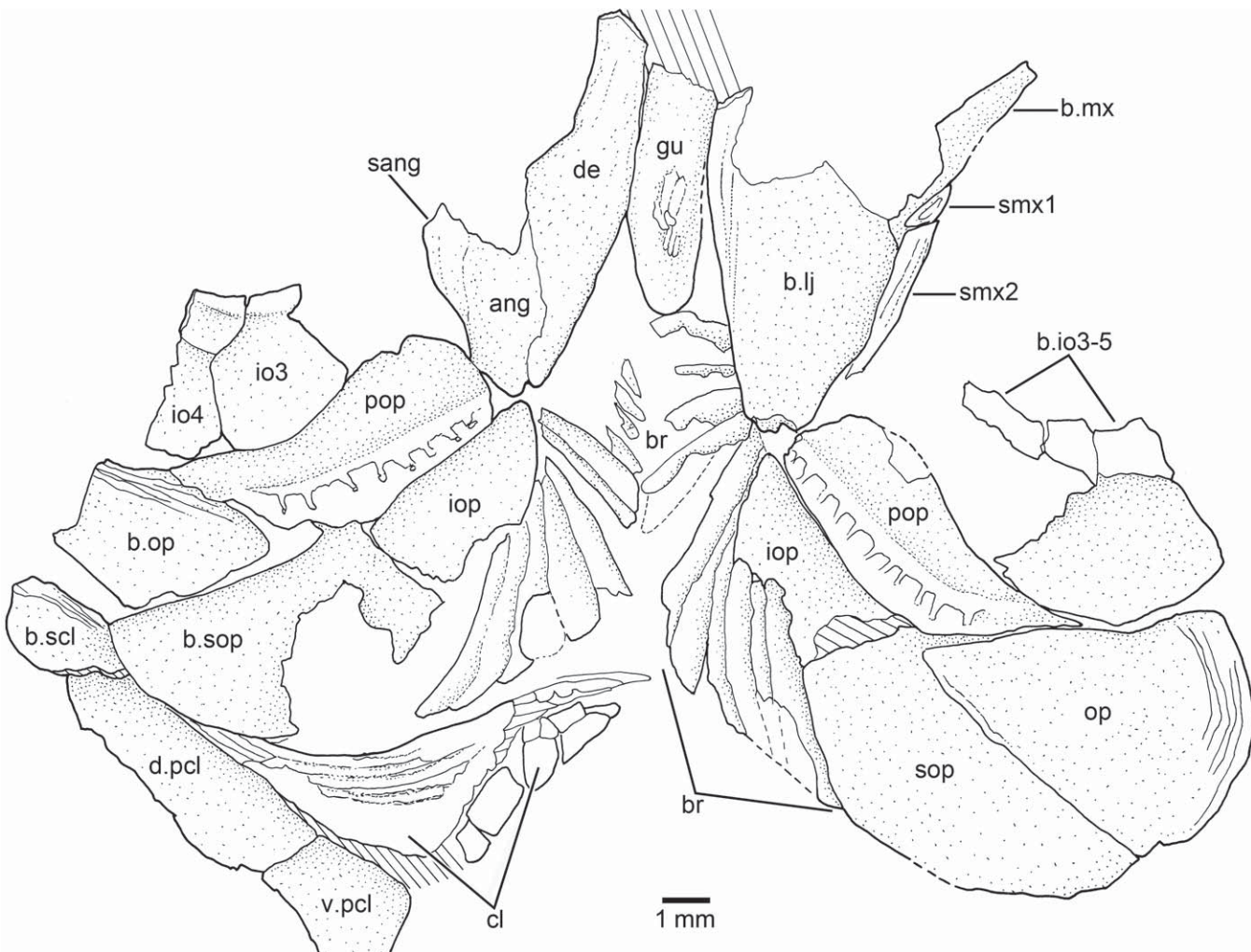


FIGURE 93. *†Pholidophoretes salvus* Griffith (paratype; NHMW 2007z0170/0094). Drawing of cranium and pectoral girdle in ventral view.

and pores is clearly visible because the ganoine is thin or almost nonexistent.

The opercle (Figs. 92A, B, 93) is a moderately large, roughly triangular bone. Its dorsal and posterior margins form a curve that continues in the posteroventral margin of the subopercle. The anterior margin is slightly wavy, and the ventral margin is long and straight, forming an oblique joint with the subopercle. The anterior margin of the opercle is markedly thickened and is covered by two or three ridges of ganoine. The ventral margin is markedly oblique. The surface of the opercle near the dorsal margin is covered by a few concentric, thin ridges of ganoine. In contrast, no ornamentation has been observed in other opercular bones.

The subopercle (Figs. 92A, B, 93) is slightly larger than the opercle. Its ventral margin is almost straight, whereas its rounded posterior margin is continuous with the posterior margin of the opercle. Its anterior margin is almost straight and joins the interopercle and a preopercle anteriorly. The anterodorsal process of the subopercle is well developed and partially exposed between the opercle and preopercle.

The interopercle (Fig. 92A, B) is a large, long, triangular bone positioned between the posteroventral margin of the preopercle

and anterior margin of the subopercle. The bone extends below the preopercle close to the posterior region of the mandible.

There are 11 or 12 branchiostegal rays (Fig. 93). The anterior-most rays are moderately narrow and long, but the breadth and length of the rays increases progressively posteriorly, with the largest ones positioned below the subopercle. The anterior-most branchiostegal rays are located below the angular region of the lower jaw, not posterior to it as illustrated by Griffith (1977:fig. 28). The gular plate (Fig. 93) is long, slightly oval-shaped, and its ventral surface is covered by a few tubercles of ganoine, which are irregularly shaped.

Vertebral Column—Remnants of a few ring-like chordacentra are observed between scales (Fig. 92A). No other elements associated with the vertebral column have been observed.

Paired Girdles and Fins—Both paired girdles and fins are poorly preserved in the available material. A description of the dermal elements (supracleithrum, cleithrum, and postcleithra) can be provided, but the chondral bones have not been observed. The supracleithrum is relatively large and narrow. The bone bears ridges of ganoine near its anterior margin, but the ridges close to the ventral margin seem to be in continuation with the serrated appendage on the cleithrum.

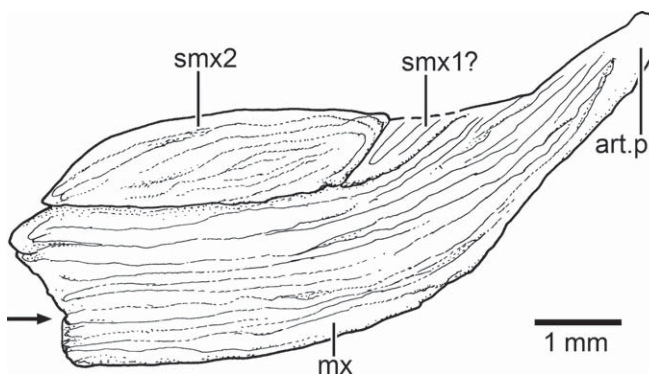


FIGURE 94. *†Pholidophoretes salvus* Griffith (NHMW 0170/0297). Drawing of right maxilla and supramaxillary bones in lateral view. Note the limit between the preserved supramaxilla 1 and maxilla is not evident, because the layer of ganoine and its ornamentation form one surface. Arrow points to characteristic notch at the posterior margin of maxilla.

The cleithrum (Fig. 93) is smaller than the supracleithrum and is slightly boomerang-shaped; its dorsal ramus is slightly shorter than the ventral one. The anterior surface of the cleithrum is covered with a series of long, toothed ridges that form the serrated appendage. It is unclear whether a clavicle was present in front of the cleithrum as is observed in other taxa described here. Two postcleithra are present; the dorsal one is large and roughly rectangular, and the ventral one is almost square.

The pectoral fin consists of about 18 lepidotrichia. The first pectoral ray has a long base and is thicker than all other rays, but it is unclear whether the ray is distally segmented and branched. A propterygium fused to the proximal region of the first ray has not been observed. The remainder rays have long bases and are distally segmented and branched. A series of small, elongate fringing fulcra is associated with the leading margin of the fin.

The relatively small pelvic fins consist of about 11 rays, which are similar to those of the pectoral fins, except for the first ray. A series of small fringing fulcra is associated with the leading margin of the fin.

Unpaired Fins—The dorsal fin, unlike other fishes studied here, is positioned posteriorly, lying opposite to the anal fin. It has about three basal fulcra and 11 to 14 principal rays with long bases that are subtly segmented and branched distally. It is unknown whether only the first principal ray forms the leading margin of the fin or whether the second principal ray takes part. A series of fringing fulcra lies between the last basal fulcrum and leading margin of the fin.

The origin of the anal fin is slightly anterior to the dorsal fin. There are nine rays preserved in one specimen, but it is possible that more rays were present. Small fringing fulcra are associated with the leading margin of the fin.

The caudal endoskeleton has not been observed, because the squamation is *in situ* in most specimens, or the caudal region of the body is missing. The hemi-heterocercal caudal fin is moderately forked, with shorter middle principal rays in comparison with the leading margins of the dorsal and ventral lobes of the fin. The area covered by ganoid scales at the base of the caudal fin ends in two lobes that are slightly separated by a notch. The epaxial scaly lobe is longer than the ventral one.

The caudal fin consists of about seven epaxial basal fulcra, 20 or 21 principal rays, and three or four hypaxial basal fulcra. It is unclear whether a rudimentary epaxial ray was present or not, and the number of hypaxial procurent rays remains unknown. Fring-

ing fulcra are present in both leading margins of the fin. The dorsal and ventral leading margins of the fin are formed by at least two principal rays.

Scales—Most scales (Figs. 90C, 92A) are partially destroyed, but as far as the preservation shows, they are ganoid with the typical peg-and-socket articulation. Their surface is smooth, including the posterior margin. The body is covered by scales of different sizes and shapes. Most scales of the dorsal and ventral rows of the flank are rhombic, slightly rectangular, or even square-shaped. In contrast, the anterior main row of the flank (the lateral line row) is formed by rectangular scales that are twice as deep as broad. Then at the center of the body, the scales become progressively smaller posteriorly. In the caudal peduncle, the scales are more uniform in size, but they are very irregular in shape—some are rhombic and others are rectangular.

The scales are arranged in 34 or 35 oblique vertical rows (including the last scale bearing the lateral line canal). Another five to seven rows of scales extend into the epaxial lobe of the caudal fin. Seven to eight vertical rows are anterior to the pelvic fins, 17 to 18 anterior to the anal fin, whereas 19 or 20 are anterior to the dorsal fin. Four or five horizontal rows of scales lie above the horizontal row of lateral line scales, and eight below in the region anterior to the insertion of the pelvic fins.

Lateral Line—The lateral line is associated with the main horizontal row of body scales. It is unknown if there are additional lateral lines in the predorsal region, near the dorsal margin of the body, as in other species described here.

PHYLOGENETIC ANALYSIS AND RESULTS

Phylogenetic Analysis

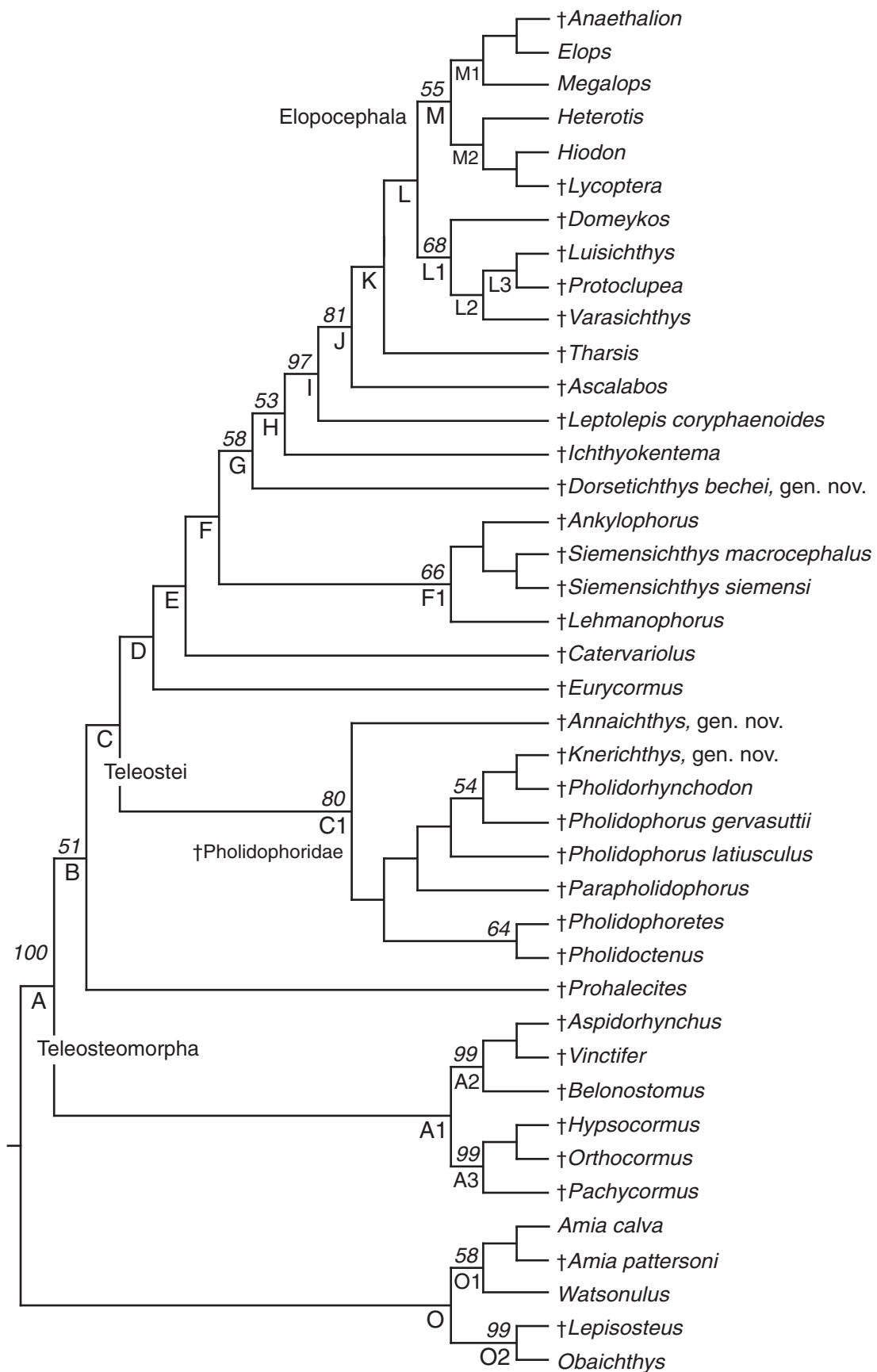
To assess the phylogenetic relationships of Triassic pholidophorids, I conducted a cladistic analysis of 41 advanced neopterygian taxa scored for 167 cranial, postcranial, and scale characters. The list of characters (Appendix 1) is modified from Arratia (2000) by the addition of 29 new characters, which reflects additional taxon sampling (e.g., the Triassic pholidophorids described here, the Middle Jurassic *†Catervariolus*, the Late Jurassic *†Lehmanophorus*). This increased taxonomic scope also required slight modification of character states, which is explained in Appendix 1. The character-taxon matrix is presented in Appendix 2. Polarization of characters is based on comparison with six outgroups, which include fossil and recent taxa.

Parsimony analysis was performed using PAUP 4.0 beta 10 (Swofford, 2000). The number of taxa necessitated a heuristic search, which used a random addition sequence with 500 replicates and the tree bisection and reconnection (TBR) branch-swapping algorithm. A bootstrap analysis was performed using 1000 to 20,000 replicates to assess for resulting clade support. The parsimony analysis recovered one equally parsimonious tree of 454 steps (retention index [RI] = 0.7769; consistency index [CI] = 0.4515; Fig. 95).

Results

The topology of the single most parsimonious tree is presented in Figure 95. Below I discuss the content and character support at each node. In some cases, identified below, the character optimization is ambiguous. In those cases, synapomorphy distribution presented assumes accelerated transformations (ACCTRAN).

Teleosteomorpha, Node A—This node, which includes total-group teleosts, is supported by a dozen characters, including two soft anatomical characters (Appendix 1: character states 164[1] and 165[1]) that cannot be scored in extinct forms but are nonetheless interpreted to have been present in members of this clade. Seven unambiguous, uniquely derived characters support this



node. An autophenotic lacking a small dermal component (char. 10[0]) is a reversal of the condition found in holosteans (see Grande, 2010). The presence of an unpaired vomer in adult individuals (char. 24[1]) is a teleostean morph synapomorphy, although many taxa cannot be scored (see Appendix 2). Other reversals supporting this node include the absence of a tube-like canal bearing the anterior arm of the antorbital bone (char. 40[0]) and the absence of two vertebral centra fused into occipital condyle in adults (char. 94[0]). The presence of a hypural articulating with a few caudal rays (char. 142[1]) is a teleostean morph synapomorphy that is further transformed in other members of the group (e.g., rays articulated with a hypural plate in pachycormiforms). Additionally, there are five homoplastic characters supporting this node. Two or three suborbital bones are positioned between the posterior margin of posterodorsal infraorbitals and the anterior margin of the opercular apparatus (char. 47[2]). Other homoplastic characters supporting this node include a complete ring formed of two sclerotic bones, which are oriented anterior and posterior to the eye (char. 50[1]), and one long, toothed, serrated appendage covering the whole medial surface of the cleithrum 1 (char. 108[1]). Ambiguous features include the presence of a compound first pectoral ray fused with basal fulcra (char. 112[1]) and a rudimentary or short neural spine of the preural centrum 1 (char. 123[1]), both of which are missing for the most basal teleostean morphs.

Node A1—This novel clade, which links †Aspidorhynchiformes and †Pachycormiformes, is supported by several homoplasies and three uniquely derived characters. In these taxa, the supramaxillary bone is positioned posterior or dorsoposterior to maxilla (char. 61[1]), whereas in other fishes the supramaxilla lies on the dorsal margin of the maxilla. The absence of a distinct coronoid process (char. 69[3]) on the lower jaw is another synapomorphy of aspidorhynchiforms and pachycormiforms. The absence of the postcleithrum (char. 107[2]) is predicted by the parsimony analysis as a synapomorphy supporting this node; however, the condition is unknown for pachycormiforms. Homoplastic features supporting this node include the presence of each vertebral centrum of the caudal region of adult individuals formed by a chordacentrum surrounded by the walls of the arcocentra (char. 96[2]), the presence of some preural neural arches modified as uroneurallike bones (char. 130[1]), and a homocercal (internally) caudal fin (char. 155[1]).

Node B—This clade unites †Prohalecites and all other teleosts. It is weakly supported by several homoplastic features that include parasphenoid without teeth (char. 25[1]); supraorbital and

otic canals with simple tubules (char. 34[1]); ascending process on premaxilla (char. 53[1]); mobile premaxilla (char. 55[1]); a moderately long maxilla reaching below the orbit (char. 56[1]); supramaxillary bone(s) absent (char. 59[1]); diplospondylous vertebrae in mid-caudal region (char. 100[1]); clavicle articulated to the anteroventral margin of the cleithrum (char. 109[1]); neural spine of preural centrum 2 shorter than neural spine of preural centrum 3 (char. 122[1]); and three rows of ganoid mid-flank scales that lie between the postcleithra and midpoint of the body length distinctively deeper than long (char. 162[1]).

Teleostei, Node C—This node includes the family †Pholidophoridae plus more advanced teleosts and is supported by nine characters. These fish share the presence of one suborbital bone positioned between the posterior margin of the posterodorsal infraorbitals and the anterior margin of the opercular apparatus (char. 47[1]), a feature that is homoplastic because the suborbital bone is lost in taxa at node J. Additionally, they have one or two additional or accessory suborbital bones positioned ventrolateral to postorbital region of skull roof (char. 48[1]), two supramaxillary bones (char. 59[2]), the quadrate-mandibular articulation positioned below the posterior half of orbit (62[1]), and the articular bone fused with both the angular and retroarticular (char. 63[1]). This latter character is homoplastic because further transformation occurs in some members of †Varasichthyidae (node L). Character state 63[2], the articular fused with just the angular, is unique to †Varasichthys within the data matrix, but this character state is more widespread, being shared with clupeocephalans (see Arratia, 2010). Node C is further supported by a ‘leptolepid’ notch in the ascending margin of the dentary (char. 65[1]), which is lost at node M. The coronoid process of the lower jaw is formed by the surangular (char. 69[1]), and further transformation of this character occurs at node H. The dorsal fin is positioned approximately in front of pelvic fins (char. 118[1]) and there is one large dorsal scute preceding the caudal fin (char. 153[1]).

†Pholidophoridae, Node C1—The monophyly of the family is supported by two uniquely derived and seven homoplastic features (Figs. 95, 96A). The tendency to have all skull roof bones fused into one bony plate (char. 1[1]) and the extrascapular with a large rollover bony layer at the anterior region of the bone (char. 17[1]) are both unique features of †Pholidophoridae. The skull roof with the orbital region slightly narrower than the postorbital region (char. 3[1]) is a feature that is further transformed within the family (Fig. 96A, node C1a). Other homoplastic features include a roughly rhomboidal rostral bone with well-developed,

← FIGURE 95. Hypothesis of phylogenetic relationships of basal teleosts based on 167 characters and using six taxa as outgroups. A single most parsimonious tree is recovered (tree length equals 454 steps). Consistency index (CI) = 0.4515; retention index (RI) = 0.7769. Numbers in italics next to nodes indicate bootstrap values (above 50%). See text and Appendix 1 for explanation of characters. Unique, derived characters are represented with an asterisk (*). Node O (outgroups). Node O1 (Halecomorpha): 11[1]. Node O2 (Lepisosteiformes): 4[1], 11[1], 31[1], 35[1]*, 47[3], 56[2], 57[3], 62[3], 69[1]*, 81[1]*, 84[1]*, 95[1]*, and 163[1]*. Node A (Teleostei or total group teleost): 10[0]*, 24[1]*, 40[0]*, 47[2], 50[1], 94[0]*, 108[1]*, 112[1], 123[1], 142[1], 164[1]*, and 165[1]*. Node A1: 49[1], 61[1], 69[3]*, 96[2], 107[2]*, 114[1], 130[1], 136[1], 137[1], 138[1], 155[1], and 160[1]. Node A2 (†Aspidorhynchiformes): 2[1], 14[1]*, 19[1]*, 30[2]*, 38[1], 54{1}*., 71[1]*, 87[1]*, 92[1], 93[1], 129[1], and 132[4]. Node A3 (†Pachycormiformes): 7[1]*, 12[1], 15[1]*, 23[1], 46[1]*, 49[2], 76[1], 110[1], 115[1]*, 118[1], 123[0], 127[2], 139[1]*, 143[2]*, 148[4], 150[1], and 153[1]. Node B: 25[1], 34[1], 53[1], 55[1], 56[1], 59[1], 100[1], 109[1], 122[1], 125[1], and 162[1]. Node C: 47[1], 48[1], 59[2], 63[1], 65[1], 69[1]*, 118[1], and 153[1]. Node C1 (†Pholidophoridae): 1[1]*, 3[1], 6[1], 17[1]*, 23[1], 70[1], 113[1], 116[1], and 122[0]. For internal nodes of †Pholidophoridae, see Figure 96. Node D (lineage of the crown group Teleostei): 78[1]*, 79[1], 102[1], 132[1], 141[1], 150[1], and 151[1]. Node E: 13[1]*, 18[1]*, 56[0], 80[1]*, 96[1]*, 103[1], 110[1], and 131[1]. Node F: 48[0], 66[1], 70[1], 82[1]*, 105[1], 108[0]*, 109[0], 127[1]*, and 129[1]*. Node G: 3[1], 25[0], 42[1], 64[1], 68[1]*, 108[3]*, 111[1]*, and 162[0]. Node H: 28[1], 30[1], 32[1], 56[1], 67[1]*, 69[2]*, 83[1]*, 100[0]*, 121[1], 124[1], 140[1]*, and 149[1]*. Node I: 50[2]*, 107[1]*, 114[1], 119[1], 120[1]*, 144[1], 148[3], 152[1]*, and 156[1]. Node J: 25[1], 29[1]*, 30[2]*, 47[0], 49[1], 70[0]*, 97[1]*, 98[1]*, and 99[1]*. Node K: 86[1], 134[1], 143[1], and 145[1]. Node L: 13[1], 33[1], 113[1], 116[1], 122[0], and 146[1]. Node L1 (†Varasichthyidae): 85[1]*, 106[1], 147[1], 148[2], 157[1], and 158[1]*. Node L2: 121[0], 122[1], 124[0], and 126[1]. Node L3: 25[0], 126[0], 132[3], 134[0], and 135[1]. Node M (Elopococephala or Teleococephala): 36[1], 63[0], 65[0], 86[0], 104[1], 117[2]*, 132[3]*, 136[1], 150[0], and 152[0]*. Node M1 (Elopomorpha): 25[0], 51[1]*, 56[0], 128[1]*, 133[1], 135[1], and 152[2]. Node M2 (Osteoglossomorpha): 31[0], 38[1], 41[1]*, 45[1], 49[2], 50[0], 59[1], 75[1]*, 91[1], 112[0], 118[0], 123[0], 129[2], and 148[0].

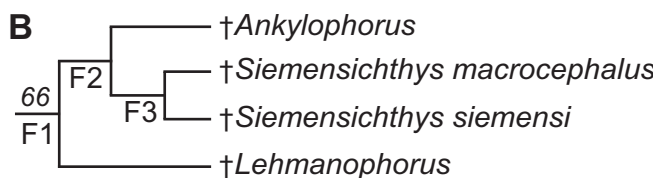
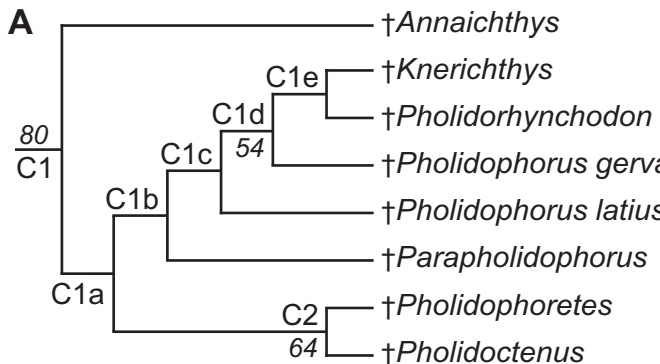


FIGURE 96. A. Hypothesis of phylogenetic intrarelationships of the family †Pholidophoridae, node C1, in Figure 95. Numbers in italics next to nodes indicate bootstrap values (above 50%). See text and Appendix 1 for explanation of characters. Unique, derived characters are represented with an asterisk (*). Node C1 (*†Pholidophoridae*): 1[1]*, 3[1], 6[1], 17[1]*, 23[1], 70[1], 113[1], 116[1], and 122[0]. Node C1a: 3[2], 42[1], 73[1], and 74[1]*. Node C1b: 5[1]. Node C1c: 21[1], 56[0], 62[0], and 89[1]. Node C1d: 37[1], 57[1], 76[1], 160[1], and 161[1]. Node C1e: 5[0], 9[1], 22[1], and 159[1]. Node C2: 21[1], 56[0], 62[0], and 89[1]. B. Hypothesis of phylogenetic relationships of the †Siemensichthys group, node F1 in Figure 95. Node F1: 9[1], 21[1], 22[1], 44[1], 45[1], 57[2], 96[2], 159[1], and 160[1]. Node F2: 5[1], 59[0], and 60[1]*. Node F3: 2[2], 49[1], 62[0], 70[0], 86[1], and 162[0].

distinct lateral processes (char. 6[1]), a contribution from the nasal bone to the orbital margin (char. 23[1]), a well-developed protruding lateral bony ridge extending along an elongate dentary and separating dental and splenial regions (char. 70[1]), the presence of pectoral (char. 113[1]) and pelvic (char. 116[1]) axillary processes, and the similarity in length of the neural spines of preural centra 2 and 3 (char. 122[0]).

Node C1a—This node distinguishes advanced pholidophorids from *†Annaichthys* (Figs. 95, 96A). It is supported by four synapomorphies: skull roof with very narrow orbital region versus a very broad postorbital region about four times broader or more (char. 3[2]); posterior region of infraorbital 3 extending below suborbital bone and reaching anterior margin of preopercle (char. 42[1]); maxilla heavily ornamented with characteristic longitudinal ridges of ganoine (char. 73[1]); and supramaxilla(e) heavily ornamented with characteristic longitudinal or concentric ridges of ganoine (char. 74[1]).

Node C1b—More advanced pholidophorids are distinguished from the *†Pholidoctenus* + *†Pholidophoretes* clade (Fig. 96A, node C2) by one synapomorphy: parietal bones [= frontals] acutely sharp anteriorly and sutured with rostral bone by a narrow contact (Char. 5[1]).

Node C1c—This clade unites *†Pholidophorus latiusculus*, *†Pholidophorus gervasutii*, and the *†Knerichthys* + *†Pholidorhynchodon* clade (Fig. 96A). Four synapomorphies support this node: nasal bone with a large foramen forming the wall of the posterior nostril (char. 21[1]); an elongate maxilla extending behind the orbit (char. 56[0]); quadrate-mandibular articulation posterior to orbit (char. 62[0]); and a notch at the posteroventral margin of preopercle (char. 89[1]).

C1d—This node includes *†Pholidophorus gervasutii* and the *†Knerichthys* + *†Pholidorhynchodon* clade, implying that the genus *†Pholidophorus* is paraphyletic (see ‘Taxonomic Comments,’ below). Features supporting this hypothesis are the presence of a large foramen in the nasal bone (char. 21[1]), which is optimized to have appeared at the basal node of *†Pholidophoridae*, reversed, and reappeared again at node C1d. Two reversals sup-

port this node: the presence of an elongate maxilla reaching behind the orbit [(char. 56[0]) and the quadrate-mandibular articulation positioned posterior to orbit (char. 62[0]). A notch at the posteroventral margin of preopercle (char. 89 [1]) is another synapomorphy supporting this node.

Node C1e—The *†Knerichthys* and *†Pholidorhynchodon* (Fig. 96) node is supported by four synapomorphies: toothed lateral dermethylmoids joined to premaxillaries laterally (char. 9[1]); lateral margin of nasal bone joining medial margin of an elongate antorbital (char. 22[1]); ganoid scales with serrated posterior margin (char. 159[1]); and parietal bones [= frontals] acutely sharp anteriorly and sutured with rostral by a narrow contact (reversal, char. 5[0]). Ganoid scales with serrated posterior margin is interpreted by the parsimony analysis as a synapomorphy due to the fact that *†Knerichthys*, gen. nov., has serrated scales; however, *†Pholidorhynchodon* has scales with smooth posterior margins.

Node C2—This clade unites *†Pholidoctenus* and *†Pholidophoretes*. This node is supported by four synapomorphies, two of which are interpreted as reversals by the parsimony analysis: roughly rhomboidal rostral bone with well-developed, distinct lateral processes (reversal, char. 6[0]); nasal bones joined in midline (reversal, char. 20[0]); posterior margin of maxilla notched or concave (char. 57[1]); and crescent-shaped preopercle (char. 90[1]).

Node D—*†Eurycormus* and more advanced teleosts (apomorphy-based teleosts to the lineage of crown group) are united by the following synapomorphies: an elongated posterodorsal or posteroventral process of quadrate (depending on the angle of the quadrate) (char. 78[1]); symplectic does not articulate with lower jaw (char. 79[1]); long epineural process of neural arch in adult individuals (char. 102[1]); seven or more neural arches modified as uroneurals (char. 132[1]); diastema between hypurals 2 and 3 (char. 141[1]); bases of the innermost principal caudal rays of dorsal lobe of caudal fin have dorsal processes (char. 150[1]); and all or some principal caudal rays with Z-like segmentation (char. 151[1]). Most of these features are still

unknown in the †Siemensichthys group (e.g., †*Ankylophorus* and †*Lehmanophorus*; see node F1).

Node E—†*Catervariolus* and more advanced teleosts are characterized by eight synapomorphies. A supraoccipital bone is present (char. 13[1]) in †*Catervariolus* (Taverne, 2011b) and more advanced teleosts, but the condition is still unknown in some members of the †Siemensichthys group (Fig. 96B, node F1). Sutures between all cartilage bones in the braincase retained throughout life, rather than being lost ontogenetically (char. 18[1]), is a unique feature of this clade. An elongate maxilla reaching behind the orbit (char. 56[0]) is a reversal at this node from the condition in †*Prohalecites* and more advanced teleosts (node B). A symplectic placed medial to posterior margin of quadrate (char. 80[1]) is another unique feature acquired at this node. Each vertebral centrum of the caudal region of adult individuals formed by a chordacentrum surrounded by an autocentrum (char. 96[1]) characterizes this clade, with further transformations in more advanced teleosts (e.g., Arratia, 1999; Arratia et al., 2001). Epipleural intermuscular bones are interpreted to be present (char. 103[1]) in this group, but epipleural data are missing from members of the †Siemensichthys group. Four pectoral proximal radials (char. 110[1]) and only ural neural arches modified as uroneurals (char. 131[1]) are features diagnosing this clade but unknown in some members.

Node F—The †Siemensichthys group (Fig. 96B, node F1) and more advanced teleosts are united by nine synapomorphies. One or two accessory suborbital bones positioned ventrolateral to postorbital region of skull roof absent (char. 48[0]) is interpreted as a reversal at this phylogenetic level. Coronoid bone(s) in the lower jaw are absent (char. 66[1]) in most members of this group, with a reversal in †*Ichthyokentema* (node H). The presence of a well-developed lateral bony ridge extending along an elongate dentary and separating dental and splenial regions (char. 70[1]) is present in this clade and also †Pholidophoridae (node C1). Two ossified hypohyals are present (char. 82[1]). The posttemporal bone has a small body and distinct, strong, sharp dorsal process to articulate with the cranium (char. 105[1]). Other synapomorphies at node F include anterior and posterior toothed elements present on the ventral arm of cleithrum (char. 108[0]), loss of the articulation between the clavicle and anteroventral margin of cleithrum (char. 109[0]), presence of two ural centra in adults (char. 127[1]), and presence three or four epurals (char. 129[1]).

†Siemensichthys Group, Node F1—The monophyly of this clade is supported by the following characters: toothed lateral dermethylmoids joined to premaxillaries laterally (char. 9[1]); nasal bone with a large foramen forming the wall of the posterior nostril (char. 21[1]); lateral margin of nasal bone joining medial margin of an elongate antorbital (char. 22[1]); fourth infraorbital an expanded, broad bone (char. 44[1]); posterior margin of maxilla acute (char. 57[2]); each vertebral centrum of the caudal region of adult individuals formed by chordacentrum surrounded by arccentra (char. 96[2]); and ganoid scales with ornamented surface (char. 160[1]).

Node G—The node joining †*Dorsetichthys bechei*, gen. nov., plus more advanced teleosts is supported by the following synapomorphies: skull roof with orbital region slightly narrower than the postorbital region (char. 3[1]); parasphenoid with small teeth (char. 25[0]; reversal from node B); well-developed postarticular process of the lower jaw (char. 64[1]); prearticular bone absent (char. 68[1]); serrated appendages absent (char. 108[3]); pectoral propterygium fused with first ray (char. 111[1]); and the three rows of mid-flank ganoid scales between the postcleithra and mid-length of the body not distinctively deeper than long (char. 162[0]). The posterior region of infraorbital 3 contacting the anterior margin of the preopercle (char. 42[1]) is homoplastic because it is present in †*Dorsetichthys bechei*, gen. nov., and

some Triassic pholidophorids (node C1). This result confirms that †*Dorsetichthys bechei*, gen. nov., is not a pholidophorid.

Node H—†*Ichthyokentema* and more advanced teleosts are united by the following 12 synapomorphies: ossified aortic canal absent (char. 28[1]); spiracular canal greatly reduced (char. 30[1]); foramen for glossopharyngeal nerve positioned in exoccipital (char. 32[1]); elongate maxilla extending below the orbit (char. 56[1]); surangular bone in lower jaw absent (char. 67[1]); coronoid process of the lower jaw formed by the dentary and angular bones (char. 69[2]); urohyal formed as an unpaired tendon bone of the sternohyoideus muscle (char. 83[1]); diplospondyl in caudal vertebral region absent (reversal of conditon; char. 100[0]); preural vertebrae (excluding preural centrum 1) of adult individuals with hemal arches laterally fused to their respective autocentra (char. 121[1]); parhypural in adults laterally fused with its centrum (char. 124[1]); bases of hypurals 1 and 2 joined by cartilage (and/or bone in some later growth stages char. 140[1]); and first and last principal caudal rays forming the leading margins of the caudal fin (char. 149[1]).

Node I—The †*Leptolepis coryphaenoides* plus more advanced teleosts node is supported by 10 synapomorphies: presence of an incomplete ring of two sclerotic bones oriented anterior and posterior to orbit (char. 50[2]); three or more postcleithra (char. 107[1]); fringing fulcra associated with the leading margin of the pectoral fin absent (char. 114[1]); fringing fulcra on leading margin of dorsal fin absent (char. 119[1]); fringing fulcra on leading margin of anal fin absent (char. 120[1]); hypaxial basal fulcra in the caudal fin absent (char. 144[1]); 19 principal caudal rays (char. 148[3]); two tendon-bone ‘urodernals’ (char. 152[1]); caudal fin homocercal (internally; char. 155[1]); and elasmoid scales of cycloid type (char. 156[2]).

Node J—†*Ascalabos* plus more advanced teleosts are supported by nine synapomorphies: toothless parasphenoid (char. 25[1]); canals for occipital arteries in basioccipital bone absent (char. 29[1]); spiracular canal absent (char. 30[2]); no suborbital bone (char. 47[0]); one supraorbital bone (char. 49[1]); a well-developed protruding lateral bony ridge extending along an elongate dentary and separating dental and splenial regions absent (char. 70[0]); mid-caudal vertebral autocentra thick and sculptured (char. 97[1]); walls of mid-caudal centra with cavities for adipose tissue (char. 98[1]); and notochord strongly constricted by the walls of the centra (char. 99[1]).

Node K—†*Tharsis dubius* and more advanced teleosts are united by four synapomorphies: preopercular sensory canal with long tubules opening on the ventral and posteroventral borders of the preopercle (char. 86[1]); uroneurals positioned at different angles (char. 134[1]); epaxial caudal basal fulcra absent (char. 143[1]); and proximity of epaxial basal fulcra or epaxial procurerent rays to neural spines, epurals, and posterior uroneurals (char. 145[1]).

Node L—Family †Varasichthyidae and more advanced teleosts are diagnosed by six synapomorphies: anterior myodome absent (char. 31[1]); foramen for vagus nerve in posterolateral face of exoccipital alone (char. 33[1]); pectoral axillary process present (char. 113[1]); pelvic axillary process present (char. 116[1]); neural spine of preural centrum 2 as long as neural spine of preural centrum 3 (char. 122[0]); and epaxial procurerent rays present (char. 146[1]). This last feature is homoplastic because epaxial procurerent rays are present in some aspidorhynchiforms.

Family †Varasichthyidae, Node L1—This node is supported by the following synapomorphies: posteroventral region of preopercle broadly expanded in a distinct pattern (char. 85[1]; see Arratia 1994, 1997); supracleithrum with main lateral line emerging at its posteroventral margin (char. 106[1]); cycloid scales with circuli crossed by transverse lines in the middle field

(char. 157[1]); and cycloid scale with crenulate posterior margin (char. 158[1]).

Elopocephala, Node M—This clade includes elopomorphs and osteoglossomorphs and is supported by 10 synapomorphies: middle pit-line groove crossing the pterotic absent (char. 36[1]); articular bone not fused with angular or retroarticular bones (char. 63[0]); ‘leptolepid’ notch absent (char. 65[0]); preopercular sensory canal with long tubules opening on the ventral and posteroventral borders of the preopercle absent (char. 86[0]); many epipleural intermuscular bones in the anterior caudal region (char. 104[1]); pelvic axillary process formed by modified scales (char. 117[2]); four or five ural neural arches modified as uroneurals (char. 132[3]); hypural 8 absent in adult individuals (char. 136[1]); dorsal processes of the bases of the innermost principal caudal rays of dorsal lobe of the caudal fin absent (char. 150[0]); and tendon-bone ‘urodermals’ absent (char. 152[0]).

Taxonomic Comments

The results of the phylogenetic analysis lead me to propose novel interrelationships amongst teleosts and their nearest relatives and consequently a novel hypothesis for the evolution of characters associated with the origin of this group. Below I discuss this new arrangement of taxa and its taxonomic implications.

Teleosteomorpha and Teleostei—The taxon Teleosteomorpha was erected by Arratia (2000:fig. 3) to identify taxa more closely related to crown-group teleosts than to their closest extant relatives (e.g., *Amia*, *Lepisosteus*).

The clade Teleosteomorpha (Fig. 95, node A) includes †Pachycormiformes, †Aspidorhynchiformes, and †Prohalecites. Pachycormiforms and aspidorhynchiforms are proposed as sister taxa. Although the oldest members of these clades are known from the Jurassic, †Prohalecites (Ladinian-Carnian boundary, 237 Ma; Tintori, 1999) is the oldest known teleosteomorph. This implies a ghost lineage preceding the appearance of the clade uniting pachycormiforms and aspidorhynchiforms.

The large clade Teleostei (Fig. 95, node C) includes †Pholidophoridae as the sister taxon to the lineage leading to the crown group (Fig. 95, node I). This clade is supported by 10 characters. The results presented here differ from previous phylogenetic hypotheses, which place †*Pholidophorus latiusculus* and †*Dorsetichthys bechei*, gen. nov., near the base of Teleostei (e.g., Arratia, 2000). The present hypothesis nests †*Ph. latiusculus* within †Pholidophoridae and †*Dorsetichthys bechei* in the lineage leading to crown teleosts, respectively. †*Annaichthys* is the most basal member of †Pholidophoridae (Fig. 95, node C; Fig. 96), and †*Eurycormus* (Fig. 95, node D) is the basal-most non-pholidophorid teleostean. The late Jurassic †*Tharsis*, which was traditionally interpreted in a more basal position than the Late Jurassic †*Ascalabos*, now appears more advanced (e.g., Arratia, 1997, 1999; Arratia and Tischlinger, 2011).

†Pholidophoriformes—This analysis includes 16 species previously included within pholidophoriforms (e.g., Lehman, 1966; Nybelin, 1968; Patterson, 1975, 1977a; Zambelli, 1986; Arratia, 2000; Arratia and Schultze, 2007; Taverne, 2011a, 2011b). The results confirm previous hypotheses that the group is not monophyletic. These 16 ‘pholidophoriform’ taxa, starting with the monophyletic family †Pholidophoridae (Fig. 95, node C), are teleosts, rather than basal teleosteomorphs.

The type species of the family †Pholidophoridae and the order †Pholidophoriformes is †*Pholidophorus latiusculus*. In the context of the phylogenetic relationships proposed here, wherein traditional pholidophoriform taxa are resolved as a non-monophyletic group, I propose to restrict the usage of the name Pholidophoriformes to include only the family †Pholidophoridae. The diagnostic characters supporting the †Pholidophoridae,

new usage, also stand for the †Pholidophoriformes, new usage.

†Pholidophoridae, new usage—The results of the phylogenetic analysis show that the Triassic pholidophorids comprise a monophyletic group, the family †Pholidophoridae (Fig. 95, node C; Fig. 96A). Other Jurassic ‘pholidophoriforms’ included in the analysis and that traditionally have been interpreted as pholidophorids (e.g., †*Pholidophorus bechei*) are resolved outside the clade formed by the Triassic forms (Fig. 95, node G). †*Annaichthys*, gen. nov., is the most basal taxon of the †Pholidophoridae.

†*Pholidophorus latiusculus* and †*Ph. gervasutii*—This analysis resolves the genus †*Pholidophorus* as not monophyletic (Figs. 95, 96). However, there is a large gap in missing data between the two species, with †*Pholidophorus latiusculus* (type species) much more incompletely known than is †*Ph. gervasutii*. Considering this, I prefer to take a conservative approach and keep both species under the same genus until †*Ph. latiusculus* is better known.

†*Pholidophorus bechei*—This species is not resolved as a member of †Pholidophoridae (Fig. 95, nodes C and G), as had been previously hypothesized (e.g., Woodward, 1895; Nybelin, 1968; Arratia, 1999). Instead, it is more closely related to crown teleosts than are pholidophorids. This taxon is interpreted here as a new genus, supported by several autapomorphies. I will revise its description in detail and discuss its taxonomic reassignment in the future, second part of this study of ‘pholidophoriforms.’

†DORSETICHTHTS gen. nov.

Pholidophorus bechei: Agassiz, 1837:2, pl. 39, figs. 1–4.

Pholidophorus bechei: Agassiz, 1844:272.

Pholidophorus bechei: Woodward, 1895:450, pl. 12, figs. 1, 2.

Pholidophorus bechei: Nybelin, 1966:357–367, pls. 1–3.

Diagnosis—Elongated teleosts of about 200 mm total length. Bones and scales covered with a thin layer of ganoine. Parietal bones [= frontals] acutely sharp anteriorly and sutured with rostral by a narrow contact. Braincase elements fuse so that there are no sutures. Supraorbital and otic canals with branched tubules. Maxilla heavily ornamented with longitudinal ridges of ganoine. Preopercle expanded anteroventrally and with a deeply notched posterior margin. Preopercular sensory canal with about 20 long tubules opening on the ventral and posteroventral borders of the preopercle. Chordacentral type of vertebrae. Diplospondyly in the caudal region. Epipleural intermuscular bones absent. Posttemporal broad, with no distinct dorsal process to articulate with cranium. Last four or five posterior ural neural arches modified as uroneurals. Tendon-bone ‘urodermals’ absent. Hemi-heterocercal caudal fin. Ganoid scales of lepisosteoid type, with smooth surface and posterior margin.

Etymology—The genus name *Dorsetichthys* refers to Dorset, England, which is an important region for fossil fish. The Greek suffix *ichthys* means fish.

Content—†*Dorsetichthys bechei*, the only known species.

Geographical Distribution and Age—Lyme Regis, Dorset, England; early Early Jurassic.

†Siemensichthys Group—The phylogenetic hypothesis proposed by Arratia (2000; Fig. 2B) included a clade of three Late Jurassic genera (†*Eurycormus*, †*Siemensichthys*, †*Ankylophorus*) that were preliminarily identified as the †Siemensichthys group. In the present study, †*Lemanophorus* from the Kimmeridgian of Cerin, France, was demonstrated to also be a member of that monophyletic group (Fig. 95, node F; Fig. 96B), but the Late Jurassic genus †*Eurycormus* was removed from the clade and into a more basal position than members of the †Siemensichthys group (see Fig. 95, node D). As in previous analyses, the †Siemensichthys group appeared as the sister group of †*Pholidophorus bechei*.

(now †*Dorsetichthys*) plus more advanced teleosts (see Fig. 2, node A; Fig. 95, nodes F, G). Members of the †*Siemensichthys* group are teleosts closely related to the crown group, not stem teleosts.

Recently, Taverne (2011a) proposed the inclusion of the †*Siemensichthys* group within the family †*Ankylophoridae* Gaudant. According to Taverne (2011a), the family †*Ankylophoridae* is included within ‘Pholidophoriformes’ (see Fig. 2C) and contains the following taxa: †*Ankylophorus*, †*Eurycornus*, †*Lemanophorus*, †‘*Pholidophorus*’ *germanicus*, †*Pholidoristion*, †*Siemensichthys*, †*Steurbautichthys*, and the Triassic pholidophorids †*Pholidorhynchodon* and †*Eopholidophorus*. One character supports the monophyly of †*Ankylophoridae* according to Taverne (2011a): posterior part of the laterodermethmoid enlarged and covering a large part of the nasal fossa, and the anterior part of the laterodermethmoid narrow, tongue-shaped, and bearing small teeth (my translation from the French text). Unfortunately, however, there is very little information concerning the structure of the laterodermethmoid in these taxa, with the exceptions of †*Siemensichthys macrocephalus* (Patterson, 1975; Arratia, 2000) and †*Pholidorhynchodon* (see description above). In the present analysis, †*Pholidorhynchodon* is nested within the family †*Pholidophoridae* rather than in the †*Siemensichthys* group (see Figs. 96, 95). To further test Taverne’s hypothesis, I scored †*Steurbautichthys*, based on Taverne’s (2011a) description, and added it to the matrix in Appendix 2. †*Steurbautichthys* does not cluster with the †*Siemensichthys* group; rather, it appeared in an unresolved position with †*Catervariolus* and more advanced teleosts. Consequently, I suggest revisions of the taxa listed as members of the †*Ankylophoridae* by Taverne (2011a).

†Eurycornus—According to the new phylogenetic hypothesis presented in Figure 95, †*Eurycornus* is the outgroup to †*Catervariolus*, the †*Siemensichthys* group, and more advanced teleosts. It is not a member of the †*Siemensichthys* group as previously hypothesized (e.g., Arratia, 2000; Taverne, 2011a), and it is not a ‘pholidophoriform.’

†Ascalabos and †Tharsis—One interesting result of the phylogenetic analysis is that the Late Jurassic †*Tharsis* appears in a more advanced phylogenetic position than the Late Jurassic †*Ascalabos*, contrary to previous hypotheses (e.g., Patterson and Rosen, 1977; Arratia, 1997, 1999). The phylogenetic position of †*Ascalabos* is strongly supported by several synapomorphies (Fig. 95, node J), four of which are uniquely derived. In contrast, the phylogenetic position of †*Tharsis* is weakly supported by four homoplastic characters. Currently, both genera are under revision by the author.

One major aspect of the phylogenetic analysis is the increased homoplasy in comparison with previous hypotheses (e.g., Arratia, 1997, 1999, 2000, etc.). The addition of the Triassic pholidophorids and of some Jurassic fishes previously interpreted as ‘pholidophoriforms’ turns many characters that were previously interpreted as uniquely derived for certain clades of teleosts into homoplasies. It is also remarkable to observe the increase of reversals in more advanced phylogenetic levels in Figure 95. For instance, there are five reversals among 10 synapomorphies supporting node M (Elopocephala).

ANALYSIS OF SOME MORPHOLOGICAL CHARACTERS USED IN DIAGNOSES AND PHYLOGENETIC ANALYSIS

Cranial Roof Bones—In general, the cranial bones in teleosts are arranged in a constant pattern, which is characterized by a cranial roof formed by the mesethmoid, nasals, parietals, autosphenotics, postparietals, pterotics, epiotics, supraoccipital, and extrascapulars. These elements are commonly independent ossifications in teleosts, but different patterns involving fusions or losses of elements may be found in a few groups. For instance, ichthyodectiforms fuse the postparietal bones (e.g.,

Bardack, 1965; Patterson and Rosen, 1977; Arratia, 1999), and catfishes fuse the postparietals and supraoccipital (e.g., Arratia and Gayet, 1995).

The skull roof of halecomorphs, including the amiiforms, comprises independent ossifications, although fusions between some skull bones have been described (e.g., between left and right parietals, left and right postparietals, or postparietals and dermopterotic; Grande and Bemis, 1998:figs. 12D–F, 13D–F). Among teleosteomorphs, fusions involving certain skull roof bones constitute unique features of pachycormiforms, such as the rostrodermethmoid-premaxilla (Lehman, 1949; Wenz, 1968) or the rostrodermethmoid (Patterson, 1975; Lambers, 1992) and of aspidorhynchiforms, such as the rostrodermethmoid-premaxilla and the postparietals fused with dermopterotics (Maisey, 1991; Brito, 1997). The bones of the skull roof are said to be fused in “different ways” in the halecostome incertae sedis †*Ligulella*; however, the skull roof was restored as separate elements by Taverne (2011c:215, figs. 6, 7).

The skull roof (Fig. 97A) of pholidophorids tends to have most bones fused into one solid plate, comprising the parietals, postparietals, autosphenotics, and dermopterotics. The fused skull roof plate never includes the rostral bone nor premaxilla as it does in pachycormiforms and aspidorhynchiforms (e.g., Mainwaring, 1978; Lambers, 1992; Brito, 1997). According to the results of the phylogenetic analysis, this fusion pattern is a unique feature of the family †*Pholidophoridae*. The skull roof of other ‘pholidophoriforms’ have independent bones forming the skull roof, such as †*Catervariolus hornemani* (Taverne, 2011b), †*Dorsetichthys bechei*, gen. nov. (Fig. 97B; Nybelin, 1966; Patterson, 1975; herein), †*Eurycornus speciosus* (pers. observ.), †*Siemensichthys macrocephalus* (Fig. 98C; Patterson, 1975; Arratia, 2000; herein), and †*Ichthyokentema purbeckensis* (Griffith and Patterson, 1963), as well as all other teleosts (Fig. 98D).

Skull Roof Shape—There is not much difference in the breadth of the skull roof between the orbital and postorbital regions in halecomorphs and teleosteomorphs; however, basal teleosts have the postorbital region slightly broader than the orbital region (e.g., Fig. 97D; †*Leptolepis coryphaenoides*). In contrast, members of the †*Pholidophoridae* have a sharp distinction between both regions, with a very narrow orbital region and a markedly broad, short rectangular postorbital region (Fig. 97A). An intermediate breadth of the postorbital relative to the preorbital region is found in †*Dorsetichthys bechei*, gen. nov., and members of the †*Siemensichthys* group (Figs. 97B, C). The shape of the skull roof plate is unique to the family †*Pholidophoridae*.

Rostral Bone—The ethmoid or snout region has a complex origin in teleosts. This region has been scarcely investigated in most recent teleosts, and there is more information available for some fossils, such as the Early Jurassic †*Dorsetichthys bechei*, gen. nov., several Jurassic ‘pholidophoriforms,’ a few Early Jurassic leptolepids (Patterson, 1975), and the Late Jurassic ichthyodectiform †*Allothrissops* (Patterson and Rosen, 1977). The ethmoid region of †*Dorsetichthys bechei*, gen. nov., comprises a well-developed rostral bone bearing the ethmoidal commissure, and this bone is not fused with underlying elements of the ethmovomerine region. In contrast, the rostral bone of †*Leptolepis coryphaenoides* is a tiny element bearing a short section of the ethmoidal commissure, and it is weakly articulated with the anterior tips of the parietal bones. Members of the †*Pholidophoridae* share large, roughly rhomboidal rostral (e.g., Figs. 14, 32, 49, 62, 98A–D) that carries the ethmoidal commissure through its middle region; the rostral may articulate directly with the anterior tip of the skull roof plate (e.g., †*Pholidophorus gervasutti* and †*Parapholidophorus*), or it may articulate with the nasals (e.g., †*Pholidoctenus* and †*Pholidophoretes*), so that a direct contact

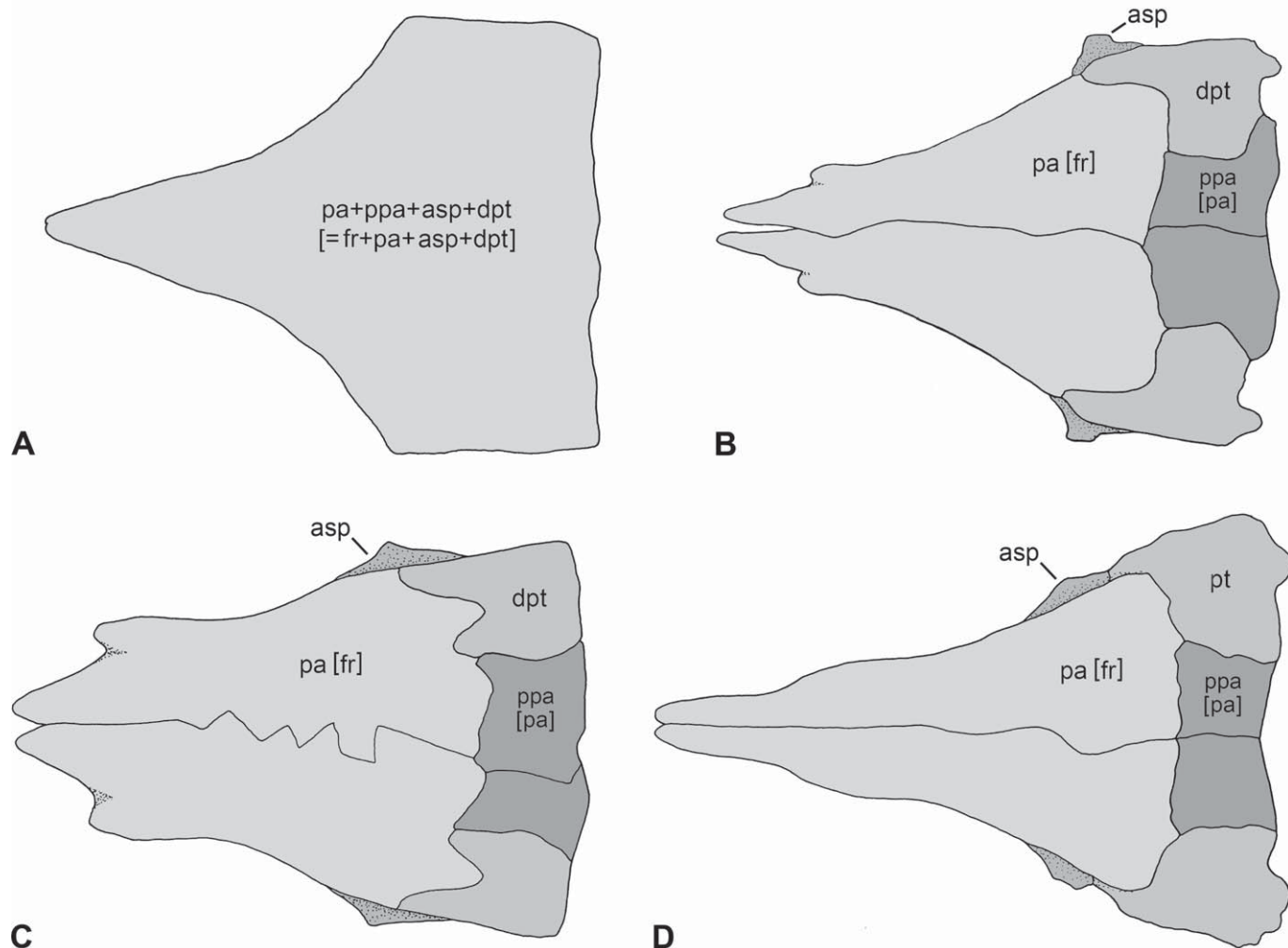


FIGURE 97. Patterns of skull roof plates in teleosts. **A**, pholidophorid pattern. **B**, *†Dorsetichthys bechei*, gen. nov. **C**, *†Siemensichthys macrocephalus*. **D**, *†Leptolepis coryphaenoides*. Not to scale.

with the skull roof plate is lost. Members of the *†Siemensichthys* group have a massive rostral that is almost rounded anteriorly, and the ethmoidal commissure runs closer to the anterior margin of the bone than to the middle region.

The rostral bone is not included in the oral margin of the upper jaw and lacks teeth, and it is dorsal to the premaxillae in most pholidophorids studied here, with the exception of *†Pholidorhynchodon*, in which the rostral is in the oral margin and bears conical teeth on its anterior margin (e.g., Fig. 49). The rostral teeth are slightly anteroventrally oriented, giving a special aspect to the upper jaw. According to the present evidence, *†Pholidorhynchodon* seems to be the only pholidophorid with a toothed rostral and toothed lateral dermethylmoids; the lateral dermethylmoids articulate with the rostral (see Figs. 49, 98D), and they displace the premaxilla posterolaterally relative to other. Dermethylmoids are also found in *†Eurycormus* (Wenz, 1968; Arratia, 2000; Arratia and Schultze, 2007) and *†Siemensichthys macrocephalus* (Patterson, 1975; Arratia, 2000), where they are positioned below the rostral bone (e.g., Patterson, 1975:fig. 145; Arratia, 2001:fig. 6), in a different position to that of *†Pholidorhynchodon*. The presence of a toothed

dermethylmoid is interpreted here as independently acquired in *†Pholidorhynchodon* and members of the *†Siemensichthys* group.

Dermethylmoid or Rostrodermethylmoid—The rostral bone is an independent bone in ‘pholidophoriforms,’ as well as in more advanced teleosts studied here. In contrast, the large rostrodermethylmoid of pachycormiforms, which projects anteriorly to the dentated ventral border of the premaxilla, is interpreted as the result of fusion between a large medial rostral and the underlying dermethylmoids (e.g., Patterson, 1975; Mainwaring, 1978; Lambers, 1992). This morphology is currently interpreted as a synapomorphy of *†Pachycormiformes* (e.g., Mainwaring, 1978; Lambers, 1992; Friedman et al., 2010). A large, long element forming the snout region in aspidorhynchiforms is currently interpreted as the result of fusion between the tube-like premaxillae and rostral region (Brito, 1992, 1997). This complex element is interpreted as a synapomorphy of *†Aspidorhynchiformes* (Brito, 1997). Dermethylmoids are also found in *†Eurycormus* and *†Siemensichthys* (Wenz, 1968; Patterson, 1975; Arratia, 2000; Arratia and Schultze, 2007). The presence of a toothed dermethylmoid is interpreted here as independently acquired in *†Pholidorhynchodon*, *†Eurycormus*, and members of the *†Siemensichthys* group.

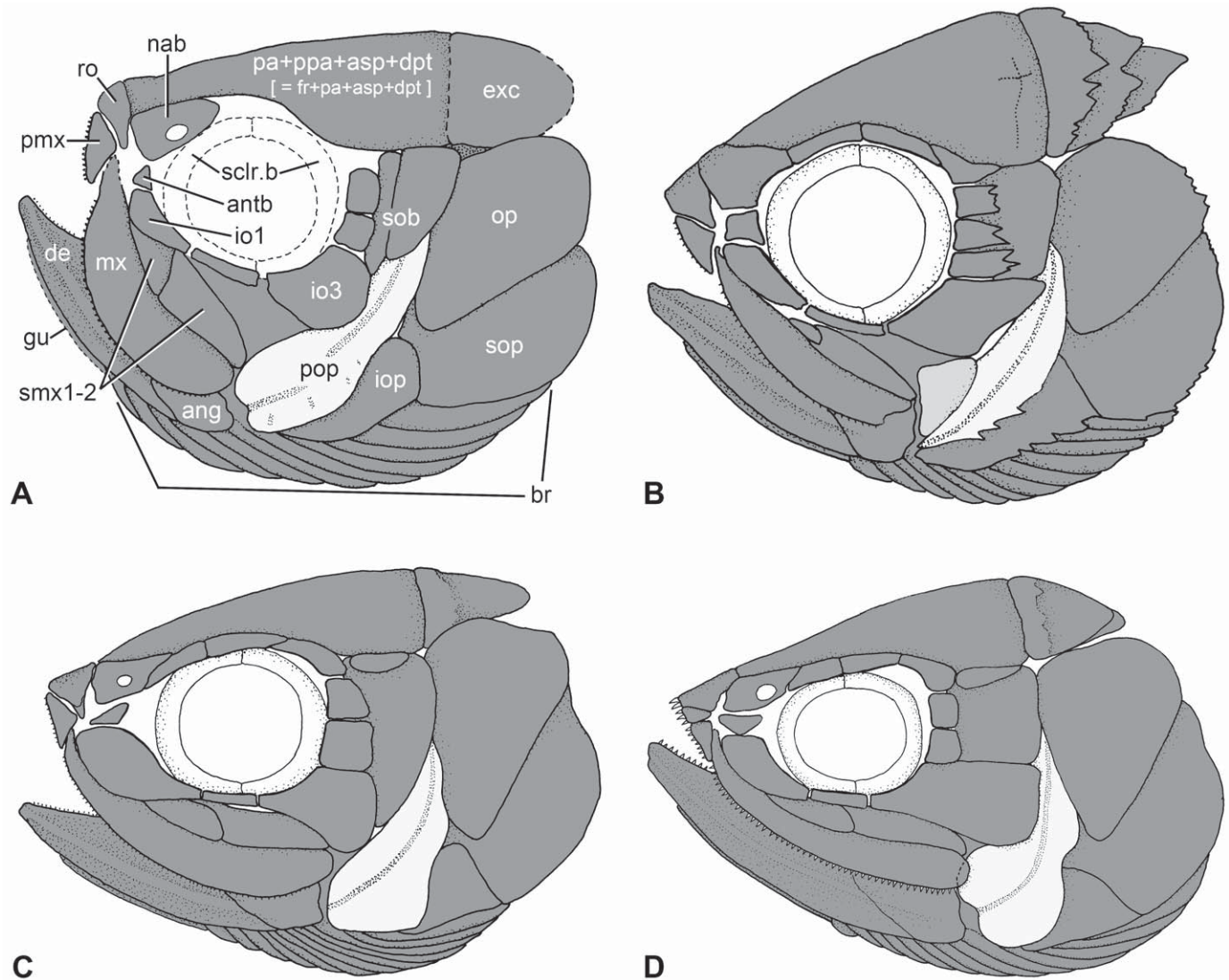


FIGURE 98. Patterns of cranial bones of some pholidophorids in left lateral view. **A**, *†Annaichthys pontegurinensis*, gen. et sp. nov. **B**, *†Pholidoctenus serianus*. **C**, *†Parapholidophorus nybelini*. **D**, *†Pholidorhynchodon malzannii*. Not to scale.

Nasal Bones—The snout region presents at least two different patterns among members of the *†Pholidophoridae*. The nasal bones in most teleosts (*†Leptolepis coryphaenoides* plus more advanced teleosts; Fig. 95, node I) are moderately small, elongate, and bilaterally positioned to the anterolateral margin of the parietal bones, but in *†Pholidophoridae* they are large elements that are separated from each other in basal forms (e.g., *†Annaichthys*; see Fig. 32) and joined in the midline in more advanced forms (e.g., *†Pholidophoretes* and *†Pholidoctenus*; see Figs. 78B, 79, 92B). Nasal bones incompletely joined at the midline is a feature found in fossil parasemionotiforms, but nasal bones completely joined at the midline is a feature found in fossil and recent amiiforms (e.g., Patterson, 1975:fig. 137; Olsen, 1984:fig. 2; Grande and Bemis, 1998:figs. 12, 13) and in *†Prohalecites* among teleosteomorphs (Fig. 95, node B). Given the distribution of this character state, nasal bones joined at the midline are interpreted here as independently acquired in some halecomorphs, some teleosteomorphs, and some pholidophorids.

The nasals of pholidophorids are characteristically large, rectangular or roughly triangular bones that are larger than those in other teleosts, including *†Dorsetichthys bechei*, gen. nov. Additionally, the nasal is characterized by the presence of the posterior nostril as a large, round foramen (e.g., *†Annaichthys*, *†Pholidophorus gervasutti*, *†Zambelichthys*, and *†Pholidophoretes*; Figs. 14, 29, 32, 92A, 98A) or a deep notch on its lateral side (e.g., *†Parapholidophorus* and *†Pholidoctenus*; Figs. 61, 79, 98B, C). The nasals of *†Dorsetichthys bechei*, gen. nov., have a small notch near the lateral wall. The nasals of *†Leptolepis coryphaenoides* and more advanced teleosts (Fig. 95, node I) are elongate bones, often tube-like, and positioned on the anterolateral margin of the parietal bones.

The lateral wall of the nasal bone forming part of the circumorbital rim (Fig. 98A–D) is an uncommon feature that is interpreted here as a unique character of *†Pholidophoridae* among teleosts. A similar condition is also found in the non-teleost *†Pachycormus* (Wenz, 1968; pers. observ.) among the fishes

studied here. It is unclear whether this feature could be an autapomorphy of *†Pachycormus* or more generally present within pachycormiforms.

Cephalic Sensory Canals—The generalized condition among teleosts is to have the components of the sensory canals interconnected (Nelson, 1972) or mostly interconnected. This is the condition in all teleosts studied here as far I can observe them. The branching or tubule system in teleosts may be simple, branched, widened, or reduced (Arratia, 1997:fig. 80A–D). According to Webb (1989), based on extant teleosts, the presence of branched tubules is primitive, and simple, widened, or reduced tubules are three apomorphic character states. When fossils are considered, the interpretation of the primitive condition may change. The supraorbital and otic canals of pholidophorids present simple tubules. The tubules are so short or almost nonexistent that it appears each pore just opens directly above the canal. In contrast, the supraorbital canal in *†Dorsetichthys bechei*, gen. nov., *†Siemensichthys macrocephalus*, and *†Euryctormus speciosus* has branches whose pores are at a distance from the main canal. Thus, the presence of simple supraorbital and otic canals is a feature interpreted as a synapomorphy of the Pholidophoridae, but it is a homoplastic feature also found outside the family.

Number of Infraorbitals—The presence of five independent infraorbital bones seems to be the generalized condition among basal teleosts, with further fusions or losses in more advanced members of the group. Five infraorbitals are also present in many halecomorphs (Grande and Bemis, 1998) and in the teleosteomorph *†Prohalecites* (Tintori, 1999). *†Pholidoctenus serianus* is unique among Triassic pholidophorids in the presence of five or six bones (e.g., Figs. 81, 98A–D), whereas *†Ichthyokentema purbeckensis* has a reduced number (Griffith and Patterson, 1963:fig. 6). Frequently, the sixth infraorbital is the result of fragmentation of some of the posterior-most infraorbitals. Seven or possibly eight infraorbitals were described and illustrated for the Early Jurassic ‘pholidophoriform’ *†Pholidophoroides crenulata* (Nybelin 1966:figs. 9, 11). This is an uncommonly high number of infraorbitals for ‘pholidophoriforms’ or teleosts in general. Considering Nybelin’s (1966:398) comments concerning the quality of preservation of the posterodorsal infraorbitals of *†Ph. crenulata*, this observation should be treated with caution and revised when more specimens are available for study. A series of six or more rectangular, small posterodorsal infraorbitals is present in some pachycormiforms (e.g., *†Hypsocormus*, *†Pachycormus*, *†Orthocormus*), but the condition is unknown in many members of the group.

Suborbital and Additional Suborbital(s)—The presence of a moderately large suborbital bone (Figs. 12, 51A, 80A, B) surrounded by the posterior margin of infraorbitals 3 to 5 and the opercle and preopercle is a feature found in the most basal teleosts studied here. This feature is lost in *†Ascalabos* plus more advanced teleosts (Fig. 95, node J). This morphology is the generalized condition in most teleosts, with the exception of *†Varasichthys* (Arratia, 1994) and the extant osteoglossomorph *Arapaima* (Taverne, 1977), which have a very small suborbital bone.

Pholidophorids may have, in addition to the large suborbital, one or more additional suborbital bones (Figs. 61, 78, 98A–D), which are positioned lateral to the dorsal surface of the suborbital and opercle. Additional suborbitals are not present in *†Dorsetichthys bechei*, gen. nov., and more advanced teleosts. Consequently, I interpret this feature as a synapomorphy of the Pholidophoridae.

Posterior Margin of Maxilla—The posterior margin of the maxilla may be slightly rounded, straight, acute (e.g., *†Annaichthys*, *†Pholidophorus latiusculus*, *†Ph. gervasutii*, *†Pholidorhynchodon*: Figs. 9, 32, 39, 51), or characteristically notched. The last condition is present at least in halecomorphs (Grande and Bemis, 1998), *†Pholidoctenus* (Fig. 81), *†Pholidophoretes* (Fig. 94), some

specimens of *†Siemensichthys macrocephalus*, and *†Varasichthys*. Grande and Bemis (1998) interpreted the presence of a maxilla with its posterior margin distinctively notched as a synapomorphy of the Halecomorpha. However, the character turns out to be homoplastic when basal teleosts are added to the phylogenetic analysis.

Number of Supramaxillae—The supramaxillae are dermal bones lying on the dorsal margin of the maxilla. One supramaxillary bone is present in various actinopterygians, such as halecomorphs, pachycormiforms, and aspidorhynchiforms (e.g., Wenz, 1968; Lambers, 1992; Brito, 1997; Arratia, 1999, 2000). The element commonly called a supramaxilla in pachycormiforms and aspidorhynchiforms is characteristically positioned posterodorsal or posterior to the maxilla.

Commonly, basal teleosts have two supramaxillae, and this feature is interpreted as a synapomorphy of Teleostei, with further transformations in more advanced taxa. Pholidophorids may have two supramaxillary bones or occasionally only one (see Figs. 5, 14, 39, 98). *†Ichthyokentema* has only one supramaxilla, and among members of the *†Siemensichthys* group, the presence of one supramaxilla is a feature shared by *†Siemensichthys* and *†Ankylophorus* (see Arratia 2000:figs. 7, 15C). Grande and Bemis (1998) interpreted the presence of one supramaxilla as a synapomorphy of the Halecomorpha. However, this feature turns out to be homoplastic when basal teleosts and teleosteomorphs are added to the comparison.

Protruding Bony Ridge on Dentary—A well-developed, bony ridge extending along the lateral wall of the dentary is present in all Triassic pholidophorids, as well as *†Dorsetichthys bechei*. The ridge separates the dental from the splenial region of the dentary, and its possible function remains unknown. This feature is considered a synapomorphy of the family Pholidophoridae (Figs. 95, 96, node C1), but it is also present in *†Dorsetichthys bechei*, gen. nov., among more advanced teleosts.

Coronoids in Lower Jaw—One or more small coronoids bearing teeth are present on the medial side of the lower jaw of halecomorphs and other neopterygians. The absence of coronoid bones was interpreted as a synapomorphy of teleosts (e.g., Patterson, 1977; Pinna, 1996; Arratia, 1997, 1999; and others). However, the addition of some ‘pholidophoriforms’ to the phylogenetic analysis changes that previous understanding. The Triassic pholidophorids, where the inner side of the jaw is known, have coronoids (*†Pholidorhynchodon* and *†Parapholidophorus*; Figs. 47, 82). Among Jurassic forms, *†Ichthyokentema* has a coronoid (Griffith and Patterson, 1963:fig. 9); in contrast, *†Leptolepis coryphaenoides* and more advanced teleosts (Arratia 1999, 2000, 2008, and others) lack coronoids (Fig. 95, node I). However, I must note that this feature is difficult to observe because, when further skeletal preparation is not allowed, it requires that the jaw be preserved in medial view.

Posterodorsal Process of Quadrato and Quadratojugal—An elongated posterodorsal (or posteroventral, depending on the angle of the quadrate in situ) process of the quadrate is a synapomorphy of *†Dorsetichthys bechei* plus more advanced teleosts (Arratia and Schultze, 1991; Arratia, 2000, 2001, 2008, and others). According to the present results, a posterodorsal process of the quadrate is a synapomorphy supporting the phylogenetic level of *†Euryctormus* plus more advanced teleosts (Fig. 95, node D).

The posterodorsal process of the quadrate has been interpreted as a quadratojugal (a dermal bone) fused to the quadrate (a chondral bone) by Patterson (1973, 1977b), Jollie (1962, 1975), and others. The quadratojugal is a dermal bone found in some sarcopterygians and primitive actinopterygians (see Arratia and Schultze, 1991:64–69, concerning the distribution of the bone). Among neopterygians, a splint-like quadratojugal is found in

lepisosteiforms, macrosemiids, and semionotids, and it is uncertain if this quadratojugal is homologous with that in other basal actinopterygians, such as the chondrostleans (Grande, 2010). There is a tendency to treat the posterodorsal process of the quadrate of teleosts as homologous with the quadratojugal of lepisosteiforms and semionotiforms. In some cases, an ontogenetic fusion between the so-called quadratojugal and quadrate has been reported (e.g., for *Esox*; Jollie, 1975), or in other cases, the process has just been assumed to be a quadratojugal (e.g., in *Salmo* and *Heterotis*; Holmgren and Stensio, 1936; Daget and d'Aubenton, 1957; Jollie, 1975) and was interpreted to be the result of phylogenetic fusion between the quadratojugal and quadrate by Patterson (1977b). Patterson (1977a) followed this interpretation and used it as one character supporting his teleostean phylogeny (quadratojugal fused with quadrate as a posterodorsal process, enclosing a groove for the symplectic, versus quadratojugal free or not recognizable). This is a curious interpretation of homology because this special ‘quadratojugal’ appears at the level of *†Ichthyokentema* plus more advanced teleosts, but it is missing in all basal teleosts and also in the Halecomorpha in Patterson’s (1977a) phylogeny (see Fig. 2A herein).

The posterodorsal (or posteroventral) process of the quadrate (Fig. 99A–C) is a membrane process that develops at the posterior or ventral margin of the pars quadrata in teleosts, as was demonstrated by Arratia and Schultze (1991:figs. 44A, B, 45A–C) and Arratia (1999:fig. 5A, B) based on ontogenetic series of extant elopiforms (e.g., *Elops*), gonorynchiforms (e.g., *Chanos*), and salmonids (e.g., *Oncorhynchus*; contra Jollie, 1975; Wiley, 1976). Such results are confirmed here based on several ontogenetic series, including other elopomorphs, ostarioclupomorphs, other salmonids, etc. (see lists of material). A membranous posteroventral process of the pars quadrata develops suddenly in the palatoquadrate of the zebrafish *Danio rerio* (Fig. 99B, C) between 5.3 and 5.5 mm notochordal length. No evidence of a separate bony splint that fuses with the pars quadrata has been observed in *Danio* or any of the teleosts studied here.

The posterodorsal process of the quadrate or a quadratojugal is missing in Triassic pholidophorids (e.g., Figs. 15, 17, 18), teleosteomorphs (e.g., *†Atacamichthys*, pachycormiforms, and aspidorhynchiforms), and halecomorphs (close relatives to teleosts), including the fossil parasemionotiforms and fossil and extant amiiforms (see for instance, Wenz, 1968; Maisey, 1990; Arratia and Schultze, 1991; Brito, 1997; Grande and Bemis, 1998; Grande, 2010; see Appendix 2), and in the basal teleosteomorph (*†Prohalecites*; Fig. 95) previously interpreted as a neopterygian incertae sedis (Arratia and Tintori, 1999). Taverne (2011a; Fig. 2C herein) interpreted this process as a synapomorphy of ‘Pholidophoriformes’ plus more advanced teleosts. However, a process is absent in the Triassic pholidophorids described here, and it is unknown for most taxa in Figure 2C. Based on the developmental formation of the quadrate and its process and on the distribution of this character in different phylogenetic hypotheses (including halecomorphs and teleosts), the posterodorsal process has to be interpreted as a new formation for teleosts. Consequently, similarities in shape (e.g., splint-like) and position of the quadratojugal of lepisosteiforms and macrosemiiforms and the posterodorsal process of teleosts can be only interpreted as independently acquired in the evolution of actinopterygians. Still the question remains whether the so-called quadratojugals of basal actinopterygians, chondrostleans, and some neopterygians are homologous structures.

Additional Preopercle—Among all fishes studied, the basal teleosteomorph *†Prohalecites* and the pholidophorid *†Pholidoctenus* have an accessory bone named ‘additional preopercle.’ The additional preopercle of *†Prohalecites* is placed ventral to the tube-like preopercle and carries the preopercular

sensory canal (Tintori, 1990; pers. observ.). In contrast, the additional preopercle of *†Pholidoctenus* is placed anteroventral to the preopercle, overlapping the quadrate, and does not carry a section of the preopercular sensory canal (Fig. 98B). Zambelli (1977) named this piece of bone ‘additional preopercle’ and I have used the name in the description above. Because this bone is only present in *†Pholidoctenus* among pholidophorids, I interpret it as an autapomorphy of this genus.

Additional Gular—The presence of a gular is a generalized feature among basal teleosts, and its loss is a character of extant osteoglossomorphs and more advanced teleosts (a homoplastic character because reappearances occur at different teleostean levels; Arratia, 1999:character 60). Triassic ‘pholidophoriforms’ with a well-preserved ventral region of the head (e.g., *†Parapholidophorus*, *†Pholidorhynchodon*, and possibly *†Pholidophorus gervasutii*; Fig. 67) show, in addition to the elongate median gular, a pair of round elements lateral to the median gular that I interpret as additional gulars. Additional gulars are covered with a thick layer of ganoine that is ornamented with tubercles and ridges, as in the median gular, and unlike the pattern in the branchiostegal rays. Zambelli (1980:fig. 3) interpreted this element as the anterior-most branchiostegal in *†Pholidorhynchodon*, despite the fact that it has a different position, size, and ornamentation than the branchiostegals. Although I have not included this feature in the diagnoses and phylogenetic analysis, I predict that this may be an additional character shared by Triassic pholidophorids.

Vertebral Column—The vertebral column and the composition of the vertebral centra are important in the evolution of teleosts, showing significant evolutionary changes from chordacentral to autocentral stages with a series of transformations, such as changes from ring-like chordacentra to chordacentra strongly constricted by the autocentrum and from thin-walled autocentra to thick-walled and ornamented autocentra.

Triassic pholidophorids, *†Eurycormus*, *†Catervariolus*, and *†Dorsetichthys bechei*, gen. nov., so far as is known, show diplospondyly in the caudal region of the vertebral column (Figs. 68, 75). The diplospondylous centra include basidorsal, basiventral, interdorsal, and interventral chordacentra, in contrast to the heavily ossified diplospondylous centra present in *Amia calva* (Schultze and Arratia, 1986; Grande and Bemis, 1998) or to the monospondylous centra of advanced teleosts. *†Pholidoctenus* is unique in possessing also the diplospondylous condition in the abdominal or precaudal region (Fig. 82). According to present evidence, this feature is interpreted as an autapomorphy of this taxon. Monospondylous centra seem to be a feature of *†Ichthyokentema* plus more advanced teleosts.

An autocentrum is a feature unquestionably found in *†Leptolepis coryphaenoides* plus more advanced teleosts (Arratia, 1991, 1997, 1999, and others; Figs. 96, 97, node C3), although the description of the centra of *†Catervariolus* can be interpreted as autocentra. All teleosts below the phylogenetic level of *†L. coryphaenoides* share ring-like chordacentra, or arcocentral type of centra, whereas all teleosts above the level of *†Tharsis* have centra with walls that constrict strongly the notochord, leaving a small notochordal foramen. These findings confirm previous results by Arratia (1997, 1999, and others) and Arratia et al. (2001).

Unfortunately, a significant amount of information concerning intermuscular bones, parapophyses, and ribs is still missing from the Triassic pholidophorids.

Clavicles and Serrated Appendages—Clavicles articulating with the anteroventral margin of the cleithrum are present in primitive actinopterygians (e.g., Jessen, 1972) and in parasemionotiforms (e.g., Olsen, 1984) among halecomorphs. Clavicles are absent in all extant teleosts, but a triangular-shaped clavicle (e.g., Fig. 69) very similar to that found in *†Watsonulus* (Olsen 1984:fig. 16)

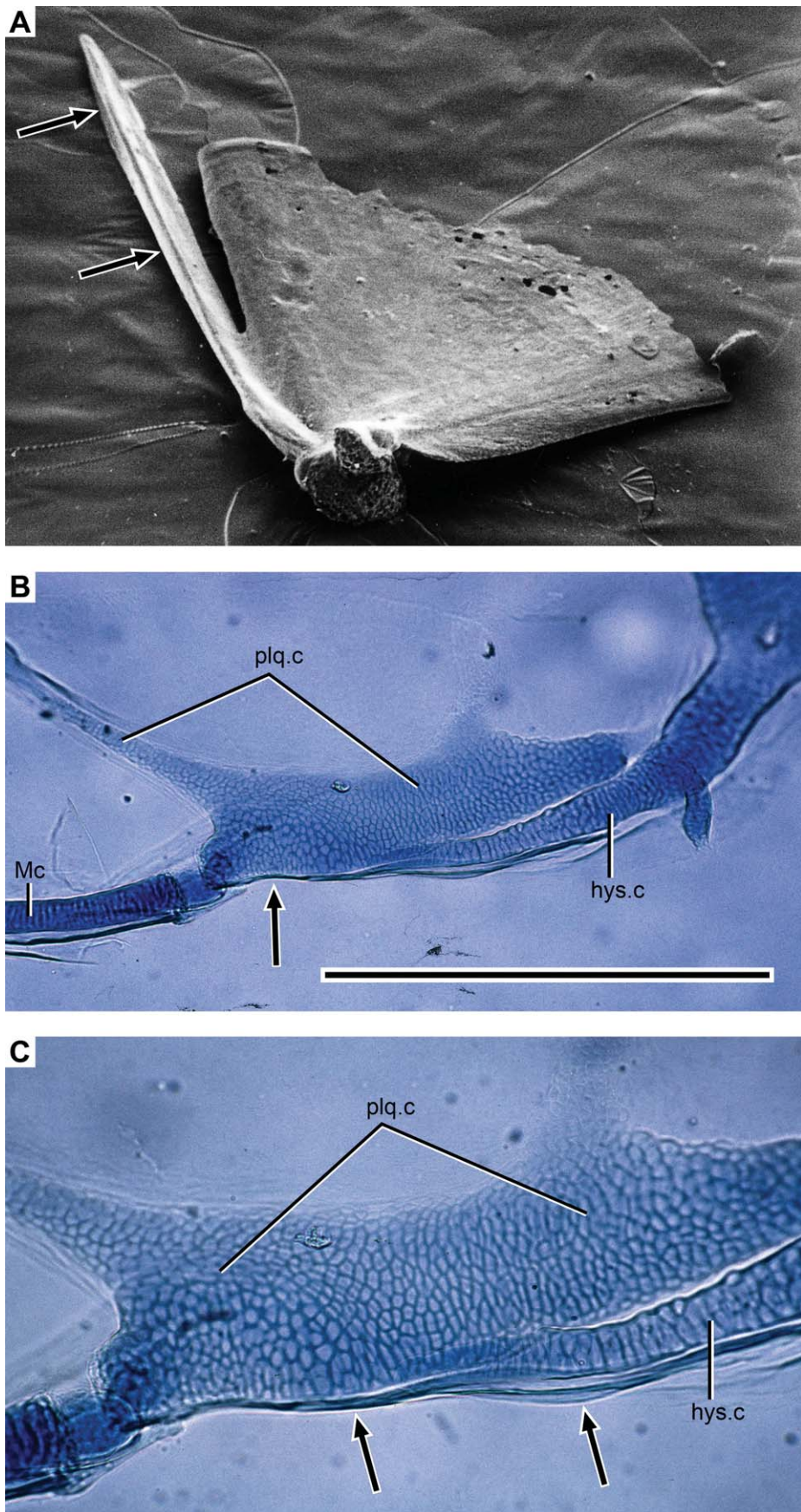


FIGURE 99. Quadrate and its posterodorsal or posteroventral process. **A**, *†Leptolepis coryphaenoides* (scanning electron micrograph of KUVP uncataloged; 55 \times). **B, C**, *Danio rerio* of 5.3 and 5.5 mm total length (KUNHM 40245). Arrows point to the membranous posterodorsal (**A**) or posteroventral (**B, C**) process of pars quadrata. Scale bar equals 0.5 mm.

articulates with the anteroventral margin of the cleithrum in Triassic pholidophorids and in the Jurassic *†Catervariolus*, giving a new scenario concerning the distribution of this element in advanced actinopterygians.

In addition to the clavicle, Triassic pholidophorids have a long, broad serrated appendage with the entire lateral surface covered in ridges bearing small denticles; this appendage abuts the medial margin of the cleithrum and extends from near the dorsal tip to the ventral tip of the cleithrum, covering about half of the cleithrum (Fig. 69). A similar serrated appendage is present in *†Watsonulus* and *†Atacamichthys* among teleostomorphs (Arratia and Schultze, 1987). A long, narrow serrated appendage, positioned along the thickened medial margin of the cleithrum, is present in *†Leptolepis coryphaenoides* (Arratia and Schultze, 1990; Fig. 100 herein). A similar element has not been observed in basal teleosts, such as *†Tharsis*, *†Ascalabos*, varasichthyids, *†Anaethalion*, *†Lycoptera*, and others. The situation is different in amiiforms and some ‘pholidophoriforms’ that have small patches bearing denticles, the so-called clavicles 1 and 2 of *†Pholidophorus germanicus* (Patterson, 1977b:fig. 6B) or the small anterior and posterior ‘clavicular’ elements of amiiforms (Grande and Bemis, 1998:figs. 87–89).

The phylogenetic analysis resolves the presence of a clavicle articulated with the anteroventral margin of the cleithrum, which is a synapomorphy of *†Prohalecites* and basal teleosts (see Fig. 95, node B). In contrast, the distribution of a long, totally serrated appendage is only known for *†Atacamichthys*, *†Pholidophoridae*, and *†Leptolepis coryphaenoides*, whereas the distribution of two serrated appendages or interclavicle elements is known for amiiforms and certain ‘pholidophoriforms.’ Based on the new information provided by the Triassic pholidophorids and the parasemionotiform *†Watsonulus* (part of the outgroup), the parsimony analysis predicts that the presence of a long, serrated appendage is a synapomorphy of teleostomorphs. It seems clear to me that we need further investigations of halecomorphs, aspidorhynchiforms, pachycormiforms, and ‘pholidophoriforms’ to assess the distribution of these elements in advanced actinopterygians.

Pelvic Axillary Process—A long, well-ossified, leaf-like pelvic axillary process is a feature found in all Triassic pholidophorids and in members of the Oxfordian family Varasichthyidae. A similar process has not been observed in *†Dorsetichthys bechei*, gen. nov., or *†Ichthyokentema*. A process formed by a combination of cycloid scales and an elongate bony splint is present in *†Leptolepis coryphaenoides* (Arratia, 2003). The process in pholidophorids is covered by a smooth layer of ganoine, whereas the process in the varasichthyids lacks ganoine. According to its distribution among basal teleosts, this feature is interpreted here as independently acquired in both groups. For information concerning the axillary processes in other teleosts, see Arratia (1997:132–135).

Caudal Skeleton—The caudal endoskeleton and the cranium are the most important sources of characters in teleostean systematics (Arratia, 2008). The morphological diversity of the caudal skeleton is enormous, as demonstrated in compilations of extant teleostean groups (Monod, 1968; Fujita, 1990) or fossil basal teleosts (e.g., Patterson, 1968; Arratia, 1991, 1997; Schultze and Arratia, 2013). Unfortunately, information on the caudal skeleton of the Triassic pholidophorids is scarce because squamation covers the region so that important questions concerning epurals, uroneurals, or hypurals cannot be addressed herein. The caudal endoskeleton of pholidophorids (see Figs. 68, 84) seems to be very fragile and not fully ossified. In contrast to the endoskeleton, the external structure of the caudal fin provides abundant new information, particularly in the number of basal fulcra and variation of the principal caudal rays.

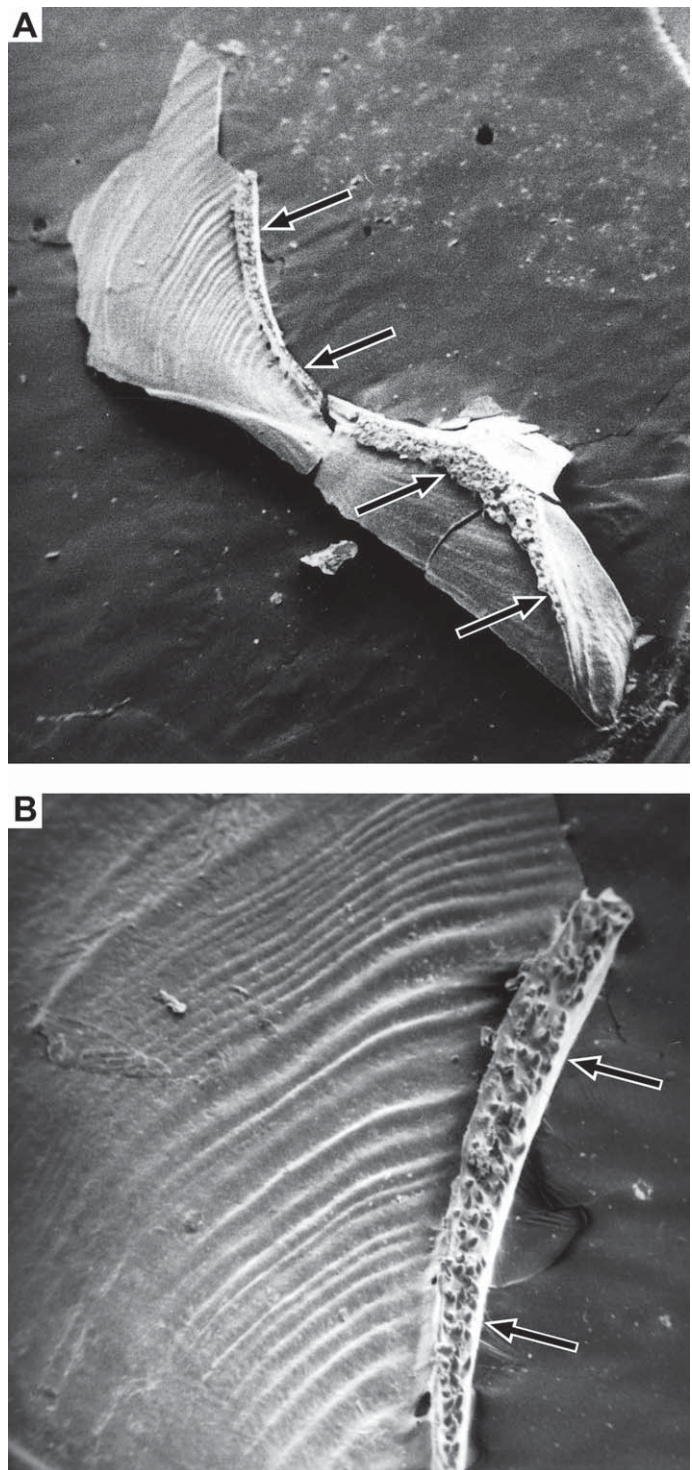


FIGURE 100. **A**, scanning electron micrograph of the cleithrum of *†Leptolepis coryphaenoides* showing the medial margin carrying the serrate appendage (SEM of KUVP uncataloged; 34 \times). **B**, enlargement of the serrated appendage showing small teeth covering its surface.

The principal rays of all Triassic pholidophorids have straight segmentation in contrast to the Z-like segmentation shown by principal rays in other species studied here (e.g., *†Eurycormus* and

\dagger *Siemensichthys*). The number of principal rays of pholidophorids spans a broad range, from 18 or 19 principal rays in \dagger *Pholidoctenus* to 28 or 29 in \dagger *Knerichthys bronni*. The latter represents the highest number ever reported for teleosts. \dagger *Dorsetichthys bechei* may have between 22 and 24, whereas \dagger *Leptolepis coryphaenoides* has 19 (occasionally 18; Arratia, 1991) principal rays, the common number in extant teleosts. Members of the \dagger *Siemensichthys* group have fewer than 19 rays. The number of principal rays and epaxial and hypaxial basal fulcra may be features of systematic value identifying certain species.

Degree of Ossification of Chondral Bones—It is important to note that the degree of ossification of the chondral bones of the Triassic pholidophorids seems to be weak, because most chondral bones are not ossified, even in the largest specimens of each taxon. This is manifest in the incomplete preservation of the hyosymplectic, branchial, hyoid arches, braincase, anguloarticular-retroarticular, and hypurals. Other chondral bones seem to remain as cartilaginous elements, because many of them have not been observed in the available material, as, for instance, the scapulocoracoid, supraneurals, and parapophyses. This condition seems to change in \dagger *Dorsetichthys bechei* and \dagger *Leptolepis coryphaenoides*, which have chondral bones that are well ossified perichondrally, but retain cartilage internally.

Layer of Ganoine on Bones and Scales—The layer of ganoine covering bones and scales may be smooth or characteristically ornamented. For instance, a smooth layer of ganoine on the scales separates \dagger *Pholidophorus latiusculus* from \dagger *Ph. gervasutii*, whereas large, round tubercles is a feature of \dagger *Annaichthys*. The characteristic plate-like ornamentation (Fig. 37) in certain cranial regions of \dagger *Knerichthys* is a unique feature of this taxon. On the other hand, the presence of distinct ornamentation on supramaxilla 1 may be characteristic of certain species (e.g., \dagger *Ph. latiusculus*; Fig. 5), whereas the characteristic elongate ridges of ganoine covering the maxilla and supramaxillae is a feature of basal members of Teleostei. According to my present understanding of basal teleosts, the presence of ganoine and its special ornamentation are features that need to be further explored as additional sources of information in the identification of ‘pholidophoriforms’ and their taxonomic status and phylogenetic relationships. Usually, descriptions of scales and bones only mention presence or absence of ganoine ornamentation. However, detailed descriptions of the ornamentation are required so that the whole array of variation in different taxa can be comparatively examined and its taxonomic and phylogenetic importance properly addressed.

The ganoid scales of all Triassic pholidophorids and of \dagger *Dorsetichthys bechei* and \dagger *Ichthyokentema* are of the lepisosteoid type (Schultze, 1966, 1996; pers. observ.), whereas scales of \dagger *Eurycornus* are of amioid type, and those of the \dagger *Siemensichthys* group are of lepisosteoid type. Thus, basal teleosts have ganoid scales of lepisosteoid type, whereas advanced teleosts (Fig. 95, node J) have exclusively elasmoid scales of cycloid type. The amioid type of scale present in \dagger *Eurycornus* is interpreted as an autapomorphy of this genus.

The differences on the ornamentation of the scales may be diagnostic for certain species (e.g., \dagger *Pholidophorus gervasutii*, \dagger *Knerichthys*, \dagger *Annaichthys*), as well as the absence of ornamentation (\dagger *Pholidophorus latiusculus*, \dagger *Pholidoctenus*). The posterior margin being smooth (most Triassic pholidophorids and \dagger *Dorsetichthys bechei*, gen. nov.; Fig. 6) or serrated (\dagger *Knerichthys* and \dagger *Pholidoctenus*; Figs. 43, 88) also may be important features of certain taxa.

DIVERSITY OF EARLY TELEOSTS

According to the evidence presented here, there are nine Triassic pholidophorid genera: \dagger *Annaichthys*, gen. nov., \dagger *Knerichthys*, gen. nov., \dagger *Parapholidophorus*, \dagger *Pholidoctenus*, \dagger *Pholidophoretes*, \dagger *Pholidophorus*, \dagger *Pholidorhynchodon*, \dagger *Zambellichthys*, gen.

TABLE 1. Late Triassic and Early Jurassic teleostean genera and their geographical occurrences (updated from Arratia, 2004).

Genus	Continent	Age
\dagger <i>Annaichthys</i> , gen. nov.	Europe	Late Triassic
\dagger <i>Elpistioichthys</i>	Europe	Late Triassic
\dagger <i>Eopholidophorus</i>	Europe	Late Triassic
\dagger <i>Knerichthys</i> , gen. nov.	Europe	Late Triassic
\dagger <i>Parapholidophorus</i>	Europe	Late Triassic
\dagger <i>Pholidoctenus</i>	Europe	Late Triassic
\dagger <i>Pholidophoretes</i>	Europe	Late Triassic
\dagger <i>Pholidophorus</i>	Europe	Late Triassic
\dagger <i>Zambellichthys</i> , gen. nov.	Europe	Late Triassic
\dagger <i>Jiangilichthys</i>	Asia	Late Triassic
\dagger <i>Dorsetichthys</i> , gen. nov.	Europe	Early Jurassic
\dagger <i>Leptolepis</i>	Europe	Early Jurassic
\dagger ‘ <i>Leptolepis</i> ’	Europe	Early Jurassic
\dagger <i>Longilepis</i>	Europe	Early Jurassic
\dagger <i>Pholidolepis</i>	Europe	Early Jurassic
\dagger <i>Pholidophoroides</i>	Europe	Early Jurassic
\dagger <i>Pholidophoropsis</i>	Europe	Early Jurassic
\dagger ‘ <i>Pholidophorus</i> ’	Europe	Early Jurassic
\dagger <i>Proleptolepis</i>	Europe, South America	Early Jurassic
\dagger <i>Hengnemia</i>	Asia	Early Jurassic

nov., and \dagger *Eopholidophorus*. This number is expected to increase with further revisions of material recovered in Lunz (Austria) and northern Italy. \dagger *Pholidophoretes* from the lower Carnian of Lunz (Austria) and \dagger *Knerichthys* from the lower Carnian of Tarvisio (Italy) are here interpreted to be the oldest known members of the family \dagger *Pholidophoridae*, new usage. They are also the oldest members of Teleostei thus far recorded. \dagger *Eopholidophorus* Zambelli, 1990, is slightly younger, late Norian, whereas the rest of the pholidophorids are from the middle to late Norian. \dagger *Prohalecites*, from the Ladinian/Carnian boundary, is the oldest teleostomorph. In contrast, the oldest pachycormiforms and aspidorhynchiforms are known from the Early and Middle Jurassic, respectively (e.g., Lambers, 1992; Brito, 1997; Arratia, 2001, 2004).

A comparison with the Early Jurassic fish faunas, especially those from Europe, which are better known than those from other continents, reveals the presence of about a dozen genera (Table 1). Together, fish such as \dagger *Dorsetichthys bechei*, gen. nov., and \dagger *Leptolepis coryphaenoides* initiate the beginning of a successful lineage that would culminate in the spectacular crown-group Teleostei represented by more than 27,000 living species today (Nelson, 2006). In addition to the ‘true’ teleosts, the predominant group during the Early Jurassic was apparently the ‘Pholidophoriformes,’ with at least six Asian and European genera of unknown relationships (Arratia, 2004). None of the Triassic pholidophorids described here has been recorded outside the Triassic. All Triassic taxa that were preliminary assigned to the genus \dagger *Pholidophorus* have been shown to belong to very different taxa (see ‘Introduction’). According to the available information, a whole replacement of fish faunas was involved at the Triassic–Jurassic boundary (see Table 1). A similar phenomenon was reported by Arratia (2004:fig. 17, table 1) for the diversity of fish faunas at the Jurassic–Cretaceous boundary.

Although the ‘pholidophoriforms’ are mainly known from Europe and Asia, ‘true’ teleosts (Fig. 95, node I) have also been reported from distant places, such as the Early Jurassic (Sinemurian) of northern Chile (Arratia and Schultze, 1999; Arratia and Hikuroa, 2010). Thus, in about 45 million years, from the Carnian to the end of the Early Jurassic, teleosts not only have diversified morphologically and taxonomically, but have a broad distribution.

Triassic pholidophorids (Fig. 95, node C) are an important component of the early diversification of teleosts, and most synapomorphies that today characterize the crown-group teleosts

(= *Teleocephala* of Pinna, 1996, or *Elopocephala* of Arratia, 1999, and Betancur-R et al., 2013) can be traced to the Early Jurassic (Fig. 95, nodes C to J). Thus, if we want to understand the evolutionary transformations present in many clades of crown group teleosts, then we need to return to the basal nodes of the teleostean tree.

CONCLUDING REMARKS

A new hypothesis of phylogenetic relationships of most basal teleosts is proposed and is the result of the most comprehensive study, including detailed morphological revision of many taxa that for the first time are included in a phylogenetic study. The monophyly of *Teleosteomorpha* (total-group teleosts) is supported by several synapomorphies (Fig. 95, node A), and pachycormiforms and aspidorhynchiforms form a novel clade that is resolved as a basal member of the group. However, without testing the role of more pachycormiform taxa, any conclusion at this moment could be premature. The Middle–Late Triassic genus *†Prohalecites* is interpreted here as a teleosteomorph based on several synapomorphies (Fig. 95, node B). *†Prohalecites* is the oldest known stem teleost or teleosteomorph.

The family *†Pholidophoridae* is interpreted as the sister of the main lineage to the teleost crown group. The new hypothesis [*†Pholidophoridae* + [*†Eurycornus* + [*†Catervariolus* + [*†Siemensichthys* group + [*†Dorsetichthys bechei* + [*†Ichthyokentema* + [*†Leptolepis coryphaenoides* + more advanced teleosts]]]]]]] has some major changes to previous hypotheses in the position of the pholidophorids and other fishes that were previously interpreted as ‘pholidophoriforms’.

The results confirm the order *†Pholidophoriformes* Berg, 1937, as a non-monophyletic group. The ‘pholidophoriform’ taxa studied herein show a paraphyletic distribution at the base of the Teleostei (Fig. 95, nodes C to H). It is proposed to reserve the name *†Pholidophoriformes* to the monophyletic family *†Pholidophoridae*. The family *†Pholidophoridae* is restricted to European Triassic pholidophorids. The family is a monophyletic group supported by several synapomorphies (Figs. 95, 96, node C1). A new diagnosis is provided. *†Pholidophorus latiusculus* is the type species of the group. The genus *†Pholidophorus* is paraphyletic, but its two Triassic species (*†Ph. latiusculus* and *†Ph. gervasutti*) are retained within the genus, although more material of the poorly known *†Ph. latiusculus* may change its status.

†Eurycornus from the Upper Jurassic of Europe is removed from the *†Siemensichthys* group and interpreted as a basal teleost (Fig. 95, node D) below the phylogenetic level of *†Catervariolus* plus more advanced teleosts.

There are a number of taxonomic changes resulting from this analysis, as well as three new genera: *†Annaichthys* and *†Zambellichthys* from the Triassic (Norian) of Italy and *†Knerichthys* from the Triassic (Carnian) of Austria. *†Annaichthys* is hypothesized as the most basal *†Pholidophoridae* because of its combination of characters (Fig. 95, node C1). *†Pholidophorus bechei*, previously interpreted as a member of the family *†Pholidophoridae*, is separate from the Triassic pholidophorids and has a more advanced position among basal forms (Fig. 95, node G). A new genus, *†Dorsetichthys*, is created here to contain *†Pholidophorus bechei*.

The results presented here demonstrate the phylogenetic importance of the earliest ‘pholidophoriforms’ as basal teleosts, especially because some of their characters combinations introduce a new perspective in understanding the origin and early radiation of the group, and indirectly provide a new scenario to interpret homologous characters. For instance, the clavicle and serrated appendage that in previous studies of *Amia* and some of the ‘pholidophoriforms’ were hypothesized as homologous features (see discussion in Grande and Bemis, 1998), but they are simultaneously

present in Triassic pholidophorids, and consequently, they cannot be interpreted as homologous.

One of the most challenging aspects of this study has been to understand the morphological diversification of the Triassic pholidophorids and the combination of characters that they exhibit. Such a scenario is not easily interpreted and involves comparisons with various disparate morphologies—such as those of holosteans, teleosteomorphs, and fossil and extant teleosts. A number of morphological interpretations are new to the concept of Teleostei: the cranial fusions in pholidophorids, the presence of the symplectic moving medial to the quadrate, the incomplete ossification of many chondral bones, diplospondylous caudal vertebrae, absence of epineural and epipleural bones, the presence of clavicles articulating with the anteroventral margin of the cleithrum, a long and broad serrated appendage covering the anteromedial region of the cleithrum, the presence of pectoral and pelvic axillary processes, and the absence of modified ural neural arches. These new descriptions and interpretations tell part of a chapter that we were missing to understand the evolutionary trends of several characters in the evolution of Teleostei.

ACKNOWLEDGMENTS

This work has been possible because of the collaboration of numerous individuals and institutions that throughout the years have supported me in different ways. I have been benefited by the cordiality, generosity, and friendly attitude of the people listed below. I thank the following individuals and institutions for permission to study material under their care: D. Berman (CM); H. Bjerring (SMNH); R. Böttcher (SMNS); D. Butt (UCLA); the late C. H. von Daniels (BGHAn); W. Eschmeyer and D. Catania (CAS); W. L. Fink and D. Nelson (UMMZ); Ursula Göhlisch (NHMW); L. Grande, W. Simpson, M. Westneat, and M. A. Rogers (FMNH); H. Jahnke (GOE); M. Koelb-Ebber and G. Viohl (JME); the late K. Liem, K. Hartel, the late F. Jenkins, and J. Cundiff (UMCZ); M. Louette and the late G. Teugels (MRAC); D. Markle (OS), the late L. Martin and D. Miao (KUVP); J. McEacharan and M. Retzer (TCWC); W. Mette and W. Resch (Innsb.); A. Paganoni (MCSNB); L. Parenti and J. Williams (NMNH); the late C. Patterson and A. Longbottom (NHMUK); T. Robins (UF); M. Röper (BMM-S); R. Rosenblatt (SIO); W. Saul (ANSP); F. J. Schwartz (UNC); A. Simons and V. Hirt (JFBM); D. Stacey and E. Holm (ROM); J. D. Stewart (formerly at LACM); M. Stiassny and B. Brown (AMNH); R. Stucky (DMNH); P. Wellhoven, R. O. Rauhut, and M. Moser (BSPG); F. Westphal and the late R. REIF (Pi); F. Witzman (MB); E. O. Wiley and A. Bentley (KUNHM); J.-Y. Zhang and Zhu M. (IVVP); and Irene Zorn (GBA). Special thanks to the late M. Coburn (John Carroll University, Cleveland, Ohio, U.S.A.), Y.-Y. Chen (Academia Sinica, Hunan, China), P. Mabee (University of South Dakota, Vermillion, South Dakota, U.S.A.), K. Matsuura (National History Museum, Tokyo, Japan), S. Poss (Gulf Coast Research Laboratory, Ocean Springs, Mississippi, U.S.A.), and H. Tischlinger (Stammham, Germany) for the gift of some important specimens.

I am especially indebted to A. Paganoni, M. Malzanni, F. Confertini, and A. Aillo for their help in different ways during my frequent visits to the fish collections of the MCSNB, and to A. Paganoni for covering part of the costs of the professional artist (Mr. J.-P. Mendau) and the costs of all photographs done by Mr. Franco Valoti from specimens deposited in the MCHNB. To J.-Y. Zhang (IVVP) for the photographs of the Chinese ‘pholidophoriform’ (Fig. 89). To W. Mette (Innsb.) who kindly did the photograph of the neotype of *†Pholidophorus latiusculus* (Fig. 1B). The photographs of specimens of *†Pholidophoretes* from NHMW were taken by Mrs. Alice Schumacher, and photographs of *†Knerichthys bronni* and *†Ph. latiusculus* deposited in the BGA were done by Mrs. Ilka Wuensche. Mr. J.-P. Mendau (Berlin,

Germany) prepared part of the final line illustrations based on my original drawings. T. J. Meehan prepared the electronic submission of all figures. K. Sturm (Lawrence, Kansas) for her editorial assistance double-checking matrices, citations, and figures. H.-P. Schultze (Lawrence, Kansas) allowed me to study his collection of peels of scales and use some of his unpublished illustrations.

My sincerest thanks to Claudio Quezada R. (Faculty of Sciences, University of Chile, Santiago, Chile), Kathryn Mickle (Lawrence, Kansas), and Matthew Davis (FMNH) for their help running the PAUP program and their willingness to analyze and discuss the results.

I thank L. Grande (Chicago, Illinois), E. Hilton (Gloucester Point, Virginia), H.-P. Schultze (Lawrence, Kansas), and L. Taverne (Brussels, Belgium) for their comments, suggestions, and constructive criticisms. I thank E. O. Wiley (Lawrence, Kansas) for comments and discussions on the phylogenetic results. My special thanks go to the editor, J. A. Wilson (Ann Arbor, Michigan), for his editorial corrections and helpful comments and criticisms that improved considerably the presentation of the memoir and to T. J. Meehan (Lawrence, Kansas) for his revisions of grammar and style of the manuscript.

This work was partially supported by the Alexander von Humboldt Foundation (Bonn), German Science Foundation (DFG SCHU 212/25-1), the German Academic Exchange Program (DAAD), and NSF EF 0431326.

LITERATURE CITED

- Agassiz, L. 1832. Untersuchungen über die fossilen Fische der Liassic-Formation. Jahrbuch für Mineralogie, Geognosie, Geologie und Petrefaktenkunde 3:139–149.
- Agassiz, L. 1833–1844. Recherches sur les Poissons Fossiles. 5 volumes. Petit Pierre, Neuchâtel and Soleure, 1798 pp.
- Airaghi, C. 1908. Di un *Pholidophorus* del Retico Lombardo. Rendiconti del Instituto Lombardo, Accademia di Scienze e Lettere, Milano 41:768–772.
- Alessandri, D. de. 1920. Sopra alcuni avanzi di pesci triasici della Lombardia. Atti della Società Italiana di Scienze naturali, Milano 59:85–104.
- Alfaro, M. E., F. Santini, C. Brock, H. Alamillo, A. Dornburg, D. L. Rabosky, G. Carnevale, and L. J. Harmon. 2009. Nine exceptional radiations plus high turnover explain species diversity in jawed vertebrates. Proceedings of the National Academy of Sciences of the United States of America 106:13410–13414.
- Allis, E. P. 1897. The cranial muscles and cranial and spinal nerves in *Amia calva*. Journal of Morphology 12:487–809.
- Arratia, G. 1981. *Varasichthys ariasi* n. gen. et sp. from the Upper Jurassic from Chile (Pisces, Teleostei, Varasichthyidae n. fam.). Palaeontographica Abteilung A 175:107–139.
- Arratia, G. 1984. Some osteological features of *Varasichthys ariasi* Arratia (Pisces, Teleostei) from the Late Jurassic of Chile. Paläontologische Zeitschrift 58:145–159.
- Arratia, G. 1991. The caudal skeleton of Jurassic teleosts: a phylogenetic analysis; pp. 249–340 in M.-M. Chang, Y.-H. Liu, and G.-R. Zhang (eds.), Early Vertebrates and Related Problems in Evolutionary Biology. Science Press, Beijing.
- Arratia, G. 1994. Phylogenetic and paleogeographic relationships of the varasichthyid group (Teleostei) from the Late Jurassic of Central and South America. Revista Geológica de Chile 21:121–165.
- Arratia, G. 1997. Basal teleosts and teleostean phylogeny. Palaeo Ichthyologia 7:1–168.
- Arratia, G. 1999. The monophyly of Teleostei and stem-group teleosts. Consensus and disagreements; pp. 265–334 in G. Arratia and H.-P. Schultze (eds.), Mesozoic Fishes 2—Systematics and Fossil Record. Verlag Dr. F. Pfeil, Munich.
- Arratia, G. 2000. New teleostean fishes from southern Germany and the systematic problems concerning the ‘pholidophoriforms.’ Paläontologische Zeitschrift 74:113–143.
- Arratia, G. 2001. The sister-group of Teleostei: consensus and disagreements. Journal of Vertebrate Paleontology 21:767–773.
- Arratia, G. 2003. *Leptolepis*, *Paraleptolepis* (Teleostei) and a new fish name. Mitteilungen aus dem Museum für Naturkunde, Berlin, Geowissenschaftliche Reihe 6:157–159.
- Arratia, G. 2004. Mesozoic halecostomes and the early radiation of teleosts; pp. 279–315 in G. Arratia and A. Tintori (eds.), Mesozoic Fishes 3—Systematics, Paleoenvironments and Biodiversity. Verlag Dr. F. Pfeil, Munich.
- Arratia, G. 2008. Actinopterygian postcranial skeleton with special reference to the diversity of fin ray elements, and the problem of identifying homologies; pp. 40–101 in G. Arratia, H.-P. Schultze, and M. V. H. Wilson, (eds.), Mesozoic Fishes 4—Homology and Phylogeny. Verlag Dr. F. Pfeil, Munich.
- Arratia, G. 2009. Identifying patterns of diversity of the actinopterygian fulcra. Acta Zoologica, Stockholm 90:220–235.
- Arratia, G. 2010. The Clupeocephala re-visited: analysis of characters and homologies. Revista de Biología Marina y Oceanografía 45:635–657.
- Arratia, G., and L. A. Cione. 1996. The fossil record of fossil fishes of southern South America; pp. 9–72 in G. Arratia (ed.), Contributions of Southern South America to Vertebrate Paleontology. Special volume of the Münchner Geowissenschaftliche Abhandlungen, A, Geologie und Paläontologie. Verlag Dr. Pfeil, Munich.
- Arratia, G., and R. Cloutier. 1996. Reassessment of the morphology of *Cheirolepis canadensis* (Cheirolepididae: Actinopterygii); pp. 165–197 in H.-P. Schultze and R. Cloutier (eds.), Devonian Fishes and Plants of Miguasha, Quebec, Canada. Verlag Dr. F. Pfeil, Munich.
- Arratia, G., and M. Gayet. 1995. Sensory canals and related bones of Tertiary siluriform crania from Bolivia and North America and comparison with Recent forms. Journal of Vertebrate Paleontology 15:482–505.
- Arratia, G., and A. Herzog. 2007. A new halecomorph fish from the Middle Triassic of Switzerland and its systematic implications. Journal of Vertebrate Paleontology 27:838–849.
- Arratia, G., and D. C. H. Hikuroa. 2010. Jurassic fishes from the Latady Group, Antarctica Peninsula, and the oldest teleosts from Antarctica. Journal of Vertebrate Paleontology 30:1331–1342.
- Arratia, G., and P. Lambers. 1996. The caudal skeleton of pachycormiform fishes: parallel evolution?; pp. 219–241 in G. Arratia and G. Viöhl (eds.), Mesozoic Fishes—Systematics and Paleoeiology. Verlag Dr. F. Pfeil, Munich.
- Arratia, G., and H.-P. Schultze. 1987. A new halecostome fish (Actinopterygii, Osteichthyes) from the Late Jurassic of Chile and its relationships; in J. E. Martin and G. Ostrander (eds.), Papers in Vertebrate Paleontology in honor of Morton Green. Dakoterra 3:1–13.
- Arratia, G., and H.-P. Schultze. 1990. The urohyal: development and homology within osteichthyans. Journal of Morphology 203:247–282.
- Arratia, G., and H.-P. Schultze. 1991. The palatoquadrate and its ossifications: development and homology within osteichthyans. Journal of Morphology 208:1–81.
- Arratia, G., and H.-P. Schultze. 1992. Reevaluation of the caudal skeleton of certain actinopterygian fishes. III. Salmonidae. Homologization of caudal skeletal structures. Journal of Morphology 214:1–63.
- Arratia, G., and H.-P. Schultze. 1999. The Mesozoic fishes from Chile; pp. 565–594 in G. Arratia and H.-P. Schultze (eds.), Mesozoic Fishes—Systematics and the Fossil Record. Verlag Dr. F. Pfeil, Munich.
- Arratia, G., and H.-P. Schultze. 2007. *Eurycormus*–*Euryponoma*, two Jurassic actinopterygian genera with mixed identity. Fossil Record 10:17–37.
- Arratia, G., and H.-P. Schultze. 2012. The macrosemiiform fish companion of the Late Jurassic tetrapod *Juravenator* from Schamhaupten, Bavaria, Germany. Fossil Record 15:5–25.
- Arratia, G., and H.-P. Schultze. 2013. Outstanding features of a new Late Jurassic pachycormiform fish from the Kimmeridgian of Brunn, Germany and comments on current understanding of pachycormiforms; pp. 87–120 in G. Arratia, H.-P. Schultze, and M. V. H. Wilson (eds.), Mesozoic Fishes 5—Global Diversity and Evolution. Verlag Dr. F. Pfeil, Munich.
- Arratia, G., and A. Tintori. 1999. The caudal skeleton of the Triassic actinopterygian *Prohalecites* and its phylogenetic position; pp. 121–142 in G. Arratia and H.-P. Schultze (eds.), Mesozoic Fishes 2—Systematics and Fossil Record. Verlag Dr. F. Pfeil, Munich.
- Arratia, G., and H. Tischlinger. 2010. The first record of Late Jurassic crossognathiform fishes from Europe and their phylogenetic importance for teleostean phylogeny. Fossil Record 13:317–341.

- Arratia, G., A. Chang, and G. Chong. 1975. *Pholidophorus domeykanus* n. sp. del Jurásico de Chile. Revista Geológica de Chile 2:1–9.
- Arratia, G., H.-P. Schultze, and J. R. Casciotta. 2001. Vertebral column and associated elements in dipnoans and comparison with other fishes. Development and homology. Journal of Morphology 250:101–172.
- Ax, P. 1987. The Phylogenetic System. The Systematization of Organisms on the Basis of Their Phylogenesis. Wiley & Sons, Chichester, U.K., 340 pp.
- Babcock, L., S. A. Leslie, D. H. Elliott, A. L. Stigall, L. A. Ford, and D. E. G. Briggs. 2006. The “Preservation Paradox”: microbes as a key to exceptional fossil preservation in the Kirkpatrick Basalt (Jurassic), Antarctica. The Sedimentary Record 4:1–8.
- Bardack, D. 1965. Anatomy and evolution of chirocentrid fishes. The University of Kansas Paleontological Contributions 10:1–88.
- Bartram, A. W. H. 1977. The Macrosemiidae, a Mesozoic family of holostean fishes. Bulletin of the British Museum of Natural History, Geology Series 29:137–234.
- Bassani, F. 1914. Sopra un *Pholidophorus* del Trias superiore del Tinnetto nel golfo della Spezia. Rendiconti della Accademia Nazionale dei Lincei, Roma 23:379–383.
- Berg, L. S. 1937. Classification of fishes, both Recent and fossil. Doklady Zoological Institute 5:85–517. [English translation by J. W. Edwards, Ann Arbor, Michigan, 1940]
- Berg, L. S., A. A. Kazantseva, and D. V. Obruchev. 1964. Superorder Palaeonisci (Archistia); pp. 528–574 in D. V. Obruchev (ed.), Fundamentals of Paleontology, Volume XI. [Translated from Russian, published for the Smithsonian Institution, U.S.A., and the National Science Foundation, Washington, D.C., by the Israel Program of Scientific Translations, 1967]
- Betancur-R., R., R. E. Broughton, E. O. Wiley, K. Carpenter, J. A. López, C. Li, N. I. Holcroft, D. Arcila, M. Sanciangco, J. Cureton, F. Zhang, T. Buser, M. Campbell, T. Rowley, J. A. Ballesteros, G. Lu, T. Grande, G. Arratia, and G. Ortí. 2013. The tree of life and a new classification of bony fishes. PLoS Currents Tree of Life. 2013 Apr 18. Edition 1. doi: 10.1371/currents.tol.53ba26640df0ccae75bb165c8c26288.
- Boni, A. 1937. Vertebrati retici italiani. Memorie della Accademia Nazionale del Lincei, Roma 6:521–719.
- Brandner, R., and W. Poleschinski. 1986. Stratigraphie und Tektonik am Kalkpensüdrand zwischen Zirl und Seefeld in Tirol (Exkursion D am 3. April 1986). Jahresberichte und Mitteilungen des Oberrheinischen Geologischen Vereines N. F. 68:67–92.
- Brito, P. 1992. L’endocrâne et le moulage endocranien de *Vinctifer compactus* (Actinopterygii, Aspidorhynchiformes) de Crétacé inférieur du Brésil. Annales de Paléontologie 78:129–157.
- Brito, P. 1997. Révision des Aspidorhynchidae (Pisces, Actinopterygii) du Mésozoïque: ostéologie et relations phylogénétiques, données environnementales et biogéographiques. Geodiversitas 19:681–772.
- Brito, P. 1999. The caudal skeleton of aspidorhynchids (Actinopterygii, Halecostomi); pp. 249–264 in G. Arratia and H.-P. Schultze (eds.), Mesozoic Fishes 2—Systematics and Fossil Record. Verlag Dr. F. Pfeil, Munich.
- Brito, P. M., and V. Gallo. 2002. A new pleuropholid, *Gondwanapleuropholis longimaxillaris* n. g., n. sp. (Actinopterygii: Teleostei) from the Jurassic of north-east Brazil. Comptes Rendus Palevol 1:697–703.
- Broughton, R. E., R. Betancur-R., C. Li, G. Arratia, and G. Ortí. 2013. Multi-locus phylogenetic analysis reveals the pattern and tempo of bony fish evolution. PLoS Currents Tree of Life. 2013 Apr 16. Edition 1. doi: 10.1371/currents.tol.2ca8041495ffaf0c92756e75247483e.
- Bürgin, T. 1992. Basal ray-finned fishes (Osteichthyes: Actinopterygii) from the Middle Triassic of Monte San Giorgio (Canton Tessin, Switzerland). Schweizerische Paläontologische Abhandlungen 114:1–164.
- Cavin, L. 2010. Diversity of Mesozoic fishes and the origin of the Lepisosteidae. Naturwissenschaften 97:1035–1040.
- Chang, M.-M., and J. Fan. 1996. Mesozoic fish faunas of China; pp. 461–478 in G. Arratia and G. Viohl (eds.), Mesozoic Fishes—Systematics and Paleoecology. Verlag Dr. F. Pfeil, Munich.
- Chiappe, L., D. Rivarola, A. L. Cione, M. Fregenal-Martínez, H. Sozzi, L. Buatois, O. Gallego, J. Laza, E. Romero, A. López-Arbarello, A. Buscalioni, C. Marsicano, S. Adamonis, F. Ortega, S. McGehee, and O. Di Iorio. 1998. Biotic association and paleoenvironmental reconstruction of the “Loma del Pterodaustro” fossil site (Early Cretaceous, Argentina). Geobios 31:349–369.
- Cloutier, R., and G. Arratia. 2004. Early diversification of actinopterygians; pp. 217–270 in G. Arratia, M. V. H. Wilson, and R. Cloutier (eds.), Recent Advances in the Origin and Early Radiation of Vertebrates. Verlag Dr. F. Pfeil, Munich.
- Coombs, S., J. Janssen, and J. F. Webb. 1988. Diversity of the lateral line system: evolutionary and functional considerations; pp. 553–593 in J. Atema, R. R. Fay, A. N. Popper, and W. N. Tavolga (eds.), Sensory Biology of Aquatic Animals. Springer, New York, Berlin, Heidelberg.
- Cope, E. D. 1887. Zittel’s Manual of Palaeontology. American Naturalist 21:1014–1019.
- Daget, J., and F. d’Aubenton. 1957. Développement et morphologie du crâne d’*Heterotis niloticus* Ehr. Bulletin de l’Institut Français de l’Afrique Noire, Série A 1:881–936.
- Danil’chenko, P. G., and V. N. Yakovlev. 1964. Order Pholidophorida; pp. 599–603 in D. V. Obruchev (ed.), Fundamentals of Paleontology, Volume XI. [Translated from Russian, published for the Smithsonian Institution, U.S.A., and the National Science Foundation, Washington, D.C., by the Israel Program of Scientific Translations, 1967]
- Della Vecchia, F. M. 2006. A new sauropterygian reptile with plesiosaurian affinity from the Late Triassic of Italy. Revista Italiana di Paleontologia e Stratigrafia 112:207–225.
- De Queiroz, K., and J. Gauthier. 1990. Phylogeny as central principle in taxonomy: phylogenetic definitions of taxon names. Systematic Zoology 39:307–322.
- Flores, M. A. 1969. El Bolsón de las Salinas en la Provincia de San Luis. Jornadas Geológicas Argentinas 4:311–327.
- Forey, P. 1973. A revision of elopiform fishes, fossil and Recent. Bulletin of the British Museum of Natural History, Geology, Supplement 10:1–222.
- Friedman, M., K. Shimada, L. Martin, M. J. Everhart, J. Liston, A. Maltese, and M. Triebold. 2010. 100-million-year dynasty of giant planktivorous bony fishes in the Mesozoic seas. Science 327:900–933.
- Fujita, K. 1990. The Caudal Skeleton of Teleostean Fishes. Tokai University Press, Tokyo, 897 pp.
- Gaudant, J. 1978. Essai de révision taxonomique des “*Pholidophorus*” (Poissons Actinopterygiens) du Jurassique supérieur de Cerin (Ain). Nouvelles Archives du Muséum d’Histoire naturelle, Lyon, fascicule 16:101–121.
- Giordano, P. G. 2010. “Pholidophoriforms” of La Cantera Formation, Lower Cretaceous, San Luis, Argentina; p. 45 in K. González-Rodríguez and G. Arratia (eds.), 5th International Meeting on Mesozoic Fishes, Global Diversity and Evolution, 2–7 August 2010. Abstract Book, Saltillo, Coahuila, Mexico.
- Giordano, P. G., and G. Arratia. 2011. Ganoid scales of “pholidophoriforms” (Actinopterygii) from La Cantera Formation, Lower Cretaceous, San Luis, Argentina. IV Latinoamerican Congress of Vertebrate Paleontology, 21 September 2011. Ameghiniana 48:232R–233R.
- Goodrich, E. S. 1909. Vertebrata Craniata (first fascicle: cyclostomates and fishes); pp. 1–518 in R. Lankester (ed.), A Treatise on Zoology. Adam and Charles Black, London.
- Gouric-Cavalli, S., and A. L. Cione. 2013. “*Pholidophorus argentinus*” Dolgopol de Saez, 1939 from the Upper Jurassic beds of the Neuquén Province of Argentina, is not a pholidophoriform but an aspidorhynchid (Actinopterygii, Aspidorhynchiformes); pp. 177–186 in G. Arratia, H.-P. Schultze, and M. V. H. Wilson (eds.), Mesozoic Fishes 5—Global Diversity and Evolution. Verlag Dr. F. Pfeil, Munich.
- Grande, L. 1985. Recent and fossil clupeomorph fishes, with materials for the revision of the subgroups of clupeids. Bulletin of the American Museum of Natural History 181:231–372.
- Grande, L. 2010. An Empirical Synthetic Pattern Study of Gars (Lepisosteiformes) and Closely Related Species, Based Mostly on Skeletal Anatomy. The Resurrection of Holosteii. American Society of Ichthyologists and Herpetologists, Special Publication 6, 871 pp.
- Grande, L., and W. E. Bemis. 1998. A Comprehensive Phylogenetic Study of Amiid Fishes (Amiidae) Based on Comparative Skeletal Anatomy. An Empirical Search for Interconnected Patterns of Natural History. Society of Vertebrate Paleontology, Memoir 4, 690 pp.

- Gregory, W. K. 1937. Fish Skull. A Study on the Evolution of Natural Mechanisms, second edition. Eric Lundberg, Laurel, Florida, 1959, 481 pp.
- Griffith, J. 1977. The Upper Triassic fishes from Polzberg bei Lunz, Austria. *Zoological Journal of the Linnean Society* 60:1–93.
- Griffith, J., and C. Patterson. 1963. The structure and relationships of the Jurassic fish *Ichthyokentema purbeckensis*. *Bulletin of the British Museum of Natural History (Geology)* 8:1–43.
- Hennig, W. 1966. Phylogenetic Systematics. University of Illinois Press, Urbana, Illinois.
- Holmgren, S., and E. A. Stensiö. 1936. Kranium und Visceralskelette der Akraniier, Cyclostomen und Fische; pp. 233–500 in L. Bolk, E. Göppert, E. Kallius, and W. Lubosch (eds.), *Handbuch der vergleichenden Anatomie*, 4. Urban und Schwarzenberg, Berlin and Vienna.
- Hubbs, C. L., and K. F. Lagler. 1947. Fishes of the Great Lakes Region. Cranbrook Institute Publication Series 26:1–186.
- Janensch, W. 1925. Fische aus dem Dysodil des Wealden vom Libanon. *Zeitschrift der Deutschen Geologischen Gesellschaft, Abhandlungen* 76:54–59.
- Jessen, H. 1972. Schultergürtel und Pectoralflosse bei Actinopterygii. *Fossil and Strata* 1:1–101.
- Jollie, M. 1962. Chordate Morphology. Reinhold Publishing, New York, 478 pp.
- Jollie, M. 1975. Development of the head skeleton and pectoral girdle in *Esox*. *Journal of Morphology* 147:61–88.
- Kner, R. 1866. Die fossilen Fische der Asphaltchiefer von Seefeld in Tirol. *Sitzungsberichte der Akademie der Wissenschaften in Wien* 54:303–334.
- Kner, R. 1867. Nachtrag zur Fossilen Fauna der Asphaltchiefer von Seefeld in Tirol. *Sitzungsberichte der Akademie der Wissenschaften in Wien* 56:898–913.
- Lambers, P. 1992. On the ichthyofauna of the Solnhofen Lithographic Limestone (Upper Jurassic, Germany). Rijksuniversiteit Groningen, Groningen, The Netherlands, 336 pp.
- Lehman, J.-P. 1966. Actinopterygii; pp. 1–243 in J. Piveteau (ed.), *Traité de Paléontologie* 4, Part 3. Masson et Cie, Paris.
- Li, G.-Q., and M. V. H. Wilson. 1996. Phylogeny of Osteoglossomorpha; pp. 167–174 in M. L. J. Stiassny, L. R. Parenti, and G. D. Johnson (eds.), *Interrelationships of Fishes*. Academic Press, San Diego.
- Lombardo, C., and A. Tintori. 2004. New perleidiforms from the Triassic of the Southern Alps and the revision of *Serrrolepis* from the Triassic of Wütemberg (Germany); pp. 179–196 in G. Arratia and A. Tintori (eds.), *Mesozoic Fishes 3—Systematics, Paleoenvironments and Biodiversity*. Verlag Dr. F. Pfeil, Munich.
- Lombardo, C., Z.-Y. Sun, A. Tintori, D.-Y. Jiang, and W.-C. Hao. 2011. A new species of the genus *Perleidus* (Actinopterygii: Perleidiformes) from the Middle Triassic of southern China. *Bollettino della Società Paleontologica Italiana* 50:75–83.
- López-Arbarello, A., O. W. M. Rauhut, and E. Cerdeño. 2010. The Triassic fish faunas of the Cuyana Basin, western Argentina. *Paleontology* 53:249–276.
- López-Arbarello, A., O. W. M. Rauhut, and K. Moser. 2008. Jurassic fishes of Gondwana. *Revista de la Asociación Geológica Argentina* 63:586–612.
- Mainwaring, A. J. 1978. Anatomical and systematic revision of the Pachycormidae, a family of Mesozoic fossil fishes. Ph.D. dissertation, Westfield College, London, 127 pp.
- Maisey, J. 1991. Santana Fossils: An Illustrated Atlas. T. F. H. Publications, Neptune City, New Jersey, 459 pp.
- McAllister, D. 1968. Evolution of branchiostegals and classification of teleostome fishes. *Bulletin of the National Museum of Canada, Ottawa* 221:1–239.
- Monod, T. 1968. Le complexe urophore des poissons téléostéens. Mémoires, Institute Fondamental d'Afrique Noire 81:1–705.
- Müller, J. 1845. Über den Bau und die Grenzen der Ganoiden, und über das natürliche System der Fische. Physikalisch-Mathematische Abhandlungen der königlichen Akademie der Wissenschaften zu Berlin 1845:117–216.
- Nelson, G. J. 1972. Cephalic sensory canals, pit-lines, and the classification of esocoid fishes, with notes on galaxiids and other teleosts. *American Museum Novitates* 2492:1–49.
- Nelson, J. S. 2006. Fishes of the World, fourth edition. J. Wiley & Sons, New York, 607 pp.
- Northcutt, G. 1989. The phylogenetic distribution and innervation of craniate mechanoreceptive lateral lines; pp. 17–78 in S. P. Coombs, P. Görner, and H. Münz (eds.), *The Mechanosensory Lateral Line*. Springer, New York.
- Nursall, R. 1996. The phylogeny of pycnodont fishes; pp. 125–152 in G. Arratia and G. Viöhl (eds.), *Mesozoic Fishes—Systematics and Paleoecology*. Verlag Dr. F. Pfeil, Munich.
- Nursall, R. 1999. The pycnodontiform bauplan; pp. 189–214 in G. Arratia and H.-P. Schultz (eds.), *Mesozoic Fishes 2—Systematics and Fossil Record*. Verlag Dr. F. Pfeil, Munich.
- Nybelin, O. 1963. Zur Morphologie und Terminologie des Schwanzskelettes der Actinopterygier. *Arkiv för Zoologi* 15:485–516.
- Nybelin, O. 1966. On certain Triassic and Liassic representatives of the family Pholidophoridae s. str. *Bulletin of the British Museum (Natural History), Geology* 11:351–432.
- Nybelin, O. 1974. A revision of the leptolepid fishes. *Acta Regiae Societatis Scientiarum et Litterarum Gothoburgensis, Zoologica* 9:1–202.
- Patterson, C. 1968. The caudal skeleton in Lower Liassic pholidophorid fishes. *Bulletin of the British Museum (Natural History), Geology* 16:202–239.
- Patterson, C. 1973. Interrelationships of holosteans; pp. 233–305 in P. H. Greenwood, R. S. Miles, and C. Patterson (eds.), *Interrelationships of Fishes*. *Zoological Journal of the Linnean Society* 53, Supplement 1.
- Patterson, C. 1975. The braincase of pholidophorid and leptolepid fishes, with a review of the actinopterygian braincase. *Philosophical Transactions of the Royal Society of London B* 269:275–579.
- Patterson, C. 1977a. The contribution of paleontology to teleostean phylogeny; pp. 579–643 in P. C. Hecht, P. C. Goody, and B. M. Hecht (eds.), *Major Patterns in Vertebrate Evolution*. NATO Advanced Study Institute, Series 14. Plenum Press, New York.
- Patterson, C. 1977b. Cartilage bones, dermal bones and membrane bones, or the exoskeleton versus the endoskeleton; pp. 77–121 in S. M. Andrews, R. S. Miles, and A. D. Walker (eds.), *Problems in Vertebrate Evolution*. Linnean Society Symposium Series, Number 4.
- Patterson, C. 1982. Morphology and interrelationships of primitive actinopterygian fishes. *American Zoologist* 22:241–259.
- Patterson, C., and G. D. Johnson. 1995. The intermuscular bones and ligaments of teleostean fishes. *Smithsonian Contributions to Zoology* 559:1–85.
- Patterson, C., and D. E. Rosen. 1977. Review of ichthyodectiform and other Mesozoic teleost fishes and the theory and practice of classifying fossils. *Bulletin of the American Museum of Natural History* 158:81–172.
- Pinna, M. de. 1991. Concepts and test of homology in the cladistic paradigm. *Cladistic* 7:367–394.
- Pinna, M. de. 1996. Teleostean monophyly; pp. 147–162 in M. L. J. Stiassny, L. R. Parenti, and G. D. Johnson (eds.), *Interrelationships of Fishes*. Academic Press, San Diego.
- Poplin, C. 2004. The dermosphenotic in early actinopterygians, a nomenclatural problem; pp. 165–178 in G. Arratia and A. Tintori (eds.), *Mesozoic Fishes 3—Systematics, Paleoenvironments and Biodiversity*. Verlag Dr. F. Pfeil, Munich.
- Regan, C. T. 1923. The skeleton of *Lepidosteus*, with remarks on the origin and evolution of the lower actinopterygian fishes. *Proceeding of the Zoological Society of London* 1923:445–461.
- Remane, A. 1952. Die Grundlagen des natürlichen Systems, der vergleichenden Anatomie und der Phylogenetik. Akademische Verlags-gellschaft Geest & Portig, Leipzig.
- Remane, A. 1955. Morphologie als Homologienforschung. *Zoologische Anzeiger*, Supplement 18:159–183.
- Rieppel, O. 1994. Homology, topology, and typology: the history of modern debates; pp. 63–100 in B. K. Hall (ed.), *Homology. The Hierarchical Basis of Comparative Biology*. Academic Press, San Diego, New York, Boston.
- Rusconi, C. 1946. Nuevos peces triásicos de El Challao, Mendoza. *Revista de la Sociedad de Historia y Geografía de Cuyo* 1:1–15.
- Rusconi, C. 1947. Mas peces triásicos de Mendoza. *Anales de la Sociedad Científica Argentina* 143:21–24.

- Saint-Seine, P. de. 1955. Poissons fossiles de l'étage de Stanleyville (Congo Belge). Première partie: la faune des argillites et schistes bitumineux. Annales du Musée Royal du Congo Belge, Tervuren (Belgique), Série in-8°, Sciences géologiques 14:1–126.
- Schaeffer, B. 1972. A Jurassic fish from Antarctica. American Museum Novitates 2495:1–17.
- Schaeffer, B., and C. Patterson. 1984. Jurassic fishes from the western United States, with comments on Jurassic fish distribution. American Museum Novitates 2796:1–86.
- Schultze, H.-P. 1966. Morphologische und histologische Untersuchungen an den Schuppen mesozoischer Actinopterygier (Übergang von Ganoid- zu Rundschuppen). Neues Jahrbuch für Geologie und Paläontologie, Abhandlungen 126:232–312.
- Schultze, H.-P. 1977. Ausgangsform und Entwicklung der rhombischen Schuppen der Osteichthyes (Pisces). Paläontologischen Zeitschrift 51:152–168.
- Schultze, H.-P. 1996. The scales of Mesozoic actinopterygians; pp. 83–93 in G. Arratia and G. Viöhl (eds.), Mesozoic Fishes—Systematics and Paleoecology. Verlag Dr. F. Pfeil, Munich.
- Schultze, H.-P. 2008. Nomenclature and homologization of cranial bones in actinopterygians; pp. 23–48 in G. Arratia, H.-P. Schultze, and M. V. H. Wilson (eds.), Mesozoic Fishes 4—Homology and Phylogeny. Verlag Dr. F. Pfeil, Munich.
- Schultze, H.-P., and Arratia, G. 1986. Reevaluation of the caudal skeleton of actinopterygian fishes. I. *Lepisosteus* and *Amia*. Journal of Morphology 190:215–241.
- Schultze, H.-P., and Arratia, G. 1988. Reevaluation of the caudal skeleton of some actinopterygian fishes. II. *Hiodon*, *Elops* and *Albula*. Journal of Morphology 195:257–303.
- Schultze, G., and G. Arratia. 1989. The composition of the caudal skeleton of teleosts (Actinopterygii, Osteichthyes). Zoological Journal of the Linnean Society 97:189–231.
- Schultze, G., and G. Arratia. 2013. The caudal skeleton of basal teleosts, its conventions, and some of its major evolutionary novelties in a temporal dimension; pp. 187–246 in Arratia, G., H.-P. Schultze, and M. V. H. Wilson (eds.), Mesozoic Fishes 5—Global Diversity and Evolution. Verlag Dr. F. Pfeil, Munich.
- Schultze H.-P., and S. Cumbara. 2001. *Dialipina* and the characters of basal actinopterygians; pp. 315–332 in P. E. Ahlberg (ed.), Major Events in Early Vertebrate Evolution, Palaeontology, Phylogeny, Genetics and Development. Taylor & Francis, London.
- Su, D. 1983. On Late Mesozoic fish fauna from Xiujiang (Sinkiang, China). Memoirs of the Institute of Vertebrate Palaeontology and Palaeoanthropology, Academia Sinica 17:61–136. [Chinese with English summary]
- Swofford, D. L. 2000. PAUP*: Phylogenetic Analysis Using Parsimony (*And Other Methods), version 4.0 beta. Sinauer Associates, Sunderland, Massachusetts.
- Taverne, L. 1975. Considérations sur la position systématique des genres fossiles *Leptolepis* et *Allotrichissops* au sein des téléostéens primatives et sur l'origine et le polyphylétisme des poissons téléostéens. Académie Royale de Belgique, Mémoires de la Classe des Sciences, série 5 61:336–371.
- Taverne, L. 1977. Ostéologie, phylogénèse et systématique des Téléostéens fossiles et actuels du super-ordre des Ostéoglossomorphes. Première partie. Ostéologie des genres *Hiodon*, *Eohiodon*, *Lycoptera*, *Osteoglossum*, *Scleropages*, *Heterotis* et *Arapaima*. Académie Royale de Belgique, Mémoires de la Classe des Sciences, Collection in-8°, 2. série 42:1–235.
- Taverne, L. 1999. Ostéologie et position systématique d'*Arratiaelops vectensis*, gen. nov., téléostéen élopiforme du Wealdien (Crétacé inférieur) d'Angleterre et de Belgique. Bulletin de l'Institut Royal des Sciences Naturelles de Belgique, Sciences de la Terre 69: 77–96.
- Taverne, L. 2011a. Ostéologie et relations phylogénétiques de *Steurbautichthys* ("*Pholidophorus*") *aequatorialis* gen. nov. (Teleostei, "Pholidophoriformes") du Jurassique moyen de Kisangani, en République Démocratique du Congo. Bulletin de l'Institut Royal des Sciences Naturelles de Belgique, Sciences de la Terre 81:129–173.
- Taverne, L. 2011b. Ostéologie et relations de *Catervariolus* (Teleostei, "Pholidophoriformes") du Jurassique moyen de Kisangani (Formation de Stanleyville) en République Démocratique du Congo. Bulletin de l'Institut Royal des Sciences Naturelles de Belgique, Sciences de la Terre 81:175–212.
- Taverne, L. 2011c. Ostéologie et relations de *Ligulella* (Halecostomi, Ligulelliformes nov. ord.) poissons du Jurassique moyen de Kisangani en République Démocratique du Congo. Bulletin de l'Institut Royal des Sciences Naturelles de Belgique, Sciences de la Terre 81:175–212.
- Tintori, A. 1990. The actinopterygian fish *Prohalecites* from the Triassic of northern Italy. Palaeontology 33:155–174.
- Tintori, A., and D. J. Sassi. 1992. *Thoracopterus* Brönn (Osteichthyes, Actinopterygii): a gliding fish from the Upper Triassic of Europe. Journal of Vertebrate Paleontology 12:265–283.
- Toombs, H. A., and A. E. Rixon. 1959. The use of acids in the preparation of vertebrate fossils. Curator 2:304–312.
- Wade, R. T. 1940. The Triassic fishes of Gosford, New South Wales. Journal and Proceedings of the Royal Society of New South Wales 73:206–217.
- Wade, R. T. 1941. The Jurassic fishes of New South Wales. Journal and Proceedings of the Royal Society of New South Wales 75:71–84.
- Waldman, M. 1971. Fish fauna from the freshwater Lower Cretaceous of Victoria, Australia with comments on the palaeoenvironment. Special Papers in Paleontology 9:1–62.
- Webb, J. F. 1989. Gross morphology and evolution of the mechanoreceptive lateral-line system in teleost fishes. Brain Behavior and Evolution 33:34–53.
- Wenz, S. 1968. Complements à l'étude des poissons actinopterygiens du Jurassique français. Centre National de la Recherche Scientifique, Paris, 276 pp.
- Westoll, T. S. 1943. The origin of the tetrapods. Biological Reviews 18:78–98.
- Wilder, B. G. 1877. On the serrated appendages of the throat of *Amia*. Proceedings of the American Association for the Advancement of Science 1877:259–263.
- Wiley, E. O. 1976. The phylogeny and biogeography of fossil and recent gars (Actinopterygii: Lepisosteidae). University of Kansas Miscellaneous Publications 64:1–111.
- Wiley, E. O., and Lieberman, B. S. 2011. Phylogenetics. The Theory of Phylogenetic Systematics. Wiley-Blackwell, Singapore, 406 pp.
- Woodward, A. S. 1890. The fossil fishes of the Hawkesbury Series at Gosford. Memoirs of the Geological Survey of New South Wales (Palaeontographic Series) 4:1–56.
- Woodward, A. S. 1895. Catalogue of the Fossil Fishes in the British Museum (Natural History). Part III (Pholidophoridae). Trustees of the British Museum of Natural History, London, 544 pp.
- Woodward, A. S. 1941. The Mesozoic ganoid fishes of the genus *Pholidophorus* Agassiz. Annals and Magazine of Natural History Series 11 8:88–91.
- Xu, G.-H., L.-J. Zhao, K.-Q. Gao, and F.-X. Wu. 2012. A new stem-neopterygian fish from the Middle Triassic of China shows the earliest over-water strategy of the vertebrates. Proceedings of the Royal Society B 280:1–7. doi: 10.1098/rspb.2012–2261.
- Zambelli, R. 1975. Note sui Pholidophoriformes. I. *Parapholidophorus nybelini* gen. n. sp. n. Rendiconti Instituto Lombardo, Accademia di Scienze e Lettere 109:3–49.
- Zambelli, R. 1977. Note sui Pholidophoriformes. II. *Pholidoctenus serianus* gen. n. sp. n. Rendiconti della Accademia Nazionale dei Lincei, Part 5 3:101–123.
- Zambelli, R. 1980a. Note sui Pholidophoriformes. III contributo: *Pholidophorus gervasutii* sp. n. Revista del Museo Civico di Science Naturali "E. Caffi," Bergamo 1:5–44.
- Zambelli, R. 1980b. Note sui Pholidophoriformes. IV contributo: *Pholidorynchodon malzannii* gen. n. sp. n. Rivista del Museo Civico di Scienze Naturali "E. Caffi," Bergamo 2:129–168.
- Zambelli, R. 1980c. Note sui Pholidophoriformes. V contributo: Pholidophoridae dell' Alta Valvestine (Brescia, Italia). "Natura Bresciana," Annali del Museo Civico di Storia Naturale, Brescia 17:77–88.
- Zambelli, R. 1986. Note sui Pholidophoriformes. VI contributo: *Pholidophorinae* subfamiglia nuova del Triassico Superiore. Revista del Museo Civico di Scienze Naturali "E. Caffi," Bergamo 10:1–32.
- Zambelli, R. 1990. Note sui Pholidophoriformes. VII contributo. *Eopholidophorus forojuiliensis* n. g., n. sp. Gortania. Atti del Museo Friulano di Storia Naturale 11:63–76.
- Zhu, M., and H.-P. Schultze. 2001. Interrelationships of basal osteichthyans; pp. 289–314 in P. E. Ahlberg (ed.), Major Events in Early

Vertebrate Evolution, Paleontology, Phylogeny, Genetics and Development. Taylor & Francis, London.

Submitted January 10, 2013; revisions received July 10, 2013; accepted August 11, 2013.

Handling editor: Jeffrey A. Wilson.

APPENDIX 1. List of characters, organized by body region. The coding of characters is based on outgroup comparison. Character states are represented by 0, 1, 2, 3, and 4. The dash [–] represents an inapplicable character state. Multistate characters are unordered. The data matrix is from Arratia (2000) with the addition of 29 new characters (1, 6, 8, 9, 10, 15, 16, 17, 20, 21, 22, 37, 42, 53, 68, 70, 73, 74, 81, 90, 108, 109, 114, 119, 120, 147, 155, 156, and 157). Characters from other authors are identified below.

Neurocranium and Skull Roof

- (1) All skull roof bones fused into a plate: absent [0]; present [1].
- (2) Postparietal [= parietal of tetrapods] bones: independent [0]; fused to each other [1]; fused with other skull bones [2].
- (3) Skull roof: no distinct broadening between orbital and postorbital regions [0]; orbital region slightly narrower than postorbital one [1]; narrow orbital region versus a broad postorbital region—about four times broader or more [2].
- (4) Ratio of preorbital snout length to postorbital head length: less than 1.2 [0]; 1.5 or greater [1] (Grande, 2010).
- (5) Parietal bones [= frontal of tetrapods] acutely sharp anteriorly and sutured with rostral by a narrow contact: absent [0]; present [1].
- (6) Roughly rhomboidal rostral bone with well-developed, distinct lateral processes: absent [0]; present [1].
- (7) Large compound rostrodermethmoid: absent [0]; present [1]. (Interpretation of rostrodermethmoid after Mainwaring, 1978, and Lambers, 1992.)
- (8) Teeth on rostrodermethmoid: uniform in size [0]; combination of large tusk-like tooth and small dentition [1].
- (9) Toothed lateral dermethmoids joined to premaxillaries laterally: absent [0]; present [1].
- (10) Autosphenotic with small dermal component: absent [0]; present [1] (Grande, 2010).
- (11) Basisphenoid: present [0]; absent [1].
- (12) Large orbitosphenoid bone: absent [0]; present [1].
- (13) Supraoccipital bone: absent [0]; present [1].
- (14) Occipital process formed by fusion of intercalar and au-topteroitic: absent [0]; present [1] (Brito, 1997).
- (15) Temporal boss (enlargement of temporal-supratemporal region): absent [0]; present [1].
- (16) Temporal boss: poorly developed, scarcely rising above the surface of the skull roof [0]; well developed, extending above and in front of postparietal region [1].
- (17) Extrascapular bone with a large rollover bony layer at the anterior region of the bone: absent [0]; present [1].
- (18) Sutures between all cartilage bones in the braincase retained throughout life, rather than being lost ontogenetically: absent [0]; present [1].
- (19) Interparietal [= interfrontal] suture: smooth [0]; serrated [1]; absent [–].
- (20) Nasal bones: joined in midline [0]; completely separated from each other by the parietal bones [= frontals of tetrapods] [1].
- (21) Nasal bone with a large foramen forming the wall of the posterior nostril: absent [0]; present [1].
- (22) Lateral margin of nasal bone joining medial margin of an elongate antorbital: absent [0]; present [1].

- (23) Nasal bone forming part of the orbital margin: absent [0]; present [1].
- (24) Vomer (in adult individuals): paired [0]; unpaired [1].
- (25) Parasphenoid: with small teeth [0]; toothless [1]; with large teeth [2].
- (26) Long parasphenoid extending posterior to basioccipital: absent [0]; present [1].
- (27) Primary bite between parasphenoid and basihyal: absent [0]; present [1].
- (28) Osified aortic canal: present [0]; absent [1].
- (29) Canals for occipital arteries in basioccipital bone: present [0]; absent [1].
- (30) Spiracular canal: developed [0]; greatly reduced [1]; absent [2].
- (31) Anterior myodome: present [0]; absent [1].
- (32) Foramen for glossopharyngeal nerve positioned in exoccipital: absent [0]; present [1].
- (33) Foramen for vagus nerve placed in posterolateral face of exoccipital alone: absent [0]; present [1].
- (34) Supraorbital canal with: branched tubules [0]; simple tubules [1].
- (35) Supraorbital canal and infraorbital canal: join within the parietal [= frontals of tetrapods] bone [0]; within the dermopterotic [1]; within the dermosphenotic [2]; do not join [3].
- (36) Middle pit-line groove crossing the dermopterotic (or pterotic): present [0]; absent [1].
- (37) Skull roof bones covered by layer of ganoine densely ornamented with ridges and/or tubercles of ganoine: absent [0]; present [1].

Circumorbital Bones

- (38) Antorbital bone: present [0]; absent [1].
- (39) Antorbital bone: carrying a bony enclosed portion of the infraorbital sensory canal (= antorbital branch) [0]; antorbital branch absent [1].
- (40) Tube-like canal bearing anterior arm of antorbital: absent [0]; present [1] (Grande, 2010).
- (41) A long, narrow tube-like infraorbital 1: absent [0]; present [1].
- (42) Posterior region of infraorbital 3 extending below suborbital bone and reaching anterior margin of preopercle: absent [0]; present [1]; no suborbital or tube-like infraorbital [–].
- (43) Narrow, long infraorbital (3 plus 4 and 5) forming the ventro-posterior part of circumorbital ring: absent [0]; present [1].
- (44) Fourth infraorbital bone: small [0]; expanded, broad bone [1]; bone is fused with another infraorbital or has some other morphology [–].
- (45) Fourth and fifth infraorbital bones: separated [0]; fused forming an expanded bone [1]; bones are fused with another infraorbital or have some other morphology [–].
- (46) More than six small, roughly posterodorsal infraorbital bones: absent [0]; present [1].
- (47) Suborbital(s): none [0]; one [1]; two or three [2]; many [3].
- (48) One or two accessory suborbital bones positioned ventrolateral to postorbital region of skull roof: absent [0]; present [1].
- (49) Supraorbital bones: two or more [0]; one [1]; none [2].
- (50) Sclerotic ring: absence of bones [0]; complete ring of two sclerotic bones oriented anterior and posterior to eye [1]; an incomplete ring of two sclerotic bones oriented anterior and posterior to eye [2].

Jaws

- (51) Elongated jaws bearing numerous villiform teeth: absent [0]; present [1].

- (52) Premaxillary teeth: placed at an angle of about 90 degrees to the premaxilla [0]; placed obliquely to the premaxilla (posteriorly directed teeth) [1].
- (53) Ascending process on premaxilla: absent [0]; present [1].
- (54) Premaxilla forming a rostral tube that projects into the ethmoidal region: absent [0]; present [1] (Brito, 1997).
- (55) Mobile premaxilla: absent [0]; present [1].
- (56) Maxilla: elongate, extending behind orbit [0]; moderately long, extending below the orbit [1]; very short, anterior to orbit [2].
- (57) Posterior margin of maxilla: rounded or straight [0]; notched or concave [1]; acute [2]; irregularly shaped [3].
- (58) Supramaxillary process on dorsal margin of maxilla: absent [0]; present [1].
- (59) Supramaxillary bone(s): one [0]; none [1]; two [2].
- (60) Long supramaxillary bone covering most of dorsal margin of maxilla: absent [0]; present [1].
- (61) Supramaxillary bone: dorsal to maxilla [0]; posterior to maxilla [1].
- (62) Quadrate-mandibular articulation: posterior to orbit [0]; below the posterior half of orbit [1]; below anterior half of orbit [2]; anterior to orbit [3].
- (63) Articular bone: not fused with angular and/or retroarticular bones [0]; fused with angular and retroarticular [1]; fused with angular forming an anguloarticular [2].
- (64) Postarticular process of lower jaw: poorly developed or not developed [0]; well developed [1].
- (65) Notch (= 'leptolepid' notch) in the ascending margin of dentary: absent [0]; present [1].
- (66) Coronoid bone(s) in lower jaw: present [0]; absent [1].
- (67) Surangular bone in lower jaw: present [0]; absent [1].
- (68) Prearticular bone in lower jaw: present [0]; absent [1].
- (69) Coronoid process of lower jaw formed by: surangular and dentary [0]; surangular [1]; dentary and angular [2]; no process [3]; only dentary [4].
- (70) A well-developed, protruding lateral bony ridge extending along the dentary and separating dental and splenial regions: absent [0]; present [1].
- (71) Toothed predentary in lower jaw: absent [0]; present [1].
- (72) Predentary: short, less than half the length of the premaxillary tube [0]; almost as long as the premaxillary tube [1].
- (73) Maxilla heavily ornamented with characteristic longitudinal ridges of ganoine: absent [0]; present [1].
- (74) Supramaxilla(e) heavily ornamented with characteristic longitudinal or concentric ridges of ganoine: absent [0]; present [1].

Palatoquadrate, Hyoid Arch, and Urohyal

- (75) Autopalatine bone: present [0]; absent [1].
- (76) Elongation of the suspensorium due to the posteroventral inclination of the hyomandibula: absent [0]; present [1].
- (77) Hyomandibular bone with a preopercular process at its posterior margin: absent [0]; present [1].
- (78) Elongated posterodorsal or posteroventral process of quadrate (depending on the angle of the quadrate): absent [0]; present [1].
- (79) Symplectic: articulates with lower jaw [0]; does not articulate with lower jaw [1].
- (80) Symplectic: posterior to the posterior margin of quadrate [0]; medial to the posterior margin of quadrate [1].
- (81) Quadrate and metapterygoid: close together and articulated with each other [0]; distant to each other [1].
- (82) Two ossified hypohyals: absent [0]; present [1].
- (83) Urohyal formed as an unpaired tendon bone of the sternohyoideus muscle: absent [0]; present [1].

Opercular Bones, Branchiostegals, and Gular Plates

- (84) Anterior extent of preopercle: not extending below anterior region of orbit [0]; extending below anterior region of orbit [1].
- (85) Posteroventral region of preopercle: narrow or slightly expanded [0]; broadly expanded in a distinct pattern [1].
- (86) Preopercular sensory canal with long tubules opening on the ventral and posteroventral borders of the preopercle: absent [0]; present [1].
- (87) Very posterior position of the preopercular sensory canal in a peculiarly shaped preopercle: absent [0]; present [1].
- (88) Preopercle with a notch at its anteroventral margin and inverted heart-like shape: absent [0]; present [1].
- (89) Notch at the posteroventral margin of preopercle: absent [0]; present [1].
- (90) Crescent-shaped preopercle: absent [0]; present [1].
- (91) Irregular parallelogram, oval, or kidney-shaped opercular bone: absent [0]; present [1] (Li and Wilson, 1996).
- (92) Interopercle: present [0]; absent [1].
- (93) Median gular plate: present [0]; absent [1].

Vertebrae and Intermuscular Bones

- (94) Two vertebral centra fused into occipital condyle in adults: absent [0]; present [1].
- (95) Opisthoceolous centra with convex anterior articular surface and concave posterior surface: absent [0]; present [1].
- (96) Each vertebral centrum of the caudal region of adult individuals formed by: chordacentrum [0]; chordacentrum surrounded by autocentra [1]; chordacentrum surrounded by arcocentra [2].
- (97) Mid-caudal vertebral autocentra: thin and smooth [0]; thick and sculptured [1].
- (98) Walls of mid-caudal centra: without cavities for adipose tissue [0]; with cavities for adipose tissue [1].
- (99) Notochord strongly constricted by the walls of the centra: absent [0]; present [1].
- (100) Diplospondyly in mid-caudal region: absent [0]; present [1].
- (101) Neural spines of caudal vertebrae: paired [0]; unpaired [1].
- (102) Long epineural process of neural arch in adult individuals: absent [0]; present [1].
- (103) Epipleural intermuscular bones: absent [0]; present [1].
- (104) Epipleural intermuscular bones: few bones in the anterior caudal region [0]; many bones [1].

Pectoral and Pelvic Girdles, and Axillary Processes

- (105) Posttemporal with a small body and distinct, strong, sharp dorsal process to articulate with cranium: absent [0]; present [1].
- (106) Supracleithrum with main lateral line emerging: at its upper half [0]; at its posteroventral margin [1].
- (107) Postcleithrum(a): one or two (0); three or more (1); none (2).
- (108) Serrated appendages: anterior and posterior toothed elements present on the ventral arm of cleithrum [0]; one long, toothed element covering the whole medial surface of cleithrum [1]; one long, narrow element covering the medial border of cleithrum [2]; absent [3].
- (109) Clavicle articulated to the anteroventral margin of cleithrum: absent [0]; present [1].
- (110) Four pectoral proximal radials: absent [0]; present [1].
- (111) Pectoral propterygium fused with first ray: absent [0]; present [1].
- (112) A compound first pectoral ray fused with basal fulcra; absent [0]; present [1].

- (113) Pectoral axillary process: absent [0]; present [1].
- (114) Fringing fulcra associated with the leading margin of the pectoral fin: present [0]; absent [1].
- (115) Pectoral fin scythe-like: absent [0]; present [1].
- (116) Pelvic axillary process: absent [0]; present [1].
- (117) Pelvic axillary process formed by: an elongate bony element [0]; a combination of bony elements and modified scales [1]; modified scales [2].

Dorsal and Anal Fins

- (118) Dorsal fin placed posteriorly, closer to caudal fins than to pelvic fins: present [0]; absent [1].
- (119) Fringing fulcra on leading margin of dorsal fin: present [0]; absent [1].
- (120) Fringing fulcra on leading margin of anal fin: present [0]; absent [1].

Caudal Skeleton

- (121) Preural vertebrae (excluding preural centrum 1) of adult individuals with haemal arches: autogenous [0]; laterally fused to their respective autocentra [1].
- (122) Neural spine of preural centrum 2: as long as neural spine of preural centrum 3 [0]; shorter than neural spine of preural centrum 3 [1].
- (123) Neural spine of preural centrum 1: long, close or extending to the dorsal margin of the body [0]; rudimentary or short [1]; absent [2].
- (124) Parhypural in adults: autogenous [0]; laterally fused with its centrum [1].
- (125) Neural spine of ural centrum 1 (diural terminology; adults): absent [0]; present [1]; fused elements [–].
- (126) Neural arch over first ural centrum (adults): complete [0]; reduced or absent [1]; fused elements [–].
- (127) Number of ural centra (in adults): more than two [0]; commonly two [1]; no ural centra [2].
- (128) Cartilaginous ‘elopomorph’ neural arch above ural centra: absent [0]; present [1].
- (129) Number of epural(s): five or more [0]; three or four [1]; one [2]; none [3].
- (130) Some of the preural neural arches modified as uroneural-like bones: absent [0]; present [1]. (For information concerning uroneural-like bones, see Arratia and Lambers, 1996; Arratia and Schultze, 2013; Schultze and Arratia, 2013.)
- (131) Only ural neural arches modified as uroneurals: absent, additional components included [0]; present [1]; uroneurals absent [–].
- (132) Number of ural neural arches modified as uroneurals: none [0]; seven or more [1]; six [2]; five or four [3]; three or less [4]; uroneurals absent [–].
- (133) Anterior most uroneurals present as: a group of three or four long separate elements [0]; one or two long, separate uroneural(s) [1]; uroneurals absent [–].
- (134) All uroneurals: inclined toward the horizontal, one beside the other [0]; at different angles [1]; uroneurals absent [–].
- (135) Two uroneurals (rather than three or four) extending beyond the second ural centrum (diural terminology): absent [1]; present [2]; another condition, e.g., absence of uroneurals [–].
- (136) Hypural 8: present in adult individuals [0]; absent [1]; another condition, e.g., fusion of elements [–].
- (137) Hypural 7: present [0]; absent [1]; fusion of elements [–].
- (138) Hypural 6: present [0]; absent [1]; fusion of elements [–].

- (139) Hypurals fused into a plate: absent [0]; present [1].
- (140) Bases of hypurals 1 and 2: not joined by cartilage [0]; joined by cartilage (and/or bone) in some growth stages [1]; fusion of elements [–].
- (141) A diastema between hypurals 2 and 3: absent [0]; present [1]; fusion of elements [–].
- (142) Arrangement of hypurals and caudal fin rays: each hypural normally articulated with one caudal ray [0]; each hypural normally articulated with a few caudal rays [1]; a hypural plate articulated with many rays [2] (modified from Grande and Bemis, 1998).
- (143) Epaxial caudal basal fulcra: present [0]; absent [1].
- (144) Hypaxial basal fulcra: present [0]; absent [1].
- (145) Epaxial basal fulcra or epaxial procurrent rays are in close proximity to: epurals and posterior uroneurals [0]; neural spines, epurals, and posterior uroneurals [1]; absence of structures, e.g., uroneurals [–].
- (146) Epaxial procurrent rays: absent [0]; present [1].
- (147) Long and narrow fringing fulcra: absent [0]; present [1].
- (148) Number of principal caudal rays: fewer than 19 [0]; 27 to 30 [1]; 20 to 26 [2]; 19 [3]; more than 40 rays [4].
- (149) First and last principal caudal rays forming the leading margins of the caudal fin: absent [0]; present [1].
- (150) Dorsal processes of the bases of the innermost principal caudal rays of dorsal lobe of the caudal fin: absent [0]; present [1].
- (151) All or some principal caudal rays with: straight segmentation [0]; Z-like segmentation [1].
- (152) Tendon-bone ‘urodermals’: none [0]; two [1]; one [2]. (For an explanation on tendon-bone urodermals see Arratia and Schultze, 1992.)
- (153) One large dorsal scute preceding caudal fin: absent [0]; present [1].
- (154) Posterior margin of caudal fin convexly rounded: absent [0]; present [1].
- (155) Caudal fin homocercal (internally): absent [0]; present [1].

Scales

- (156) Scales: ganoid of lepisosteoid type [0]; elasmoid of amioid type [1]; elasmoid of cycloid type [2].
- (157) 157. Cycloid scales with circuli crossed by transverse lines in the middle field: absent [0]; present [1]; other type of scale [–].
- (158) 158. Cycloid scale with crenulate posterior margin: absent [0]; present [1]; other type of scale [–].
- (159) Ganoid scales with posterior margin: smooth [0]; serrated [1]; other type of scale [–].
- (160) Ganoid scales with: smooth surface [0]; ornamented surface [1]; other type of scale [–].
- (161) Layer of ganoine on scales densely ornamented with ridges and/or tubercles of ganoine: absent [0]; present [1]; other type of scale [–].
- (162) Three rows of ganoid mid-flank scales distinctively deeper than long between the postcleithra and midpoint of the body length: absent [0]; present [1]; other type of scale [–].

Miscellaneous Characters

- (163) Narrow separation between olfactory organ and eye: present [0]; absent [1].
- (164) Accessory nasal sacs: absent [0]; present [1].
- (165) Craniotemporal muscle: absent [0]; present [1].
- (166) Very elongate, needle-like body: absent [0]; present [1].
- (167) Body: covered with scales [0]; devoid of squamation [1].

APPENDIX 2. Character-taxon matrix for 167 morphological characters in 41 taxa. Outgroups include halecomorphs (*Amia calva* and †*A. pattersoni*), lepisosteiforms (*Lepisosteus* and †*Obaichthys*), and a parasemionotid (†*Watsonulus*), and a neopterygian incertae sedis (†*Prohalecites*). Symbols for polymorphic conditions: \$ = 0/1; # = 1/2; * = 0/2; ^ = 0/3. See Appendix 1 for character list.

	0	0	0	0	0
	1	2	3	4	5
	0	0	0	0	0
<i>Amia calva</i>	0\$00000-01	00000-0000	0100000000	0000000001	0-01000020
<i>Amia pattersoni</i>	0000000-01	00000-0000	010000??0	?0?000001	0-01000020
<i>Anaethalion</i>	0010000-00	001?0-0101	0001000??2	?11300000	0-00000002
<i>Annaichthys</i>	1-10010-0?	?00?0-??1	101??0???	?????01010	0000001071
<i>Ankylophorus</i>	00001?0-1?	???0-0201	110???????	??\$2000?0	000-10100?
<i>Ascalabos</i>	0010000-00	201?0-0101	0001?00?22	?1?1?000?0	0-0000002?
<i>Aspidorhynchus</i>	02000-0-00	00010-0011	0001000???	00?0?00?-	0000002001
<i>Belonostomus</i>	02010-0-00	20010-0011	000?000???	0001?001--	0000002011
<i>Catervariolus</i>	0000000-00	01100-0?00	0001100???	?11302000	0-1-0210?
<i>Domeykos</i>	00100?0-00	001?0-0101	?01100??2	?1?1?20???	0-0?0000?2
<i>Elops</i>	0010000-00	00100-0101	0001000112	1111310000	0-01000012
<i>Eurycormus</i>	0000000-10	?0000-00?1	010?100???	?0?200000	0000001101
<i>Ichthyokentema</i>	0010000-10	00100-0100	00010001??	0111300000	0000-01001
<i>Heterotis</i>	0000000-00	00100-0100	0001100012	01113101--	1-0-100020
<i>Hiodon</i>	0010000-00	00100-0101	0001201112	01113101--	1-0-100020
<i>Hypsocormus</i>	00000-11?0	01000110001	00????00??0	0000?00???	0000012021
<i>Knerichthys</i>	1-200?0-??	?00?0-??1	???????????	?????1?0???	???????????
<i>Lehmanophorus</i>	00000?0-1?	???0-0??1	110???????	?0?1?000?0	020?????0?
<i>Leptolepis coryphaenoides</i>	0010000-00	00100-0001	0001000001	0001300000	0100001002
<i>Lepisosteus</i>	0001000-01	10000-0001	0000000000	1000100001	--0-03-00
<i>Luisichthys</i>	0010000-00	?0100-0101	2001000112	?111?10???	?-000000?2
<i>Lycoptera</i>	0010000-00	001?0-0101	0001201?22	?0?1?001--	1-0-100020
<i>Megalops</i>	0010000-00	00100-01?1	0001000112	1111310000	0-00000012
<i>Obaichthys</i>	0001000-01	10000-0001	00000000??	1?0?1001-1	-?0-0?20
<i>Orthocormus</i>	00000-11?0	01000180001	00????00??0	0?0?0?0???	0000012021
<i>Pachycormus</i>	00000-10?0	01000100001	0011?00??0	00?030000?	0000012021
<i>Parapholidophorus</i>	1-20110-00	?00?0-1?1	001?1?0???	?0?1310000	0\$00001101
<i>Dorsetichthys</i>	0010100-00	00100-0001	0001000000	0000300000	0100001001
<i>Pholidophorus gervasutti</i>	1-20110-00	?00?0-1?1	101?1?0???	?0?1?0000	0000001101
<i>Pholidophorus latiusculus</i>	1-201?0-20	???0-1?1	?1?1?00???	?0?130000?	010000100?
<i>Pholidophoretes</i>	1-200?0-20	??0?0-1?0	\$?1????0???	?0?130000?	010000100?
<i>Pholidoctenus</i>	1-20000-00	?00?0-1?0	001?1?0???	?0?1300000	0100001101
<i>Pholidorhynchodon</i>	1-20010-10	?00?0-1?1	111?1000??	?0?1301000	0100001101
<i>Prohalecites</i>	0\$00000-0?	20000-0000	010?100???	?0?13\$0000	0-0000200?
<i>Protoclupea</i>	0010?0?-20	?01?0-0101	0?0?200??2	?0?130000?	?-000000?2
<i>Siemensichthys macrocephalus</i>	0200100-10	?0100-0101	1101100?0?	000\$3000?0	0001\$00011
<i>Siemensichthys siemensi</i>	?000100-10	?00?0-0?01	???????????	????\$000???	?0?1?00???
<i>Tharsis</i>	0010000-00	00100-0101	000110011#	0101300000	0-00000012
<i>Varasichthys</i>	0010000-00	00100-0101	000?110112	1111300000	0-00000012
<i>Vinctifer</i>	02000-0-00	00010-0111	0001100?02	000?001--	0000002011
<i>Watsonulus</i>	0000000-01	11000-0000	00000000?0	0??3011-1	000000000?

	0	0	0	0	1
	6	7	8	9	0
	0	0	0	0	0
<i>Amia calva</i>	0000001100	0000000000	0-00000000	0000000001	00010????11
<i>Amia pattersoni</i>	0000001100	0000000000	0-00000000	0000000001	000?0????11
<i>Anaethalion</i>	1010180020	0?1?11120	0-00000111	0110000000	0000011110
<i>Annaichthys</i>	0010110020	02101?0?11	0-00?0????	0?20000100	00?200-0?
<i>Ankylophorus</i>	0010102?01	01?0?????1	0-00?????1	??0?00000	00?????????
<i>Ascalabos</i>	0010110020	0111111120	0-00000111	0110000000	0010011110
<i>Aspidorhynchus</i>	0001000000	1000000?30	1000?000?0	0000001000	\$1?02-000
<i>Belonostomus</i>	0001000000	1000000?30	1100?00010	0000001000	\$1?02-000
<i>Catervariolus</i>	001010\$000	0100\$0000	0-?2000111	00?2000000	0000011?01
<i>Domeykos</i>	0010?20020	0111111120	0-00?0?111	0?2?0110000	00?2011110
<i>Elops</i>	1010100020	0001011120	0-00000111	01100\$0000	0000011110
<i>Eurycormus</i>	0000010020	01?00?00?0	0-00?00?0	?000000000	000000-001
<i>Ichthyokentema</i>	0010110000	011?101121	0-00000111	0?20000001	000?20?0?
<i>Heterotis</i>	001012001-	-101011140	0-00100111	011000000?	1010011110
<i>Hiodon</i>	001011001-	-101011120	0-00100111	0110000000	1010011110
<i>Hypsocormus</i>	01000000??	?00000?030	0-00?1?0???	??20000000	000?------
<i>Knerichthys</i>	00?0?0#?00	00?01????1	0-11??????	??20000000	00?????????
<i>Lehmanophorus</i>	0010102?20	01?2?????1	0-?20?0?0??	??20000000	00?????????
<i>Leptolepis coryphaenoides</i>	0010110020	0111111121	0-00000111	0110000000	0000010000
<i>Lepisosteus</i>	20000230*0	0300000010	0-00?00000	1001000000	01011?000
<i>Luisichthys</i>	00?01?0020	01?1?11?20	0-00?0?111	0?2?0110000	0000011110
<i>Lycoptera</i>	00101?001-	-1?0011120	0-00100111	0?2?000000	100?01\$0
<i>Megalops</i>	1010100020	0111011120	0-00000111	0110000000	0000011110
<i>Obaichthys</i>	0000023000	03000?0?10	0-00?00000	1001000000	00011?000
<i>Orthocormus</i>	01000000??	?0?000?0???	0-00?0?0???	??20000000	000?------
<i>Pachycormus</i>	0000?000???	10?0000030	0-00?1?0???	??20000000	000?------
<i>Parapholidophorus</i>	0010110020	01?0100?11	0-11?00?00	0?00000100	000?00-001
<i>Dorsetichthys</i>	0010100020	0111110111	0-10?00111	0?00010010	000?00-00
<i>Pholidophorus gervasutii</i>	001010#020	00?01?0?11	0-11?100\$	0?02000010	000?00-001
<i>Pholidophorus latiusculus</i>	00?0100020	00?01????1	0-11?0????	??20000010	000?0?0???
<i>Pholidophoretes</i>	00?0?110*0	01?0?????1	0-11?0????	??20000001	000?0?0???
<i>Pholidoctenus</i>	001011\$020	01?01?0?11	0-11?0?0\$?	??20000001	000?00-001
<i>Pholidorhynchodon</i>	0010100020	0010100011	0-11?100??	0?00000110	000?00-002
<i>Prohalecites</i>	0010?10010	-0000?0?00	0-00?000??	?000000001	00?200--1
<i>Protoclupea</i>	00?0??0?020	-111111120	0-00?00111	01?0110000	00?2011110
<i>Siemensichthys macrocephalus</i>	0010102001	-0101?0010	0-00?0?111	01?0010000	000002-0?
<i>Siemensichthys siemensi</i>	00?0100001	-010?0010	0-00?0?1?1	0?2?0010000	000???????
<i>Tharsis</i>	0010110020	-111111120	0-00001111	0110011000	0000011110
<i>Varasichthys</i>	001011020	-120111120	0-00001111	0110110000	0000011110
<i>Vinctifer</i>	0001000020	-000011?30	1000?00000	0000001000	?11002-000
<i>Watsonulus</i>	00000001100	0000000000	0-00?00000	0000000000	100?0???????

	1	1	1	1	1
	1	2	3	4	5
	0	0	0	0	0
<i>Amia calva</i>	100-000000	000100-011	00000-0010	-0---0000	0011-1-000
<i>Amia pattersoni</i>	100-0?0000	000100-011	00000-0010	-0---0000	0011-1?-00
<i>Anaethalion</i>	1110101301	1??10??111	1111101110	1310100001	1101100311
<i>Annaichthys</i>	??????011?	??20010100	???????????	???????????	?200?00200
<i>Ankylophorus</i>	???????????	??200?100	???????????	???????????	?200?0020?
<i>Ascalabos</i>	1110101301	1?0100-111	1111101010	1100000001	110100-311
<i>Aspidorhynchus</i>	\$00-002?0?	0?0100-000	\$0#0000030	140001110?	0100-10200
<i>Belonostomus</i>	100-002?0?	??1?0-000	0020000031	0400011100	\$100-01000
<i>Catervariolus</i>	111001011?	01000?100	00?0100000	1300000000	0?00?0030?
<i>Domeykos</i>	1110?130?	?211010111	1011101010	1101000001	111101-211
<i>Elops</i>	1111111301	1111012111	0110101110	1310110001	111111-310
<i>Eurycormus</i>	110-?00?20	010000-100	0120010001	0100000000	1100100001
<i>Ichthyokentema</i>	?0??1?030?	??2000-100	???????????	???????????	?200?022?
<i>Heterotis</i>	11111?0301	10?10?2011	1000002030	20?-01101	111111-010
<i>Hiodon</i>	1111101301	1011012011	1001101020	1300?10001	111111-010
<i>Hypsocormus</i>	#00-0?????	0?0?10-1??	0000-2-01	00----1-	-200-0040?
<i>Knerichthys</i>	?????0?0???	??200?100	?????----?	???????????	?200?00100
<i>Lehmanophorus</i>	???????????	??200?2100	???????????	???????????	?200?0020?
<i>Leptolepis coryphaenoides</i>	1101111201	1101011111	1111101010	1110000001	0101000311
<i>Lepisosteus</i>	\$00-000000	0000000-000	0000100000	-0---0000	0000-00000
<i>Luisichthys</i>	111-1?1???	1?11010111	0110011010	131010000?	111111-?1?
<i>Lycoptera</i>	111-?0130?	??1?0?2011	100110\$020	120001000?	111111-010
<i>Megalops</i>	1111101301	1111012111	1011101110	1310110001	111111-310
<i>Obaichthys</i>	100-000000	0000000-000	0?200?0000	-0---?200	0000-00000
<i>Orthocormus</i>	100-0?????	??0110-1??	0000-2-01	00----1-	-200-00401
<i>Pachycormus</i>	100-0????1	0?0?110-1??	0000-2-01	00----1-	-200-0040?
<i>Parapholidophorus</i>	100-00011?	0110010100	00?01000?0	00---?200	0?00?00200
<i>Dorsetichthys</i>	120-000?21	1100010100	011010?080	1?2?0?00000	1100000201
<i>Pholidophorus gervasutii</i>	100-00011?	0110010100	???????????	???????????	?200?00200
<i>Pholidophorus latiusculus</i>	??2-?201??	??200?100	???????????	???????????	?200?00200
<i>Pholidophores</i>	??2-?201??	??200?2000	???????????	???????????	?200?002??
<i>Pholidoctenus</i>	100-00011?	0110010100	00101000?0	00---?200	0?00?00'00
<i>Pholidorhynchodon</i>	200-000110	0110010100	???????????	???????????	?200?00200
<i>Prohalecites</i>	100-000???	??2000-000	0110100000	----00000	0100-00000
<i>Protoclupea</i>	111-111?0?	??11010111	0110?11010	130010000?	111101-21?
<i>Siemensichthys macrocephalus</i>	11??1000??	01000?2100	0??0???????	???????????	?200?000?1
<i>Siemensichthys siemensi</i>	??????0???	??200?100	???????????	???????????	?200?002??
<i>Tharsis</i>	1110101301	110100-111	0110101010	1101000001	0111100311
<i>Varasichthys</i>	1110111301	1?11010111	02001110?0	11010?2001	111111121?
<i>Vinctifer</i>	100-002?00	0?0100-000	0010111030	1400111101	0101?10000
<i>Watsonulus</i>	?00-000?10	0?0000-000	???????????	???????????	?000?00?0?

	1	1
	6	6
	0	7
<i>Amia calva</i>	000101----	0-0000?
<i>Amia pattersoni</i>	000101----	0-0??0?
<i>Anaethalion</i>	12101200--	0-0??0?
<i>Annaichthys</i>	001000-01	110??0?
<i>Ankylophorus</i>	?01000-11	010??0?
<i>Ascalabos</i>	11101210--	0-0??0?
<i>Aspidorhynchus</i>	000010--01	110??0?
<i>Belonostomus</i>	000010-01	000??1?
<i>Catervariolus</i>	?0?000-00	010??00
<i>Domeykos</i>	1??01211--	0-0??0?
<i>Elops</i>	12101200--	0-0110?
<i>Eurycormus</i>	101001----	0-0??00
<i>Ichthyokentema</i>	10?000-00	000??00
<i>Heterotis</i>	10101200--	0-01100
<i>Hiodon</i>	10101200--	0-01100
<i>Hypsocormus</i>	0010?-----	0-0??00
<i>Knerichthys</i>	001000-11	1-0??00
<i>Lehmanophorus</i>	?0?000-11	110??00
<i>Leptolepis coryphaenoides</i>	?1101200--	0-0??00
<i>Lepisosteus</i>	000000-00	0010000
<i>Luisichthys</i>	?2?01211--	0-0??00
<i>Lycoptera</i>	00101200--	0-0??00
<i>Megalops</i>	12001200--	0-01100
<i>Obaichthys</i>	000000-01	001??00
<i>Orthocormus</i>	0010?-----	0-0??00
<i>Pachycormus</i>	0010?-----	0-0??00
<i>Parapholidophorus</i>	001000-00	010??00
<i>Dorsetichthys</i>	0010?0-00	000??00
<i>Pholidophorus gervasutii</i>	001000-01	110??00
<i>Pholidophorus latiusculus</i>	001000-00	010??00
<i>Pholidophoretes</i>	001000-00	010??00
<i>Pholidoctenus</i>	001000-10	010??00
<i>Pholidorhynchodon</i>	001000-11	110??00
<i>Prohalecites</i>	00000-----	- -0?01
<i>Protoclupea</i>	1?101211--	0-0??00
<i>Siemensichthys macrocephalus</i>	101000-11	000??00
<i>Siemensichthys siemensi</i>	101000-00	000??00
<i>Tharsis</i>	11101200--	0-0??00
<i>Varasichthys</i>	11101211--	0-0??00
<i>Vinctifer</i>	100010-00	000??00
<i>Watsonulus</i>	00?000-00	000??00